CRYSTAL STRUCTURES OF
$CsCH_3SO_3$, $LiN_2H_5SO_4$, AND $K_2Cr_2O_7$

THE CRYSTAL STRUCTURES

OF

$CsCH_3SO_3$, $LiN_2H_5SO_4$, AND $K_2Cr_2O_7$

By

JAMES KENNETH BRANDON, B. Sc.

A Thesis
Submitted to the Faculty of Graduate Studies
in Partial Fulfilment of the Requirements
for the Degree
Doctor of Philosophy

McMaster University
October 1967

DOCTOR OF PHILOSOPHY (1967)
(Physics)

McMASTER UNIVERSITY
Hamilton, Canada

TITLE: The Crystal Structures of $CsCH_3SO_3$, $LiN_2H_5SO_4$, and $K_2Cr_2O_7$

AUTHOR: James Kenneth Brandon, B.Sc. (McMaster University)

SUPERVISOR: Dr. I. D. Brown

NUMBER OF PAGES: xi, 175

SCOPE AND CONTENTS: X-ray diffraction experiments have been used to determine the structures of cesium methylsulfonate ($CsCH_3SO_3$), lithium hydrazinium sulfate ($LiN_2H_5SO_4$) above 160°C, and triclinic potassium dichromate ($K_2Cr_2O_7$). The solved $CsCH_3SO_3$ structure is compared with $BaSO_4$ and the $CH_3SO_3^{-1}$ ion stereochemistry is discussed in terms of a current theory of bonding for such groups. The previously known structure of room temperature ferroelectric $LiN_2H_5SO_4$ has received additional refinement and a comparison is made with the structure determined above 160°C. The symmetry and structure found for $K_2Cr_2O_7$ are compared with similar compounds and predictions are given for the yet unsolved structures of other $K_2Cr_2O_7$ phases. The first accurate data for the $Cr_2O_7^{-2}$ ion stereochemistry is presented. This ion is compared to similar ones, and the possibility of extending a bonding theory to such ions involving chromium is discussed.

ACKNOWLEDGEMENTS

The author expresses thanks to Dr. I. D. Brown for his encouragement, advice, and criticism so kindly offered during his supervision of this research. The author is also grateful to other members of the crystallography group, especially to Dr. C. Calvo for useful discussions, and to fellow graduate students for their contributions to the pool of crystallographic computer programs.

The author is grateful to the Ontario Government and the National Research Council of Canada for personal financial support.

TABLE OF CONTENTS

TABLE OF CONTENTS (Continued)

TABLE OF CONTENTS (Continued)

TABLE OF CONTENTS (Continued)

LIST OF FIGURES

LIST OF FIGURES (Continued)

LIST OF TABLES

LIST OF TABLES (Continued)

CHAPTER 1 INTRODUCTION

The crystal structures of the three materials to be described in this thesis are each of interest for a variety of reasons. These reasons will be outlined in detail in the separate chapters dealing with their structures. There is, however, one common feature of all three compounds which makes them of current interest. They all contain atomic groups in which either sulfur or chromium atoms are found in at least approximate tetrahedral coordinations.

The interest in this feature arises because Cruickshank (1) has described a mechanism for π-bonding among the atoms in tetrahedral groups where the central atom is one of Si, P, S, or Cl, and the surrounding atoms are O or N. This π-bonding occurs in addition to the basic σ-bond mechanism which arises through the tetrahedral arrangement of sp^3 hybrid orbitals around the central atom (2, Ch.4). In the theory, the π-bonding orbitals are formed by the $3d_{x^2-y^2}$ and $3d_{z^2}$ orbitals of the central atom together with the appropriate p orbitals of the four surrounding atoms. If for any reason strict tetrahedral symmetry should be lost, it is then proposed that the $3d_{xy}$, $3d_{yz}$, and $3d_{xz}$ orbitals can also add to the π-bonding strength. Cruickshank also discusses the distortions from tetrahedral symmetry to be expected when some of the surrounding atoms are not suited to take part in any π-bonding. This is the case for the methylsulfonate ion in $CsCH_3SO_3$ where a methyl group has replaced one of the oxygen atoms of a sulfate ion. $LiN_2H_5SO_4$ contains the sulfate ion itself, and Cruickshank has considered this ion as a basic example in developing his theory of π-bonding. Because sulfur and chromium are chemically similar and because they both can be found with tetrahedral oxygen coordinations, the dichromate ion $Cr_2O_7^{-2}$ in potassium dichromate might be expected to be similar to the pyrosulfate ion $S_2O_7^{-2}$ (3). Since much of the $S_2O_7^{-2}$ ion stereochemistry can be accounted for (1) on the π-bonding theory, a comparison with the $Cr_2O_7^{-2}$ ion ought to indicate experimentally the extent to which the theory is applicable when chromium is the central atom of a distorted oxygen tetrahedron.

Further discussion of the π-bonding theory will be postponed to later chapters where the details arise in explaining some experimental observations.

CHAPTER 2 THEORY

2.1 Introduction

The use of x-ray diffraction as a tool to investigate the arrangement of atoms in a crystal dates back to 1912 when an experiment suggested by P. M. Laue demonstrated that x-rays could be diffracted by the three dimensional periodic array of matter in a crystal. Since that date, theory and experimental techniques have been developed to a state far superior to that available when the first few simple crystal structures were determined. Today's students of crystallography are fortunate to have available a large number of reference works and texts which describe the theory and techniques of x-ray diffraction and crystal structure analysis (4)-(12). Therefore this present discussion will only outline very briefly the methods used. A relatively complete description is presented for the least squares refinement techniques.

2.2 Crystal Structure Determination

In single crystal x-ray diffraction experiments, a monochromatic x-ray beam interacts with the electrons in a crystal and is scattered by them. Since the electrons are concentrated mainly around the nuclei of the atoms which comprise the crystal, the scattering can be considered to arise from atoms and can be described in terms of atomic scattering factors (7, Ch.3) for the different species of atom present.

Since the arrangement of atoms in a crystal is periodic, interference of the scattered x-rays produces diffracted beams in well defined directions. From the geometry of diffraction patterns, as detected on photographic film by special x-ray cameras, one can determine the unit cell parameters $\underline{a}$ $\underline{b}$ $\underline{c}$ α β γ of the crystal lattice. The concepts of the reciprocal lattice (with unit cell parameters $\underline{a}^*$ $\underline{b}^*$ $\underline{c}^*$ α^* β^* γ^*) (7, Ch.1) and the Ewald sphere construction (7, Ch.1) are valuable in analysing the geometry of these diffraction patterns. It is customary to assign to each diffracted beam or reflection a set of Miller indices $(hk\ell)$ corresponding to the set of lattice planes which have produced the reflections (13, Ch.1).

From the symmetry of the diffraction patterns and from systematic absences (8, Ch.2). one can determine much about the space group symmetry of the unit cell. The relative integrated intensities of the diffracted beams contain part of the data necessary to determine the arrangement of atoms within the unit cell. These intensities $I(hk\ell)$ are real numbers and are related to the magnitudes of the structure factors. The structure factors are complex numbers of the form $F(hk\ell) = A(hk\ell) + i\,B(hk\ell)$ where A and i B are the real and imaginary parts of F and $\phi \equiv \tan^{-1}\frac{B}{A}$ is the phase of the structure factor. If both the magnitude and phase of each structure factor were known, it would be possible to determine the periodic electron density $\rho(x,y,z)$ in the unit cell according to the three dimensional Fourier series (8,Ch.1)

$$\rho(x,y,z) = \frac{1}{V} \sum_{h} \sum_{k} \sum_{\ell=-\infty}^{+\infty} F(hk\ell) \exp\{-2\pi i(hx + ky + \ell z)\} \quad [2\text{-}1]$$

where x,y,z are fractional coordinates along $\underline{a}$ $\underline{b}$ $\underline{c}$ and V is the unit cell volume.

Simplifications of [2-1] are possible in which projections of electron density are calculated. For example a projection down $\underline{b}$ of the unit cell electron density is

$$\rho(x,z) = \frac{1}{A'} \sum_{h} \sum_{\ell=-\infty}^{+\infty} F(h0\ell) \exp\{-2\pi i(hx + \ell z)\} \quad [2\text{-}2]$$

where A' is the area of the unit cell projection.

A direct calculation of ρ by [2-1] or [2-2] is not possible since the phases of the structure factors $F(hk\ell)$ are not measurable in diffraction experiments. This lack of knowledge is called the phase problem of crystallography. If the structure is centrosymmetric, the imaginary part of the structure factor is identically zero and the phase problem reduces to a problem of determining the sign of A.

It is common practice to devise a model for the structure and calculate the magnitudes and phases of the structure factors for this model. These complex numbers $F_c(hk\ell)$ usually involve a scale factor K and a temperature factor T which allows $|F_c(hk\ell)|$ to be fitted to the observed

$F_o(hk\ell)$. Frequently $1/K$ is applied to the set $F_o(hk\ell)$.

$$F_c(hk\ell) = K \sum_{i=1}^{N} f_i(hk\ell)\ T_i(hk\ell)\ \exp 2\pi i\ (hx_i + ky_i + \ell z_i) \quad [2\text{-}3]$$

where $f_i(hk\ell)$ is the atomic scattering factor of atom i (7,Ch.3)

$T_i(hk\ell)$ is the Debye Waller temperature factor (7, Ch.5)

i is an index running over the N atoms in a unit cell

and $x_i y_i z_i$ are the fractional coordinates of atom i.

The temperature factor

$$T_i = \exp \left\{- B_i \frac{\sin^2\Theta}{\lambda^2}\right\} \quad [2\text{-}4]$$

adjusts the calculated structure factors to account for the thermal motion of the atoms about their mean positions. B_i is an adjustable parameter for each atom and can be related to an isotropic root mean square displacement $\{\overline{u_i^2}\}^{1/2}$ of atom i according to (7, Ch.5)

$$B_i = 8\pi^2\ \overline{u_i{}^2}\ . \quad [2\text{-}5]$$

Since $B \dfrac{\sin^2\Theta}{\lambda^2} = \dfrac{B}{4} \{h^2a^{*2} + k^2b^{*2} + \ell^2c^{*2} + 2hka^*b^* \cos \gamma^*$

$+ 2h\ell a^*c^*\cos\beta^* + 2k\ell b^*c^*\cos\alpha^*\}$

an anisotropic temperature factor conveniently takes the form of an ellipsoid according to

$$T = \exp\text{-}\{\beta_{11}h^2 + \beta_{22}k^2 + \beta_{33}\ell^2 + 2\beta_{12}hk + 2\beta_{13}h\ell + 2\beta_{23}k\ell\} \quad [2\text{-}6]$$

with six adjustable thermal parameters β_{11} β_{22} β_{33} β_{12} β_{13} and β_{23}. The directions and magnitudes of the three principal axes of these ellipsoids can be found and the root mean square displacements along these three perpendicular directions can be calculated analogously to [2-5].

If the magnitudes $|F_c(hk\ell)|$ calculated by eqn [2-3] for the model are similar to the experimental set $F_o(hk\ell)$, then the model is considered a reasonable approximation of the true structure. The phases of the calculated $F_c(hk\ell)$ may then be used with the observed magnitudes $F_o(hk\ell)$ to calculate an electron density function. A plot of this function or one of its projections usually suggests adjustments which will improve the model, and the whole procedure can be repeated.

A difference electron density function uses the coefficients $F_o(hk\ell) - F_c(hk\ell)$ in place of $F(hk\ell)$ in eqn [2-1], with $F_o(hk\ell)$ taking the calculated phases of $F_c(hk\ell)$ when their magnitudes are reasonably similar. This function is a more sensitive indicator of the changes necessary to improve the model structure.

At each stage one can examine how well the proposed model structure fits the observed data by calculating an agreement index R

$$R = \left[\frac{\Sigma\ \omega\ (|F_o(hk\ell)| - |F_c(hk\ell)|)^2}{\Sigma\ \omega\ |F_o(hk\ell)|^2}\right]^{1/2} \qquad [2\text{-}7]$$

where the summations are over all reflections $(hk\ell)$ and ω is a weighting factor for each reflection customarily taken as

$1/\sigma^2$, where σ is the estimated standard error for $F_o(hk\ell)$. A decreasing R value indicates an improved fit between observed and calculated structure amplitudes.

A common method of initially devising a model structure is that introduced by Patterson (14) where the squares of the experimental diffraction amplitudes are used as coefficients in a Fourier series

$$P(u,v,w) = \frac{1}{V} \sum_h \sum_k \sum_{\ell=-\infty}^{+\infty} |F_o(hk\ell)|^2 \exp\{-2\pi i(hu + kv + \ell w)\} \quad [2\text{-}8]$$

where $P(u,v,w)$ is the Patterson function at u,v,w and u,v,w are fractional coordinates along $\underline{a}$ $\underline{b}$ $\underline{c}$. This Patterson function may be shown (8,Ch.1) to be equal to

$$V \int_0^1 \int_0^1 \int_0^1 \rho(x,y,z)\ \rho(x+u,\ y+v,\ z+w)\ dx\ dy\ dz$$

It will therefore have large values at positions $u\underline{a} + v\underline{b} + w\underline{c}$ corresponding to vectors in the unit cell connecting regions of large electron density. From such vector maps a model structure can often be found (10). For projections, say down $\underline{b}$, the Patterson function reduces to the form

$$P(u,w) = \frac{1}{A'} \sum_h \sum_{\ell=-\infty}^{+\infty} |F_o(h0\ell)|^2 \exp\{-2\pi i(hu + \ell w)\} \quad [2\text{-}9]$$

where A' is the area of the unit cell projection.

To obtain a set of experimental structure amplitudes $F_o(hk\ell)$ from the observed intensities $I(hk\ell)$, it is necessary to apply some geometrical correction factors. These are:

I) The Lorentz correction which compensates for variations in the time periods for which different crystal planes are moving through their reflecting positions. This factor does depend on camera geometry.

II) The polarization correction which compensates for the fact that different polarization components of the incident beam are not scattered equally.

Corrections I and II are commonly seen combined for a given x-ray camera technique. The squares of the experimental structure amplitudes are $|F_o(hk\ell)|^2 \propto \frac{1}{Lp} I(hk\ell)$ where L is the Lorentz factor, and p is the polarization factor. For unpolarized incident radiation $\frac{1}{p} = \frac{2}{1 + \cos^2 2\Theta}$ (11,Ch.7) where Θ is the Bragg scattering angle of the reflection. The Lorentz factor for various camera geometries is quoted in reference (11,ch.7).

There is another group of effects for which corrections may be necessary. These include absorption, primary extinction and secondary extinction (11,Ch.8). Usually one arranges by experimental design that these effects are small compared to the expected random errors of intensity measurements. These effects are therefore frequently ignored, at least during the preliminary stages of a structure determination.

2.3 Least Squares Refinement of Structure Parameters

With large memory high speed computers available, a convenient procedure for refining a promising model structure is a least squares analysis. In this approach, one adjusts the parameters in the model to minimize the sum of the squares of the differences between the observed and calculated structure factors. Since the observed values usually contain certain unavoidable inaccuracies, and since these are usually random in nature, it is necessary in using a least squares refinement to provide a large overdeterminacy of observed data.

The steps involved in a crystallographic least squares refinement process will now be described. For a given model a set of structure factors is calculated according to the function f, one for each measured reflection hkℓ.

i.e. $$F_c(\underline{h}) = f(\underline{h},p_i)$$

where the vector notation $\underline{h}$ denotes the set of indices hkℓ of the reflection and where p_i are the parameters of the model. The set p_i, $i = 1 \ldots N$, contain the x,y,z, β_{11}, β_{22}, β_{33}, β_{12}, β_{13}, β_{23}, and a multiplicity factor for each atom. In addition, layer scaling constants are also considered as adjustable parameters and may be included in the p_i list. The six anisotropic β's may be replaced by one parameter B for isotropic temperature factor refinement.

The parameters in the model structure are assumed to have approximately correct values given by p_i whereas the true values are considered to be the set $p_i + \Delta p_i$. In a linear approximation using the first two terms of a Taylor series expansion one has the relation

$$f\ (p_i + \Delta p_i) \simeq f\ (p_i) + \sum_i \Delta p_i \frac{\partial f(p_i)}{\partial p_i} .$$

The discrepancy between the structure factors calculated from the true parameters and from the approximate set is then

$$\Delta_T F(\underline{h}) = |F_T(\underline{h})| - |F_c(\underline{h})|$$

$$= |F_c(\underline{h})| + \sum_{i=1}^{N} \{\Delta p_i \frac{\partial |F_c(\underline{h})|}{\partial p_i}\} - |F_c(\underline{h})|$$

or

$$\Delta_T F(\underline{h}) = \sum_{i=1}^{N} \{\Delta p_i \frac{\partial |F_c(\underline{h})|}{\partial p_i}\} .$$

Ideally if one knew exact values for $|F_o|-|F_c|$ these could be substituted into the left hand side and one could solve any set of N such equations for the N unknown Δp_i values. However if the measurements of $|F_o(\underline{h})|$ are subject to random errors, each may be considered to be in discrepancy from $F_T(\underline{h})$ by an amount $E(\underline{h})$

$$E(\underline{h}) = |F_T(\underline{h})| - |F_o(\underline{h})| .$$

Therefore we have in the actual situation

$$\Delta_T F(\underline{h}) = |F_o(\underline{h})| - |F_c(\underline{h})| + E(\underline{h}) .$$

Hence

$$E(\underline{h}) = \left[\sum_{i=1}^{N} \Delta p_i \frac{\partial |F_c(\underline{h})|}{\partial p_i}\right] - |F_o(\underline{h})| + |F_c(\underline{h})| .$$

Using the usual principle of least squares one requires for a sufficiently large number of reflections that the sum of the squares of the values $E(\underline{h})$ should be a minimum, i.e. that

$$\sum_{\underline{h}} \omega(\underline{h})\, E^2(\underline{h})$$

$$= \sum_{\underline{h}} \omega(\underline{h}) \left[\left\{\sum_{i=1}^{N} \Delta p_i \frac{\partial |F_c(\underline{h})|}{\partial p_i}\right\} - |F_o(\underline{h})| + |F_c(h)|\right]^2$$

be minimized. Here $\omega(\underline{h})$ is a factor used to weight the individual reflections.

This function is a minimum when its N first order partial derivatives with respect to each of the p_i parameters are all zero.

i.e. $$\frac{\partial}{\partial p_{i'}} \{\sum_{\underline{h}} \omega(\underline{h})\, E^2(\underline{h})\} = 0 \text{ for all } i' = 1....N ,$$

i.e.

$$0 = \sum_{\underline{h}} \omega(\underline{h}) \left[2[\{\sum_{i=1}^{N} \Delta p_i \frac{\partial |F_c(\underline{h})|}{\partial p_i}\} - |F_o(\underline{h})| + |F_c(\underline{h})|] \frac{\partial |F_c(\underline{h})|}{\partial p_{i'}}\right] \qquad i' = 1....N ,$$

using the fact that second order derivatives $\frac{\partial^2 |F(\underline{h})|}{\partial p_{i'}\, \partial p_i}$ disappear in the linear approximation.

These N equations may be rewritten to give

$$\sum_{\underline{h}} \omega(\underline{h}) \left\{ \sum_{i=1}^{N} \Delta p_i \frac{\partial |F_c(\underline{h})|}{\partial p_i} \right\} \frac{\partial |F_c(\underline{h})|}{\partial p_{i'}}$$

$$= \sum_{\underline{h}} \omega(\underline{h}) \left\{ |F_o(\underline{h})| - |F_c(\underline{h})| \right\} \frac{\partial |F(\underline{h})|}{\partial p_{i'}}$$

or

$$\sum_{i=1}^{N} \left\{ \sum_{\underline{h}} \omega(\underline{h}) \frac{\partial |F_c(\underline{h})|}{\partial p_i} \frac{\partial |F_c(\underline{h})|}{\partial p_{i'}} \right\} \Delta p_i$$

$$= \sum_{\underline{h}} \omega(\underline{h}) \Delta F(\underline{h}) \frac{\partial |F_c(\underline{h})|}{\partial p_{i'}} \qquad i' = \ldots.N$$

where $\Delta F(\underline{h}) \equiv |F_o(\underline{h})| - |F_c(\underline{h})|$. These are N linear equations in the N unknowns Δp_i $i = 1,\ldots.N$.

In matrix notation these become

$$(A)_{N\mathrm{x}N} (\Delta P)_{N\mathrm{x}1} = (B)_{N\mathrm{x}1}$$

with matrix elements defined by

$$(A)_{ij} = \sum_{\underline{h}} \omega(h) \frac{\partial |F_c(\underline{h})|}{\partial p_i} \frac{\partial |F_c(\underline{h})|}{\partial p_j}$$

$$(\Delta P)_i = \Delta p_i$$

$$(B)_j = \sum_{\underline{h}} \omega(\underline{h}) \Delta F(\underline{h}) \frac{\partial |F_c(\underline{h})|}{\partial p_j}$$

for i,j = 1 .... N.

Calculating A^{-1}, the inverse of the matrix A, one then uses matrix multiplication to solve for the matrix ΔP,

$$\Delta P = A^{-1} A \, \Delta P = A^{-1} B \, .$$

This yields directly the components of ΔP and hence the required adjustments for the set of approximate parameters in the model.

During least squares refinement, a calculation of estimated standard errors for the refined parameters p_i is possible. The formula applicable would normally be

$$\sigma_{p_i}^{2} = \frac{\{\sum_{\underline{h}} \omega(\underline{h}) \, [\Delta' F(\underline{h})]^2\} \, (A^{-1})_{ii}}{N_u - N}$$

where N_u is the number of reflections with non zero weight used during refinement, and $\Delta' F(\underline{h})$ are the differences between observed structure factors and those calculated with the new parameters $p_i + \Delta p_i$. Since these new structure factors are not usually calculated until a later refinement cycle, the $\sigma_{p_i}^{2}$ are approximated according to

$$\sigma_{p_i}^{2} \doteq \frac{\{ \sum_{\underline{h}} \omega(\underline{h}) \, [\Delta F(\underline{h})]^2 - \sum_{i'} B_{i'} \, \Delta p_{i'}\} \, (A^{-1})_{ii}}{N_u - N} \, .$$

From the definition of $B_{i'}$, the correction term in this form can be seen to provide a valid approximation for $\Delta' F(\underline{h})$ in terms of the values $\Delta F(\underline{h})$ available during the present cycle of refinement.

During refinement it is hoped that parameters to be simultaneously refined do not have large correlations between them. Large correlations between two parameters in a model structure imply that either or both of them may undergo a coupled adjustment in improving the least squares fit and are not strictly refining as independent variables. In this case there arises some uncertainty whether the proper adjustment to either parameter has been determined. Large correlations may also point out the unsuitable nature of the model and in some cases may even indicate the structure to be indeterminate. A relative measure of the strength of interaction between any two parameters p_i and p_j may be inspected from the C_{ij} element of the correlation matrix defined by

$$C_{ij} = \frac{[A^{-1}]_{ij}}{\{[A^{-1}]_{ii}\ [A^{-1}]_{jj}\}^{1/2}} \quad .$$

These elements are normalized to unity for $i=j$ and one hopes that elements for $i \neq j$ in any refinement remain small fractions of unity.

CHAPTER 3 THE CRYSTAL STRUCTURE OF CESIUM METHYLSULFONATE

3.1 Introduction

The interest in cesium methylsulfonate $CsCH_3SO_3$ (hereafter abbreviated as CsMS), and specifically in the methylsulfonate ion, arises from a discussion by Cruickshank (1) about possible π-bonding between a central silicon, phosphorous, sulfur, or chlorine atom and surrounding oxygen or nitrogen atoms when these substances form a tetrahedral group. Cruickshank also considers the case where the four ligands are not all identical either in chemical species or position, and suggests what resulting distortions from tetrahedral symmetry might be expected. Since no bond lengths and angles have been determined for the methylsulfonate ion, study of this group is of value as an experimental test of Cruickshank's theories for an example where sulfur is the central atom.

In addition, a comparison of the CsMS structure to a similar one such as $BaSO_4$ points out differences in the two crystal structures attributable to the different stereochemistries of the methylsulfonate and sulfate groups.

3.2 Experimental

3.2 A Sample Preparation

Several samples containing cesium methylsulfonate crystals (CsMS) were supplied during the course of this work by Dr. E. A. Robinson of the University of Toronto. The crystals were prepared (15),(16*) from cesium carbonate and an aqueous solution of methansulfonic acid. Equimolar quantities of the reagents were used and the solution evaporated nearly to dryness. The salt was filtered off and washed with methanol. It was dissolved in a small quantity of water and reprecipitated by addition of methanol. Recrystallization was from aqueous methanol.

The samples contained white amorphous lumps as well as a few colourless crystals of CsMS. As was discovered during x-ray investigations there were clear colourless crystals of cesium sulfate Cs_2SO_4 also present in the samples. However, the desired CsMS crystals could easily be distinguished from cesium sulfate by their x-ray diffraction patterns.

3.2 B Crystal Data

The colourless cesium methylsulfonate (CsMS) crystals were frequently needle shaped, elongated in the b direction. They were found to be deliquescent and in humid weather would often deteriorate before a full set of x-ray intensity

---

*In this reference, the material is called "Caesium methanesulphonate".

photographs could be collected.

The unit cell parameters were measured from hk0 and 0kℓ precession camera photographs taken with Zr-filtered Mo-radiation ($\lambda_{MoK\alpha_1}$ = 0.70930 Å (17)). The observed systematic absences were consistent with either the centrosymmetric Pnma (D_{2h}^{16}) or the noncentrosymmetric $Pn2_1a$ (C_{2v}^{9}) space group. The structure analysis shows that the correct space group is probably Pnma. The density of CsMS crystals was measured by floatation in a density column of tetrabromoethane and trichloroethylene calibrated using crystals of CaF_2, $CaCl_2$ and NaCl. The measured density agrees with the value calculated assuming four formula units per unit cell. The crystal data are summarized in Table 3-1.

3.2 C Intensity Data

The crystal selected for x-ray intensity photographs was a rectangular parallelepiped with dimensions 0.07 x 0.15 x 0.07 mm elongated in the [010] direction. It was mounted externally on a capillary since the photographs were being taken during a season of low atmospheric humidity. Equi-inclination Weissenberg photographs of the layers hkℓ k = 0,1,2,3,4, and 5 were taken using Ni-filtered Cu-radiation ($\lambda_{CuK\bar{\alpha}}$ = 1.54184 Å (17)). Each layer was recorded on five photographs of varying exposure times ($\frac{1}{3}$, 1, 3, 9 and 27 hours) and each film was developed under identical conditions. Collection of this many exposures

TABLE 3-1

Crystal data for $CsCH_3SO_3$

System	Orthorhombic
Systemmatic absences	hk0 h = 2n + 1
	0kℓ k + ℓ = 2n + 1
Space group	Pnma (D_{2h}^{16})
Cell constants	
a	9.526 ± 0.005 Å
b	6.264 ± 0.006 Å
c	8.692 ± 0.008 Å
Unit cell volume	518.7 ± 0.7 $Å^3$
Reciprocal cell constants	
a*	0.1046 ± .0001 $Å^{-1}$
b*	0.1596 ± .0002 $Å^{-1}$
c*	0.1150 ± .0001 $Å^{-1}$
Density	
Measured	2.90 ± 0.06 gm cm^{-3}
Calculated	2.920 ± 0.004 gm cm^{-3}
Number of formula units per unit cell	4
X-ray absorption coefficients	MoKα 75.2 cm^{-1} CuKα 586. cm^{-1}

per layer allowed easy measurement of the weakest and strongest reflections and also provided more than one independent intensity measurement which could be averaged for the majority of the reflections.

A lattice row template was used to index the Weissenberg films and the intensities were measured visually by comparison with a calibrated wedge film. The wedge was prepared by exposing a film to a diffracted beam of x-rays for successively longer time intervals, the film holder being displaced slightly between each exposure. Each intensity measurement was assigned a standard error which could be used for weighting the individual reflections during least squares refinement of the structure.

The intensities were then corrected for the Lorentz and polarization effects. The form of these corrections for the equi-inclination Weissenberg method is given in (11, Ch.7). No absorption corrections were attempted even though μR for Cu radiation was about 2.0 (5, Table 5.3.5B).

3.3 Structure Determination and Refinement

3.3 A Solution in the [010] Projection

For both of the possible space groups Pnma and $Pn2_1a$ the projection down [010] is a centrosymmetric one having plane group symmetry pgg. A solution for the structure in this centrosymmetric projection using the $h0\ell$ data was attempted first. This projection was selected because the problem of determining the phases of the structure factors reduces to one of determining only the signs (+ or -) of the real part of each structure amplitude since the imaginary parts are identically zero. Also, since Z = 4 (Z ≡ the number of formula units per unit cell) the Cs and S atoms are restricted to lie on mirror planes in Pnma and the orientation of the methylsulfonate group is similarly restricted by the mirror planes perpendicular to [010]. Hence a solved [010] projection could possibly distinguish the correct space group for the observed methylsulfonate group orientation.

The h0ℓ observed structure amplitudes were used to calculate a Patterson function projection down [010], according to equation [2-9]. This function revealed probable positions for the large cesium atoms but little else, so a sharpened Patterson function (10, Ch.4) was calculated in order to increase the resolution. Figure 3-1 shows this sharpened Patterson function. It was solved by the method of superposition (8,Ch.7) to give the four Cs atoms and the four S atoms in the unit cell. With these proposed x and z atom coordinates and with a temperature factor and scale factor provided by Wilson's method (8, Ch.4), structure factors $F_c(h0\ell)$ were calculated according to eqn.[2-3]. These were found to be close

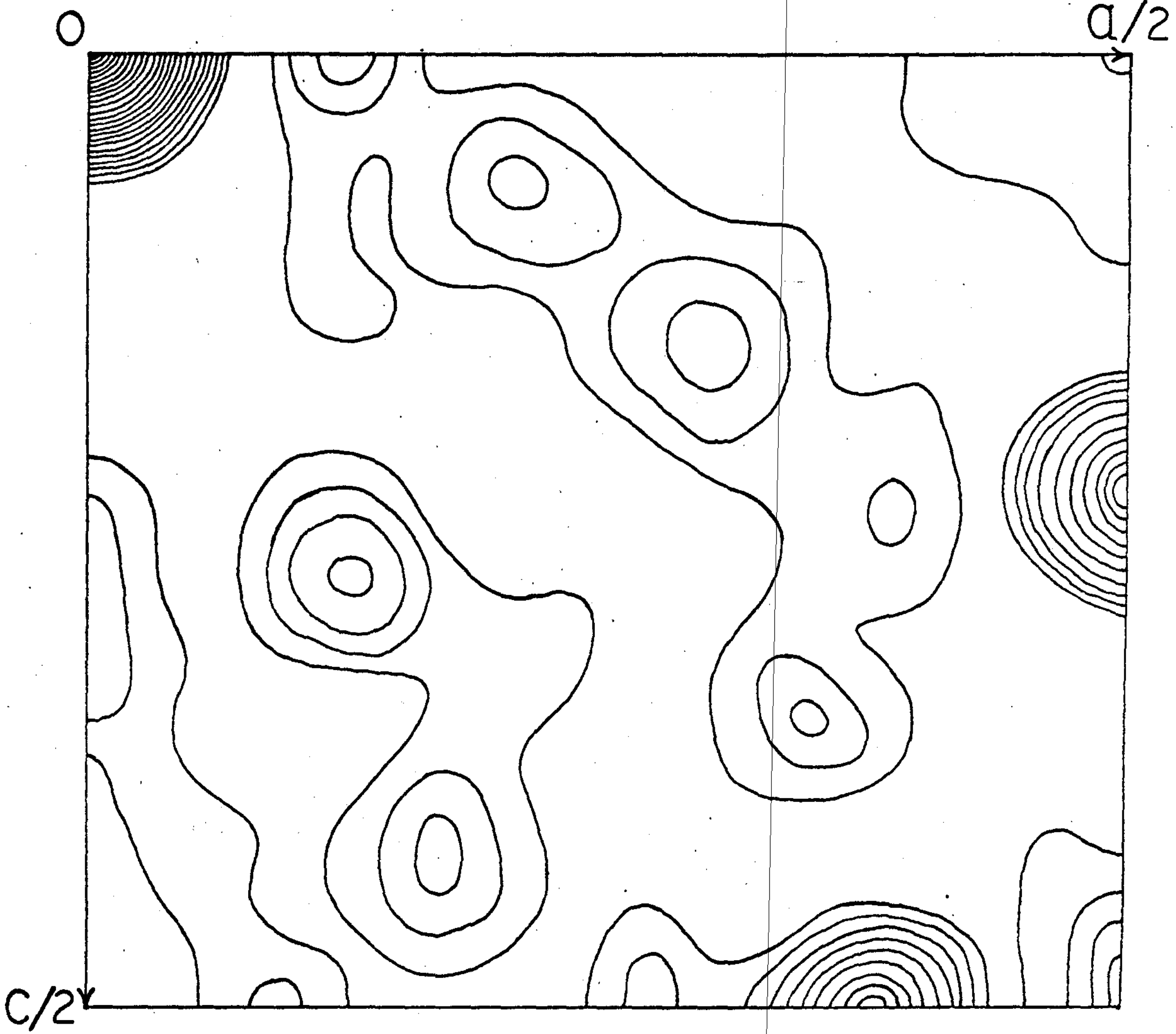

FIGURE. 3-1

Sharpened Patterson Function Projection Down [010]. Contours are Drawn at Equal Intervals in Arbitrary Units.

enough to the observed structure factor magnitudes $|F_o(h0\ell)|$ to allow a [010] electron density projection to be calculated according to eqn.[2-2]. The signs of the $F_o(h0\ell)$ were considered to be known if $|F_c(h0\ell)|$ was not less than $\frac{1}{2}$ $|F_o(h0\ell)|$.

This electron density function, shown in Figure 3-2, revealed three possible positions close to the S atom for the O and C atoms. Further Fourier syntheses indicated one of these positions to be the C atom since it was at least 1.7 Å from the S atom and S-O distances were not expected to be this long. One of the two remaining positions did not show spherical contours and this was interpreted to be two O atoms which were partially superposed in this projection. The third position was interpreted to be the remaining O atom. No H atom positions could be seen in any of these initial electron density projections.

3.3 B Refinement of Trial Three Dimensional Structures

Since there was some doubt that two of the O atoms overlapped exactly in the [010] projection, it was proposed that there was no mirror plane through the methylsulfonate group perpendicular to [010] and that the noncentrosymmetric space group $Pn2_1a$ should be used for a trial three dimensional structure. If Pnma should

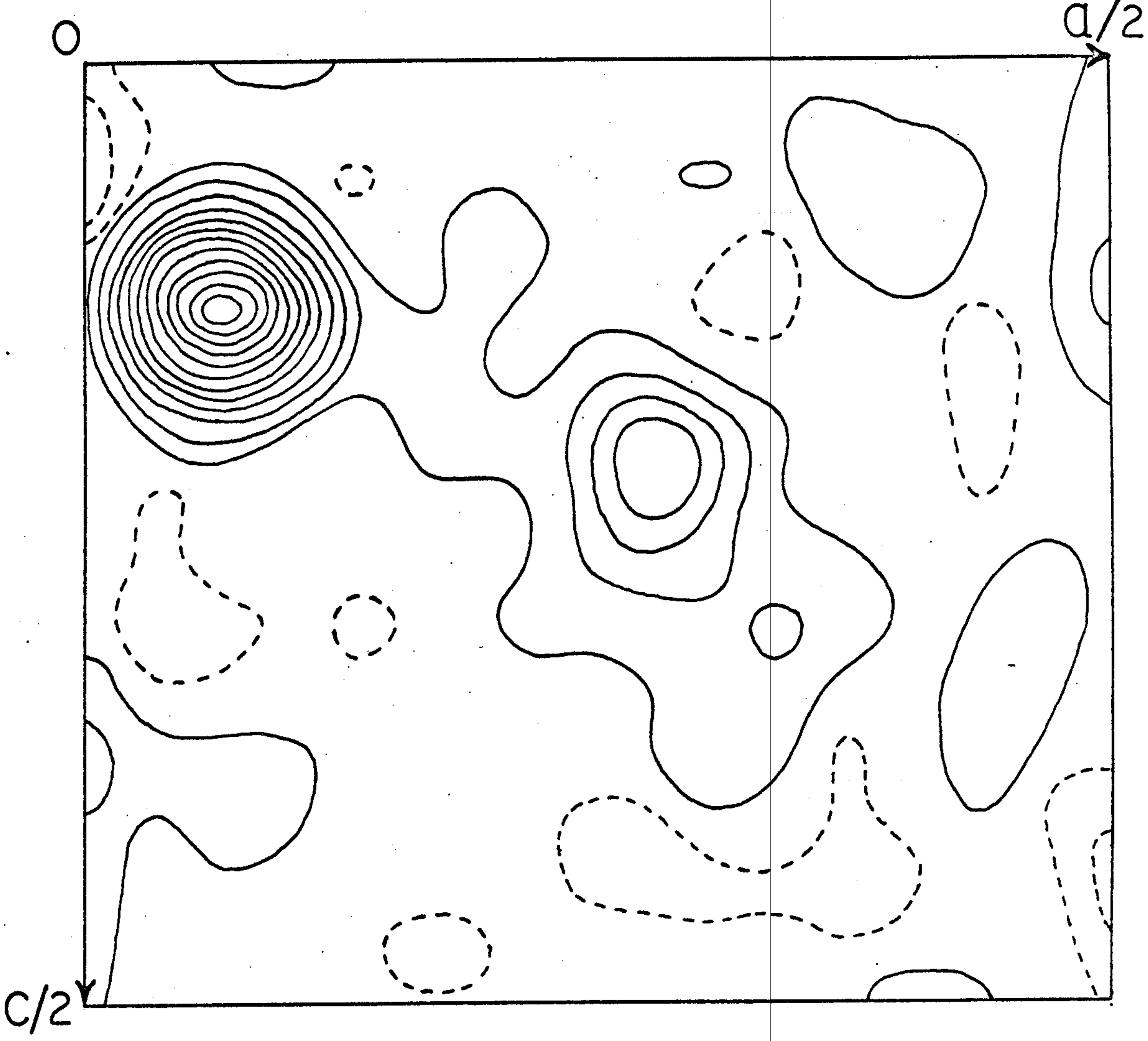

FIGURE 3-2

Initial Electron Density Function Projection Down [010]. Contours are Drawn at Equal Intervals in Arbitrary Units. Dashed Lines Denote Negative Contours.

be the true space group then the $Pn2_1a$ refinement should indicate this fact by generating the mirror plane. A trial three dimensional structure was obtained by calculating appropriate y coordinates for a possible structure, making use of the known x and z values. This trial structure was used as a starting point for least squares refinement.

The least squares program allowed adjustment of x, y, z and six anisotropic temperature factor components for each atom along with scale factors for each of the layers of data. In $Pn2_1a$ the y coordinate of one atom must be chosen arbitrarily and so the Cs atom was given the value $y = \frac{1}{4}$ corresponding to its constrained value in Pnma space group. After a few refinement cycles the atom positions in the $Pn2_1a$ model were not very much different from those required by the centrosymmetric Pnma space group. Hence the structure was also refined in Pnma. The best weighted agreement index, R as defined by eqn. [2-7], obtainable in Pnma was 0.1206 compared to 0.1199 in $Pn2_1a$. Hence there was not very much difference in the fits to the observed data given by these two models. Since Pnma used 37 variable parameters compared to 59 for $Pn2_1a$, one would normally prefer the Pnma model which uses fewer variables to obtain a nearly equivalent fit. However the real question at this point seemed to be whether small deviations from a centrosymmetric structure actually exist in CsMS.

3.3 C Tests for the Correct Space Group

An attempt to detect piezoelectricity was made in order to investigate further the question of the correct space group. The presence of a piezoelectric effect would indicate that the noncentrosymmetric $Pn2_1a$ space group was correct. The equipment constructed for this purpose was essentially the transmission type piezoelectricity detector described by Blume (18) except that a commercial signal generator was used as the FM source with frequency modulation chosen as 1000 c.p.s. A differential input oscilloscope with sensitivity of 0.1 mv. was used to display the detector output. No piezoelectric resonances were observed in CsMS over the frequency range 1×10^6 to 50×10^6 c.p.s. The absence of an observable piezoelectric effect is consistent with either space group so these measurements failed to resolve the question.

Hamilton's tables for significance tests (19) on the crystallographic R factors were also used in an attempt to determine the correct space group. These significance tests indicate the statistical chance of error if one accepts an unrestrained model with a lower R factor in preference to a restrained model with larger R factor. Since the R factor ratio for the two refinements was small ($R(Pnma)/R(Pn2_1a) = 1.006$), it was necessary to extend the series of tables given by Hamilton to higher levels of significance. This was done using Hamilton's relation between the R factor ratio and the F table values (19,Eqn.24), and Merrington and Thompson's relation (20) which gives the F values for significance levels greater than 0.5 in terms of those less than 0.5. Only the necessary table values were calculated corresponding to $R_{20,366,\alpha}$ for the significance levels $\alpha = 0.750, 0.900, 0.950, 0.975, 0.990$, and 0.995, and these were examined as a function of α. Since the observed ratio of 1.006 still lay below the lowest of these calculated values (1.010 calculated for $\alpha = 0.995$), there is statistically more than 99.5% chance of error if one excluded the Pnma refinement and proposed that only the $Pn2_1a$ refinement is correct. Hamilton's test therefore indicates a very remote chance of the space group being $Pn2_1a$, and the rest of the discussion will be based on the structure refined in Pnma space group.

3.3 D Possible Hydrogen Positions

In an attempt to detect hydrogen atom positions, a difference electron density projection down [010] was calculated. The Fourier coefficients used were the differences between the observed $h0\ell$ structure factors and those calculated from parameters refined in Pnma with three dimensional data. The function is shown in Figure 3-3. The broken straight lines enclose regions in which

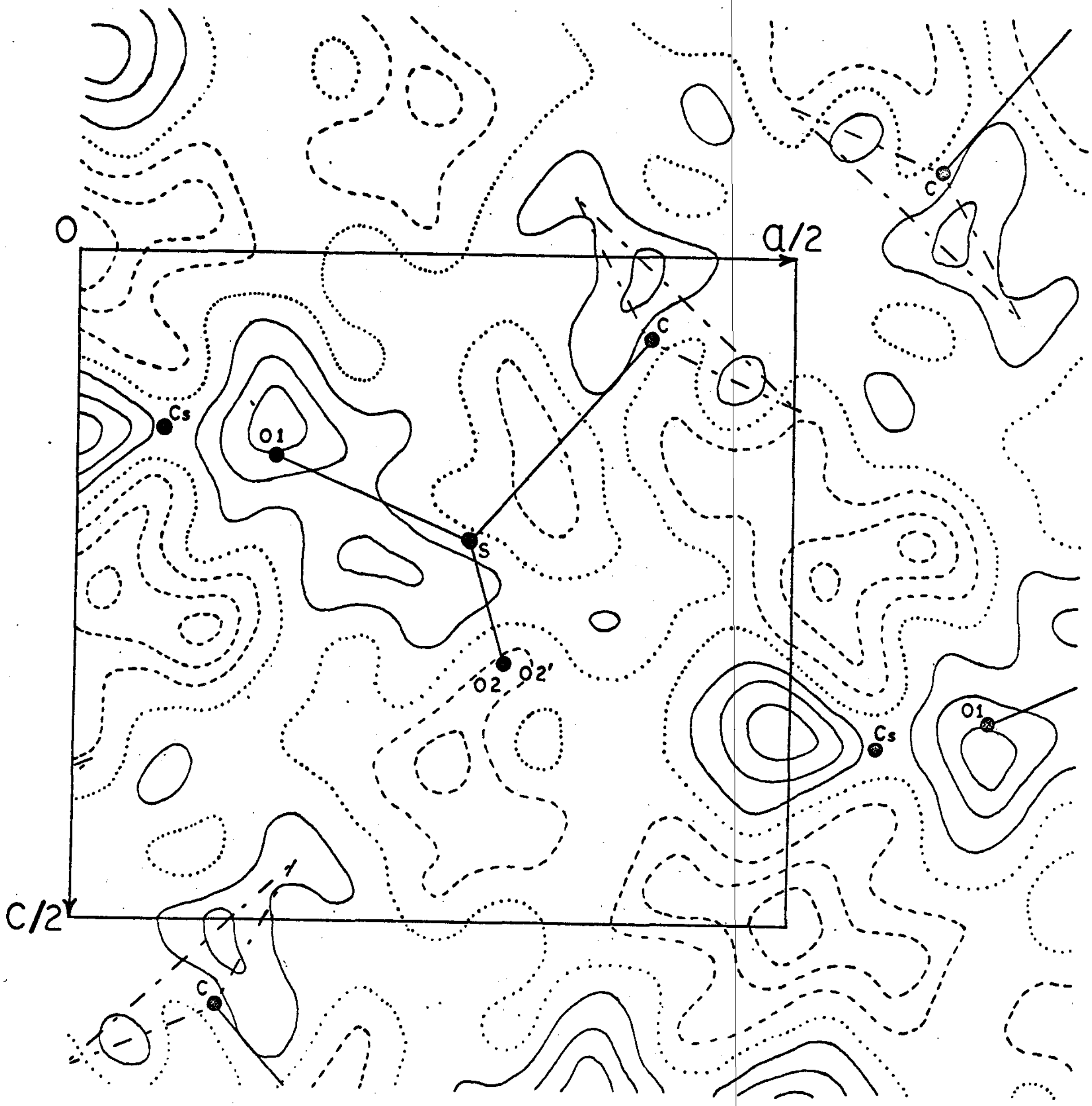

FIGURE 3-3

Final Difference Electron Density Function Projection Down [010]. Contours are Drawn at Equal Intervals in Arbitrary Units. Atom Positions Used to Calculate F_c are Shown. The Dotted Lines are Zero Contours and the Dashed Lines are Negative Contours. The Broken Straight Lines Enclose Regions in which H Atoms Might be Expected.

hydrogen peaks might be expected, assuming tetrahedral S-C-H angles and C-H bond lengths of 1.10 Å or less. Some density is found in this region, but the peaks are smaller than other difference Fourier peaks in this projection and it would be unwise to draw any conclusions in such circumstances.

Another attempt to detect hydrogen atoms was made by including them in the model at likely positions and examining any improvement in the agreement between calculated and observed structure factors. Three hydrogen atoms were included in the model assuming that they were part of a rotating methyl group. The structure factor contribution for each such atom may be calculated like any other atom in eqn.[2-3] but with a modified atomic scattering factor (see Appendix I). The rotating hydrogen atoms were constrained to make tetrahedral S-C-H angles and to have C-H distances of 1.10 Å (6, Table 4.2.3). The calculation was insensitive to this small addition of scattering matter as R only decreased by 0.001. Consequently from this analysis and from the [010] difference electron density, no hydrogen positions could be confirmed in this x-ray analysis.

Table 3-2 gives the final atomic coordinates and anisotropic temperature factors in space group Pnma together with the standard errors calculated during the least squares refinement.

TABLE 3-2

Atomic parameters for $CsCH_3SO_3$ in space group Pnma. (Figures in parantheses are the standard errors in the last digits quoted.)

Atom	Multiplicity and site†	x	y	z
Cs	4(c)	0.0610 (2)	1/4	0.1324 (2)
S	4(c)	0.2740 (7)	3/4	0.2182 (7)
O1	4(c)	0.1366 (17)	3/4	0.1538 (22)
O2	8(d)	0.3015 (14)	0.5569(25)	0.3072 (18)
C	4(c)	0.4015 (32)	3/4	0.0647 (39)

Temperature factor components*

Atom	β_{11}	β_{22}	β_{33}	β_{12}	β_{13}	β_{23}
Cs	88 (2)	215 (7)	116 (2)	0	-10 (2)	0
S	63 (7)	224 (28)	84 (7)	0	-10 (6)	0
O1	55 (18)	310 (80)	129 (30)	0	3 (18)	0
O2	118 (18)	187 (55)	171 (22)	40 (22)	-21 (18)	97 (31)
C	97 (37)	623(165)	147 (42)	0	113 (37)	0

*Anisotropic temperature factors appear in the structure factor calculations in the form

$$T = \exp[-10^{-4}(\beta_{11}h^2 + \beta_{22}k^2 + \beta_{33}{}^2 + 2\beta_{12}hk + 2\beta_{13}h\ell + 2\beta_{23}k\ell)].$$

†Site symbol as defined for the space group Pnma in International Tables (4).

Table 3-3 presents the observed structure amplitudes F_o together with their estimated standard errors σ and the structure factors, F_c, calculated from the parameters of Table 3-2. The atomic scattering factors used throughout these calculations were taken from (6, Table 3.3.1A) for S ref. SXC-69, O ref. SX-8, C ref. SX-6, and H ref. Q-1; and from (6, Table 3.3.1B) for Cs.

3.4 Description of the Structure

Figure 3-4 shows the structure of one unit cell of cesium methylsulfonate (CsMS) projected down [010]. The two mirror planes perpendicular to b are at y = 1/4 and y = 3/4. The n and a glide planes perpendicular to a and c respectively are shown by broken lines. The groups shown in heavy outline lie on the mirror plane at y = 3/4, while those in fainter outline are below on the mirror plane at y = 1/4. The oxygen atom O2 is situated below the mirror plane in each methylsulfonate group and is related to another oxygen atom by reflection in the mirror plane. O2 and O2' its mirror image,are superposed when viewed down [010] as in Fig. 3-4. By operation of the n and a glide plane symmetry elements on the atoms of any asymmetric unit, the complete unit cell and its neighbouring cells can be generated. Fig. 3-5(a) shows an extended diagram of the [010] projection. Here the anions have been drawn as projections of triangular pyramids with the carbon atoms marked as black circles. The

TABLE 3-3

H	K	L	FO	FC	σ
2	0	0	414	475	27
4	0	0	130	197	26
6	0	0	808	-336	55
8	0	0	649	-688	66
10	0	0	353	-331	44
12	0	0	119	-90	40
1	0	1	1217	1279	90
2	0	1	760	-676	46
3	0	1	307	311	21
4	0	1	1381	-1548	70
5	0	1	168	-210	28
6	0	1	110	-133	28
7	0	1	451	-477	25
8	0	1	294	-337	44
9	0	1	411	-422	43
10	0	1	350	315	44
11	0	1	103	-122	26
12	0	1	180	158	24
0	0	2	1016	-1034	90
1	0	2	986	-832	80
2	0	2	687	598	43
3	0	2	1603	-1639	96
4	0	2	410	-360	29
5	0	2	1056	-1107	98
6	0	2	114	95	28
7	0	2	125	-231	31
8	0	2	133-	57	66
9	0	2	132-	88	66
10	0	2	121-	47	61
11	0	2	311	321	31
12	0	2	55-	54	28
1	0	3	1756	-1453	159
2	0	3	922	-902	52
3	0	3	187	-174	31
4	0	3	459	-427	42
5	0	3	231	287	38
6	0	3	599	-620	48
7	0	3	399	438	31
8	0	3	134	106	33
9	0	3	431	450	39
10	0	3	115-	56	58
11	0	3	90-	100	45
0	0	4	1337	-1227	85
1	0	4	89-	79	44
2	0	4	1414	-1184	76
3	0	4	100	105	25
4	0	4	187	198	31
5	0	4	220	251	31
6	0	4	389	454	31
7	0	4	133-	1	66
8	0	4	548	590	48
9	0	4	125-	121	62
10	0	4	301	292	28
11	0	4	76-	-61	38
1	0	5	521	-491	31
2	0	5	912	937	62
3	0	5	263	-239	36
4	0	5	785	750	45
5	0	5	125	143	32
6	0	5	407	429	32
7	0	5	327	355	27
8	0	5	129-	-7	64
9	0	5	115-	91	58
10	0	5	93-	-79	46
0	0	6	297	299	23
1	0	6	235	241	29
2	0	6	208	182	35
3	0	6	819	871	56
4	0	6	129-	-38	64
5	0	6	430	472	31
6	0	6	134-	30	67
7	0	6	343	328	37
8	0	6	119	-120	30
9	0	6	100-	-144	50
10	0	6	70-	-89	35
1	0	7	731	704	46
2	0	7	245	261	35
3	0	7	187	175	47
4	0	7	232	226	39
5	0	7	133-	-127	66
6	0	7	128	155	32
7	0	7	383	-413	37
8	0	7	102-	-38	51
9	0	7	172	-134	17
0	0	8	527	461	34
1	0	8	134-	44	67
2	0	8	411	420	33
3	0	8	310	-320	42
4	0	8	129-	11	65
5	0	8	123-	-2	62
6	0	8	253	-243	51
7	0	8	120	-136	20
8	0	8	305	-237	18
1	0	9	126	124	32
2	0	9	361	-342	43
3	0	9	120-	102	60
4	0	9	329	-306	39
5	0	9	145	-157	36
6	0	9	271	-259	28
7	0	9	63-	-27	32
0	0	10	149	-109	37
1	0	10	255	-218	32
2	0	10	142	-169	36
3	0	10	163	-141	41
4	0	10	83-	40	42
5	0	10	327	-271	27
1	0	11	275	-210	36
2	0	11	53-	-20	27
2	1	0	1192	-1455	131
4	1	0	1134	-1250	99
6	1	0	1150	-1143	74
8	1	0	187	223	37
10	1	0	156	200	39
12	1	0	371	324	43
0	1	1	484	-438	34
1	1	1	220	-242	21
2	1	1	1568	-1544	138
3	1	1	806	-867	99
4	1	1	77	98	19
5	1	1	906	-808	86
6	1	1	343	395	29
7	1	1	328	-340	38
8	1	1	665	614	66
9	1	1	146	157	36
10	1	1	279	254	22
11	1	1	220	224	18
12	1	1	38-	-9	19
1	1	2	1728	-1575	133
2	1	2	374*	117	0
3	1	2	871	-760	51
4	1	2	141	-131	23
5	1	2	324	372	20
6	1	2	355	366	26
7	1	2	773	892	83
8	1	2	119	-132	30
9	1	2	417	457	42
10	1	2	76-	89	38
11	1	2	160	159	34
0	1	3	1461	-1185	150
1	1	3	289	241	20
2	1	3	258	-268	15
3	1	3	1161	1046	69
10	1	3	176	198	29
4	1	3	271	-298	22
5	1	3	706	773	52
6	1	3	413	457	21
7	1	3	329	364	26
8	1	3	281	348	32
9	1	3	182	-182	37
11	1	3	220	-204	21
1	1	4	57-	102	29
2	1	4	741	704	42
3	1	4	198	181	16
4	1	4	1250	1183	96
5	1	4	106	125	27
6	1	4	511	547	64
7	1	4	188	-223	38
8	1	4	84-	106	42
9	1	4	78-	-17	39
10	1	4	351	-350	46
11	1	4	102	-119	20
0	1	5	1229	1030	88
1	1	5	372	400	30
2	1	5	606	577	31
3	1	5	322	298	28
4	1	5	187	187	31
5	1	5	541	485	54
6	1	5	411	-502	43
7	1	5	85-	27	42
8	1	5	352	-387	28
9	1	5	72-	-33	36
10	1	5	227	-194	18
1	1	6	704	743	40
2	1	6	77-	-56	38
3	1	6	463	428	68
4	1	6	201	-197	34
5	1	6	267	-290	27
6	1	6	146	-166	37
7	1	6	310	-341	21
8	1	6	74-	-88	37
9	1	6	581	-439	25
10	1	6	41-	58	21
0	1	7	353	367	19
1	1	7	412	-402	21
2	1	7	220	207	31
3	1	7	386	-379	28
4	1	7	85-	-83	42
5	1	7	627	-620	42
6	1	7	80-	-120	40
7	1	7	74-	-93	37
8	1	7	141	-144	28
9	1	7	46-	85	23
1	1	8	146	-138	37
2	1	8	253	-307	42
3	1	8	186	-186	37
4	1	8	426	-455	39
5	1	8	77-	101	38
6	1	8	244	-248	20
7	1	8	60-	-3	30
8	1	8	45-	-40	22
0	1	9	476	-446	26
1	1	9	111	45	28
2	1	9	268	-260	22
3	1	9	294	-279	19
4	1	9	70-	-56	35
5	1	9	63-	3	32
6	1	9	193	197	11
7	1	9	36-	-29	18
1	1	10	308	-278	17
2	1	10	62-	59	31
3	1	10	58-	-50	29
4	1	10	157	161	17
5	1	10	38-	16	19
0	1	11	39-	-35	19
1	1	11	36-	3	18
2	2	0	891	-1020	64
4	2	0	85-	-38	43
6	2	0	884	822	88
8	2	0	446	479	37
10	2	0	378	383	26
1	2	1	949	-777	94
2	2	1	966	965	59
3	2	1	390	-426	35
4	2	1	881	870	54
5	2	1	300	326	17
6	2	1	398	388	80
7	2	1	370	364	31
8	2	1	223	210	37
9	2	1	357	388	22
10	2	1	277	-286	23
11	2	1	89-	112	44
0	2	2	291	271	19
1	2	2	1355	1064	111
2	2	2	71-	-71	36
3	2	2	1269	1152	91
4	2	2	217	201	20
5	2	2	953	975	57
6	2	2	116	-164	29
7	2	2	217	281	36
8	2	2	129-	50	65
9	2	2	124-	-142	62
10	2	2	109-	-98	55
11	2	2	250	-251	14
1	2	3	1299	1053	116
2	2	3	625	525	55
3	2	3	520	483	40
4	2	3	557	573	46
5	2	3	528	-498	47
6	2	3	468	436	47
7	2	3	239	-267	17
8	2	3	129-	-70	64
9	2	3	418	-432	26
10	2	3	103-	-44	51
11	2	3	73-	-100	37
0	2	4	1342	1131	91
1	2	4	512	-477	41
2	2	4	1136	959	57
3	2	4	103-	103	51
4	2	4	156	-167	39
5	2	4	206	-224	17
6	2	4	356	-368	22
7	2	4	129-	-80	65
8	2	4	541	-548	29
9	2	4	114-	-26	57
10	2	4	270	-248	16
11	2	4	52-	12	26
1	2	5	654	534	86
2	2	5	878	-724	68
3	2	5	114-	-6	57
4	2	5	691	-627	105
5	2	5	126-	57	63
6	2	5	408	-416	41
7	2	5	382	-408	32
8	2	5	119-	25	59
9	2	5	103-	-64	51
10	2	5	77-	64	38
0	2	6	167	-148	42
1	2	6	119-	-21	59
2	2	6	243	-252	30
3	2	6	956	-860	49
4	2	6	128-	72	64
5	2	6	419	-427	30
6	2	6	127-	-17	64
7	2	6	208	-233	35
8	2	6	107-	90	54
9	2	6	86-	83	43
1	2	7	723	-651	56
2	2	7	129-	-168	64
3	2	7	129-	-78	65
4	2	7	288	-283	29
5	2	7	125-	41	63
6	2	7	118-	-77	59
7	2	7	418	398	27
8	2	7	88-	4	44
9	2	7	106*	124	0
0	2	8	587	-513	70
1	2	8	128-	-78	64
2	2	8	284	-294	28
3	2	8	305	297	38
4	2	8	120-	-33	60
5	2	8	112-	19	56
6	2	8	201	207	38
7	2	8	83-	103	42
8	2	8	98*	241	0
1	2	9	116-	-105	58
2	2	9	276	263	23
3	2	9	108-	-97	54
4	2	9	300	327	17
5	2	9	125	141	31
6	2	9	141	192	26
0	2	10	129	143	32
1	2	10	156	182	13
2	2	10	86-	118	43
3	2	10	135	142	11
4	2	10	64-	-24	32
2	3	0	579	753	44
4	3	0	1022	1179	73
6	3	0	591	713	41
8	3	0	119-	-121	60
10	3	0	136	-142	34
0	3	1	843	804	43
1	3	1	86	79	7
2	3	1	636	787	38
3	3	1	608	740	59
4	3	1	88-	-38	44
5	3	1	575	605	70
6	3	1	248	-231	12
7	3	1	204	222	17
8	3	1	590	-557	60
9	3	1	112-	-97	55
10	3	1	164	-155	27
11	3	1	208	-190	21
1	3	2	1252	1194	83
2	3	2	72-	36	36
3	3	2	382	365	22
4	3	2	93-	-82	47
5	3	2	127	-135	21
6	3	2	150	-175	40
7	3	2	714	-746	40
8	3	2	118-	88	59
9	3	2	393	-353	23
10	3	2	91-	-84	46
11	3	2	142	-120	18
0	3	3	808	765	73
1	3	3	79	66	20
2	3	3	273	301	20
3	3	3	852	-906	49
4	3	3	174	199	29
5	3	3	600	-595	30
6	3	3	428	-398	24
7	3	3	207	-220	17
8	3	3	232	-239	29
9	3	3	104-	87	52
10	3	3	167	-168	21
1	3	4	173	-186	12
2	3	4	590	-551	32
3	3	4	102-	49	51
4	3	4	845	-893	63
5	3	4	270	-222	25
6	3	4	438	-408	24
7	3	4	237	238	15
8	3	4	111-	-98	56
9	3	4	96-	4	48
10	3	4	302	285	17
0	3	5	853	-857	95
1	3	5	471	-463	24
2	3	5	389	-375	23
3	3	5	159	-163	40
4	3	5	201	-170	34
5	3	5	421	-366	42
6	3	5	412	383	26
7	3	5	114-	-71	57
8	3	5	389	324	20
9	3	5	83-	74	42
1	3	6	605	-547	33
2	3	6	117-	6	59
3	3	6	452	-399	23
4	3	6	293	230	37
5	3	6	355	295	20
6	3	6	114-	76	57
7	3	6	303	246	18
8	3	6	88-	89	44
9	3	6	320	347	18
0	3	7	159	-186	42
1	3	7	359	351	30
2	3	7	239	-234	30
3	3	7	346	284	20
4	3	7	116-	80	58
5	3	7	507	472	30
6	3	7	101-	116	51
7	3	7	123	100	31
8	3	7	91	94	23
1	3	8	114-	111	57
2	3	8	287	291	22
3	3	8	109	152	27
4	3	8	342	312	23
5	3	8	94-	-79	47
6	3	8	228	233	14
7	3	8	58-	-7	29
0	3	9	297	310	17
1	3	9	98-	-20	49
2	3	9	212	239	11
3	3	9	199	205	20
4	3	9	80-	39	40
5	3	9	56-	7	33
1	3	10	173	220	13
2	3	10	67-	-62	31
2	4	0	419	472	31
4	4	0	104	136	26
6	4	0	512	-546	31
8	4	0	449	-381	26
10	4	0	270	-243	20
1	4	1	631	643	75
2	4	1	502	-487	29
3	4	1	195	248	22
4	4	1	743	-723	38
5	4	1	205	-197	34
6	4	1	200	-174	40
7	4	1	317	-281	25
8	4	1	214	-185	35
9	4	1	278	-260	21
10	4	1	243	219	14
0	4	2	359	-353	38
1	4	2	619	-523	64
2	4	2	198	168	20
3	4	2	810	-786	45
4	4	2	223	-175	28
5	4	2	638	-652	43
6	4	2	128-	107	64
7	4	2	158	-196	26
8	4	2	121-	-1	61
9	4	2	105-	97	53
10	4	2	77-	39	38
1	4	3	773	-693	59
2	4	3	444	-428	23
3	4	3	258	-267	23
4	4	3	279	-309	25
5	4	3	257	257	30
6	4	3	366	-360	23
7	4	3	253	245	32
8	4	3	116-	82	58
9	4	3	345	291	28
10	4	3	62-	34	31
0	4	4	659	-654	45
1	4	4	222	186	28
2	4	4	639	-692	51
3	4	4	120-	18	60
4	4	4	126	118	31
5	4	4	182	143	45
6	4	4	287	275	29
7	4	4	122	35	31
8	4	4	404	364	22
9	4	4	85-	37	43
1	4	5	300	-335	25
2	4	5	459	493	25
3	4	5	128-	-70	64
4	4	5	419	405	30
5	4	5	128-	38	64
6	4	5	349	318	25
7	4	5	275	247	23
8	4	5	95-	-12	47
9	4	5	61-	68	30
0	4	6	129-	103	64
1	4	6	129-	106	64
2	4	6	158	175	25
3	4	6	508	550	33
4	4	6	127-	-33	64
5	4	6	272	305	27
6	4	6	112-	-10	56
7	4	6	166	181	42
8	4	6	71-	-59	35
1	4	7	390	424	21
2	4	7	125-	123	63
3	4	7	122-	109	61
4	4	7	165	190	41
5	4	7	107-	-67	54
6	4	7	93-	75	47
7	4	7	221	-255	22
0	4	8	280	338	23
1	4	8	114-	17	57
2	4	8	221	237	41
3	4	8	210	-188	39
4	4	8	95-	3	43
5	4	8	82-	-17	41
6	4	8	107	-148	27
1	4	9	88-	84	44
2	4	9	165	-199	41
3	4	9	73-	50	37
4	4	9	115*	-210	0
2	5	0	643	-514	118
4	5	0	502	-473	47
6	5	0	602	-571	48
8	5	0	104-	115	52
0	5	1	200*	-213	0
1	5	1	165	-173	21
2	5	1	853	-658	102
3	5	1	360	-402	33
4	5	1	110-	93	55
5	5	1	344	-361	41
6	5	1	170	195	43
7	5	1	164	-152	41
8	5	1	283	275	28
9	5	1	80-	86	40
1	5	2	994	-639	92
2	5	2	95-	119	47
3	5	2	348	-328	40
4	5	2	114-	-94	57
5	5	2	169	192	42
6	5	2	169	194	42
7	5	2	376	395	43
8	5	2	99-	-84	50
9	5	2	205*	245	0
0	5	3	757	-582	130
1	5	3	176	178	44
2	5	3	107-	-105	53
3	5	3	629	443	51
4	5	3	118-	-119	59
5	5	3	361	358	30
6	5	3	166	221	42
7	5	3	109	192	27
8	5	3	159	189	40
9	5	3	55-	-104	27
1	5	4	113-	65	57
2	5	4	393	323	34
3	5	4	119-	101	59
4	5	4	577	565	63
5	5	4	119-	-0	59
6	5	4	195	242	49
7	5	4	100-	-81	50
8	5	4	78-	57	39
0	5	5	609	486	59
1	5	5	120-	136	60
2	5	5	340	263	53
3	5	5	120-	178	60
4	5	5	118-	82	59
5	5	5	225	244	55
6	5	5	177	-226	44
7	5	5	85-	-3	43
1	5	6	429	381	49
2	5	6	117-	-50	59
3	5	6	198*	164	0
4	5	6	109-	-96	54
5	5	6	100-	-121	50
6	5	6	85-	-89	43
7	5	6	130*	-189	0
0	5	7	189	195	47
1	5	7	188	-169	47
2	5	7	106-	85	53
3	5	7	174	-195	43
4	5	7	91-	-20	45
5	5	7	153	-311	34
1	5	8	87-	-82	44
2	5	8	82-	-151	41
3	5	8	73-	-77	35
4	5	8	122*	-257	0

Observed and calculated structure factors (F_o and F_c) in units of 1/10 electron per unit cell with estimated relative standard errors (σ) in F_o. A minus sign following F_o indicates an unobserved reflection; an asterisk indicates an unreliable F_o measurement which was not used in the least squares refinement.

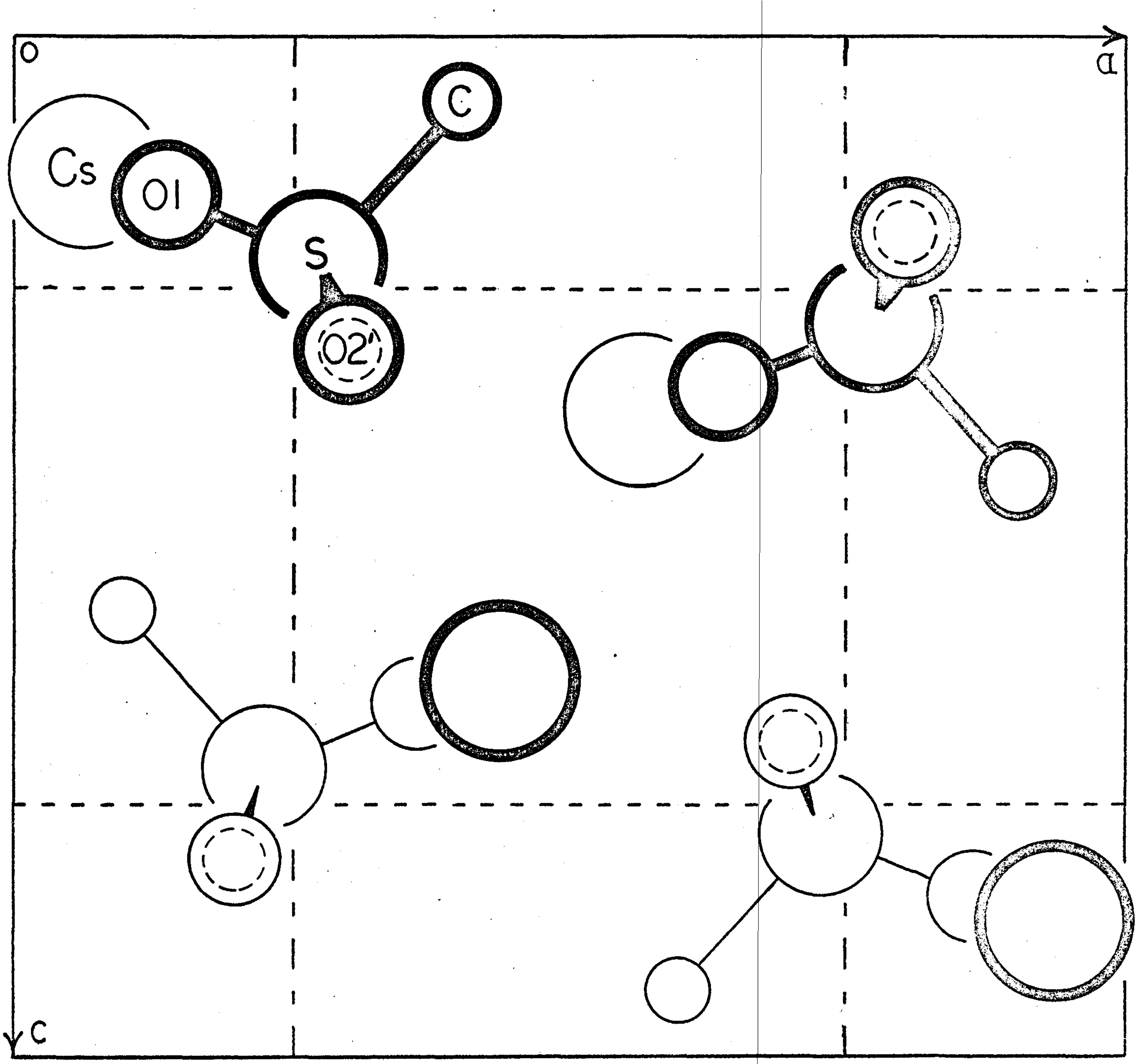

FIGURE 3-4

Structure of cesium methylsulfonate viewed down [010].

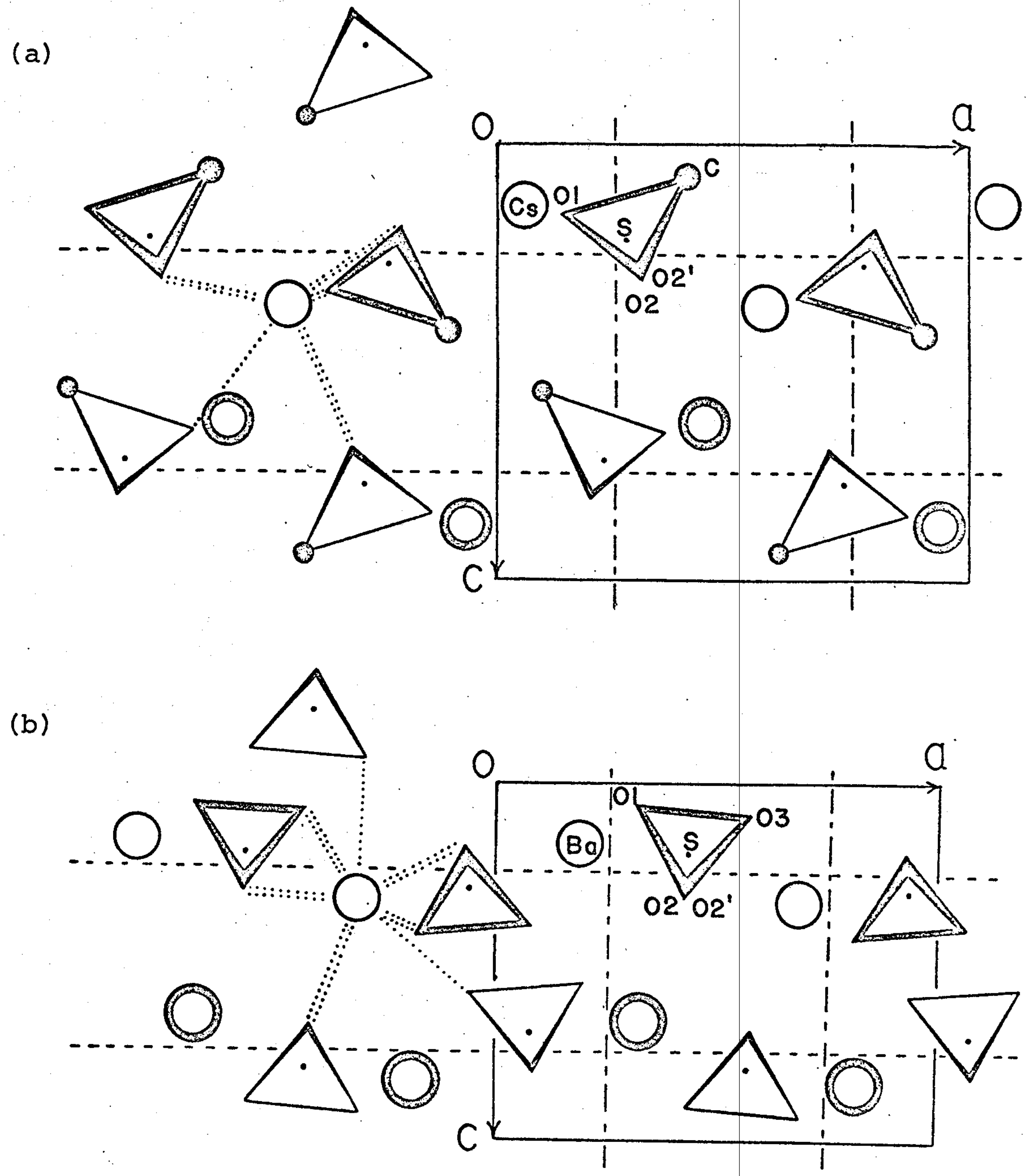

FIGURE 3-5

The structures of (a) cesium methylsulfonate and (b) barium sulfate projected down [010]. The groups in heavy outline lie on the mirror plane at y = 3/4; those in faint outline lie on the one at y = 1/4. The atoms O2 and O2' are related by reflection in the mirror plane at y = 3/4.

dark and light shading is again used to indicate groups on the y = 3/4 and y = 1/4 mirror planes respectively.

Figure 3-6 shows the environment of a cesium ion, with the distances in Å marked for each neighbour. Six of the nine oxygen atom neighbours can be considered as forming a slightly distorted triangular prism which is shown by dotted lines. Two more O atoms lie outside the triangular faces. The ninth O neighbour is situated outside one of the rectangular faces. The nearest C atom at 3.77 Å is found outside one of the other rectangular faces. All other C atoms are more than 4.36 Å away. The dotted lines drawn around one Cs atom in Fig. 3-5(a) describe this same set of O neighbours viewed in the [010] projection.

The environment found for a carbon atom is shown in Fig. 3-7 with distances marked in Å units. This figure does not explicitly show the O and S atoms belonging to the same methylsulfonate group as the C atom, nor does it show any H atoms of the methyl group since these could not be located. The C atom lies approximately in the plane formed by the three oxygen neighbours. The oxygen atom O1 and the Cs atom are coplanar with the C-S bond since all these atoms lie in the same mirror plane. No other C-O distance is less than 4.15 Å except of course those O atoms belonging to the same methylsulfonate group. Each C atom is related to two others by centres of symmetry.

FIGURE 3-6

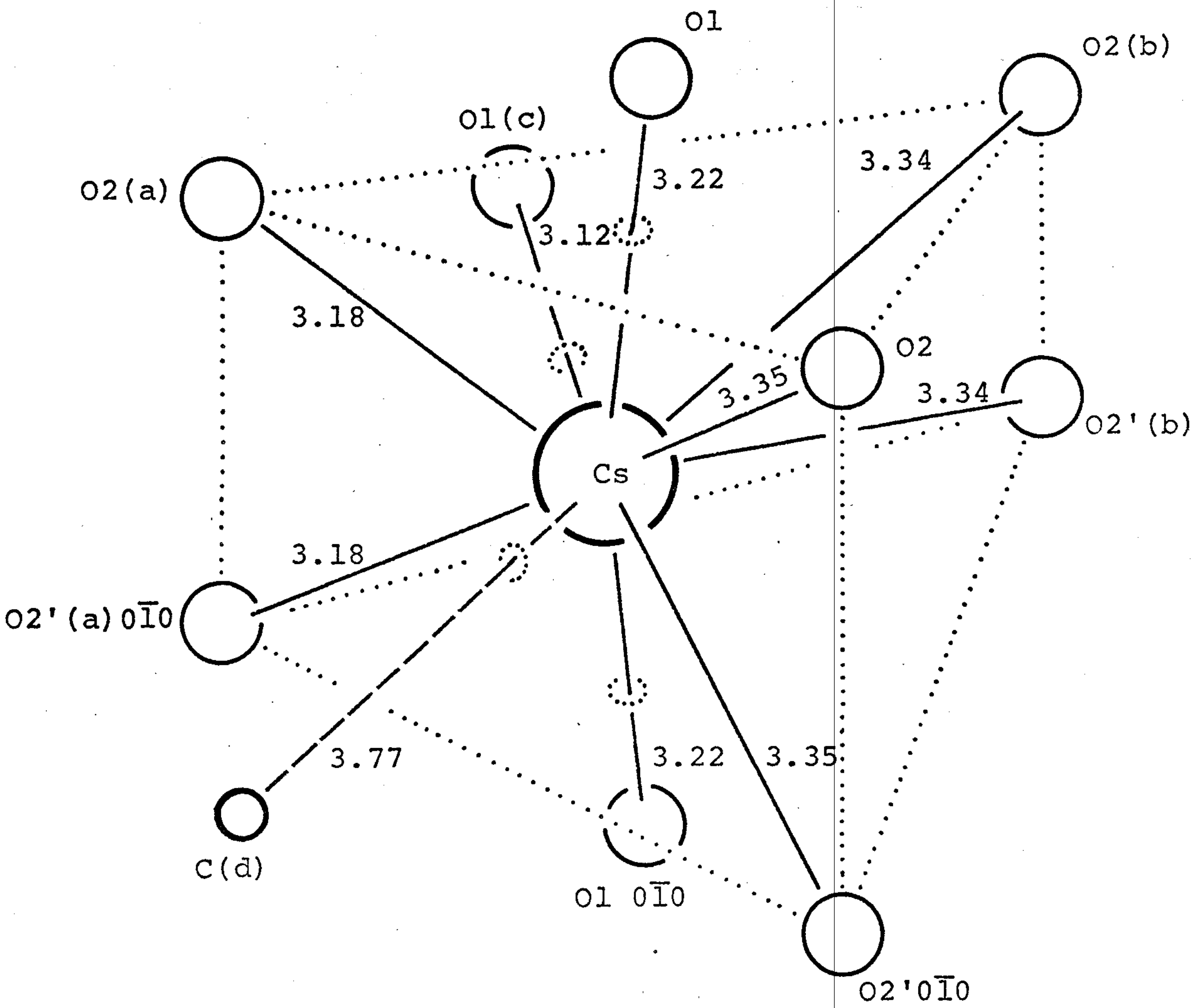

Environment of a cesium ion in cesium methylsulfonate. Distances are marked in Å. Atom labels are as defined in Table 3-4.

FIGURE 3-7

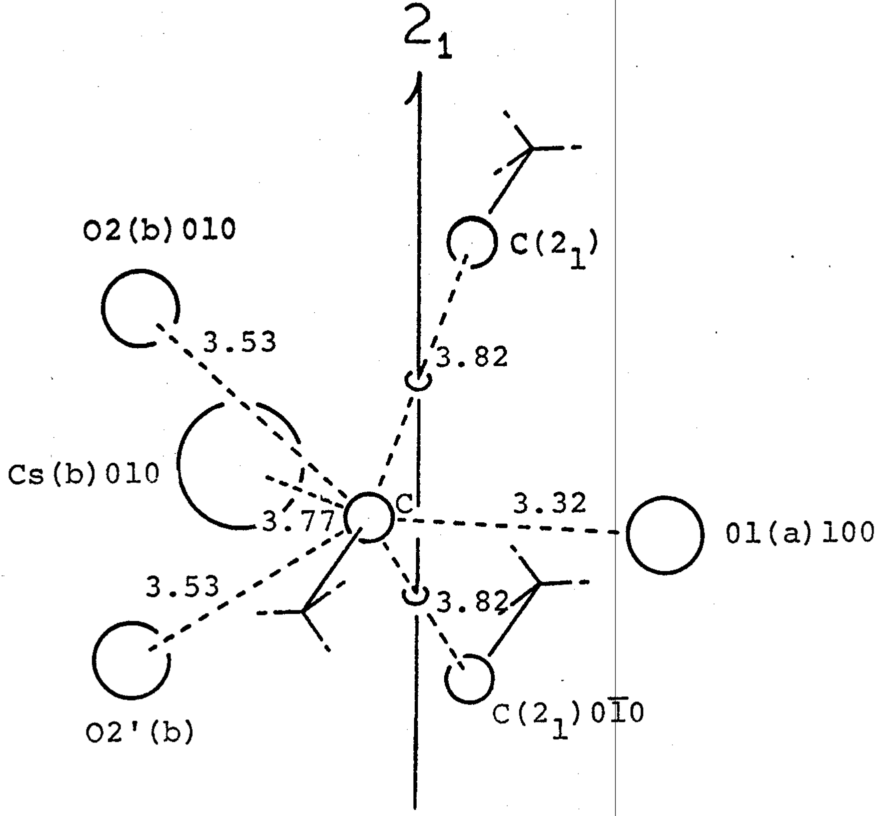

Environment of a carbon atom in cesium methylsulfonate. Distances are shown in Å. Sulfur and oxygen atoms belonging to the same CH_3SO_3 ion are not shown, nor are the hydrogen atoms since these were not located. Atom labels are as defined in Table 3-4 with the additional 2_1 axis through (x,z) = (1/2,0).

These features of the C atom environment are also evident from the [010] projection in Fig. 3-5(a).

Table 3-4 gives the interatomic distances and angles in CsMS together with their standard errors. In certain cases distances are also given after applying corrections for thermal motion (21) assuming a riding motion of the O and C atoms on the heavier central S atom. The significance of these corrections and the standard errors will be discussed in Section 3.5 C.

3.5 Discussion and Conclusions

3.5 A Comparison of $CsCH_3SO_3$ and $BaSO_4$

In discussing many of the features of the CsMS structure it is useful to make a comparison with the structure of the isoelectronic compound barium sulfate, $BaSO_4$. Barium sulfate also crystallizes in space group Pnma with four formula units per unit cell, and has cell constants a = 8.86, b = 5.44, c = 7.14 Å. The barium sulfate structure was studied by James and Wood (22) in 1925 as one member of an isostructural series which they suggest includes strontium and lead sulfate, strontium and barium selenate and chromate, potassium and rubidium permanganate, and potassium fluoborate. More recent neutron diffraction work on barium sulfate (23) has yielded more reliable values for some of the oxygen coordinates. The fact that barium sulfate and CsMS crystallize in the same space group with similar cell constants

TABLE 3-4

Interatomic distances and angles in cesium methylsulfonate. (Figures in parantheses are the standard errors in the last digits quoted.)

		Uncorrected[*]	Corrected[*]
S-O1		1.424(18) Å	1.434(19) Å
S-O2	X2[†]	1.460(16) Å	1.485(18) Å
S-C		1.804(33) Å	1.846(38) Å
Mean S-O		1.448(12) Å	1.468(17) Å
O1-S-O2	X2	111.9 (8)°	
O2-S-O2'[‡]		111.9(13)°	
O1-S-C		109.2(16)°	
O2-S-C	X2	105.8(11)°	
Cs-O1	X2	3.22 (1) Å	
Cs-O2	X2	3.35 (2) Å	
Cs-O2(a)[§]	X2	3.18 (2) Å	
Cs-O2(b)	X2	3.34 (2) Å	
Cs-O1(c)		3.12 (2) Å	
Cs-C (d)		3.77 (3) Å	

[*] For a discussion of these corrections for thermal motion, see text.

[†] The multiplicity X2 indicates that two equivalent bonds exist related by the mirror plane through the central atom.

[‡] The atom O2' is related to O2 by reflection in the mirror plane y = 3/4.

[§] The following are symmetry transformations applied to the coordinates of Table 3-2.

(a): x-1/2, y, -z + 1/2;
(b): -x + 1/2, y - 1/2, z - 1/2;
(c): -x, -y + 1, -z;
(d): -x + 1/2, y - 1/2, z + 1/2.

might lead one to expect that they were isostructural. However a detailed comparison indicates that this is not the case even though the structures are closely related.

Fig. 3-5(b) shows the structure of barium sulfate projected down [010] and may be compared to the [010] projection of CsMS in Fig. 3-5(a). In both structures, the a glide planes and b translations generate layers perpendicular to the c axis. The structure of an individual layer is very similar in the two materials with only a slight difference occurring in the orientation of the anions within a layer.

However the stacking of the layers relative to each other is quite different in the two crystals. Adjacent layers in CsMS are displaced relative to one another by about a/4 compared to the positions of the corresponding adjacent layers in barium sulfate. This displacement may alternatively be seen as a difference in the positions of the atoms along the a direction when measured from the centre of symmetry at the origin, or when measured from the n glide planes. The particular arrangement of the layers in CsMS is seen to provide channels in the structure running parallel to b. Since the S-C bonds are directed into these channels, the methyl groups are expected to occupy these relatively open regions, and in so doing they avoid close contacts with Cs ions. On the other hand this arrangement of the layers is observed to retain close contacts between O atoms and Cs ions.

In both barium sulfate and CsMS each O atom has three neighbouring cations. The Ba ion has twelve O neighbours at distances ranging from 2.7 Å to 3.3 Å (22), whereas the Cs ion has only nine O neighbours at distances between 3.12 Å and 3.35 Å. The nearest O neighbours to the Cs and Ba ions have been indicated by dotted lines in Fig. 3-5(a) and (b).

Since barium sulfate and CsMS are isoelectronic compounds whose forms can be pictured as compact ionic structures, one might expect to be able to relate any prominent structural differences to the differences in the constituent ions. Since Ba and Cs are neighbouring elements in the periodic table they are expected to have similar effects on the packing even though they carry different charges when ionized and have different ionic radii (1.35 Å for Ba^{+2}, 1.69 Å for Cs^{+1} (2, Table 13-3)). However, in considering the differences between the two anions, one would not be surprised to find them in quite different environments as a result of their interactions in a structure. There are two points of difference that are relevant. The first is a difference observed in the geometry of the anion when a methyl group replaces an O atom. The elongation of the anion along the S-C direction and the addition of three H atoms is expected to increase the volume of the anion. The second difference is one of charge distribution. In both the SO_4^{-2} ion and the $CH_3SO_3^{-1}$ ion the negative charge is expected to be evenly distributed among the oxygen atoms of the ion. However the methyl group will probably carry very little negative charge and when viewed externally would appear to carry a slightly positive charge since the H atoms have their electrons mainly in bonding orbitals between the protons and the C atom. The differences in the structures observed for $BaSO_4$ and $CsCH_3SO_3$ can be explained in terms of these simple pictures of volume and charge distribution differences for the two anions. The volume difference results in a structure for cesium methylsulfonate which has relatively open regions to accommodate the methyl groups. The arrangement of the methyl groups in these regions results in only a small amount of contact between the methyl groups and positive cesium ions.

The stable configuration adopted by CsMS is one which maintains three cation contacts for each oxygen atom as is the case in barium sulfate. Local charge neutrality may be demonstrated by assuming that electron charges on each oxygen atom are $-2e \times 1/4 = -0.5e$ in $BaSO_4$, and $-1e \times 1/3 = -0.33e$ in $CsCH_3SO_3$. Each Ba^{+2} is then surrounded by 12 oxygens each contributing 1/3 of its $-0.5e$, or a total of $12 \times -0.5e \times 1/3 = -2e$, to balance the $+2e$ charge on the barium ion.

Each Cs^{+1} is surrounded by 9 oxygens each contributing 1/3 of its -0.33e, or a total of 9 x -0.33e x 1/3 = -1e, to balance the +1e charge on the cesium ion.

3.5 B Possibility of Hydrogen Bonding

Although no hydrogen atoms were located by this x-ray analysis, possible hydrogen bonds could be inferred if short C-O distances were observed. Any hydrogen bonding between carbon and oxygen is expected to be quite weak, and examples known to exhibit such hydrogen bonds are comparatively few. The three closest oxygens to each carbon atom (excluding those on the same anion) have been shown in Fig. 3-7 and lie at distances of 3.32, 3.53 and 3.53 Å. The first of these is within the value 3.4 Å found for the sum of Van der Waal radii for the methyl group and the oxygen atom (2.0 Å and 1.40 Å (2, Table 7-20)), and might suggest a hydrogen bond. However the C-O1 direction seems unsuitable since it gives a S-C-O1 angle of 85°. The other two oxygen neighbours, while probably too distant to consider, also are unsuitably located as they both have S-C-O angles of 96°.

It seems very unlikely that the strong covalent C-H bonds which are expected to form tetrahedral S-C-H angles (109.5°) would distort by 25° or so in favour of any weak hydrogen bonding interaction with the neighbouring oxygen atoms. For this reason no hydrogen bonds are likely to exist in CsMS. Indeed the lack of close interactions for the H atoms with the rest of the structure suggests that the methyl group may be rotating about the S-C axis at room temperature.

3.5 C Bondlength Errors and Thermal Corrections

Standard errors have been given in Table 3-4 for the bond lengths and angles. These include the standard errors in the atom coordinates provided by the least squares refinement and the standard errors in the cell constants. This error does not include possible systematic errors such as those caused by the thermal motion of the atoms. It is possible to correct the S-O and S-C distances for temperature effects (21) by making assumptions about their relative motions. The values of the thermally corrected bond lengths are given assuming that the methylsulfonate group is undergoing a riding or librational type of motion. The standard errors quoted for corrected distances take into account the standard errors in the uncorrected values and the standard errors calculated by the least squares program for the temperature factors.

However, since the intensity data were not corrected for absorption, these temperature factors may contain systematic errors which would not appear in the standard errors derived during their least squares refinement.
In addition the methylsulfonate group may not be undergoing a riding motion but instead the relative motions of the sulfur,

oxygen and carbon atoms might be uncorrelated. In this event the corrected values in Table 3-4 are 0.05 Å too small. The assumption of a riding motion is probably a better one to make for a group such as the methylsulfonate ions since it is more likely that a covalently bonded group would undergo a rigid body type motion rather than a random motion of the individual atoms. However, with possible uncertainties of 0.05 Å in any of the corrected bondlengths, the difference between the distances S-O1 and S-O2 is probably not significant. The mean values for the observed S-O bondlengths as quoted in Table 3-4 should provide the most reliable values for these distances in the methylsulfonate ion.

The neglect of the H atoms might be expected to affect the position and the temperature factor of the C atom. However, when the rotating charge distribution was included in the model to take account of H atom scattering (see Section 3.3D), no significant shortening of the S-C bond could be observed. Hence the atomic coordinates used in calculating the thermally uncorrected S-C distance were probably not affected by the omission of H atoms in the model. However it seems quite likely that the C atom anisotropic temperature factors would be affected by this omission. Hence the thermally corrected S-C bondlength value could be less reliable than its standard error would indicate.

3.5 D The Methylsulfonate Ion

Certain features of the methylsulfonate ion have previously been described, particularly those which influence the crystal structure as a whole. The following discussion deals with the stereochemistry of the ion and its chemical significance.

The methylsulfonate ion is only required by the crystallographic space group to have C_s point symmetry (S, C, and O lie on a mirror plane, H neglected). However, within the accuracy of our results it probably has the higher C_{3v} symmetry. An idealized diagram of the ion in this symmetry is shown in Fig. 3-8.

The bond distances and angles in the methylsulfonate ion agree fairly well with values found in the literature for similar groups involving S-O and S-C bonds. The mean S-O bond distances of 1.448 ± .012 Å or 1.468 ± .017 Å * (see Table 3-4) can be compared to the following values:

1.461 ± .005 Å * in potassium methylenedisulfonate, $K_2\ [CH_2(SO_3)_2]$ (24);

1.44 ± .02 Å in sulfanilic acid monohydrate $NH_3^+C_6H_4SO_3^- \cdot H_2O$ (25);

1.44 ± .01 Å in metanilic acid $NH_3^+C_6H_4SO_3^-$ (26);

---

* The values marked with an asterisk include corrections for thermal motion.

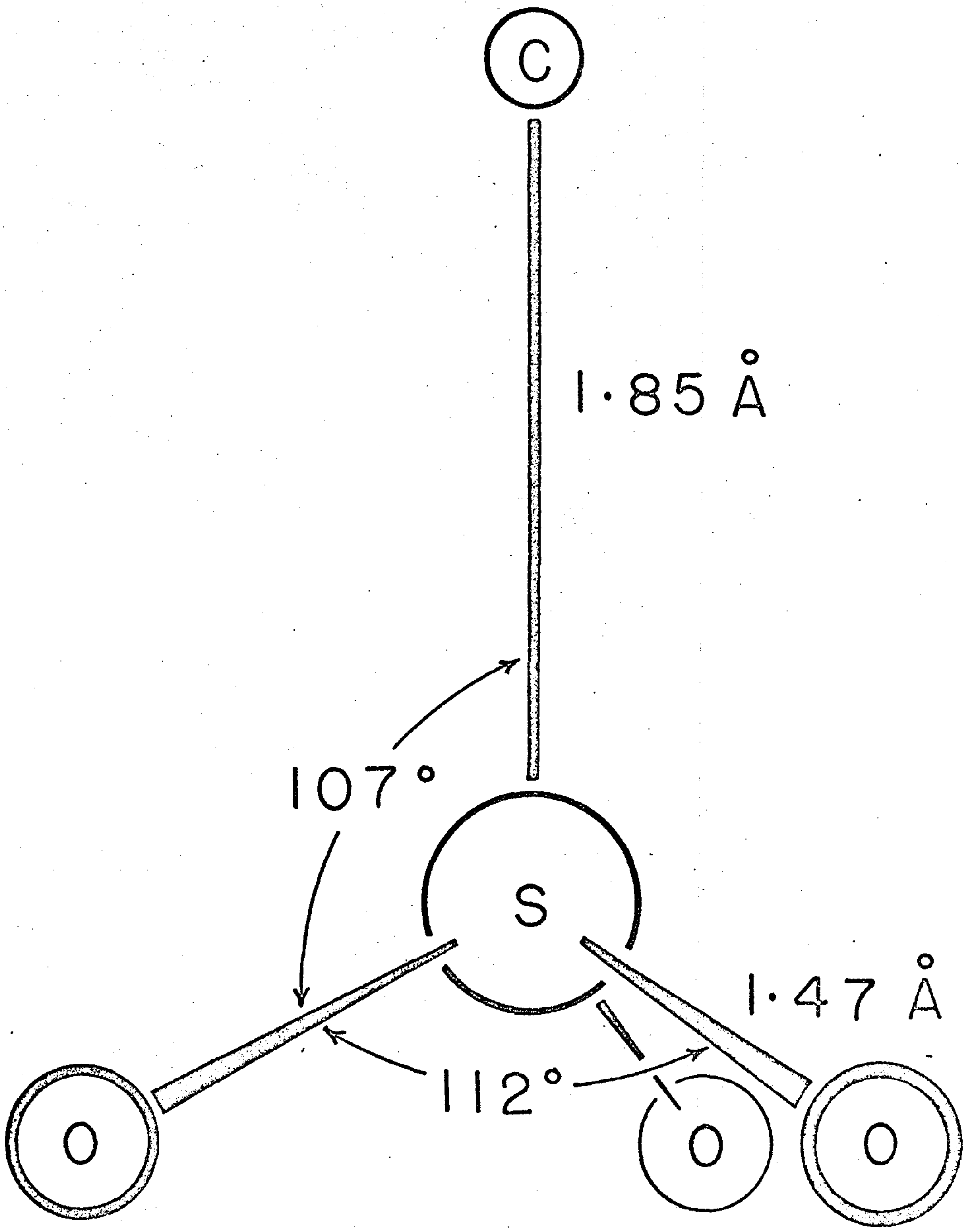

FIGURE 3-8

The structure of the methylsulfonate ion shown in the idealized symmetry C_{3v}.

and

1.454 Å in sodium napthionate tetrahydrate
$NH_2C_{10}H_6SO_3Na \cdot 4H_2O$ (27).

The uncorrected S-C bondlength of 1.80 ± .03 Å can be compared with the following values quoted for S-C single bonds which are also uncorrected for thermal motion:

1.770 ± .007 Å in the bridged carbon of $K_2\ [CH_2(SO_3)_2]$ (24),
1.77 ± .02 Å in $NH_3^+\ C_6H_4SO_3^- \cdot H_2O$ (25);
1.80 ± .01 Å in $NH_3^+C_6H_4SO_3^-$ (26); and
1.766 Å in $NH_2C_{10}H_6SO_3\ Na \cdot 4H_2O$ (27).

The thermally corrected S-C bondlength value of 1.85 ± .04 Å may not be too reliable because of unusual carbon atom temperature factor effects (see discussion in previous section).

3.5 E Comparison of the $CH_3SO_3^{-1}$ Ion and a Related Series

It is useful to compare the bondlengths and angles of the methylsulfonate ion with others in the isoelectronic series containing the sulfate ion SO_4^{-2} (1), the dimethyl sulfone molecule $(CH_3)_2SO_2$ (28), the trimethyloxosulfonium ion $(CH_3)_3SO^+$ (29)(30), and the hypothetical $(CH_3)_4S^{+2}$ ion. This comparison is presented in Table 3-5. The bond lengths used in this comparison have been corrected for thermal motion. For dimethyl sulfone these corrections have been made using the average of the temperature factors quoted by Sands (28) and assuming a riding motion for the molecule.

TABLE 3-5

Comparison of the interatomic distances and angles in SO_4^{2-}, $CH_3SO_3^-$, $(CH_3)_2SO_2$, $(CH_3)_3SO^+$, and the hypothetical $(CH_3)_4S^{2+}$. (Figures in parentheses are the standard errors in the last digits quoted.)

	SO_4^{2-}	$CH_3SO_3^-$	$(CH_3)_2SO_2$	$(CH_3)_3SO^+$	$(CH_3)_4S^{2+}$
Bonds (Å)					
S-O	1.49(1)	1.47(2)	1.47(2)	1.47(2)	
S-C		1.85(4)	1.79(2)	1.79	1.79
Angles (°)					
O-S-O	109.5	111.9(13)	117.9(8)		
O-S-C		106.9(16)	108.8(8)	112.7(7)	
C-S-C			103.0(8)	106.1(8)	109.5

Certain trends are apparent as successive O atoms are replaced by methyl groups:

1. With methyl groups present the angles at the S atom deviate from the tetrahedral value of 109.5°. Angles which are subtended by O atoms increase at the expense of angles involving the C atoms. The experimental errors indicate that these observed differences are significant.
2. None of the S-C distances differ too significantly from 1.80 Å.
3. The S-O bond distances appear to decrease as more methyl groups are substituted for O atoms. However this decrease may not be significant.

The configurations for this series can be understood in terms of the theory proposed by Cruickshank (1). The theory suggests that appreciable π-bonding exists in certain tetrahedral groups in addition to the usual σ bonding. This π-bonding arises from overlap of d_{z^2} and $d_{x^2-y^2}$ electron orbitals of the central atom with p orbitals of the four surrounding atoms. When one or more methyl groups are substituted, this hypothesis suggests the following effects:

1. The S-C distance will be that of a single σ-bond since the C atom has no p electrons available for π-bonding.

(2) If the arrangement is not strictly tetrahedral, say if the angles deviate from tetrahedral values, still stronger π-bonding can arise from the d_{xy}, d_{yz}, and d_{xz} orbitals of the central atom. With methyl groups present the O-S-O angles can open because the C atoms are more distant and the negatively charged O atoms can repel one another by electrostatic forces. The angle changes which are observed when methyl groups are present satisfy this criterion necessary for even stronger π-bonding and the remaining S-O distances are expected to be shortened.

The data of Table 3-5 appear to verify these predictions. Hence these results are in accord with the predictions of Cruickshank regarding the nature of the bonding in compounds of this type with S as the central atom.

CHAPTER 4 STRUCTURAL INVESTIGATIONS ON LITHIUM HYDRAZINIUM SULFATE

4.1 Introduction

4.1 A Literature Survey

The preparation of lithium hydrazinium sulfate, $LiN_2H_5SO_4$ (hereafter referred to as LiHzS), was described in 1916 by Sommer and Weise (32). Crystals of LiHzS at room temperature belong to the orthorhombic space group $Pbn2_1$ (C_{2v}^9) with cell constants a = 8.99, b = 9.94, c = 5.18 Å, and four formula units per cell. In 1958 these crystals were reported by Pepinsky, Vedam, Okaya, and Hoshino (33) to exhibit good ferroelectric hysteresis loops over the range -15°C to 80°C, but no dielectric anomalies were observed between -196°C and 140°C. Excessive conductivity interfered with both the ferroelectric and dielectric measurements above these two temperatures. In 1963 Cuthbert and Petch (34) reported the results of proton and Li^7 nuclear magnetic resonance studies. This work indicated the probable hydrogen atom configurations and motions in the crystal, and suggested from the Li^7 signals the possible existence of a high temperature polymorph above 160°C. Also in 1963 Blinc, Schara and Poberaj (35) used electron spin resonance experiments to study paramagnetic centres produced in γ-irradiated LiHzS.

Crystal structure analyses of room temperature ferroelectric LiHzS were reported simultaneously in 1964 by Brown (36) and by Van den Hende and Boutin (37) and a two dimensional structure was reported by Niizeki and Koizumi (38) which agreed with the other two determinations. Also in 1964 Vanderkooy, Cuthbert, and Petch (39) reported the results of conductivity experiments on LiHzS crystals and suggested that the large conductivity in the $\underline{c}$ direction was caused by proton transfer along the sequence of hydrogen bonds linking the hydrazinium groups. Studies of Raman spectra from LiHzS were published in 1965 by Krishnan and Krishnan (40). A neutron diffraction study on LiHzS published in 1967 by Padmanabhan and Balasubramanian (41) describes a crystal structure in agreement with the x-ray results. These authors also report hydrogen atom positions and prefer a static model rather than their attempted refinement* of a dynamic model in which the NH_3^+ groups of the hydrazinium ions would be rotating. A recent paper by MacClement, Pintar and Petch (42) reports measurements of the proton spin-lattice relaxation time along with improved

---

*The dynamic model structure factor contribution formula which these authors report they have used is either in error or suffers from a misprint. See Appendix I.

proton magnetic resonance measurements. These results contradict the interpretation from the neutron diffraction experiments that the hydrogen positions of the NH_3 groups are static.

4.1 B Description of the Structure

The x-ray, neutron, and NMR experiments have given considerable information about the room temperature structure of LiHzS. Fig. 4-1 shows the structure in the [001] projection. The sulfur and lithium atoms are each surrounded by four oxygen atoms at the corners of a tetrahedron. These tetrahedra form a framework by sharing corner oxygen atoms. The hydrazinium groups, $NH_2—NH_3^+$, are situated in channels running through the framework along c and have their N-N bonds approximately perpendicular to c. The earlier proton magnetic resonance studies (34) have shown that the atoms N2 are part of the NH_3^+ groups and that these hydrogen atoms are probably rotating at room temperature about the N1-N2 direction. The neutron diffraction results (41) have been interpreted as favouring a static model for these hydrogens, but this interpretation has since been challenged (42). The atoms N1 are part of the NH_2 groups and each N1 is hydrogen bonded to the adjacent N1 atom within the same channel. Each N1 is also hydrogen bonded to the oxygen atom O4 of the framework. Fig. 4-2(a) and (b) show the two possible configurations

FIGURE 4-1

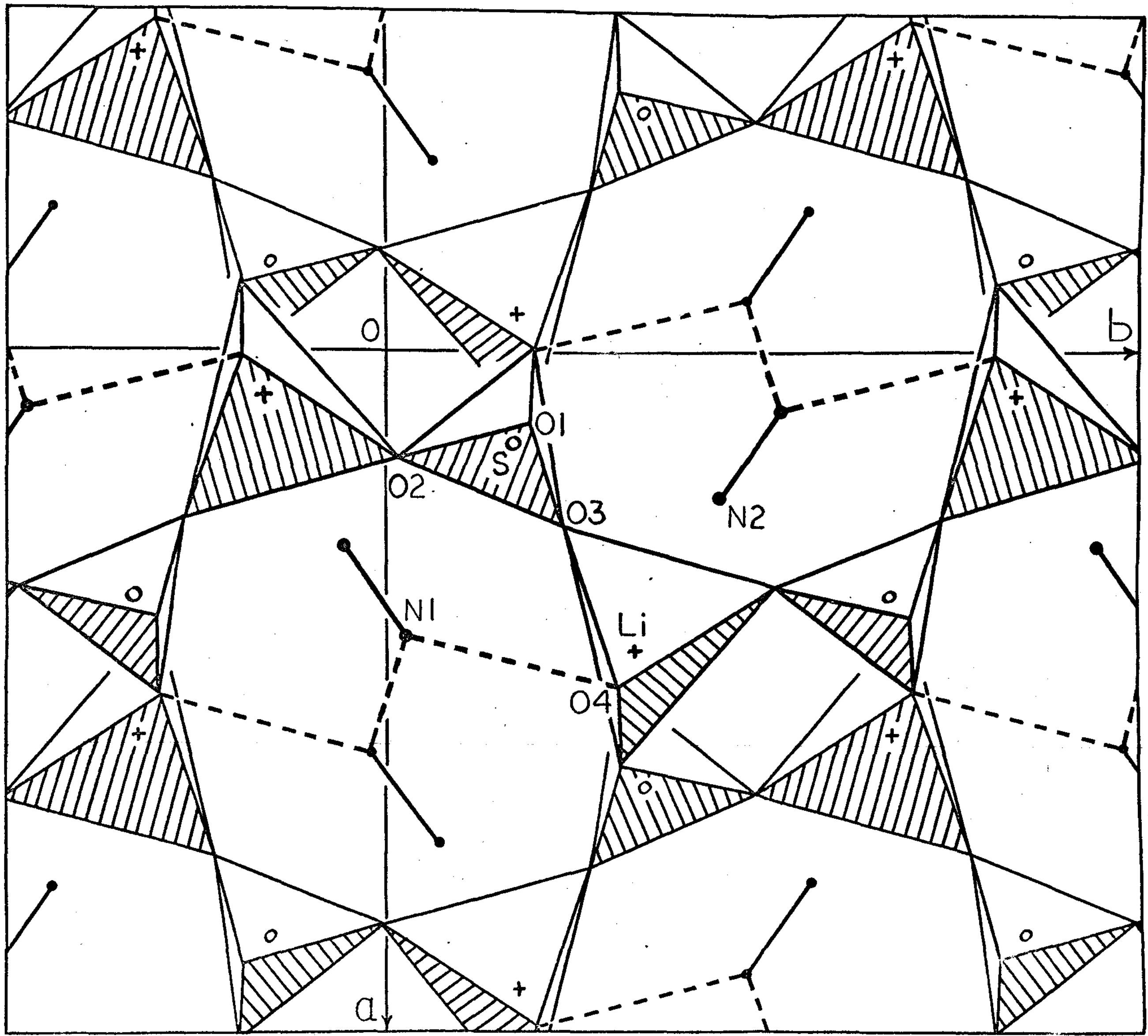

[001] Projection of LiHzS Structure. Broken lines indicate hydrogen Bonds Involving the NH_2 Groups.

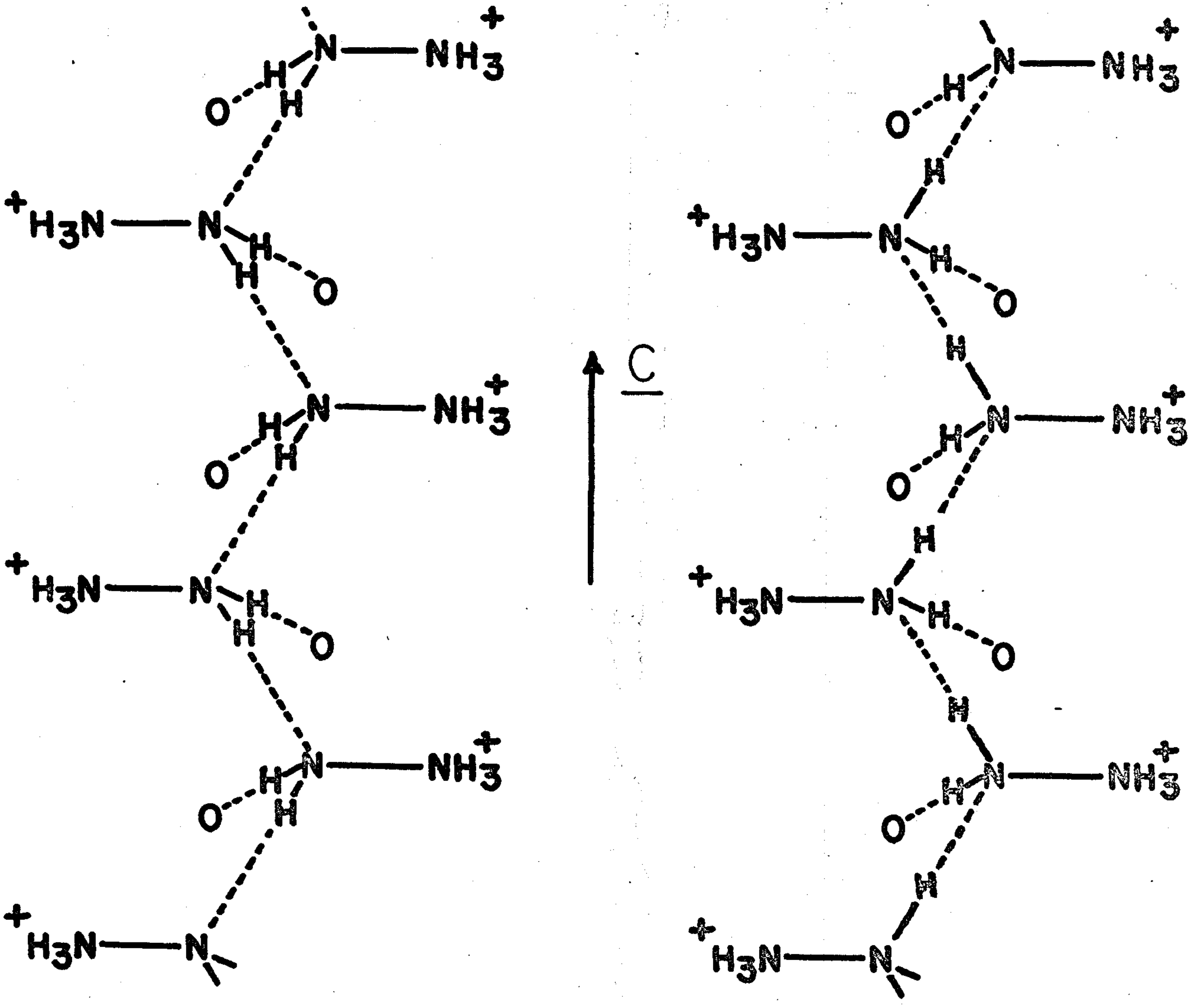

(a) (b)

FIGURE 4-2

Two Alternative Configurations for an Ordered Series of Hydrogen Bonds Linking the Hydrazinium ions:

(a) N — H ··· N directed toward - c ;

(b) N — H ··· N directed toward + c.

for the hydrogen bonds linking adjacent NH_2 groups of the hydrazinium ions. On the assumption of tetrahedral N2-N1-H and H-N1-H angles the proton resonance results would favour the hydrogen bond configuration of Fig. 4-2(b). However the neutron diffraction results, while confirming that the hydrogen bonds are ordered in the crystal, favour the configuration of Fig. 4-2(a).

4.1 C Possible Ferroelectric Mechanisms

Possible theories for ferroelectric behaviour in LiHzS must explain the origin of permanent electric dipole moments along the c direction and the mechanism for reversal of the direction of these moments upon reversal of an applied electric field. Since $Pbn2_1$ space group has b and n glide planes perpendicular to a and b, the c axis is the only possible direction in which any net dipole moment can occur. The ferroelectricity in LiHzS might arise in one of, or a combination of, three possible ways:

I The noncentrosymmetric structure may possess a permanent net dipole moment which can be reversed exactly by a change of the crystal to its enantiomorphous (opposite handed) structure.

II The polar hydrogen bonds between nitrogen atoms can contribute a dipole moment to the structure. This moment could be reversed by an interchange in the roles of the donor and acceptor nitrogen atoms in each hydrogen bond, i.e. a switch between the two structures shown in Fig. 4-2.

III There may exist some molecule or ion such as the sulfate ion which, because of its own electronic configuration, may possess a dipole moment. These dipoles might be reversed by a change in orientation of the group itself or by a change to another degenerate state of the group in which the polarization direction is different.

4.1 D Difficulties with Mechanisms Assigned to LiHzS

To date there seems to be no conclusive experimental evidence explaining the ferroelectric mechanism in LiHzS. For any ferroelectric crystal, a mechanism of type I above is an obvious choice to consider. The simplest framework change to produce the enantiomorphous structure involves a rotation of about 46° for the sulfate group about an axis close to the S-O2 direction. This involves a change of about 1.1 Å in the position of O1. Simultaneously the enantiomorph would have its N1— H ···N2 hydrogen bonds reversed and the N1 — H ··· O hydrogen bonds would have to change from O4 to what had previously been O1. Other ways of switching to the enantiomorph require even larger motions for the oxygen atoms and seem less probable than the method described. In any case the atomic shifts necessary to reach the enantiomorphous structure are quite large. The mechanism of type I therefore seems unlikely, especially in view of the relatively low coercive field necessary to produce ferroelectric switching in LiHzS (320 volts/cm. at room temperature (33)). Furthermore Niizeki and Koizumi (38) mention dielectric studies which have shown an increase in the saturation polarization with applied electric field. They claim that this phenomenon does not support a mechanism involving a reversible framework polarization, hence making a type I mechanism unlikely.

In ferroelectric crystals known to contain hydrogen bonds, the type II mechanism is another obvious one to examine. If the series of polar hydrogen bonds which connects separate N1 atoms into a chain is an ordered series, it can contribute to a net spontaneous polarization along the c axis. The neutron diffraction work (41) indicates that the series is an ordered one. A reversal in the roles of acceptor and donor nitrogen atoms is equivalent to moving each proton about 1.0 Å along the chain (see Fig. 4-2). So far this corresponds to a type II mechanism, but suffers from the objection that the two structures are crystallographically distinct and probably have different energies. Any polarization arising from the framework and N1 — H···O4 hydrogen bonds does not change when the N1 — H···N1 polarization reverses, and therefore asymmetric hysteresis loops might be expected. These have not been reported, and a simple type II mechanism seems doubtful.

Cuthbert and Petch (34) have discussed an explanation wherein a type II switch triggers a type I mechanism. They suggest that if the N1 — H···N1 hydrogen bonds reverse from the NMR favoured configuration shown in Fig. 4-2(b), then the assumed tetrahedral N2-N1-H and H1-N1-H2 angles no longer allow nearly linear N1 — H···N1 and N1 — H···O4 hydrogen bonds. Cuthbert and Petch suggest that in such circumstances the structure is not in its lowest energy form and the framework must switch as well to its enantiomorph. The net result is a type I mechanism. The following objections may be raised for this compound mechanism:

(a) The framework reversal still requires large atom shifts and it is uncertain whether the energy of reversing the N1 — H···N1 hydrogen bonds is a large enough triggering energy to induce a framework reversal.

(b) The NH_2 group hydrogen positions reported in the neutron diffraction study (41) do not confirm that nearly linear N1 — H···N1 and N1 — H···O4 hydrogen bonds are necessary for a stable structure. If one accepts these results, then the assertion is suspect that the framework would choose to reverse in an electric field in order to achieve nearly linear hydrogen bonds.

Van den Hende and Boutin (37) examined a possible mechanism of type III where a polarization might arise from distorted sulfate ions. Their x-ray structure analysis indicated that the S-O1 bond was significantly longer (1.55 ± .01 Å) than the other S-O bonds (mean 1.47 ± .01 Å), and they considered that the sulfate ion might have a permanent dipole moment. It would be extremely surprising if such a distortion in a SO_4^{-2} ion were real. Brown's refinement (36) indicated that all S-O distances were equal within experimental errors. In fact S-O1 was reported by Brown to be the shortest of the four distances. Padmanabhan and Balasubramanian (41) find a slightly distorted ion with a S-O1 distance of 1.51 ± 0.02 Å. However their standard errors cannot definitely confirm that a real distortion has been observed. Krishnan and Krishnan (40) in their Raman scattering experiments have concluded that the sulfate ion has tetrahedral symmetry. Hence a mechanism of type III involving the SO_4^{-2} ion seems very unlikely. It is possible that the anomalies seen for S-O1 distances are the result of parameters such as O1(z) not being ideally suited to refinement by least squares.

An alternative mechanism of type III might involve dipole moments arising from the lithium atom occupying different degenerate sites within its approximately tetrahedral oxygen environment. This proposal is not supported by arguments based on the ionic radii of lithium and oxygen which suggest that the lithium ion is snugly bound by the four oxygen atoms. The sum of oxygen and lithium radii (2, Table 13-3) is 1.40 Å + 0.60 Å = 2.00 Å compared to a mean Li-O distance of 1.94 Å (36). If such a mechanism did exist it would be a difficult one to detect by x-ray analysis because the weakly scattering Li atom position cannot be as accurately resolved as the larger atoms.

4.1 E Further X-ray Analysis

Since the work of Cuthbert and Petch (34) had suggested the existence of a high temperature polymorph above 160°C, an attempt was made to examine by x-ray analysis the space group and crystal structure above this temperature. The Li^7 results above 160°C indicated that the orientations of the principal axes of the electric field gradient tensors are coincident with the crystal axes. While this could be just coincidental it suggested that a higher crystallographic symmetry might exist for the Li sites and hence a high temperature space group different from $Pbn2_1$ or Pbnm which could be detected by different systematic absences. It is possible that such a polymorph might be a paraelectric form but since excessive conductivity interferes with ferroelectric measurements above 80°C (33), no evidence for a Curie point above this temperature can be obtained directly.

Prior to examining the high temperature structure the two sets of room temperature x-ray data (36)(43) were subjected to further refinement. This seemed advisable since there were significant differences in some features of these two reported structures, particularly the SO_4^{-2} ion distortions.

4.2 Continued Refinements of Room Temperature Structures

4.2 A Description and Comparison of Continued Refinements

Additional full matrix least squares refinement was carried out on each of the two room temperature structures. The structure factor data* published by Brown (36) together with his published atomic parameters and cell constants were used as a starting point for one refinement (hereafter referred to as the B refinement). A similar set of data† (43)(37) was used for the continued refinement of Van den Hende and Boutin's structure (hereafter referred to as the V refinement). In each refinement the atomic coordinates, anisotropic temperature factor components and layer line scaling constants were varied.

In their original refinement, Van den Hende and Boutin assigned a weighting factor of $1/F_o$ to each reflection. As Brown had estimated standard errors (σ) for his data, these were used to give a weighting scheme based on

---

*Misprints appear in Brown's reflections 941, 951 and 961 for which F_o should appear as <1.4, 2.7 and 2.0.

†The observed structure factors (43) of Van den Hende and Boutin are given in Appendix II.

$\omega = 1/\sigma^2$. Since Brown's standard errors had nearly a constant value for all observed reflections, this weighting scheme was essentially one of unit weights. In order to produce comparable refinements, the present analysis used unit weights ($\omega = 1$) during the continued refinements of the V data.

Table 4-1 gives the atom coordinates and anisotropic temperature factors together with their standard errors as determined in the final cycle of each refinement. The weighted R factor for the B data was reduced from 0.111 to 0.071 and for the V data from 0.164 to 0.124.

Table 4-2 gives the bond distances and angles calculated for the two sets of atom coordinates in Table 4-1. The standard errors in these values take account of standard errors in the coordinates and cell constants. The other entries in Table 4-2 give the differences in the distances and angles, the standard errors in these differences, and the ratio of the difference to the standard error. Here and in other tables in this chapter the following subscript convention denotes atoms related by symmetry to those for which x, y and z appear in the coordinate tables:

$$\begin{array}{lclll}
\mathrm{Aabc} & \longrightarrow & x + a, & y + b, & z + c; \\
\mathrm{Babc} & \longrightarrow & -x + \frac{1}{2} + a, & y + \frac{1}{2} + b, & z + c; \\
\mathrm{Cabc} & \longrightarrow & x + \frac{1}{2} + a, & -y + \frac{1}{2} + b, & z + \frac{1}{2} + c; \\
\mathrm{Dabc} & \longrightarrow & -x + 1 + a, & -y + 1 + b, & z + \frac{1}{2} + c.
\end{array}$$

TABLE 4-1

STRUCTURAL PARAMETERS FOLLOWING CONTINUED REFINEMENTS

Atom	Structure Factor Data†	Coordinates			Temperature Factor Components (x 10^4)					
		x	y	z	β_{11}	β_{22}	β_{33}	β_{12}	β_{13}	β_{23}
S	B	.1281(3)	.1581(2)	.2500(0)	74(3)	48(2)	74(15)	- 5(3)	2(12)	- 1(7)
	V	.1285(4)	.1591(4)	.2500(0)	13(4)	1(3)	37(12)	- 4(3)	-3(10)	-20(9) *
O1	B	.1075(10)	.1889(9)	.5130(26)	99(12)	79(9)	191(62)	-15(9)	-50(26)	- 4(20)
	V	.1069(13)	.1883(14)	.5416(22)	21(15)	43(15)	-71(37)	- 8(12)	10(24)	28(21)*
O2	B	.1537(8)	.0101(6)	.2194(30)	121(11)	39(6)	376(68)	-16(7)	42(31)	18(23)
	V	.1519(14)	.0128(12)	.2333(38)	58(18)	9(11)	76(49)	8(11)	7(36)	-46(31)*
O3	B	.2598(10)	.2299(7)	.1487(22)	78(10)	78(9)	283(74)	-21(8)	-5(19)	32(18)
	V	.2566(16)	.2338(12)	.1628(31)	38(16)	10(12)	149(52)	-9(12)	-18(26)	77(26)*
O4	B	.4958(10)	.3021(9)	.5981(23)	86(12)	106(10)	183(54)	-22(10)	-37(19)	35(19)
	V	.4941(17)	.3035(17)	.6061(36)	28(18)	60(17)	231(77)	-3(16)	5(29)	54(31)
N1	B	.4176(10)	.0235(9)	.7492(38)	99(13)	83(10)	330(76)	-30(9)	60(38)	37(37)
	V	.4188(17)	.0297(17)	.7482(55)	36(19)	46(17)	184(64)	-5(14)	-25(54)	59(50)
N2	B	.2176(9)	.4401(8)	.7384(40)	94(13)	60(8)	279(70)	2(8)	81(36)	49(30)
	V	.2144(15)	.4448(16)	.7353(47)	23(18)	58(18)	34(51)	-9(13)	7(38)	-66(39)*
Li	B	.4341(20)	.3306(17)	.2670(66)	89(21)	72(16)	-42(75)	16(18)	-44(62)	-45(44)*
	V	.4344(49)	.3224(41)	.2377(224)	82(52)	45(44)	842(356)	-24(39)	-103(173)	166(161)

* Denotes a non positive definite temperature factor matrix.

† The symbol B refers to the data of Brown (36) , while V refers to that of Van den Hende and Boutin (43)

TABLE 4-2

COMPARISON OF BOND LENGTHS AND ANGLES IN THE CONTINUED REFINEMENTS

Bonds (Å)	Refinement B	Refinement V	Δ	|Δ|/σ
S-O1	1.408(13)	1.550 (12)	-0.142 (18)	7.9
O2	1.498 (7)	1.471 (13)	0.027 (15)	1.8
O3	1.479 (9)	1.443 (15)	0.036 (18)	2.0
$O4_{C\bar{1}0\bar{1}}$	1.480(10)	1.467 (10)	0.013 (19)	.7
$Li-O1_{C00\bar{1}}$	2.050(28)	1.857 (74)	0.193 (79)	2.4
$O2_{B000}$	1.966(19)	2.046 (43)	-0.080 (47)	1.7
O3	1.957(22)	1.866 (51)	0.091 (56)	1.6
O4	1.825(35)	1.991(113)	-0.166(118)	1.4
$N1-N2_{B0\bar{1}0}$	1.472(12)	1.467 (21)	0.005 (24)	.2
O4	2.962(14)	2.899 (25)	0.063 (29)	2.2
$N1_{D0\bar{1}0}$	3.021(25)	3.031 (37)	-0.010 (45)	.2
N2-O1	2.929(15)	2.905 (22)	0.024 (27)	.9
$O1_{B000}$	3.155(15)	3.074 (21)	0.081 (26)	3.1
$O2_{B000}$	3.008(24)	2.944 (30)	0.072 (38)	1.9
$O2_{B001}$	2.834(24)	2.925 (30)	-0.091 (38)	2.4
$O3_{A001}$	3.004(19)	3.073 (26)	-0.069 (32)	2.2
O4	2.944(14)	2.958 (22)	-0.014 (26)	.5

Angles (°)	Refinement B	Refinement V	Δ	|Δ|/σ
O1-S-O2	109.6 (4)	105.1 (7)	4.5 (8)	5.6
O3	110.1 (6)	108.0 (8)	2.1 (10)	2.1
$O4_{C\bar{1}0\bar{1}}$	110.5 (7)	110.1 (9)	0.4 (11)	.4
O2-S-O3	108.3 (9)	112.1 (20)	-3.8 (22)	1.7
$O4_{C\bar{1}0\bar{1}}$	109.3 (6)	109.8 (11)	-0.5 (13)	.4
$O3-S-O4_{C\bar{1}0\bar{1}}$	109.0 (5)	111.5 (8)	-2.5 (10)	2.5
$O1_{C00\bar{1}}-Li-O2_{B000}$	108.1(15)	111.3 (67)	-3.2 (69)	.5
O3	111.1(30)	125.1(191)	-14.0(193)	.7
O4	110.9(24)	107.1(101)	3.8(104)	.4
$O2_{B000}-Li-O3$	95.9 (8)	96.3 (20)	-0.4 (22)	.2
O4	112.4(10)	101.6 (35)	10.8 (36)	3.0
O3-Li-O4	117.3(21)	112.7 (92)	4.6 (94)	.5
$N2_{B0\bar{1}0}-N1-O4$	135.4(10)	136.0 (19)	-0.6 (21)	.3
$-N1_{D0\bar{1}0}$	110.5(14)	108.7 (16)	1.8 (21)	.9
$-N1_{D0\bar{1}\bar{1}}$	106.6(13)	104.0 (16)	2.6 (21)	1.2
$O4-N1-N1_{D0\bar{1}0}$	104.8 (4)	106.7 (6)	-1.9 (7)	2.7
$-N1_{D0\bar{1}\bar{1}}$*	78.6 (4)	81.6 (6)	-3.0 (7)	4.3
$N1_{D0\bar{1}0}-N1-N1_{D0\bar{1}\bar{1}}$	118.1(13)	117.4 (16)	0.7 (21)	.3

*This angle should appear in reference (36) as 80°.

The subscript A000 is always deleted.

4.2 B Discussion of Continued Refinements

The bondlengths in Table 4-2 suggest that each set of data refines to a structure with distorted sulfur-oxygen and lithium-oxygen tetrahedra, assuming significant bond differences to exist where the discrepancy is more than twice the standard error. The directions of these distortions do not agree since the B refinement gives a significantly short S-O1 distance of 1.408 ± .013 Å compared to the significantly long distance of 1.550 ± .012 Å for the same bond in the V refinement. The respective Li-O1 distances are 2.05 ± .03 Å and 1.87 ± .07 Å .

Such distortions, if real, might suggest some contribution to the ferroelectricity in LiHzS from a mechanism of type III. One could suppose the opposite distortions to represent two possible configurations with opposite permanent dipole moments. If this were true, then both structure analyses must have been carried out on single domain crystals which were by chance spontaneously polarized in opposite directions.

While both sets of data after continued refinement indicate a possible mechanism of type III for both the sulfate ions and the lithium sites, it would be extremely surprising if these effects were real. In particular the indicated shortening and lengthening of a S-O distance in the covalently bonded sulfate ion cannot be explained by any accepted theory of chemical bonding. A change in the S-O1 distance from 1.41 to 1.55 Å could not represent a switch between two states of equivalent energy of the sulfate ion. The large change in the energy of the SO_4^{-2} ion would have to be exactly balanced by a corresponding large energy change elsewhere in the structure. It is much more reasonable to suppose that the S-O1 bondlength discrepancies arise from some systematic errors in the data or that they occur because of unusual behaviour of the least squares refinement. Difficulties in refinement of the z coordinate of O1 would be sufficient to cause the problem. Since the refined z coordinates of O1 and Li are suspect, no conclusive assessment of a type III mechanism for the lithium ion site can be made either.

4.2 C Analysis of Anisotropic Temperature Factors

The anisotropic temperature factors derived during the continued refinements can be analysed to give the root mean square displacement tensors and the direction cosines for their principal axes. This has been done for the B refinement and the results are given in Table 4-3. No such analysis is presented for the V refinement since the temperature factors are non positive definite for the atoms S, O1, O2, O3, and N2, probably indicating some systematic errors in the data. Non positive definite values are

TABLE 4-3

Principal Axes Analysis for Anisotropic Temperature Factors

Atom	R.M.S. Displacements (Å)	Direction Cosines With Respect to a	b	c
S	0.166	-.949	.315	-.026
	0.144	-.316	-.949	.010
	0.094	.021	-.017	-.999
O1	0.212	.795	-.481	-.370
	0.182	-.323	-.852	.413
	0.128	.513	.209	.833
O2	0.232	-.691	.040	-.721
	0.196	.672	-.331	-.662
	0.120	-.266	-.943	.202
O3	0.212	.398	-.735	-.549
	0.176	-.565	.275	-.778
	0.148	-.723	-.619	.306
$O4_{C\bar{1}0\bar{1}}$	0.234	-.419	.852	-.314
	0.170	-.802	.510	.312
	0.132	.425	-.121	-.897
N1	0.226	-.730	.229	-.644
	0.216	.240	-.797	-.555
	0.124	-.640	-.559	.527
N2	0.232	.630	.313	.710
	0.168	.586	-.792	-.171
	0.110	-.509	-.524	.683
Li	0.206	-.673	-.686	.279
	0.162	-.718	.696	-.022
	imaginary	(.178	.215	.960)*

*Non positive definite case.

inconsistent with physically possible motions. Since it is difficult to assess intensity measurements of other workers no further attempts have been made to trace the source of these errors. The B refinement has one atom (Li) with a non positive definite temperature factor but this could be made positive definite by increasing β_{33} by less than its standard error.

The thermal motions described in Table 4-3 are roughly consistent with the motions observed by Brown (36) for the oxygen atoms in a difference electron density projection calculation based on an isotropic temperature factor model. While this projection had indicated a librational motion of the SO_4^{-2} group around an axis parallel to $\underline{c}$, the three dimensional motions for the oxygens in Table 4-3 suggest a motion more complicated than a libration about any single axis. The root mean square displacements for the oxygen atoms seem too small to suggest that the crystal might easily be transformed to a centrosymmetric one or completely reversed to its enantiomorph. O1 was seen (Section 4.1 D) to require a motion of 1.1 Å in changing the crystal to its enantiomorph whereas the maximum RMS displacements at room temperature are only about 0.23 Å. These estimates of RMS displacements are valid provided the refinement of temperature factors has not been greatly influenced by systematic errors in the intensity data. It is quite unlikely that they could be in error here by a factor of four.

4.2 D Hydrogen Positions

Prior to the recent study of Padmanabhan and Balasubramanian (41) which reports hydrogen positions, some attempts were made to locate these atoms from the x-ray data of Brown (36). One attempt placed a ring of charge density beyond N2 with the plane of the ring perpendicular to the N1-N2 direction. This model was an approximation for the three hydrogen atoms of the NH_3^+ group reported by Cuthbert and Petch (34) to be rotating at room temperature. Appendix I discusses the modified structure factor formula used in this calculation. An N-H distance of 1.01 Å (6, Table 4.1.2) and tetrahedral N1-N2-H angles were assumed. The R factor decreased by only 0.001 when these atoms were included indicating that the refinement was relatively insensitive to the addition of these hydrogen atoms on a rotating model.

A second attempt placed hydrogen atoms of the NH_2 group in positions calculated from the data of Cuthbert and Petch, again assuming N-H distances of 1.01 Å. The two atoms were placed at the following positions in accordance with the ordered configuration of Fig. 4-2(b):

N1 — H1···N1; H1 : x = .471 y = .015 z = .923

N1 — H2···O4; H2 : x = .388 y = .120 z = .712

In addition to refining positions and isotropic temperature factors of H1 and H2, the coordinates of N1 and O4 were allowed to vary from their best values found prior to including H1 and H2. No significant changes occurred for N1 or O4. Since the hydrogen atom temperature factors underwent large fluctuations over several cycles of refinement, it was difficult to assess whether the lowering of R by 0.002 actually indicated that hydrogen atoms were at these places. The refined parameters gave

H1: $x = .467$ (17) $y = .050$ (15) $z = .887$ (45)

$B = 1.1$ (4.9)

H2: $x = .353$ (26) $y = .087$ (25) $z = .704$ (103)

$B = 12.6$ (104)

These may be compared to the more recent neutron diffraction results which favour the reversed configuration along the hydrogen bond chain (see Fig. 4-2(a)).

H1: $x = .467$ (4) $y = .036$ (4) $z = .571$ (4)

$B = 5.15$ (34)

H2: $x = .381$ (4) $y = .118$ (3) $z = .796$ (3)

$B = 3.56$ (33)

No further attempts to locate hydrogen positions were made from the x-ray data.

4.3 Structure of High Temperature $LiN_2H_5SO_4$

4.3 A Experimental

The crystals used were kindly supplied by J. Cuthbert. These crystals were from the same batch used in the NMR experiments (34) and had been prepared by evaporating an aqueous solution of $(N_2H_6)SO_4$ and Li_2CO_3 with purification by one cycle of recrystallization.

Early diffraction experiments at temperatures above about 75°C indicated a rapid decomposition of the crystals was occurring. The decomposition product appeared first on the surface of the crystals and rapidly spread throughout their volume. The effect of the decomposition product remained in the diffraction patterns when the temperature was lowered. It produced Weissenberg diffraction spots typical of a crystal with a large mosaic spread. Cell constants were roughly measured as $a = 8.88$ Å, $b = 8.79$ Å, $c = 5.30$ Å with $V = 413$ Å^3 . All axes were parallel to the corresponding axes in LiHzS, at least to the accuracy with which the centres of the broad spots could be determined. No change in systematic absences from those of LiHzS was noticed. The decomposition product was not identified.

In order to slow down this decomposition, silicon oil was used to coat the LiHzS crystal surfaces. Large crystals were necessary in order to achieve reasonable lifetimes even with the coated samples. A coated needle shaped crystal of mean diameter 0.75 mm was mounted with high temperature glue inside a Lindeman glass capillary. This sample was used to obtain intensity measurements with a Nonius Weissenberg camera equipped with apparatus for achieving exposures at high temperatures.

The size of this crystal was quite large compared to what one would normally select for negligible absorption and extinction effects. To overcome the large difficulties of absorption and extinction in a crystal this size, films were double exposed to obtain both the room temperature and high temperature diffraction patterns from the same crystal together on the same film. The film carriage was displaced slightly between exposures to separate the high and room temperature reflections. Since both exposures suffered approximately the same absorption and extinction effects, the ratio of the intensities of the high and room temperature forms would not depend to first order on these effects. These ratios could be measured and applied to a set of room temperature intensities collected under normal conditions, thus giving a true set of high temperature data.

Ni-filtered Cu-radiation was used to obtain double exposures for the layers hk0 and hk1. Because of deterioration in the first crystal, a second one of similar size was used for the hk1 photographs. The desired temperature of 180 ± 5°C was attained during the high temperature exposures by bathing the crystal mount in a stream of hot air. The air was heated by an electrical element while it flowed through an insulated tube. The exhaust nozzle of this tube was designed to fit inside the end of the Nonius camera layer line screens. The temperature was controlled by adjusting either the air flow rate or the heater voltage. A thermocouple and potentiometer were used to measure the temperature of the air flow close to the position of the crystal. The accuracy of this temperature measuring arrangement was verified prior to the diffraction experiments by mounting a second thermocouple on a goniometer head in the exact crystal position.

The high and room temperature double exposures indicated that the cell constants undergo slight changes due to thermal expansion. Accurate measurements of these increases were not made since the effects were small ones. No changes in systematic absences were observed indicating that the space group must still be either $Pbn2_1$ or Pbnm.

For each double exposed reflection, the ratio of the high to low temperature intensity was determined by measuring each intensity visually with a calibrated wedge film. The ratios were then applied to a set of room temperature intensities (hereafter referred to as room temperature data RT) derived by independent measurements of Brown's original hk0 and hkl photographs. The choice of a set of room temperature intensities is not too critical.

Parameter shifts between the room temperature and high temperature structures are related in a first approximation only to the changes in intensities, and these can be derived from the measured intensity ratios. Hence all that is required is a set of room temperature intensities which adequately describe the room temperature structure.

Table 4-4 gives the measured intensity ratios (I_{HT}/I_{RT}), their standard errors, the room temperature intensities, and their standard errors.

Table 4-5 gives the high temperature intensity data and standard errors as calculated from the data of Table 4-4. The high and room temperature data of Tables 4-4 and 4-5 were then corrected for Lorentz and polarization effects for the equi-inclination Weissenberg method (11,Ch. 7).

4.3 B Structure Refinement

Least squares refinement was carried out in the space group $Pbn2_1$ using the high temperature observed structure amplitudes (HT data). For comparison a similar refinement was done using the room temperature data (RT data). In each case isotropic temperature factors were used since the amount of data was insufficient to allow enough overdeterminacy if an anisotropic model were used. The final weighted R factors for these refinements were 0.129 for the high temperature data and 0.113 for the room temperature data. Since the high temperature structure fit the data just about

TABLE 4-4

Measured Intensity Ratios $R \equiv (I_{HT}/I_{RT})$ with Standard Errors and Room Temperature Intensities with Standard Errors.

The letters U, L, and G after the ratio column denote the following cases for the reflections on the doubly exposed (HT and RT) films:

U — both I_{HT} and I_{RT} were unobservable,

L — I_{HT} was unobservable and I_{RT} was observable,

G — I_{HT} was observable and I_{RT} was unobservable.

Minus signs after the I_{RT} column denote unobserved reflections on the room temperature films and asterisks denote unreliable I_{RT} measurements which were deleted during least-squares refinement.

TABLE 4-4 (Continued)

H	K	L	R	σ(R)	I(RT)	σ(I)
0	2	0	1.15	0.20	756	162
0	4	0	1.00	0.30	540	108
0	6	0	1.00	0.25	972	162
0	8	0	0.90	0.20	25	5
0	10	0	1.20	0.20	30	6
0	12	0	0.65	0.15	108	20
1	1	0	1.25	0.25	2106	486
1	2	0	1.15	0.25	2106	486
1	3	0	1.35	0.25	5022	972
1	4	0	1.00	0.20	1458	270
1	5	0	1.05	0.20	729	162
1	6	0	1.50	0.30	22	4
1	7	0	1.15	0.20	31	5
1	8	0	1.00	0.20	48	12
1	9	0	0.85	0.15	54	10
1	10	0	L		6	3
1	11	0	0.50	0.15	24	5
1	12	0	U		3	1
2	0	0	0.40	0.15	216	36
2	1	0	1.30	0.30	4320	1080
2	2	0	1.15	0.20	216	36
2	3	0	U		9	2
2	4	0	1.50	0.40	84	18
2	5	0	0.60	0.15	486	108
2	6	0	1.15	0.20	180	54
2	7	0	1.10	0.20	153	36
2	8	0	1.00	0.20	17	4
2	9	0	1.00	0.40	7	3
2	10	0	0.45	0.10	21	5
2	11	0	0.50	0.10	91	18
2	12	0	U		3	1
3	1	0	0.55	0.15	486	108
3	2	0	1.15	0.25	1782	486
3	3	0	U		5	2
3	4	0	1.25G	0.50	2	1
3	5	0	1.00	0.25	48	9
3	6	0	1.00	0.35	12	2
3	7	0	0.80	0.15	261	54
3	8	0	0.75	0.15	138	36
3	9	0	0.85	0.20	12	3
3	10	0	0.85	0.20	19	5
3	11	0	L		6	3
3	12	0	U		1-	1
4	0	0	1.15	0.25	459	81
4	1	0	L		14	3
4	2	0	1.20	0.25	108	27
4	3	0	0.75	0.20	207	36
4	4	0	1.00	0.35	216	45
4	5	0	2.00	0.40	12	3
4	6	0	0.80	0.20	594	135
4	7	0	0.50	0.15	24	6
4	8	0	U		1	1
4	9	0	0.65	0.20	15	3
4	10	0	0.75	0.20	38	7
4	11	0	U		1	1
4	12	0	0.30	0.15	1*	*****
5	1	0	1.10	0.25	48	9
5	2	0	0.65	0.15	351	81
5	3	0	1.15	0.20	261	54
5	4	0	0.60	0.15	36	6
5	5	0	0.75	0.25	1*	*****
5	6	0	0.40	0.20	9	2
5	7	0	0.50	0.25	3	1
5	8	0	0.65	0.15	150	36
5	9	0	0.70	0.20	72	14
5	10	0	0.40	0.15	54	9
5	11	0	U		1	1
6	0	0	1.60	0.40	20	4
6	1	0	0.65	0.15	387	72
6	2	0	2.50	0.70	12	2
6	3	0	0.50	0.20	18	4
6	4	0	0.50	0.30	10	2
6	5	0	0.75	0.15	270	63
6	6	0	0.40	0.20	14	4
6	7	0	0.75	0.20	72	18
6	8	0	U		1-	1
6	9	0	0.50	0.20	16	3
6	10	0	0.65	0.20	9	3
7	1	0	0.50	0.10	243	54
7	2	0	0.90	0.20	108	36
7	3	0	0.55	0.15	24	5
7	4	0	0.75	0.15	102	24
7	5	0	0.40	0.10	66	15
7	6	0	L		6	3
7	7	0	0.50	0.15	24	6
7	8	0	1.00	0.35	20	5
7	9	0	0.55	0.10	27	6
7	10	0	1.00	0.25	15	5
8	0	0	0.60	0.15	243	72
8	1	0	U		1-	1
8	2	0	0.60	0.15	108	27
8	3	0	U		1-	1
8	4	0	0.60	0.15	17	4
8	5	0	U		1-	1
8	6	0	0.55	0.10	63	15
8	7	0	U		1-	1
8	8	0	L		4	2
8	9	0	0.40	0.15	57	13
9	1	0	U		1-	1
9	2	0	0.40	0.10	58	12
9	3	0	0.65	0.15	99	24
9	4	0	0.40	0.10	32	8
9	5	0	0.55	0.20	13	4
9	6	0	0.50	0.20	9	3
9	7	0	1.00	0.20	14	3
9	8	0	0.50	0.15	1*	*****
10	0	0	U		1-	1
10	1	0	0.50	0.15	60	12
10	2	0	U		1-	1
10	3	0	0.40	0.15	19	5
10	4	0	U		1-	1
10	5	0	0.50	0.15	81	21
10	6	0	U		1-	1
11	1	0	0.40	0.15	20	6
11	2	0	1.00	0.25	22	5
11	3	0	L		15	4
11	4	0	0.50	0.10	1*	*****

TABLE 4-4 (Continued)

H	K	L	R	σ(R)	I(RT)	σ(I)
0	2	1	1.00	0.20	2754	891
0	4	1	1.00	0.20	252	54
0	6	1	1.30	0.20	15	6
0	8	1	1.00	0.20	36	9
0	10	1	0.67	0.20	6	3
0	12	1	0.57	0.20	45	12
1	0	1	1.00	0.25	1944	648
1	1	1	1.00	0.25	1134	324
1	2	1	1.20	0.20	945	216
1	3	1	0.75	0.15	15	6
1	4	1	1.30	0.25	30	6
1	5	1	0.90	0.20	30	6
1	6	1	1.00	0.20	162	36
1	7	1	1.00	0.25	48	12
1	8	1	0.70	0.14	21	6
1	9	1	0.42	0.12	12	3
1	10	1	0.90	0.18	6	3
1	11	1	0.75	0.25	9*	*****
1	12	1	0.70	0.15	45	12
2	1	1	1.00	0.20	3078	1053
2	2	1	0.70	0.15	198	45
2	3	1	1.00	0.20	216	45
2	4	1	1.17	0.20	90	18
2	5	1	1.00	0.25	162	45
2	6	1	0.65	0.13	24	6
2	7	1	0.75	0.15	153	36
2	8	1	U		4-	4
2	9	1	0.85	0.20	33	9
2	10	1	L		4-	4
2	11	1	U		4-	4
2	12	1	L		4	4
3	0	1	1.00	0.20	540	108
3	1	1	0.83	0.17	337	81
3	2	1	1.00	0.20	234	54
3	3	1	0.52	0.11	51	12
3	4	1	1.00	0.25	324	81
3	5	1	0.58	0.15	108	27
3	6	1	1.45	0.25	57	12
3	7	1	1.00	0.20	18	6
3	8	1	0.75	0.15	9	3
3	9	1	0.65	0.13	33	12
3	10	1	0.55	0.13	21	6
3	11	1	0.50	0.20	18	6
3	12	1	0.80	0.25	27	9
4	1	1	1.00	0.25	21	6
4	2	1	1.00	0.25	162	45
4	3	1	1.75	0.35	6	3
4	4	1	1.00	0.30	180	45
4	5	1	1.00	0.20	4	4
4	6	1	0.55	0.11	78	18
4	7	1	U		4-	4
4	8	1	0.65	0.20	78	18
4	9	1	U		4-	4
4	10	1	0.75	0.18	9	3
4	11	1	U		4-	4
5	0	1	0.75	0.15	234	54
5	1	1	1.00	0.25	120	30
5	2	1	0.65	0.14	108	27
5	3	1	0.75	0.15	57	12
5	4	1	0.80	0.18	6	3
5	5	1	2.00	0.50	3-	3
5	6	1	0.80	0.16	75	18
5	7	1	0.90	0.20	15	6
5	8	1	U		4-	4
5	9	1	0.40	0.15	18	9
5	10	1	0.47	0.17	9	3
5	11	1	0.80	0.20	27	9
6	1	1	0.75	0.25	21	6
6	2	1	0.55	0.15	24	6
6	3	1	1.00	0.25	66	15
6	4	1	0.55	0.13	6	3
6	5	1	1.00	0.22	9	4
6	6	1	0.55	0.15	4	4
6	7	1	0.62	0.12	30	9
6	8	1	0.30	0.06	15	6
6	9	1	1.00	0.25	9	3
6	10	1	U		4-	4
7	0	1	1.55	0.30	21	6
7	1	1	0.75	0.17	108	27
7	2	1	0.90	0.20	33	9
7	3	1	0.80	0.28	4	4
7	4	1	0.75	0.15	6	4
7	5	1	0.67	0.14	18	6
7	6	1	1.10	0.20	4	4
7	7	1	0.70	0.14	18	6
7	8	1	L		4-	4
7	9	1	L		4-	4
8	1	1	U		4-	4
8	2	1	0.70	0.14	48	12
8	3	1	U		4	4
8	4	1	0.82	0.17	39	9
8	5	1	L		4	4
8	6	1	L		4-	4
8	7	1	L		4	4
8	8	1	0.67	0.14	36	9
9	0	1	0.50	0.10	54	12
9	1	1	1.10	0.20	9	3
9	2	1	U		4-	4
9	3	1	U		4-	4
9	4	1	U		4-	4
9	5	1	0.80	0.18	36	9
9	6	1	0.30	0.12	18	9
9	7	1	1.00	0.20	6	3
10	1	1	0.65	0.20	9*	*****
10	2	1	U		4-	4
10	3	1	0.75	0.18	24	6
10	4	1	U		4-	4
10	5	1	U		4-	4
11	0	1	U		4	4
11	1	1	0.67	0.30	9	3
11	2	1	L		4	4
11	3	1	U		4-	4

TABLE 4-5

High Temperature Intensity Data with Standard Errors.

Minus signs after the I_{HT} column denote that the intensities are less than the value quoted. Asterisks denote unreliable I_{HT} values which were deleted during least-squares refinement.

TABLE 4-5 (Continued)

H	K	L	I(HT)	σ(I)
0	2	0	869	338
0	4	0	540	270
0	6	0	972	405
0	8	0	23	10
0	10	0	36	13
0	12	0	70	29
1	1	0	2633	1134
1	2	0	2422	1085
1	3	0	6780	2568
1	4	0	1458	562
1	5	0	765	316
1	6	0	33	13
1	7	0	36	12
1	8	0	48	22
1	9	0	46	17
1	10	0	6-	3
1	11	0	12	6
1	12	0	3*	****
2	0	0	86	47
2	1	0	5616	2700
2	2	0	248	85
2	3	0	9*	****
2	4	0	126	61
2	5	0	292	138
2	6	0	207	98
2	7	0	168	70
2	8	0	17	7
2	9	0	7	6
2	10	0	9	4
2	11	0	46	18
2	12	0	3*	****
3	1	0	267	132
3	2	0	2049	1004
3	3	0	5*	****
3	4	0	3*	****
3	5	0	48	21
3	6	0	12	6
3	7	0	209	82
3	8	0	104	48
3	9	0	10	5
3	10	0	16	8
3	11	0	6-	3
3	12	0	2-	2
4	0	0	528	208
4	1	0	14-	3
4	2	0	130	59
4	3	0	155	68
4	4	0	216	121
4	5	0	24	11
4	6	0	475	227
4	7	0	12	7
4	8	0	2*	****
4	9	0	10	5
4	10	0	29	13
4	11	0	2*	****
4	12	0	0*	****
5	1	0	53	22
5	2	0	228	105
5	3	0	300	114
5	4	0	22	9
5	5	0	1*	****
5	6	0	4	3
5	7	0	2	1
5	8	0	98	46
5	9	0	50	24
5	10	0	22	12
5	11	0	2*	****
6	0	0	32	14
6	1	0	252	105
6	2	0	30	13
6	3	0	9	6
6	4	0	5	4
6	5	0	203	88
6	6	0	6	4
6	7	0	54	28
6	8	0	2-	2
6	9	0	8	5
6	10	0	6	4
7	1	0	122	51
7	2	0	97	54
7	3	0	13	6
7	4	0	77	33
7	5	0	26	13
7	6	0	6-	3
7	7	0	12	7
7	8	0	20	12
7	9	0	15	6
7	10	0	15	9
8	0	0	146	80
8	1	0	2-	2
8	2	0	65	32
8	3	0	2-	2
8	4	0	10	5
8	5	0	2-	2
8	6	0	35	15
8	7	0	2-	2
8	8	0	4-	2
8	9	0	23	14
9	1	0	2-	2
9	2	0	23	11
9	3	0	64	30
9	4	0	13	6
9	5	0	7	5
9	6	0	5	3
9	7	0	14	6
9	8	0	1*	****
10	0	0	2-	2
10	1	0	30	15
10	2	0	2-	2
10	3	0	8	5
10	4	0	2-	2
10	5	0	41	23
10	6	0	2-	2
11	1	0	8	5
11	2	0	22	11
11	3	0	15-	4
11	4	0	1*	****

TABLE 4-5 (Continued)

H	K	L	I(HT)	σ(I)
0	2	1	2754	1442
0	4	1	252	104
0	6	1	20	11
0	8	1	36	16
0	10	1	4	3
0	12	1	26	16
1	0	1	1944	1134
1	1	1	1134	608
1	2	1	1134	448
1	3	1	11	7
1	4	1	39	15
1	5	1	27	11
1	6	1	162	68
1	7	1	48	24
1	8	1	15	7
1	9	1	5	3
1	10	1	5	4
1	11	1	7*	****
1	12	1	32	15
2	1	1	3078	1669
2	2	1	139	61
2	3	1	216	88
2	4	1	105	39
2	5	1	162	86
2	6	1	16	7
2	7	1	115	50
2	8	1	5-	5
2	9	1	28	14
2	10	1	5-	5
2	11	1	5-	5
2	12	1	5-	5
3	0	1	540	216
3	1	1	280	125
3	2	1	234	101
3	3	1	27	12
3	4	1	324	162
3	5	1	63	32
3	6	1	83	32
3	7	1	18	10
3	8	1	7	4
3	9	1	21	12
3	10	1	12	6
3	11	1	9	7
3	12	1	22	14
4	1	1	21	11
4	2	1	162	86
4	3	1	11	7
4	4	1	180	99
4	5	1	4	5
4	6	1	43	18
4	7	1	5-	5
4	8	1	51	27
4	9	1	5-	5
4	10	1	7	4
4	11	1	5-	5
5	0	1	176	76
5	1	1	120	60
5	2	1	70	33
5	3	1	43	18
5	4	1	5	3
5	5	1	6-	6
5	6	1	60	26
5	7	1	14	8
5	8	1	5-	5
5	9	1	7	6
5	10	1	4	3
5	11	1	22	13
6	1	1	16	10
6	2	1	13	7
6	3	1	66	32
6	4	1	3	2
6	5	1	9	6
6	6	1	2	3
6	7	1	19	9
6	8	1	5	3
6	9	1	9	5
6	10	1	5-	5
7	0	1	33	16
7	1	1	81	39
7	2	1	30	15
7	3	1	3	4
7	4	1	5	4
7	5	1	12	7
7	6	1	5	6
7	7	1	13	7
7	8	1	5-	5
7	9	1	5-	5
8	1	1	5-	5
8	2	1	34	15
8	3	1	4*	****
8	4	1	32	14
8	5	1	5-	5
8	6	1	5-	5
8	7	1	5-	5
8	8	1	24	11
9	0	1	27	11
9	1	1	10	5
9	2	1	5-	5
9	3	1	5-	5
9	4	1	5-	5
9	5	1	29	14
9	6	1	5	5
9	7	1	6	4
10	1	1	6*	****
10	2	1	5-	5
10	3	1	18	9
10	4	1	5-	5
10	5	1	5-	5
11	0	1	5*	****
11	1	1	6	5
11	2	1	5-	5
11	3	1	5-	5

as well as the $Pbn2_1$ room temperature structure, $Pbn2_1$ space group was considered to be the correct one for the high temperature structure. Hence no trial structure in Pbnm needed to be examined. At some stages during the high temperature refinement the Li(z) coordinate oscillated between 0.20 and 0.30 with R as low as 0.139. By setting it at the mean value 0.25 and refining it further, it stayed nearly fixed and R decreased to the 0.129 value quoted above.

The atom parameters from the high (HT) and room temperature (RT) refinements are compared in Table 4-6 and their calculated bond distances and angles are compared in Table 4-7.

Table 4-8 gives the differences in the coordinates in Å units for the two structures. Since the standard errors for the high temperature structure are a composite of the errors present in the room temperature structure together with the errors in the intensity ratios, the standard errors in the differences of Table 4-8 are calculated according to $\sigma_D^2 = \sigma_{HT}^2 - \sigma_{RT}^2$. Table 4-9 gives the differences in bond lengths and angles between the two structures with standard errors calculated in the same way. Here also ratios of differences to standard errors are given.

In Figure 4-3 the dots show the room temperature atom positions as projected down [001]. The directions of the observed shifts for the high temperature structure are

TABLE 4-6

Comparison of HT and RT Refinement Parameters

Atom	Structure	x	y	z	B
S	HT	.1256 (4)	.1594 (4)	.2500 (0)	2.49(11)
	RT	.1286 (3)	.1582 (3)	.2500 (0)	1.62 (5)
O1	HT	.0995(18)	.1911(19)	.5071(153)	4.62(52)
	RT	.1053(11)	.1909(10)	.5189(119)	3.16(29)
O2	HT	.1563(13)	.0153(12)	.2036(154)	3.96(29)
	RT	.1539 (8)	.0099 (7)	.2134(121)	2.48(16)
O3	HT	.2570(15)	.2324(11)	.1384(136)	3.72(29)
	RT	.2585 (8)	.2294 (6)	.1468(117)	2.42(16)
O4	HT	.4952(20)	.3085(14)	.5904(135)	4.54(37)
	RT	.4954(10)	.3057 (8)	.5866(109)	2.67(17)
N1	HT	.4141(17)	.0223(16)	.7272(191)	4.60(38)
	RT	.4166(11)	.0242 (9)	.7299(164)	2.63(20)
N2	HT	.2145(16)	.4394(15)	.7171(210)	3.82(31)
	RT	.2187(10)	.4400 (9)	.7338(190)	2.40(17)
Li	HT	.4347(41)	.3386(27)	.2558(500)	3.72(59)
	RT	.4294(27)	.3338(18)	.2596(403)	2.80(43)

TABLE 4-7

Comparison of Bond Distances and Angles from HT and RT Refinements

Bonds (Å)	HT	RT	Angles (°)	HT	RT
S-O1	1.389 (76)	1.445 (60)	O1-S-O2	114.0 (14)	113.3 (7)
O2	1.479 (18)	1.504 (11)	O3	113.1 (33)	111.0 (24)
O3	1.502 (30)	1.466 (23)	$O4_{C\bar{1}O\bar{1}}$	110.8 (40)	111.9 (30)
$O4_{C\bar{1}O\bar{1}}$	1.470 (42)	1.509 (33)	O2-S-O3	105.0 (14)	107.9 (10)
$Li\text{-}O1_{COO\bar{1}}$	1.986(178)	2.029(136)	$O4_{C\bar{1}O\bar{1}}$	105.5 (11)	106.4 (7)
$O2_{BOOO}$	1.956 (48)	1.919 (34)	$O3\text{-}S\text{-}O4_{C\bar{1}O\bar{1}}$	107.8 (30)	108.2 (23)
O3	2.008 (88)	1.944 (69)	$O1_{COO\bar{1}}\text{-}Li\text{-}O2_{BOOO}$	110.9 (78)	109.7 (65)
O4	1.841(253)	1.816(202)	O3	108.6(153)	111.5(140)
$N1\text{-}N2_{BO\bar{1}O}$	1.421 (22)	1.477 (13)	O4	111.5(167)	107.5(144)
O4	3.021 (35)	2.980 (28)	$O2_{BOOO}\text{-}Li\text{-}O3$	95.6 (16)	98.1 (12)
$N1_{DO\bar{1}O}$	3.048(119)	3.031(103)	O4	113.5 (67)	112.5 (57)
N2-O1	2.888 (55)	2.900 (46)	O3-Li-O4	115.8(145)	117.2(132)
$O1_{BOOO}$	3.200 (51)	3.156 (43)	$N2_{BO\bar{1}O}\text{-}N1\text{-}O4$	137.2 (23)	137.0 (16)
$O2_{BOOO}$	2.998(120)	3.011(105)	$\text{-}N1_{DO\bar{1}O}$	111.1 (70)	107.8 (55)
$O2_{BOO1}$	2.876(119)	2.823(103)	$\text{-}N1_{DO\bar{1}\bar{1}}$	107.2 (68)	109.2 (56)
$O3_{AOO1}$	3.024 (95)	3.015 (82)	$O4\text{-}N1\text{-}N1_{DO\bar{1}O}$	102.4 (18)	104.1 (14)
O4	2.914 (37)	2.925 (32)	$\text{-}N1_{DO\bar{1}\bar{1}}$	79.4 (18)	80.0 (14)
			$N1_{DO\bar{1}O}\text{-}N1\text{-}N1_{DO\bar{1}\bar{1}}$	116.4 (67)	117.4 (54)

TABLE 4-8

Coordinate Changes from RT to HT Refined Structure

Atom	ΔX (Å)	ΔY (Å)	ΔZ (Å)
S	-.032 (3)	.012 (5)	.000 (0)
O1	-.052(13)	.002(16)	-.061 (50)
O2	.022 (9)	.054(10)	-.051 (50)
O3	-.013(11)	.030 (9)	-.044 (36)
O4	-.002(15)	.028(12)	.020 (41)
N1	-.022(12)	-.019(13)	-.014 (51)
N2	-.038(12)	-.006(12)	-.087 (47)
Li	.048(28)	.048(20)	-.020(153)

TABLE 4-9

Bond Length and Angle Changes From RT to HT Refined Structure

Bonds	Δ(Å)	Δ/σ	Angles	Δ(°)	Δ/σ
S-O1	-0.056 (47)	-1.2	O1-S-O2	2.7(12)	2.3
O2	-0.025 (14)	-1.8	O3	2.1(23)	1.2
O3	0.036 (19)	1.9	O4	-1.1(26)	-0.4
$O4_{C\bar{1}0\bar{1}}$	-0.039 (28)	-1.4	O2-S-O3	-2.9(10)	-2.9
			O4	-0.9 (9)	-1.0
$Li\text{-}O1_{C00\bar{1}}$	-0.043(114)	-0.4	O3-S-O4	-0.4(19)	-0.2
$O2_{B000}$	0.037 (34)	1.1			
O3	0.064 (55)	1.2	O1-Li-O2	1.2(44)	0.3
O4	0.025(152)	0.2	O3	-2.9(62)	0.5
			O4	4.0(85)	0.5
$N1\text{-}N2_{B0\bar{1}0}$	-0.056 (18)	-3.1	O2-Li-O3	-2.5(11)	-2.3
O4	0.041 (21)	2.0	O4	1.0(33)	0.3
$N1_{D0\bar{1}0}$	0.017 (60)	0.3	O3-Li-O4	-1.4(60)	-0.2
N2-O1	-0.012 (30)	-0.4	$N2_{B0\bar{1}0}\text{-}N1\text{-}O4$	0.2(17)	0.1
$O1_{B000}$	0.044 (27)	1.6	$N1_{D0\bar{1}0}$	3.3(43)	0.8
$O2_{B000}$	-0.013 (58)	-0.2	$N1_{D0\bar{1}\bar{1}}$	-2.0(38)	-0.5
$O2_{B001}$	0.053 (60)	0.9	$O4\text{-}N1\text{-}N1_{D0\bar{1}0}$	-1.7(11)	-1.5
$O3_{A001}$	0.009 (48)	0.2	$N1_{D0\bar{1}\bar{1}}$	-0.6(11)	-0.5
O4	-0.011 (19)	-0.6	$N1_{D0\bar{1}0}\text{-}N1\text{-}N1_{D0\bar{1}\bar{1}}$	-1.0(40)	-0.3

FIGURE 4-3

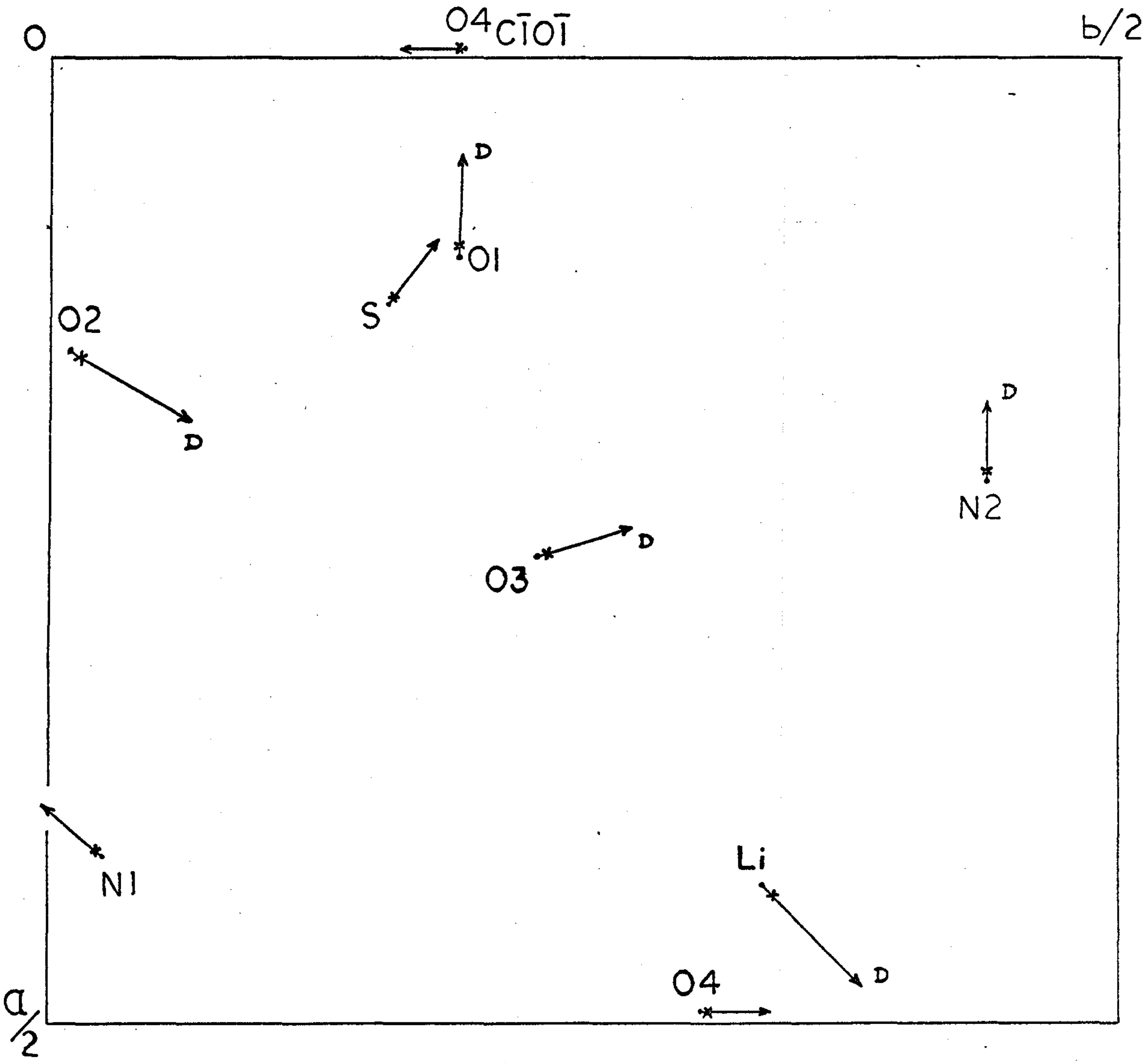

Observed atom shifts in [001] projection between room temperature positions (dots) and high temperature positions (crosses). Arrows show schematically the shift directions and are scaled ten times longer than the actual shifts. U or D at a vector tip denotes a significant shift up or down the c direction.

shown schematically by vectors which have a length scaled ten times larger than the actual observed shift in the projection. The letters "U" and "D" at the vector tip denote significant shifts up or down the c axis respectively.

Another attempt to display these shifts was made by calculating a [001] difference electron density projection using (F_{HT} - F_{RT}) and the sign of F_{calc} as the Fourier coefficients in eqn. [2-1]. No definite shifts could be seen in the plot of this function since they were masked by the differences in temperature factors.

4.3 C Conclusions from High Temperature Analysis

Systematic absences indicate that the high temperature space group is either $Pbn2_1$ or Pbnm. The refinement of the available high temperature data indicates that at 180°C the space group of LiHzS remains $Pbn2_1$. This result fails to explain on the basis of any change to a higher crystallographic symmetry why the electric quadrupole coupling tensors at all four lithium sites are identical in magnitude and orientation as reported in the nuclear magnetic resonance studies of Cuthbert and Petch (34). Such a high symmetry would not be required crystallographically even if the space group did change to Pbnm.

The slight increase in cell constants at high temperatures is due to thermal expansion. The small magnitudes observed for atom shifts when the temperature is raised to 180°C suggest that no significant changes occur for the heavy atoms in the crystal structure. If there is a distinctly different structure above 160°C it must differ primarily in the hydrogen configurations which were not seen, or possibly in the nitrogen and lithium z coordinates the latter of which was the least accurately determined parameter in this analysis.

The increase in all the temperature factors reflects the general decrease of the intensities observed on the films and results from increased thermal motion of the atoms at higher temperatures. An oxygen isotropic temperature factor of $B = 4.6 \text{ Å}^2$ in the high temperature refinement suggests isotropic root mean square thermal displacements of 0.24 Å (see eqn.[2-5]) assuming that no large systematic effects are influencing the temperature factors. Although this is an isotropic or average estimate of the O motions it is still below the value 1.1 Å estimated in Section 4.1 D as being necessary for easy excursion of the structure to its enantiomorph.

4.3 D Discussion of Experimental Difficulties and Possible Improvements

This high temperature analysis might be criticized on the grounds that the refinement has used only a limited amount of three dimensional data. This limitation might explain the oscillations of the lithium z coordinate at certain stages of the refinement, but even here the excursions did not exceed the range of the standard error given for the parameter. However, since a similar quantity of data for the room temperature form refined to a structure which agrees with that found using Brown's full set of data, the available high temperature data was expected to give a structure that would agree within its limits of error with a more accurate refinement.

Greater criticism can probably be directed at the accuracy of the film data which was collected. The absorption effects for large crystals, while not directly influencing the ratio method of intensity measurement, did produce film spots of irregular shapes sometimes making accurate comparisons with the wedge film quite difficult. Hence the general accuracy of the measurements was probably decreased even though the method eliminated the large systematic error of absorption. The spot shape problem was enhanced by the surface decomposition product which contributed diffraction spots with a large mosaic spread to certain of the high temperature low angle reflections. The amount of decomposition was observed to increase during each high temperature exposure, thus introducing a systematic error into the comparison of low and high temperature exposures.

It was felt, however, that if prominent structural differences did occur for the heavy atoms above 160°C then an analysis using this data would at least indicate their presence. Certainly a change to any symmetry higher than

Pbnm would be visible as a change in the systematic absences. Since no such indications were found, further efforts to improve the x-ray diffraction experiments seemed unjustifiable.

If further x-ray work could be justified it would seem advisable to solve first the problem of keeping small crystals stable for extended time periods at high temperatures.

CHAPTER 5 THE CRYSTAL STRUCTURE OF TRICLINIC POTASSIUM DICHROMATE

5.1 Introduction

Potassium dichromate $K_2Cr_2O_7$ is one of the most familiar crystalline solids. As early as 1833 Mitscherlich (44) observed that it undergoes a phase transition close to 250°C. This was one of the first solid state phase transitions to be noted in the scientific literature. In spite of continued interest since that date in its crystallography, the structure of even its room temperature phase had never been solved. In 1959, Klement and Schwab (45) reviewed what was then known about potassium dichromate and concluded that it exists in at least three different forms, namely a triclinic room temperature phase, a monoclinic high temperature phase, and a metastable monoclinic room temperature phase. The similarity found for the unit cells of these forms suggests a similarity in their structures and indeed a similarity with other structures such as ammonium dichromate and potassium pyrosulfate. Details concerning these and other related structures will be described in later sections.

Although no structure had been proposed for triclinic $K_2Cr_2O_7$, there was considerable controversy through the years as to whether the triclinic space group is noncentrosymmetric

(P1) or centrosymmetric ($P\bar{1}$). Brief reviews of the controversy appear in the papers of Klement and Schwab (45) and Rao (46). After reviewing conflicting evidence from crystal growth and etch figure experiments on the one hand and the absence of any observable piezoelectric effect on the other, Klement and Schwab declare themselves in favour of $P\bar{1}$. Rao (46) also favours $P\bar{1}$ on the additional basis of his statistical analysis of the x-ray diffraction intensity data. On the other hand the recent Russian studies of crystal growth and etch figures by Podisco (47), and Parvov and Shubnikov (48) continue to favour the noncentrosymmetric P1 choice. An obvious step toward resolving this controversy would be to determine the crystal structure.

A structure determination was considered of value also for determining accurate distances and angles for the dichromate ion. Some values had previously been reported in the paper describing the structure of $(NH_4)_2Cr_2O_7$ (49) but these were not very accurate. The unexpected large discrepancies reported there among apparently equivalent Cr-O distances were difficult to explain chemically and were possibly due to large parameter errors in the structure determination. More accurate studies of the dichromate ion might be of value in assessing the applicability of Cruickshank's theories (1) to chromium in tetrahedral arrangements. In particular a comparison to the pyrosulfate ion, $S_2O_7^{-2}$, is of interest.

There has also been recent interest in the geometry of groups of the type X_2O_7 (50),(51),(52) and in the variety of structures they can form. An accurate knowledge of the dichromate ion geometry would add valuable information to the study of these groups.

At an advanced stage in the writing of this thesis a structure determination of triclinic $K_2Cr_2O_7$ was published by Kuzmin, Iliukhin, and Belov (53). While they reported essentially the same structure as had been determined by this author, their refinement accuracy was not as great. In comparison to the more accurate results given here,their determination of the dichromate ion stereochemistry is somewhat misleading. Consequently no extensive changes in this thesis have been made aside from pointing out their different cell convention and comparing the final atom parameters.

5.2 Experimental

5.2 A General Crystal Data

Crystals of triclinic potassium dichromate were grown by slowly evaporating at room temperature a saturated solution of technical grade potassium dichromate in distilled water. The clear orange seed crystals which formed, while occasionally platelike, were more frequently needle shaped along [010]. Several large crystals were grown with dimensions up to 2 cm from plate and needle seeds and all of these large samples had the characteristic habit shown in Fig. 5-1. The choice of axis senses and face names in Fig. 5-1 corresponds to those of the actual crystal which was indexed by the diffraction photographs. Table 5-1 gives the transformations between this convention and those of other workers.

Accurate cell parameters were measured using precession camera photographs taken with Zr-filtered Mo-radiation. The films were calibrated by recording on them an exposure from a single crystal of rutile (59), ($a = 4.59373 \pm 5$, $c = 2.95812 \pm 5$ Å). A pycnometer calibrated for ρ(water) = 1 gm. cm.$^{-3}$ at 0°C was used to measure the density of a mixture of carbon tetrachloride and bromoform in which $K_2Cr_2O_7$ crystals neither sank nor floated. The choice of $P\bar{1}$ as the correct space group is described in detail in a later section. The crystal data are given in Table 5-2.

5.2 B Intensity Data

The crystal selected for intensity measurements was of typical shape and approximated a cylinder with mean diameter of 0.25 mm and with length 0.46 mm along b. An integrating precession camera was used to obtain exposures of 1, 3, 9 and 27 integration cycles for each of the layers hk0, hk1, hk2, hk3, $0k\ell$, $1k\ell$, and $2k\ell$. All photographs were taken with Zr-filtered Mo-radiation. The integrated intensities were measured from these films by

FIGURE 5-1

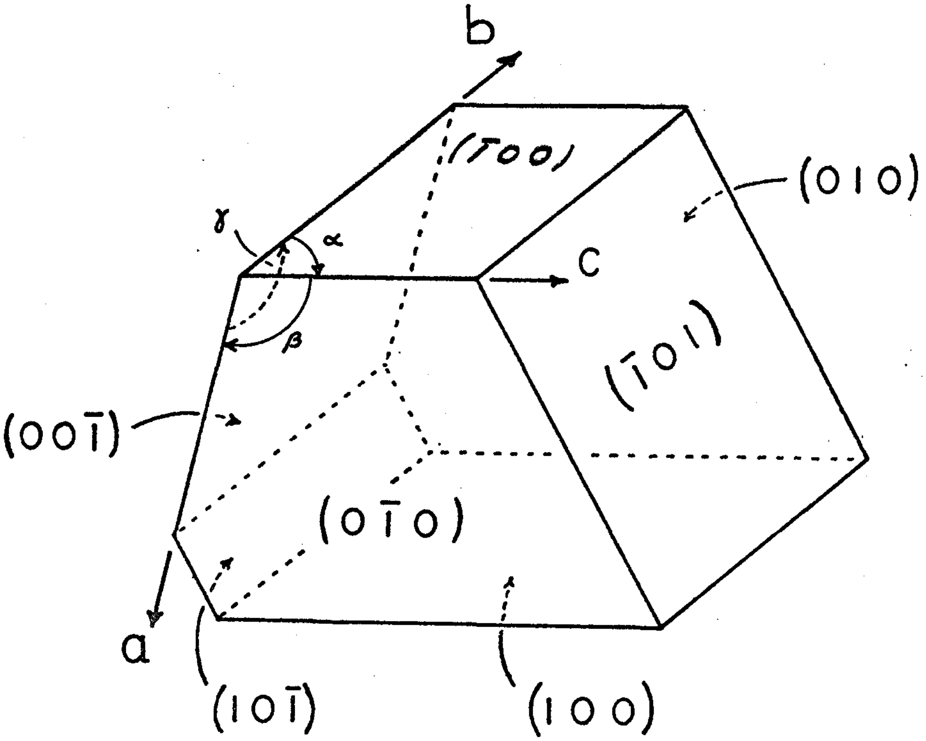

Characteristic Habit of Triclinic Potassium Dichromate Crystals. Other Small Faces Occasionally Present are (001), $(\bar{2}\bar{1}0)$, and $(\bar{1}10)$.

TABLE 5-1

Transformations Among Various Unit Cell Conventions[*†]

	$(hk\ell)^1$ x	$(hk\ell)^2$ x	$(hk\ell)^2$ x	$(hk\ell)^4$ x
$(hk\ell)^1$ =	1	$\begin{matrix}0 & 0 & -1\\ 0 & -1 & 0\\ -1 & 0 & 0\end{matrix}$	$\begin{matrix}0 & 0 & 1\\ 1 & 0 & 0\\ 0 & 1 & 0\end{matrix}$	$\begin{matrix}0 & 1 & 0\\ 0 & 0 & -1\\ -1 & 0 & 0\end{matrix}$
$(hk\ell)^2$ =	$\begin{matrix}0 & 0 & -1\\ 0 & -1 & 0\\ -1 & 0 & 0\end{matrix}$	1	$\begin{matrix}0 & -1 & 0\\ -1 & 0 & 0\\ 0 & 0 & -1\end{matrix}$	$\begin{matrix}1 & 0 & 0\\ 0 & 0 & 1\\ 0 & -1 & 0\end{matrix}$
$(hk\ell)^3$ =	$\begin{matrix}0 & 1 & 0\\ 0 & 0 & 1\\ 1 & 0 & 0\end{matrix}$	$\begin{matrix}0 & -1 & 0\\ -1 & 0 & 0\\ 0 & 0 & -1\end{matrix}$	1	$\begin{matrix}0 & 0 & -1\\ -1 & 0 & 0\\ 0 & 1 & 0\end{matrix}$
$(hk\ell)^4$ =	$\begin{matrix}0 & 0 & -1\\ 1 & 0 & 0\\ 0 & -1 & 0\end{matrix}$	$\begin{matrix}1 & 0 & 0\\ 0 & 0 & -1\\ 0 & 1 & 0\end{matrix}$	$\begin{matrix}0 & -1 & 0\\ 0 & 0 & 1\\ -1 & 0 & 0\end{matrix}$	1

Superscripts denote the conventions of various authors:

1. Present work.
2. Parvov and Shubnikov 1964 (48),
   Shubnikov 1911 (54), 1931 (55).
3. Klement and Schwab 1960 (45).
4. Groth 1908 (56),
   Stedehouder and Terpstra Fig. 3(a) 1930 (57).

[*] Kuzmin, Iliukhin, and Belov (53) use convention 3 but minus signs and origin shifts become necessary in converting their diagrams of the structure to those of the present work.

[†] The present work confirms that Gossner and Mussnug (58) have an error in one of their angle measurements.

TABLE 5-2

Crystal Data for Triclinic $K_2Cr_2O_7$

System		Triclinic
Space Group		$P\bar{1}$
Cell Constants	a	13.367 (11) Å
	b	7.376 (5)
	c	7.445 (6)
	α	90.75 (5) °
	β	96.21 (7)
	γ	97.96 (5)
Unit Cell Volume		722.3 Å^3
Reciprocal Cell Constants		
	a^*	0.07601 (6) Å^{-1}
	b^*	0.13696 (9)
	c^*	0.13517 (10)
	α^*	88.37 (5) °
	β^*	83.63 (5)
	γ^*	81.91 (5)
Density Measured		2.66 ± .05 gm cm^{-3}
Calculated		2.704 ± .003 gm cm^{-3}
Number of Formula Units per Unit Cell		4
X-ray Absorption Coefficient (MoKα)		42.4 cm^{-1}

using a recording photomicrodensitometer. The individual film intensities were scaled and averages taken for each reflection. A standard error was estimated for each intensity for use in weighting the data during least squares refinement.

Unobserved intensities were labelled and were assigned the local minimum observable intensity value. Unreliable intensity measurements (e.g.cases with beamstop interference, cases close to the edge of the film, etc.) were labelled to allow assignment of zero weights (i.e. deleted during least squares refinement). The full set of data consisted of 3221 measured reflections of which 617 were classified as unreliable and 324 had intensities too small to be observed. During the last stages of refinement an additional 25 low angle reflections suspected of showing extinction effects were classified with the unreliable ones so that they would not contribute in the final refinement.

The intensity data and their estimated standard errors were then corrected for Lorentz and polarization effects (12,Ch. 11). Absorption corrections were not considered necessary since μR was only 0.5 (5, Sec. 5.3).

5.2 C Attempts to Determine Space Group by Direct Experiment

Toward the final stages of the refinement, it became clear that the structure was quite close to being centrosymmetric. Anomalous dispersion experiments (6, Sec. 3.3.2), (8, Ch. 14) were performed to resolve this question.

Calculations performed with the best refined P1 parameters (isotropic model, R = .0754, see Sec. 5.3) and with complex scattering factors for Cr and K species (6, Sec. 3.3.2) indicated that appreciable intensity differences between $hk\ell$ and $\bar{h}\bar{k}\bar{\ell}$ should be observable for some reflections with Co or Cu-radiation if the space group were P1. Precession camera photographs were taken for the $hk0$ and $0k\ell$ layers with Fe-filtered Co-radiation. Weissenberg photographs were taken of the $h0\ell$ layer with Ni-filtered Cu-radiation. The Weissenberg films were double exposed in a way which gave the reflections $h0\ell$ and $\bar{h}0\bar{\ell}$ close to one another on the film for easier comparison of their intensities. Visual comparison of the pairs $hk\ell$ and $\bar{h}\bar{k}\bar{\ell}$ indicated no marked intensity differences among the pairs as expected from the calculations. Some small intensity differences were observed, but these were systematic effects attributable to different crystal absorption in the two reflecting positions. These observed inequalities had a random direction compared to the directions of the calculated inequalities. Hence the anomalous dispersion experiments were interpreted as favouring P$\bar{1}$.

At the suggestion of Dr. C. V. Stager and with his kind cooperation in performing the experiments, nuclear magnetic resonance techniques were used in an effort to determine the number of crystallographically distinct sites for Cr and K atoms. These attempts failed to detect any signals from either the 9.5% abundant Cr^{53} isotope or from the 93% K^{39} isotope, and hence this experiment was inconclusive.

5.3 Solution and Refinement of the Structure

A Patterson function was calculated using the hk0 intensity data. This function is shown in Fig. 5-2. About half of the large Cr atoms were located by identifying Patterson peaks which correspond to the Cr-Cr interatomic vectors in the same projection of the monoclinic ammonium dichromate structure (49). This comparison to an ammonium dichromate Patterson projection illustrated that the Cr-Cr vectors appear as satellite peaks at the edges of larger compound peaks. Trial solutions choosing Cr-Cr vectors at the centres of these large peaks had previously failed to yield a promising structure, but with the satellite positions and several cycles of electron density and structure factor calculations, the x and y coordinates for the remaining atoms were found.

The z coordinates were then determined from a Patterson function calculated with the $0k\ell$ data and a trial three dimensional structure was formulated in space group P1 with 44 independent atoms in the unit cell. This trial structure possessed approximate centres of symmetry but further refinement was performed without imposing any such constraints.

A three dimensional full matrix least squares

FIGURE 5-2

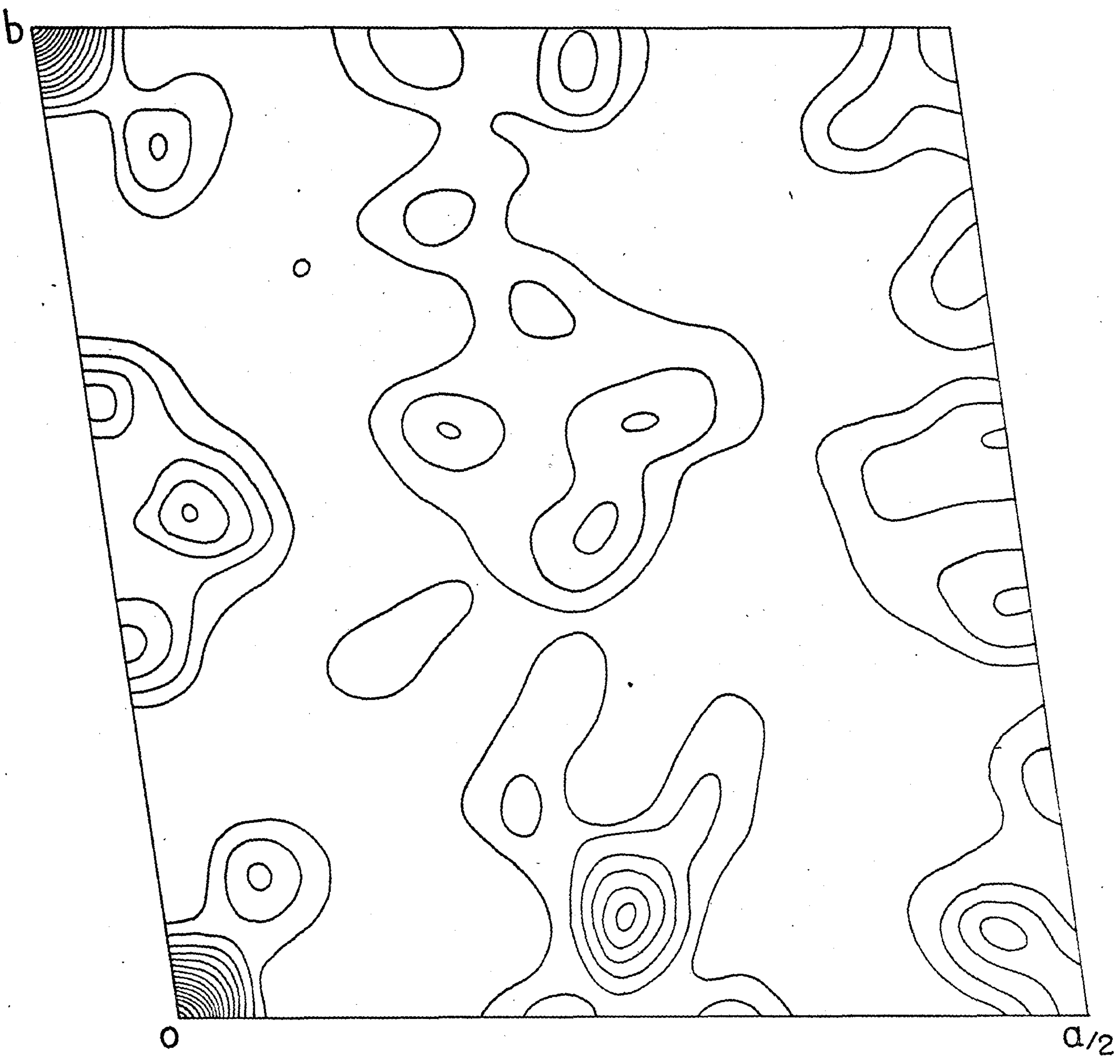

[001] Projection of Patterson Function for Triclinic $K_2Cr_2O_7$

computer program was used to refine the atom coordinates and isotropic temperature factors together with separate scale constants for the seven layers of data. The coordinates of Cr1 were held fixed in this P1 refinement and $\omega = 1/\sigma^2$ weights were used. Unobserved reflections in agreement (F(calc) $\leq F_{min}$, the local minimum observable value) were given zero weight. Those calculating larger than F_{min} were refined as though F_o was equal to F_{min}. The best weighted agreement index (R) obtained in P1 space group with isotropic temperature factors was 0.0754. This P1 isotropic model had 180 variable parameters and approximately 2300 reflections contributed to the refinement with non zero weights. Examination of the refined structure revealed an approximate centrosymmetric arrangement. Consequently refinement was also performed in $P\bar{1}$ space group giving a final R of 0.0963 using isotropic temperature factors. This $P\bar{1}$ isotropic model had 95 variable parameters and approximately 2300 reflections contributed with non zero weight.

The coordinates and their standard errors suggested that the P1 and $P\bar{1}$ structures were different particularly for the potassium and oxygen positions. Hamilton's significance test (19), when applied to the R factors for these two models, indicated less than 0.5% chance of the $P\bar{1}$ refinement being correct. However anomalous dispersion experiments (see Sec.5.2 C) failed to show any of the large differences between the $hk\ell$ and $\bar{h}\bar{k}\bar{\ell}$ intensities which had been expected from calculations based on the P1 coordinates. A second problem which arose if P1 were accepted as correct was that of understanding the systematic features of the distortions from $P\bar{1}$. There are four nonequivalent dichromate groups in P1 but each deviated from C_{2v} symmetry in a different way.

Detailed comparison of results from the P1 and $P\bar{1}$ isotropic refinements led to a suggestion which resolved the problem in assigning a space group. Pseudo-centrosymmetric O-Cr-O bond angles in P1 were found to differ markedly (about 7°) from each other while their mean value was very close to the corresponding angle found in $P\bar{1}$. This was consistent with pairs of the pseudo-centrosymmetric oxygen atoms in P1 having positions displaced in random but opposite directions from their $P\bar{1}$ positions. The question then arises whether the isotropic P1 model might have simply compensated for anisotropic thermal motion of both the oxygen and potassium atoms. The mathematics of the problem was appropriate for such a situation to arise; the insertion in P1 of two atoms almost related by a centre of symmetry gives nearly the same intensity as inserting in $P\bar{1}$ two half atoms each slightly displaced in opposite directions from their mean position (see Appendix III for proof). This latter situation is analogous to the physical case where an atom undergoes anisotropic thermal motion.

It was proposed that even though the isotropic P1 refinement had resulted in a significantly improved R factor compared to the isotropic $P\bar{1}$ model, the P1 structure was incorrect because it was using extra degrees of freedom to fit anisotropic thermal effects in the data.

Three tests were investigated to show this proposal to be correct. In the first test a $P\bar{1}$ refinement was performed with anisotropic temperature factors for the oxygen and potassium atoms. This particular model was chosen since with 185 variables it could be closely compared to the best fit allowed by the isotropic P1 model with 180 variables. The chosen anisotropic $P\bar{1}$ refinement gave a decrease in R from 0.0963 to 0.0633 in the first cycle, thus verifying the new $P\bar{1}$ model to be better than the isotropic P1 (R = 0.0754) with a similar number of variables. Further refinement cycles adding anisotropic temperature factors for chromium atoms gave a final $1/\sigma^2$ weighted R index of 0.054 in $P\bar{1}$.

The second test involved checking the least squares correlations (see Sec. 2.3) to confirm the suspected situation truly existed in the mathematics of the P1 model. Indeed large positive elements (0.6 to 0.9) were found in the P1 correlation matrix for pairs of coordinates related by the pseudo-centre of symmetry. Hence the P1 model had been adjusting the atoms in pairs in the manner suspected, keeping the members of each pair on opposite sides of the

$P\bar{1}$ positions. Correlations in the anisotropic $P\bar{1}$ model were no larger than 0.3 among atom coordinates indicating this to be a more suitable model for refinement.

As a third test of the $P\bar{1}$ anisotropic model, the temperature factor ellipsoids were examined to see if they corresponded to any physically reasonable type of thermal motion. This was indeed found to be the case, and details concerning the thermal parameter analysis are presented in Section 5.4 D. Hence triclinic $K_2Cr_2O_7$ is found within the accuracy of this structure analysis to be centrosymmetric.

The possibility of extending the model to test an anisotropic P1 structure seems inadvisable. The large correlations expected during least squares refinement would cast doubt on any results, and the refinement with existing computer memory size could only be performed in block diagonal matrix fashion. Furthermore the agreement (R = .054) obtained in $P\bar{1}$ anisotropic seems to be approaching closely the expected limits available with the intensity data used. The rest of this chapter will describe only the $P\bar{1}$ structure.

The atomic coordinates and anisotropic temperature factors are given in Table 5-3 for the final refinement (R = 0.054). Also given are the independently determined $P\bar{1}$ coordinates of Kuzmin, Iliukhin, and Belov (53) with R = 0.161. The latter have been converted from the published values to the convention of this author by moving their origin to

TABLE 5-3

Refined $P\bar{1}$ Coordinates and Temperature Factors
Compared to Transformed Values of Kuzmin et al.

Atom	x	y	z
K1	.15845 (7)	.16251(10)	.91463(16)
	.159	.160	.916
K2	-.13591 (8)	.19591(12)	.65275(19)
	-.136	.198	.656
K3	.64056 (7)	.60346(12)	.66946(18)
	.639	.604	.668
K4	.34939 (8)	.75019(11)	.76701(16)
	.348	.749	.768
Cr1	.11332 (5)	.31682 (7)	.42610(11)
	.113	.318	.426
Cr2	-.08334 (5)	.31361 (7)	.15240(11)
	-.083	.312	.154
Cr3	.60718 (5)	.09201 (7)	.76914(11)
	.608	.092	.768
Cr4	.41379 (5)	.29304 (7)	.80714(11)
	.414	.293	.808
OB1	.02283(21)	.42955(30)	.29483(52)
	.024	.433	.303
O11	.19970(22)	.47632(34)	.51664(57)
	.199	.453	.517
O12	.16358(25)	.18614(36)	.29483(54)
	.168	.199	.295
O13	.06054(25)	.19409(40)	.57663(58)
	.064	.194	.584
O21	-.14893(28)	.45840(36)	.06270(62)
	-.145	.463	.067
O22	-.15170(24)	.17519(33)	.27537(54)
	-.150	.176	.279

(continued next page)

TABLE 5-3 (Continued)

Refined P$\bar{1}$ Coordinates and Temperature Factors
Compared to Transformed Values of Kuzmin et al.

Atom	x	y	z
O23	-.04319(24)	.19264(39)	-.00185(56)
	-.043	.187	-.005
OB3	.52748(23)	.20950(37)	.89187(55)
	.522	.210	.893
O31	.70143(26)	.05349(40)	.91201(61)
	.696	.050	.905
O32	.64874(29)	.22010(38)	.61033(57)
	.651	.209	.613
O33	.54493(26)	-.09817(34)	.68346(62)
	.546	-.083	.673
O41	.36029(28)	.36600(38)	.97283(58)
	.365	.364	.975
O42	.33655(26)	.13702(36)	.69261(61)
	.340	.142	.701
O43	.44272(24)	.46064(34)	.67255(57)
	.443	.470	.675

Refined Temperature Factor Components* (x 10^5)

Atom	β_{11}	β_{22}	β_{33}	β_{12}	β_{13}	β_{23}
K1	286 (4)	916(11)	879(19)	99 (6)	-17(12)	-28(12)
K2	302 (5)	1364(14)	1111(22)	90 (7)	32(14)	393(16)
K3	253 (4)	1376(14)	1124(23)	71 (6)	87(13)	-244(16)
K4	309 (4)	1274(13)	931(20)	221 (7)	35(13)	-125(15)
Cr1	198 (3)	738 (8)	667(13)	30 (4)	15 (8)	-54 (9)
Cr2	206 (3)	654 (7)	668(13)	87 (4)	17 (8)	22 (8)
Cr3	198 (3)	723 (8)	753(13)	103 (4)	52 (8)	68 (9)

(continued next page)

TABLE 5-3 (Continued)

Refined Temperature Factor Components* (x 10^5)

Atom	β_{11}	β_{22}	β_{33}	β_{12}	β_{13}	β_{23}
Cr4	195 (3)	696 (8)	725(13)	89 (4)	76 (8)	73 (9)
OB1	288(14)	735(34)	1093(66)	42(18)	-55(39)	104(40)
O11	276(15)	1049(40)	1375(76)	18(21)	-45(42)	-215(49)
O12	354(16)	1263(43)	1043(69)	208(23)	128(45)	-333(49)
O13	347(17)	1585(52)	1241(76)	65(26)	95(48)	629(57)
O21	448(18)	1214(48)	1737(95)	289(25)	-115(50)	130(56)
O22	326(15)	1026(41)	1149(75)	-1(21)	198(44)	136(47)
O23	305(16)	1619(51)	1027(71)	121(24)	18(45)	-398(53)
OB3	319(16)	1539(50)	918(65)	363(24)	36(43)	51(51)
O31	349(15)	1717(51)	1265(80)	373(26)	-83(46)	146(58)
O32	468(20)	1255(46)	1242(78)	70(26)	114(55)	331(53)
O33	397(17)	993(42)	1731(93)	14(23)	41(49)	-75(53)
O41	420(18)	1442(48)	1177(76)	213(25)	269(50)	88(53)
O42	368(17)	1182(44)	1496(84)	-29(24)	36(47)	-259(53)
O43	313(15)	1085(41)	1358(77)	75(21)	173(43)	371(48)

---

*Kuzmin et al. used the isotropic values $B_K = 1.4\ \AA^2$, $B_{Cr} = 1.1\ \AA^2$, and $B_O = 1.7\ \AA^2$

TABLE 5-4

Observed and calculated structure factors (F_o and F_c) in units of 1/10 electron per unit cell with estimated relative standard errors (σ) in F_o. A minus sign following F_o indicates an unobserved reflection; an asterisk indicates an unreliable F_o measurement which was not used in the least-squares refinement; an x indicates a reflection which was suspected of showing extinction effects and was therefore not used during the final stages of refinement.

TABLE 5-4 (Continued)

H	K	L	FØ	FC	σ
0	0	0	0*	5640	***
18	0	0	105*	-102	***
17	0	0	119*	108	***
16	0	0	268	-252	20
15	0	0	36	34	15
14	0	0	130	127	16
13	0	0	32	-26	16
12	0	0	111	110	13
11	0	0	36-	6	18
10	0	0	184	-184	13
9	0	0	65	-60	11
8	0	0	255	257	15
7	0	0	66	27	12
6	0	0	163	160	11
5	0	0	138*	116	***
4	0	0	1226*	-2193	***
3	0	0	45*	-30	***
2	0	0	366*	413	***
1	0	0	9*	-22	***
18	-1	0	120*	116	***
17	-1	0	127	-128	15
16	-1	0	405	-393	23
15	-1	0	40-	33	20
14	-1	0	266	-265	20
13	-1	0	368	375	27
12	-1	0	198	200	14
11	-1	0	262	-274	26
10	-1	0	306	304	26
9	-1	0	554	-593	32
8	-1	0	288	297	21
7	-1	0	274	280	20
6	-1	0	30	35	8
5	-1	0	26	30	7
4	-1	0	561	-579	68
3	-1	0	23*	-24	***
2	-1	0	203*	-237	***
1	-1	0	249*	-209	***
0	-1	0	67*	-90	***
-1	-1	0	318*	-328	***
-2	-1	0	111	-95	11
-3	-1	0	141	-147	13
-4	-1	0	576	606	96
-5	-1	0	26-	-8	13
-6	-1	0	248	266	15
-7	-1	0	309	323	17
-8	-1	0	298	-304	17
-9	-1	0	253	-267	15
-10	-1	0	283	-291	17
-11	-1	0	251	-262	29
-12	-1	0	216	-224	13
-13	-1	0	178	179	13
-14	-1	0	79	-80	7
-15	-1	0	220	223	12
-16	-1	0	285	288	16
-17	-1	0	36-	-2	18
-18	-1	0	164*	180	***
18	-2	0	27*	2	***
17	-2	0	211	-206	12
16	-2	0	308	308	16
15	-2	0	100	98	12
14	-2	0	126	126	8
13	-2	0	303	295	20
12	-2	0	395	-394	22
11	-2	0	428	-439	36
10	-2	0	144	-135	10
9	-2	0	390	-406	28
8	-2	0	298	-301	15
7	-2	0	641	672	41
6	-2	0	186	-175	18
5	-2	0	722	754	96
4	-2	0	959X	1044	172
3	-2	0	492	-489	50
2	-2	0	619	625	74
1	-2	0	929X	-1026	176
0	-2	0	1030*	-1320	***
-1	-2	0	176	165	9
-2	-2	0	959X	-1107	178
-3	-2	0	723	775	76
-4	-2	0	719	760	89
-5	-2	0	118	119	8
-6	-2	0	317	329	18
-7	-2	0	464	-493	26
-8	-2	0	102	108	18
-9	-2	0	157	149	12
-10	-2	0	409	419	38
-11	-2	0	530	555	31
-12	-2	0	161	-167	11
-13	-2	0	59	62	9
-14	-2	0	339	-339	17
-15	-2	0	131	-132	20
-16	-2	0	38-	22	19
-17	-2	0	117*	-117	***
18	-3	0	101*	-99	***
17	-3	0	303	295	18
16	-3	0	40-	-16	20
15	-3	0	116	120	9
14	-3	0	44	48	12
13	-3	0	507	-501	36
12	-3	0	536	537	32
11	-3	0	91	-93	6
10	-3	0	499	506	30
9	-3	0	923	979	106
8	-3	0	674	-689	64
7	-3	0	245	241	20
6	-3	0	819	-841	94
5	-3	0	635	-671	59
4	-3	0	267	256	15
3	-3	0	617	621	59
2	-3	0	198	194	12
1	-3	0	101	97	5
0	-3	0	291	-297	23
-1	-3	0	433	-435	37
-2	-3	0	339	331	25
-3	-3	0	493	516	36
-4	-3	0	567	-600	56
-5	-3	0	86	-94	6
-6	-3	0	809	-879	89
-7	-3	0	737	-793	79
-8	-3	0	651	682	77
-9	-3	0	184	-178	24
-10	-3	0	558	577	42
-11	-3	0	423	423	26
-12	-3	0	215	-224	12
-13	-3	0	40-	31	20
-14	-3	0	114	-117	14
-15	-3	0	230	-234	25
-16	-3	0	46*	28	***
18	-4	0	76*	-80	***
17	-4	0	125*	129	***
16	-4	0	264	-250	23
15	-4	0	40-	-20	20
14	-4	0	327	-312	18
13	-4	0	298	-303	26
12	-4	0	160*	137	***
11	-4	0	59	72	8
10	-4	0	560	571	41
9	-4	0	477	483	33
8	-4	0	157*	-146	***
7	-4	0	164	-165	9
6	-4	0	595	-603	49
5	-4	0	222	-218	32
4	-4	0	131*	-103	***
3	-4	0	61	56	8
2	-4	0	147	139	8
1	-4	0	57	-63	6
0	-4	0	125	-118	10
-1	-4	0	81	83	4
-2	-4	0	128	-119	7
-3	-4	0	189	-180	12
-4	-4	0	455	474	32
-5	-4	0	35-	46	17
-6	-4	0	420	423	30
-7	-4	0	205	211	13
-8	-4	0	229	-227	13
-9	-4	0	38-	-41	19
-10	-4	0	458	-458	33
-11	-4	0	215	-212	17
-12	-4	0	39-	-4	20
-13	-4	0	78*	-81	***
-14	-4	0	389	398	39
-15	-4	0	126	129	14
-16	-4	0	124*	175	***
17	-5	0	137*	147	***
16	-5	0	215	208	20
15	-5	0	148	-141	15
14	-5	0	253	253	19
13	-5	0	40-	16	20
12	-5	0	222	-216	12
11	-5	0	127	120	8
10	-5	0	607	-620	48
9	-5	0	367	-367	26
8	-5	0	167	162	9
7	-5	0	102	-109	13
6	-5	0	848	892	100
5	-5	0	530	529	37
4	-5	0	177	177	12
3	-5	0	36	-20	11
2	-5	0	139	-135	13
1	-5	0	189	-182	11
0	-5	0	321	-336	23
-1	-5	0	576	583	58
-2	-5	0	370	-378	29
-3	-5	0	65	64	13
-4	-5	0	322	310	19
-5	-5	0	505	-514	36
-6	-5	0	643	671	62
-7	-5	0	38-	-22	19
-8	-5	0	48	58	10
-9	-5	0	108	115	9
-10	-5	0	516	-528	35
-11	-5	0	39-	-16	20
-12	-5	0	105	-113	12
-13	-5	0	37-	14	18
-14	-5	0	146*	154	***
16	-6	0	115*	120	***
15	-6	0	60	-66	10
14	-6	0	269	263	16
13	-6	0	39-	39	20
12	-6	0	151*	122	***
11	-6	0	154	-145	10
10	-6	0	389	-380	26
9	-6	0	48	42	10
8	-6	0	323	-311	18
7	-6	0	186*	148	***
6	-6	0	257	240	22
5	-6	0	468	-462	30
4	-6	0	175	174	9
3	-6	0	719	-721	71
2	-6	0	35	27	13
1	-6	0	505	486	32
0	-6	0	164	161	15
-1	-6	0	764	799	80
-2	-6	0	56	-70	9
-3	-6	0	391	-385	22
-4	-6	0	337	-356	19
-5	-6	0	304	-300	16
-6	-6	0	295	-282	15
-7	-6	0	188	167	24
-8	-6	0	47	46	11
-9	-6	0	53	52	10
-10	-6	0	303	302	19
-11	-6	0	41	41	11
-12	-6	0	120*	106	***
-13	-6	0	52*	35	***
15	-7	0	218*	-222	***
14	-7	0	92*	-81	***
13	-7	0	37-	43	18
12	-7	0	292	287	18
11	-7	0	95	85	13
10	-7	0	175	168	18
9	-7	0	39*	46	***
8	-7	0	39-	24	20
7	-7	0	39-	17	20
6	-7	0	74*	-46	***
5	-7	0	97	-97	10
4	-7	0	274	-270	15
3	-7	0	44	46	12
2	-7	0	76	-71	13
1	-7	0	215	198	13
0	-7	0	88	83	7
-1	-7	0	90*	-66	***
-2	-7	0	180	173	17
-3	-7	0	90	-99	9
-4	-7	0	160	156	11
-5	-7	0	131	127	15
-6	-7	0	93	-86	9
-7	-7	0	194	184	18
-8	-7	0	204	-199	12
-9	-7	0	70	68	10
-10	-7	0	84	-81	10
-11	-7	0	110*	-122	***
13	-8	0	40*	27	***
12	-8	0	215	-215	21
11	-8	0	63	64	7
10	-8	0	215	-210	12
9	-8	0	76	74	19
8	-8	0	277	252	18
7	-8	0	349	-338	19
6	-8	0	388	387	32
5	-8	0	39-	-6	20
4	-8	0	39-	52	20
3	-8	0	509	506	35
2	-8	0	363	-359	20
1	-8	0	87	-89	12
0	-8	0	403	-390	38
-1	-8	0	536	-534	47
-2	-8	0	39-	19	19
-3	-8	0	38-	0	19
-4	-8	0	271	266	14
-5	-8	0	278	275	17
-6	-8	0	79	75	9
-7	-8	0	48	-52	9
-8	-8	0	187	-182	16
-9	-8	0	28*	-10	***
11	-9	0	88*	89	***
10	-9	0	78*	-76	***
9	-9	0	57*	43	***
8	-9	0	90*	71	***
7	-9	0	117	-121	13
6	-9	0	76*	-63	***
5	-9	0	90*	-94	***
4	-9	0	33	29	14
3	-9	0	49	49	9
2	-9	0	160	174	10
1	-9	0	88	93	7
0	-9	0	38-	11	19
-1	-9	0	84*	39	***
-2	-9	0	36-	20	18
-3	-9	0	35-	-1	17
-4	-9	0	33-	-3	17
-5	-9	0	124*	-120	***
-6	-9	0	131*	-136	***
7	-10	0	57*	-63	***
6	-10	0	267*	-278	***
5	-10	0	22*	-5	***
4	-10	0	136*	-130	***
3	-10	0	24*	-17	***
2	-10	0	134*	134	***
1	-10	0	54*	-59	***
0	-10	0	244*	223	***
-1	-10	0	20*	-11	***
-2	-10	0	91*	101	***
13	-10	1	37*	39	***
12	-10	1	71*	86	***
11	-10	1	36*	-48	***
10	-10	1	195	200	11
9	-10	1	204	-214	11
8	-10	1	48-	-16	24
7	-10	1	49-	19	24
6	-10	1	181	-180	18
5	-10	1	250	262	13
4	-10	1	50-	-16	25
3	-10	1	76	-75	13
2	-10	1	91	89	11
1	-10	1	189	-186	10
0	-10	1	106	103	20
-1	-10	1	147	154	11
-2	-10	1	174	172	14
-3	-10	1	176*	159	***
15	-9	1	125*	133	***
14	-9	1	107*	121	***
13	-9	1	58	-60	19
12	-9	1	88	88	9
11	-9	1	133	-138	12
10	-9	1	112	-112	9
9	-9	1	111*	-106	***
8	-9	1	169	-166	10
7	-9	1	42	-41	21
6	-9	1	46	-42	19
5	-9	1	243	238	13
4	-9	1	206	205	11
3	-9	1	159	144	8
2	-9	1	141	135	9
1	-9	1	268	-260	13
0	-9	1	53	-39	17
-1	-9	1	209	-201	10
-2	-9	1	126	-127	10
-3	-9	1	103	96	10
-4	-9	1	232	-244	12
-5	-9	1	143	142	9
-6	-9	1	51	-43	16
-7	-9	1	49-	5	24
-8	-9	1	220	221	14
-9	-9	1	99	-99	7
-10	-9	1	131*	122	***
-11	-9	1	90*	-90	***
17	-8	1	91*	-97	***
16	-8	1	86*	86	***
15	-8	1	47-	-3	24
14	-8	1	180	-188	11
13	-8	1	50-	-29	25
12	-8	1	253	-255	14
11	-8	1	85	85	10
10	-8	1	112	104	9
9	-8	1	247	235	14
8	-8	1	377	378	21
7	-8	1	44	33	20
6	-8	1	51-	-30	25
5	-8	1	185	-170	12
4	-8	1	266	-270	15
3	-8	1	51	41	17
2	-8	1	70	75	12
1	-8	1	132*	120	***
0	-8	1	62	67	14
-1	-8	1	125	-106	13
-2	-8	1	99	-101	14
-3	-8	1	65	63	16
-4	-8	1	50	-40	18
-5	-8	1	127	116	10
-6	-8	1	127	131	7
-7	-8	1	94*	-78	***
-8	-8	1	166	164	11
-9	-8	1	69	-72	12
-10	-8	1	80	-88	10
-11	-8	1	72	-71	10
-12	-8	1	178	-185	9
-13	-8	1	30*	-28	***
18	-7	1	68*	80	***
17	-7	1	190*	-193	***
16	-7	1	49-	15	24
15	-7	1	208	209	11
14	-7	1	151	-156	12
13	-7	1	271	276	19
12	-7	1	72	-75	12
11	-7	1	192	-200	11
10	-7	1	225	236	11
9	-7	1	180	-170	13
8	-7	1	289	284	17
7	-7	1	49-	7	25
6	-7	1	212	-215	11
5	-7	1	187	-187	11
4	-7	1	520	-515	31
3	-7	1	49-	-44	24
2	-7	1	329	-314	19
1	-7	1	449	446	28
0	-7	1	118	117	11
-1	-7	1	75	82	11
-2	-7	1	386	382	21
-3	-7	1	270	-284	13
-4	-7	1	159	168	8
-5	-7	1	119	122	7
-6	-7	1	259	-251	13
-7	-7	1	51-	33	26
-8	-7	1	264	-274	13
-9	-7	1	127	-132	8
-10	-7	1	204	195	13
-11	-7	1	100	102	10
-12	-7	1	276	270	21
-13	-7	1	82	83	14
-14	-7	1	45*	-35	***
-15	-7	1	64*	-65	***
18	-6	1	76*	-68	***
17	-6	1	50-	-8	25
16	-6	1	101	95	9
15	-6	1	86	-84	10
14	-6	1	271	278	26
13	-6	1	116	110	10
12	-6	1	179	177	9
11	-6	1	67	66	12
10	-6	1	273	-268	20
9	-6	1	323	-316	24
8	-6	1	164	-160	11
7	-6	1	187	-177	14
6	-6	1	80	67	9
5	-6	1	448	440	22
4	-6	1	81	-77	9
3	-6	1	548	558	45
2	-6	1	161	154	11
1	-6	1	127	-122	14
0	-6	1	89	72	8
-1	-6	1	714	-739	50
-2	-6	1	124	-110	12
-3	-6	1	166	-174	11
-4	-6	1	48-	-24	24
-5	-6	1	473	478	24
-6	-6	1	49-	-31	24
-7	-6	1	180	174	9
-8	-6	1	134	-129	12
-9	-6	1	157	-156	11
-10	-6	1	41	36	21
-11	-6	1	70	-57	18
-12	-6	1	254	249	13
-13	-6	1	49	-12	18
-14	-6	1	60	-60	14
-15	-6	1	71	-71	10
-16	-6	1	266*	-259	***
18	-5	1	174*	173	***
17	-5	1	119	-115	7
16	-5	1	52-	27	26
15	-5	1	448	-452	28
14	-5	1	175	-169	10
13	-5	1	124	-119	13
12	-5	1	146	-152	11
11	-5	1	378	372	19
10	-5	1	193	-195	13
9	-5	1	155	156	9
8	-5	1	40	32	17
7	-5	1	315	-309	20
6	-5	1	527	516	35
5	-5	1	90	89	13
4	-5	1	284	292	25
3	-5	1	133	-133	8
2	-5	1	202	-190	17
1	-5	1	268	-260	22
0	-5	1	138	-144	11
-1	-5	1	406	391	22
-2	-5	1	121	-133	6
-3	-5	1	44-	36	22
-4	-5	1	56*	38	***
-5	-5	1	155	-142	10
-6	-5	1	377	387	19
-7	-5	1	220	222	11
-8	-5	1	150	153	13
-9	-5	1	156	165	15
-10	-5	1	121	-116	20
-11	-5	1	268	-260	16
-12	-5	1	75	-70	11
-13	-5	1	187	-191	12
-14	-5	1	86	-75	10
-15	-5	1	245	234	12
-16	-5	1	48-	-27	24
-17	-5	1	189*	189	***
-18	-5	1	54*	92	***
18	-4	1	42*	37	***
17	-4	1	52-	-38	26
16	-4	1	52-	11	26
15	-4	1	72	79	12
14	-4	1	115	-118	7
13	-4	1	48-	-26	24
12	-4	1	47-	2	23
11	-4	1	158	150	8
10	-4	1	189	-185	14
9	-4	1	454	450	29
8	-4	1	77	68	15
7	-4	1	113	-105	8
6	-4	1	641	649	64
5	-4	1	587	-602	59
4	-4	1	194	-200	10
3	-4	1	68	-61	8
2	-4	1	887	-927	72
1	-4	1	465	464	24
0	-4	1	37-	-21	19
-1	-4	1	442	443	28
-2	-4	1	1133X	1231	196
-3	-4	1	482	-467	30
-4	-4	1	265	273	18
-5	-4	1	948	-1013	108
-6	-4	1	676	-676	64
-7	-4	1	244	-242	13
-8	-4	1	124	-133	8
-9	-4	1	310	315	21
-10	-4	1	89	-91	8
-11	-4	1	189	190	10
-12	-4	1	101	-101	8
-13	-4	1	49	42	17
-14	-4	1	175	170	13
-15	-4	1	50	-57	18
-16	-4	1	114	114	10
-17	-4	1	47	-36	17
-18	-4	1	70*	-73	***
18	-3	1	319	-322	36
17	-3	1	89	78	20
16	-3	1	153	151	8
15	-3	1	184	180	9
14	-3	1	277	286	20
13	-3	1	123	130	9
12	-3	1	44	-38	16
11	-3	1	60	-44	15
10	-3	1	190	-199	12
9	-3	1	180	-189	12
8	-3	1	378	-392	20
7	-3	1	261	-253	17
6	-3	1	98	-88	5
5	-3	1	629	624	61
4	-3	1	547	502	56
3	-3	1	556	524	56
2	-3	1	513	494	51
1	-3	1	351	-340	25
0	-3	1	64	8	5
-1	-3	1	61	56	7
-2	-3	1	54*	-38	***
-3	-3	1	258	-270	26
-4	-3	1	209	200	24
-5	-3	1	267	-263	15
-6	-3	1	177	-167	9
-7	-3	1	232	238	18
-8	-3	1	201	-203	12
-9	-3	1	358	344	23
-10	-3	1	37*	-9	***
-11	-3	1	38*	-34	***
-12	-3	1	163	167	11
-13	-3	1	211	-204	10
-14	-3	1	330	325	23
-15	-3	1	51-	-31	26
-16	-3	1	48	-49	18
-17	-3	1	51	-47	17
-18	-3	1	334	-328	18
18	-2	1	52-	-17	26
17	-2	1	151	156	18
16	-2	1	150	153	8
15	-2	1	223	-228	15
14	-2	1	88	87	9
13	-2	1	359	-371	18
12	-2	1	44-	-15	22
11	-2	1	72	-71	8
10	-2	1	57*	33	***
9	-2	1	616	609	55
8	-2	1	232	-231	12
7	-2	1	501	491	35
6	-2	1	758	-747	81
5	-2	1	739	-745	80
4	-2	1	36*	7	***
3	-2	1	679	-699	77
2	-2	1	991*	1221	***
1	-2	1	39	-25	6
0	-2	1	918*	-1095	***
-1	-2	1	31	17	6
-2	-2	1	1238*	-1660	***
-3	-2	1	216	-218	17
-4	-2	1	622	641	63
-5	-2	1	315	301	18
-6	-2	1	723	798	71
-7	-2	1	529	563	34
-8	-2	1	83	86	10
-9	-2	1	144	-150	8
-10	-2	1	190	-193	10
-11	-2	1	307	-317	21
-12	-2	1	201	-193	10
-13	-2	1	48-	1	24
-14	-2	1	118	-112	10
-15	-2	1	163	162	11
-16	-2	1	127	119	7
-17	-2	1	95	91	13
-18	-2	1	155	151	8
18	-1	1	52-	-37	26
17	-1	1	109*	94	***
16	-1	1	115	-116	12
15	-1	1	76	-83	11
14	-1	1	39*	36	***
13	-1	1	213	-219	11
12	-1	1	39*	-22	***
11	-1	1	234	248	13
10	-1	1	71*	74	***
9	-1	1	719	740	64
8	-1	1	278	286	15
7	-1	1	220	-219	12
6	-1	1	525	515	45
5	-1	1	1097X	-1266	202
4	-1	1	89	-85	5
3	-1	1	724	-750	131
2	-1	1	353*	-354	***
-2	-1	1	160*	-168	***
-3	-1	1	858X	1019	154
-4	-1	1	218	221	14
-5	-1	1	340	341	23
-6	-1	1	146	151	8
-7	-1	1	836	-909	98
-8	-1	1	217	-216	24
-9	-1	1	75	-78	6
-10	-1	1	223	-233	15
-11	-1	1	851	881	85
-12	-1	1	199	-206	10
-13	-1	1	47-	12	23
-14	-1	1	48-	6	24
-15	-1	1	482	-444	35
-16	-1	1	127	127	7
-17	-1	1	48*	-54	***
-18	-1	1	111	104	16
18	0	1	133	-132	12
17	0	1	74	-71	18
16	0	1	259	-260	13
15	0	1	280	283	15
14	0	1	39*	36	***
13	0	1	412	432	21
12	0	1	382	395	19
11	0	1	663	-671	54
10	0	1	36*	12	***
9	0	1	954	-1002	108
8	0	1	444	-443	42
7	0	1	298	298	21
6	0	1	30-	-3	15
5	0	1	405	393	30
4	0	1	325	310	23
3	0	1	203*	169	***
-3	0	1	13*	17	***

TABLE 5-4 (Continued)

H	K	L	F0	FC	σ
-4	0	1	66*	68	***
-5	0	1	126	-120	8
-6	0	1	49	-46	6
-7	0	1	117	-131	7
-8	0	1	149	-158	8
-9	0	1	33	48	14
-10	0	1	38	-48	13
-11	0	1	602	636	40
-12	0	1	254	263	19
-13	0	1	160	161	6
-14	0	1	80	81	10
-15	0	1	414	-411	39
-16	0	1	156	-154	8
-17	0	1	115	-115	8
-18	0	1	43	-42	21
18	1	1	58*	51	***
17	1	1	77	81	12
16	1	1	191	-188	14
15	1	1	43	38	20
14	1	1	145	-157	10
13	1	1	91*	-84	***
12	1	1	246	259	14
11	1	1	338	-344	18
10	1	1	243	269	19
9	1	1	66	-66	8
8	1	1	595	-607	45
7	1	1	732	748	102
6	1	1	45	-44	8
5	1	1	714	739	80
4	1	1	984X	1090	186
3	1	1	190	-183	13
2	1	1	614*	616	***
-3	1	1	167*	-214	***
-4	1	1	597*	-962	***
-5	1	1	316*	466	***
-6	1	1	211*	-274	***
-7	1	1	363*	491	***
-8	1	1	479*	638	***
-9	1	1	398*	-493	***
-10	1	1	291*	287	***
-11	1	1	610*	-650	***
-12	1	1	556	-543	50
-13	1	1	45-	17	23
-14	1	1	132	-143	10
-15	1	1	203	200	12
-16	1	1	245	245	18
-17	1	1	52-	22	26
-18	1	1	88	76	10
18	2	1	86*	65	***
17	2	1	52-	24	26
16	2	1	102	96	12
15	2	1	210	-214	10
14	2	1	153	-151	11
13	2	1	89	-101	9
12	2	1	312	-298	15
11	2	1	152	157	16
10	2	1	156	156	10
9	2	1	158	162	13
8	2	1	640	628	73
7	2	1	164	170	9
6	2	1	71	-72	6
5	2	1	105	-103	6
4	2	1	961X	-1069	175
3	2	1	301	-285	28
2	2	1	355	-342	26
1	2	1	306	-287	19
0	2	1	820	927	151
-1	2	1	1038*	1337	***
-2	2	1	134	-144	12
-3	2	1	988X	1208	177
-4	2	1	801	-860	152
-5	2	1	861	-953	164
-6	2	1	377*	387	***
-7	2	1	416*	-498	***
-8	2	1	532*	660	***
-9	2	1	191	-177	11
-10	2	1	39-	10	20
-11	2	1	238	-246	12
-12	2	1	140	-142	7
-13	2	1	250	254	17
-14	2	1	48-	4	24
-15	2	1	325*	370	***
-16	2	1	59*	72	***
-17	2	1	48*	-30	***
-18	2	1	165	167	11
18	3	1	74*	67	***
17	3	1	50-	-34	25
16	3	1	104	105	9
15	3	1	346	349	23
14	3	1	51-	-17	25
13	3	1	211	214	11
12	3	1	49-	10	24
11	3	1	44	46	17
10	3	1	207	204	13
9	3	1	300	-309	26
8	3	1	45	-32	13
7	3	1	559	-556	40
6	3	1	167	-157	17
5	3	1	187	181	9
4	3	1	389	-381	20
3	3	1	771	786	94
2	3	1	579	-566	64
1	3	1	66*	-30	***
0	3	1	172	164	9
-1	3	1	561	-558	57
-2	3	1	133	127	7
-3	3	1	197	187	17
-4	3	1	59	62	6
-5	3	1	75	-73	13
-6	3	1	366	-378	22
-7	3	1	277	-278	14
-8	3	1	469	-467	46
-9	3	1	127	131	7
-10	3	1	177*	188	***
-11	3	1	134*	164	***
-12	3	1	273	284	13
-13	3	1	151	152	8
-14	3	1	106	93	18
-15	3	1	43	-37	19
-16	3	1	150	-145	9
-17	3	1	329	-321	27
-18	3	1	77*	-55	***
17	4	1	50	66	15
16	4	1	87	-78	12
15	4	1	44*	-1	***
14	4	1	64	-29	14
13	4	1	71	-68	12
12	4	1	115	113	9
11	4	1	66	-69	12
10	4	1	112	112	7
9	4	1	165	-170	11
8	4	1	37	-32	18
7	4	1	263	-253	27
6	4	1	162	-167	8
5	4	1	260	270	13
4	4	1	71	67	11
3	4	1	1002	1024	116
2	4	1	44	-29	12
1	4	1	88	-92	5
0	4	1	49	-41	12
-1	4	1	1122X	-1249	186
-2	4	1	139	142	7
-3	4	1	112	-111	8
-4	4	1	102	-76	7
-5	4	1	983	1060	114
-6	4	1	71	63	9
-7	4	1	715	731	73
-8	4	1	237	244	12
-9	4	1	238	-243	15
-10	4	1	210	196	13
-11	4	1	333	-342	17
-12	4	1	75*	-74	***
-13	4	1	122*	-155	***
-14	4	1	125	-118	10
-15	4	1	51-	-32	25
-16	4	1	84	-79	10
-17	4	1	240	234	23
-18	4	1	155	-154	9
17	5	1	126*	-132	***
16	5	1	134	137	8
15	5	1	207	-217	16
14	5	1	81	-85	11
13	5	1	62	-46	14
12	5	1	297	-292	15
11	5	1	132	130	6
10	5	1	94	94	9
9	5	1	202	200	10
8	5	1	251	242	13
7	5	1	238	243	22
6	5	1	189	-186	11
5	5	1	237	-235	13
4	5	1	200	-196	17
3	5	1	612	-618	45
2	5	1	66	55	15
1	5	1	43-	-2	21
0	5	1	49*	-32	***
-1	5	1	117	119	6
-2	5	1	148	145	10
-3	5	1	42-	-32	21
-4	5	1	442	437	23
-5	5	1	46	38	13
-6	5	1	249	-258	20
-7	5	1	44-	16	22
-8	5	1	305	-308	19
-9	5	1	87	-92	9
-10	5	1	403	410	20
-11	5	1	192	-193	10
-12	5	1	48-	6	24
-13	5	1	49-	9	25
-14	5	1	411*	-394	***
-15	5	1	162*	213	***
-16	5	1	52-	-11	26
-17	5	1	249	244	14
-18	5	1	189	186	11
16	6	1	28*	22	***
15	6	1	37*	31	***
14	6	1	173	173	9
13	6	1	248	258	14
12	6	1	122	-116	7
11	6	1	92	97	9
10	6	1	314	-314	16
9	6	1	129	-131	7
8	6	1	191	188	13
7	6	1	83	-83	10
6	6	1	364	363	22
5	6	1	82	-81	10
4	6	1	48-	23	24
3	6	1	58	67	13
2	6	1	277	-272	19
1	6	1	426	413	31
0	6	1	41*	-29	***
-1	6	1	376	374	34
-2	6	1	399	400	21
-3	6	1	254	-246	15
-4	6	1	254	237	15
-5	6	1	576	-593	37
-6	6	1	151	-143	9
-7	6	1	200	-208	10
-8	6	1	368	-373	18
-9	6	1	101	101	8
-10	6	1	80	63	10
-11	6	1	172	173	28
-12	6	1	285	287	20
-13	6	1	108	109	8
-14	6	1	51*	-41	***
-15	6	1	93	-100	10
-16	6	1	103	-97	9
-17	6	1	124*	-124	***
-18	6	1	66*	-56	***
14	7	1	70*	80	***
13	7	1	46-	13	23
12	7	1	49-	-1	24
11	7	1	41	31	21
10	7	1	183	-181	14
9	7	1	154	-160	8
8	7	1	89	-84	25.
7	7	1	127	-119	7
6	7	1	110	109	8
5	7	1	172	177	8
4	7	1	50-	-25	25
3	7	1	319	324	26
2	7	1	50-	-15	25
1	7	1	136	131	12
0	7	1	85	80	10
-1	7	1	481	-478	27
-2	7	1	166	-171	12
-3	7	1	452	-442	23
-4	7	1	49-	-19	24
-5	7	1	49	49	16
-6	7	1	344	339	33
-7	7	1	313	323	21
-8	7	1	78	-70	10
-9	7	1	310	329	21
-10	7	1	344	-358	27
-11	7	1	112	-106	12
-12	7	1	144	142	12
-13	7	1	263	-270	27
-14	7	1	328	327	17
-15	7	1	47	-49	18
-16	7	1	63	-64	13
-17	7	1	138	131	10
-18	7	1	145*	-150	***
13	8	1	143*	-173	***
12	8	1	80*	67	***
11	8	1	46-	20	23
10	8	1	102	98	8
9	8	1	304	313	19
8	8	1	75	-74	11
7	8	1	184	181	14
6	8	1	51-	0	26
5	8	1	241	-255	12
4	8	1	146	150	11
3	8	1	308	-304	16
2	8	1	108	-109	10
1	8	1	55	48	16
0	8	1	76	-62	12
-1	8	1	157	160	11
-2	8	1	109	105	8
-3	8	1	51-	-2	26
-4	8	1	179	-182	9
-5	8	1	92	64	9
-6	8	1	51-	-22	25
-7	8	1	164	149	8
-8	8	1	134	121	6
-9	8	1	77	-79	11
-10	8	1	134	-128	6
-11	8	1	215	-200	16
-12	8	1	107	-114	8
-13	8	1	74	-72	12
-14	8	1	96	81	10
-15	8	1	66	58	19
-16	8	1	82	80	8
-17	8	1	125*	121	***
11	9	1	60*	80	***
10	9	1	47*	-47	***
9	9	1	64*	66	***
8	9	1	120	-117	15
7	9	1	61	-64	13
6	9	1	53	45	15
5	9	1	153	-160	10
4	9	1	139	144	7
3	9	1	185	-180	9
2	9	1	59	-48	18
1	9	1	62	63	14
0	9	1	136	-133	10
-1	9	1	291	295	17
-2	9	1	102	96	9
-3	9	1	191	199	9
-4	9	1	140	137	8
-5	9	1	177	-184	9
-6	9	1	51-	-32	26
-7	9	1	274	-288	14
-8	9	1	46	-33	19
-9	9	1	81	68	11
-10	9	1	50-	-23	25
-11	9	1	282	298	21
-12	9	1	49-	-23	24
-13	9	1	212	211	25
-14	9	1	38	28	17
-15	9	1	111*	-111	***
-16	9	1	17*	21	***
3	10	1	87*	131	***
2	10	1	135	145	6
1	10	1	112	-110	9
0	10	1	190	-204	10
-1	10	1	64	-51	15
-2	10	1	172	-186	9
-3	10	1	50-	-22	25
-4	10	1	104	107	8
-5	10	1	127	-134	8
-6	10	1	127	126	6
-7	10	1	49-	23	25
-8	10	1	79	-79	12
-9	10	1	224	210	34
-10	10	1	85	-77	9
-11	10	1	41	36	16
-12	10	1	37*	-4	***
-13	10	1	116*	-117	***
16	-10	2	76*	-91	***
15	-10	2	35*	3	***
14	-10	2	46-	32	23
13	-10	2	48-	-27	24
12	-10	2	145	163	10
11	-10	2	92	82	15
10	-10	2	51-	-10	26
9	-10	2	72	-75	12
8	-10	2	184	-188	16
7	-10	2	254	-263	21
6	-10	2	51	-57	18
5	-10	2	52-	-22	26
4	-10	2	122	120	8
3	-10	2	237	220	14
2	-10	2	53-	18	26
1	-10	2	139	131	17
0	-10	2	69	-61	13
-1	-10	2	53-	-6	26
-2	-10	2	84	-78	13
-3	-10	2	113*	-117	***
17	-9	2	265*	225	***
16	-9	2	81*	-81	***
15	-9	2	54	46	15
14	-9	2	85	-89	10
13	-9	2	248	-252	14
12	-9	2	123	122	15
11	-9	2	122	-112	15
10	-9	2	106	95	10
9	-9	2	115	111	8
8	-9	2	67	-64	13
7	-9	2	197	197	16
6	-9	2	52-	0	26
5	-9	2	145	142	12
4	-9	2	61	60	15
3	-9	2	77	-65	12
2	-9	2	52-	17	26
1	-9	2	213	-208	13
0	-9	2	52-	50	26
-1	-9	2	117	-120	12
-2	-9	2	53-	-7	26
-3	-9	2	79	76	12
-4	-9	2	138	-142	13
-5	-9	2	53-	14	26
-6	-9	2	52-	-17	26
-7	-9	2	52-	7	26
-8	-9	2	147	140	7
-9	-9	2	102	93	10
-10	-9	2	50-	-8	25
-11	-9	2	49-	-39	24
-12	-9	2	111	-107	16
-13	-9	2	133*	-134	***
17	-8	2	92	-96	22
16	-8	2	51-	-38	25
15	-8	2	51-	29	26
14	-8	2	52-	-20	26
13	-8	2	55	-47	16
12	-8	2	52-	34	26
11	-8	2	124	-122	7
10	-8	2	98	91	11
9	-8	2	155	144	17
8	-8	2	106	-105	8
7	-8	2	361	349	30
6	-8	2	184	-185	9
5	-8	2	52	61	16
4	-8	2	174	180	17
3	-8	2	429	-437	39
2	-8	2	59	26	14
1	-8	2	283	-294	24
0	-8	2	197	-191	12
-1	-8	2	265	268	26
-2	-8	2	135	137	10
-3	-8	2	339	349	18
-4	-8	2	157	149	20
-5	-8	2	52-	-6	26
-6	-8	2	99	-94	13
-7	-8	2	270	-274	20
-8	-8	2	52-	11	26
-9	-8	2	181	-168	12
-10	-8	2	187	177	19
-11	-8	2	99	91	9
-12	-8	2	51-	-21	25
-13	-8	2	181	173	16
-14	-8	2	108	-108	8
-15	-8	2	85*	75	***
17	-7	2	139	-137	14
16	-7	2	52-	-18	26
15	-7	2	154	159	9
14	-7	2	109	110	8
13	-7	2	351	315	32
12	-7	2	47	-38	18
11	-7	2	123	119	8
10	-7	2	93	-93	9
9	-7	2	267	-237	36
8	-7	2	48-	31	24
7	-7	2	205	-187	13
6	-7	2	244	-238	17
5	-7	2	57	52	16
4	-7	2	93	-93	16
3	-7	2	117	115	11
2	-7	2	409	404	22
1	-7	2	134	131	7
0	-7	2	49	16	15
-1	-7	2	64	-69	12
-2	-7	2	309	-305	19
-3	-7	2	131	-136	12
-4	-7	2	80	-71	10
-5	-7	2	118	-120	17
-6	-7	2	81	66	10
-7	-7	2	102	-105	10
-8	-7	2	64	65	13
-9	-7	2	51-	4	26
-10	-7	2	52-	-24	26
-11	-7	2	99	104	11
-12	-7	2	80	-89	11
-13	-7	2	142	140	13
-14	-7	2	51-	2	26
-15	-7	2	49-	0	25
-16	-7	2	89	92	8
-17	-7	2	143*	-133	***
17	-6	2	139	141	13
16	-6	2	52-	3	26
15	-6	2	207	206	10
14	-6	2	140	-128	11
13	-6	2	133	-125	11
12	-6	2	233	-245	15
11	-6	2	339	-339	27
10	-6	2	160	153	14
9	-6	2	131	-124	12
8	-6	2	492	508	42
7	-6	2	45-	14	22
6	-6	2	297	-298	15
5	-6	2	267	285	19
4	-6	2	547	-554	29
3	-6	2	353	373	35
2	-6	2	329	327	17
1	-6	2	79	65	20
0	-6	2	460	473	23
-1	-6	2	322	-311	19
-2	-6	2	186	-167	12
-3	-6	2	206	-205	13
-4	-6	2	200	-204	21
-5	-6	2	268	258	13
-6	-6	2	193	185	10
-7	-6	2	270	273	14
-8	-6	2	73	77	13
-9	-6	2	119*	112	***
-10	-6	2	50-	-18	25
-11	-6	2	101	-100	12
-12	-6	2	51-	-21	26
-13	-6	2	223	-220	18
-14	-6	2	108	-108	8
-15	-6	2	52-	-1	26
-16	-6	2	51-	-22	25
-17	-6	2	112	110	8
-18	-6	2	94*	83	***
18	-5	2	126	143	15
17	-5	2	52-	-26	26
16	-5	2	69	-60	13
15	-5	2	50-	3	25
14	-5	2	155	-151	15
13	-5	2	138	-133	14
12	-5	2	157	169	28
11	-5	2	157	-163	15
10	-5	2	38*	-39	***
9	-5	2	172	163	13
8	-5	2	42-	-25	21
7	-5	2	285	293	22
6	-5	2	228	219	13
5	-5	2	172	-169	9
4	-5	2	277	-293	27
3	-5	2	444	-451	28
2	-5	2	364	-354	19
1	-5	2	376	-363	26
0	-5	2	387	381	20
-1	-5	2	326	-327	16
-2	-5	2	654	627	64
-3	-5	2	426	423	22
-4	-5	2	236	-225	13
-5	-5	2	756	761	71
-6	-5	2	487	-493	26
-7	-5	2	116	-102	11
-8	-5	2	62	-60	17
-9	-5	2	514	-519	28
-10	-5	2	48-	37	24
-11	-5	2	49	-46	16
-12	-5	2	97	95	10
-13	-5	2	222	228	17
-14	-5	2	51-	-26	26
-15	-5	2	52	43	17
-16	-5	2	126	-126	7
-17	-5	2	51	3	17
-18	-5	2	49-	51	25
17	-4	2	345	-333	19
16	-4	2	51-	29	25
15	-4	2	168	-170	9
14	-4	2	98	-97	8
13	-4	2	549	541	28
12	-4	2	142	148	7
11	-4	2	511	522	26
10	-4	2	111	108	6
9	-4	2	352	-336	27
8	-4	2	194	-205	13
7	-4	2	707	-727	66
6	-4	2	256	262	17
5	-4	2	43	28	11
4	-4	2	614	624	61
3	-4	2	304	292	23
2	-4	2	39	-24	9
1	-4	2	284	283	24
0	-4	2	226	-219	13
-1	-4	2	137	135	9
-2	-4	2	103	95	9
-3	-4	2	207	-207	11
-4	-4	2	36-	-19	18
-5	-4	2	90	109	5
-6	-4	2	72	-66	14
-7	-4	2	127	-117	11
-8	-4	2	38*	-42	***
-9	-4	2	267	-272	14
-10	-4	2	45-	-11	22
-11	-4	2	75*	72	***
-12	-4	2	88	78	26
-13	-4	2	215	212	17
-14	-4	2	50-	10	25
-15	-4	2	77	66	17
-16	-4	2	130	-137	14
-17	-4	2	129	-131	10
-18	-4	2	75	-77	12
18	-3	2	186	192	24
17	-3	2	51-	16	26
16	-3	2	105	108	8
15	-3	2	84	-87	9
14	-3	2	358	-356	20
13	-3	2	196	200	15
12	-3	2	201	-193	12
11	-3	2	195	182	12
10	-3	2	39-	32	20
9	-3	2	437	-441	32
8	-3	2	123	123	10
7	-3	2	315	-322	16
6	-3	2	344	332	20
5	-3	2	523	509	68
4	-3	2	41	-41	6
3	-3	2	266	300	13
2	-3	2	412	-416	54
1	-3	2	74*	-69	***
0	-3	2	394*	-399	***
-1	-3	2	84*	-101	***
-2	-3	2	297	315	15
-3	-3	2	982	-1112	182
-4	-3	2	114	119	9
-5	-3	2	703	-739	69
-6	-3	2	267	-259	18
-7	-3	2	935	996	118
-8	-3	2	133	139	8
-9	-3	2	788	828	75
-10	-3	2	165	166	14
-11	-3	2	369	-360	19
-12	-3	2	45-	10	23
-13	-3	2	368	-361	18
-14	-3	2	79	-76	12
-15	-3	2	73	71	20
-16	-3	2	71	60	17
-17	-3	2	63	72	14
-18	-3	2	134	137	13
18	-2	2	208	-207	17
17	-2	2	182	186	10
16	-2	2	99	90	12
15	-2	2	48-	52	24
14	-2	2	287	286	16
13	-2	2	447	-450	28
12	-2	2	228	-229	15
11	-2	2	106	-108	6
10	-2	2	280	-260	28
9	-2	2	602	609	41
8	-2	2	684	666	68
7	-2	2	44*	71	***
6	-2	2	668	684	85
5	-2	2	224	203	24
4	-2	2	873*	-970	***
3	-2	2	99*	104	***
-3	-2	2	558*	633	***
-4	-2	2	175*	-164	***
-5	-2	2	59	56	16
-6	-2	2	307	-333	19
-7	-2	2	177	-191	12
-8	-2	2	228	-242	14
-9	-2	2	84	87	5
-10	-2	2	95	96	19
-11	-2	2	198	-207	17
-12	-2	2	271	263	18
-13	-2	2	427	-426	22
-14	-2	2	198	197	13
-15	-2	2	87	85	9
-16	-2	2	68	-73	24
-17	-2	2	240	250	22
-18	-2	2	162	-165	9
18	-1	2	217	-211	19
17	-1	2	253	-254	15
16	-1	2	187	193	10
15	-1	2	93	-95	8
14	-1	2	390	383	20
13	-1	2	43-	-8	22
12	-1	2	95	89	15
11	-1	2	81	78	13
10	-1	2	379	-358	36
9	-1	2	378	372	21

TABLE 5-4 (Continued)

H	K	L	F0	FC	σ
8	-1	2	461	-465	26
7	-1	2	425	-433	21
6	-1	2	316	-320	24
5	-1	2	921X	-1016	170
4	-1	2	234•	209	•••
-5	-1	2	91•	-91	•••
-6	-1	2	142	157	11
-7	-1	2	356	-366	20
-8	-1	2	227	-237	19
-9	-1	2	105	-105	9
-10	-1	2	172	-187	21
-11	-1	2	201	202	15
-12	-1	2	217	219	13
-13	-1	2	180	173	12
-14	-1	2	258	252	16
-15	-1	2	117	109	10
-16	-1	2	117•	-105	•••
-17	-1	2	51-	-36	25
-18	-1	2	184	-195	15
18	0	2	119•	115	•••
17	0	2	76•	56	•••
16	0	2	71	78	12
15	0	2	111	113	10
14	0	2	46	-31	15
13	0	2	48	-42	13
12	0	2	80•	-81	•••
11	0	2	161	-168	8
10	0	2	61	66	9
9	0	2	245	241	12
8	0	2	158	-152	14
7	0	2	391	-386	24
6	0	2	22•	-17	•••
5	0	2	1098•	-1241	•••
-5	0	2	192•	188	•••
-6	0	2	300	314	16
-7	0	2	350	375	18
-8	0	2	37•	-44	•••
-9	0	2	83•	-52	•••
-10	0	2	84•	-70	•••
-11	0	2	232	235	12
-12	0	2	436	-446	30
-13	0	2	94	-96	6
-14	0	2	115	-116	7
-15	0	2	397	-398	20
-16	0	2	275	262	14
-17	0	2	72	-65	12
-18	0	2	58	68	15
-19	0	2	260	255	25
17	1	2	249	247	32
16	1	2	77	-95	13
15	1	2	281	-273	28
14	1	2	57	-56	13
13	1	2	197	-198	10
12	1	2	43-	-21	21
11	1	2	139	-147	10
10	1	2	109	113	6
9	1	2	90	-81	20
8	1	2	326	334	16
7	1	2	819	847	104
6	1	2	29•	10	•••
5	1	2	780•	809	•••
4	1	2	422•	-413	•••
-5	1	2	377•	-475	•••
-6	1	2	215•	280	•••
-7	1	2	69•	-85	•••
-8	1	2	318•	-433	•••
-9	1	2	118•	150	•••
-10	1	2	219•	-252	•••
-11	1	2	152•	165	•••
-12	1	2	127•	105	•••
-13	1	2	243•	-238	•••
-14	1	2	44-	0	22
-15	1	2	286	-280	15
-16	1	2	62	-61	12
-17	1	2	235	229	18
-18	1	2	62	71	14
-19	1	2	283	284	19
17	2	2	111•	-112	•••
16	2	2	236	-240	12
15	2	2	115	-108	7
14	2	2	160	155	15
13	2	2	177	177	16
12	2	2	471	534	31
11	2	2	137	138	11
10	2	2	88•	-81	•••
9	2	2	86•	-82	•••
8	2	2	875	-903	82
7	2	2	478	488	25
6	2	2	62•	29	•••
5	2	2	393	391	23
4	2	2	442	456	36
3	2	2	1041•	-1242	•••
2	2	2	216•	-182	•••
-4	2	2	356•	-381	•••
-5	2	2	364•	-363	•••
-6	2	2	113	123	12
-7	2	2	413•	-471	•••
-8	2	2	55•	37	•••
-9	2	2	453•	-465	•••
-10	2	2	83•	71	•••
-11	2	2	40	36	12
-12	2	2	253	258	32
-13	2	2	375	421	24
-14	2	2	186	192	14
-15	2	2	213	217	17
-16	2	2	147	-146	16
-17	2	2	163•	-161	•••
-18	2	2	44•	-70	•••
-19	2	2	142•	-145	•••
17	3	2	47•	62	•••
16	3	2	42•	-43	•••
15	3	2	60	58	14
14	3	2	42•	-14	•••
13	3	2	48-	11	24
12	3	2	190	196	17
11	3	2	97•	94	•••
10	3	2	105	-98	12
9	3	2	106	104	5
8	3	2	430	-414	27
7	3	2	178	-172	24
6	3	2	142	145	14
5	3	2	93	-99	8
4	3	2	367	362	19
3	3	2	727	722	74
2	3	2	116	-97	8
1	3	2	287	277	28
0	3	2	351	339	37
-1	3	2	186	-176	10
-2	3	2	285	-279	31
-3	3	2	147	-158	11
-4	3	2	1035X	-1226	191
-5	3	2	531	-544	51
-6	3	2	492	504	47
-7	3	2	160	-146	17
-8	3	2	1207X	1368	221
-9	3	2	156•	153	•••
-10	3	2	175•	-206	•••
-11	3	2	333•	339	•••
-12	3	2	756	-771	76
-13	3	2	148	151	15
-14	3	2	52	59	13
-15	3	2	169	-174	17
-16	3	2	260	255	21
-17	3	2	149	-158	10
-18	3	2	51-	-26	26
-19	3	2	101•	-94	•••
17	4	2	105	104	10
16	4	2	141	141	22
15	4	2	255	247	16
14	4	2	302	-299	17
13	4	2	115	-114	18
12	4	2	407	-416	25
11	4	2	414	-413	25
10	4	2	359	360	19
9	4	2	88	-96	9
8	4	2	383	377	19
7	4	2	331	326	18
6	4	2	270	-260	15
5	4	2	149	155	10
4	4	2	409	-395	29
3	4	2	320	-321	19
2	4	2	123	-124	13
1	4	2	368	-375	23
0	4	2	268	270	19
-1	4	2	43	-33	10
-2	4	2	166	151	9
-3	4	2	214	213	11
-4	4	2	77	76	7
-5	4	2	90	91	9
-6	4	2	137	-132	11
-7	4	2	334	352	17
-8	4	2	68•	-54	•••
-9	4	2	325	332	16
-10	4	2	41	31	13
-11	4	2	154	-158	13
-12	4	2	251•	-230	•••
-13	4	2	122•	-130	•••
-14	4	2	46-	-4	23
-15	4	2	48-	22	24
-16	4	2	180	183	14
-17	4	2	51-	-25	25
-18	4	2	124	123	15
17	5	2	50-	-26	25
16	5	2	70	-64	13
15	5	2	142	131	16
14	5	2	53	54	17
13	5	2	51-	3	26
12	5	2	97	94	10
11	5	2	137	-139	11
10	5	2	228	224	24
9	5	2	100	90	15
8	5	2	62	56	12
7	5	2	47•	50	•••
6	5	2	472	-471	35
5	5	2	97	-106	10
4	5	2	56	-54	11
3	5	2	195	198	15
2	5	2	423	406	31
1	5	2	362	-355	23
0	5	2	106	100	17
-1	5	2	496	-468	40
-2	5	2	303	294	16
-3	5	2	679	659	73
-4	5	2	305	308	20
-5	5	2	637	619	64
-6	5	2	545	-553	49
-7	5	2	250	-258	14
-8	5	2	596	-597	63
-9	5	2	648	-638	65
-10	5	2	321	332	19
-11	5	2	142	-148	12
-12	5	2	227	230	12
-13	5	2	355	357	21
-14	5	2	249•	-255	•••
-15	5	2	193•	234	•••
-16	5	2	107	-103	10
-17	5	2	89•	-89	•••
-18	5	2	52-	-20	26
17	6	2	81•	-86	•••
16	6	2	49-	-10	24
15	6	2	95	-95	9
14	6	2	58	55	15
13	6	2	112	109	16
12	6	2	44•	-62	•••
11	6	2	280	284	28
10	6	2	143	-136	15
9	6	2	112	-106	11
8	6	2	49-	-5	25
7	6	2	459	-448	31
6	6	2	48-	-40	24
5	6	2	56	-53	13
4	6	2	46-	-12	23
3	6	2	399	386	31
2	6	2	550	536	49
1	6	2	71	68	9
0	6	2	385	372	32
-1	6	2	374	-365	20
-2	6	2	577	-573	44
-3	6	2	110	117	7
-4	6	2	279	-274	32
-5	6	2	173	169	11
-6	6	2	285	272	23
-7	6	2	174	-171	13
-8	6	2	137	134	12
-9	6	2	73•	66	•••
-10	6	2	123	126	20
-11	6	2	120	120	12
-12	6	2	48-	6	24
-13	6	2	49-	-29	24
-14	6	2	183	-182	9
-15	6	2	49	46	18
-16	6	2	139•	-129	•••
-17	6	2	48•	71	•••
-18	6	2	50•	79	•••
17	7	2	11•	5	•••
16	7	2	34•	17	•••
15	7	2	47-	19	23
14	7	2	157	-143	10
13	7	2	97	93	9
12	7	2	130	-138	14
11	7	2	68	-76	13
10	7	2	52-	3	26
9	7	2	123•	-125	•••
8	7	2	318	306	17
7	7	2	126	125	10
6	7	2	299	290	23
5	7	2	59	64	14
4	7	2	151	-147	19
3	7	2	46•	-39	•••
2	7	2	478	-459	49
1	7	2	142	139	11
0	7	2	141	-143	11
-1	7	2	44	-42	17
-2	7	2	185	183	12
-3	7	2	410	-401	22
-4	7	2	46	57	16
-5	7	2	108	-100	17
-6	7	2	44	-31	17
-7	7	2	271	274	22
-8	7	2	68•	-72	•••
-9	7	2	86	76	9
-10	7	2	80•	86	•••
-11	7	2	81•	-87	•••
-12	7	2	41•	29	•••
-13	7	2	173	-170	9
-14	7	2	168	-169	10
-15	7	2	130	-134	14
-16	7	2	54	37	17
-17	7	2	146	139	15
-18	7	2	148	189	14
15	8	2	37•	-37	•••
14	8	2	69•	37	•••
13	8	2	41•	38	•••
12	8	2	70	81	12
11	8	2	51-	28	26
10	8	2	46•	-36	•••
9	8	2	116	-108	23
8	8	2	52-	-2	26
7	8	2	83	90	18
6	8	2	204	210	18
5	8	2	161	162	14
4	8	2	130	-126	17
3	8	2	136	-141	7
2	8	2	436	-432	36
1	8	2	51-	-31	26
0	8	2	158	158	19
-1	8	2	49•	41	•••
-2	8	2	505	508	27
-3	8	2	43•	-31	•••
-4	8	2	50-	-9	25
-5	8	2	189	192	13
-6	8	2	333	-336	18
-7	8	2	208	213	16
-8	8	2	173	-169	22
-9	8	2	159	-163	13
-10	8	2	51-	20	26
-11	8	2	194	-193	18
-12	8	2	222	204	28
-13	8	2	127	123	7
-14	8	2	250	244	21
-15	8	2	52-	23	26
-16	8	2	46•	-33	•••
-17	8	2	50•	-37	•••
-18	8	2	189	-192	33
12	9	2	43•	23	•••
11	9	2	126	126	6
10	9	2	49-	-26	24
9	9	2	41•	-43	•••
8	9	2	109	-114	16
7	9	2	197	-188	14
6	9	2	138	-136	17
5	9	2	66	-64	14
4	9	2	130	127	21
3	9	2	59	40	16
2	9	2	178	175	13
1	9	2	111	101	21
0	9	2	72	-62	13
-1	9	2	154	155	13
-2	9	2	218	-219	21
-3	9	2	102	-108	13
-4	9	2	156	-164	12
-5	9	2	175	-183	14
-6	9	2	104	99	13
-7	9	2	158	146	17
-8	9	2	52•	51	•••
-9	9	2	98	95	9
-10	9	2	52-	-20	26
-11	9	2	180	-168	20
-12	9	2	131	134	10
-13	9	2	52-	7	26
-14	9	2	51	48	20
-15	9	2	169	165	22
-16	9	2	148	-144	13
-17	9	2	37•	-11	•••
-18	9	2	125•	-107	•••
2	10	2	74•	-66	•••
1	10	2	174	171	18
0	10	2	177	-179	18
-1	10	2	53-	8	26
-2	10	2	53-	18	26
-3	10	2	74	-76	12
-4	10	2	132	135	17
-5	10	2	135	-141	17
-6	10	2	82	83	11
-7	10	2	52-	6	26
-8	10	2	82•	70	•••
-9	10	2	224	241	24
-10	10	2	79•	-78	•••
-11	10	2	51-	16	26
-12	10	2	177	-176	19
-13	10	2	158	-167	15
-14	10	2	52	-46	15
-15	10	2	69•	-59	•••
-16	10	2	64•	59	•••
-17	10	2	23•	27	•••
14	-10	3	58•	52	•••
13	-10	3	35•	-5	•••
12	-10	3	129•	-129	•••
11	-10	3	49•	43	•••
10	-10	3	212	-218	17
9	-10	3	50-	-22	25
8	-10	3	51-	28	25
7	-10	3	51-	-22	25
6	-10	3	301	299	29
5	-10	3	88	-84	12
4	-10	3	70	59	15
3	-10	3	58	-46	18
2	-10	3	174	-163	18
1	-10	3	181	192	11
0	-10	3	52-	-14	26
-1	-10	3	111	112	10
-2	-10	3	48•	-44	•••
-3	-10	3	164	-167	16
16	-9	3	30•	5	•••
15	-9	3	36•	5	•••
14	-9	3	71•	-79	•••
13	-9	3	55	-52	17
12	-9	3	70•	-55	•••
11	-9	3	84	-77	12
10	-9	3	69	67	15
9	-9	3	51-	-6	26
8	-9	3	48•	43	•••
7	-9	3	117	104	19
6	-9	3	104	93	10
5	-9	3	61	57	17
4	-9	3	147	148	12
3	-9	3	49•	-46	•••
2	-9	3	192	-190	14
1	-9	3	51-	-6	26
0	-9	3	197	-195	18
-1	-9	3	51-	8	26
-2	-9	3	186	193	17
-3	-9	3	89	-80	20
-4	-9	3	293	297	21
-5	-9	3	52-	15	26
-6	-9	3	76	76	14
-7	-9	3	124	130	11
-8	-9	3	224	-227	17
-9	-9	3	50-	12	25
-10	-9	3	200	-201	13
-11	-9	3	46•	-43	•••
-12	-9	3	46•	54	•••
17	-8	3	124•	126	•••
16	-8	3	85•	-89	•••
15	-8	3	105	-105	9
14	-8	3	50	51	20
13	-8	3	186	-191	10
12	-8	3	204	203	21
11	-8	3	264	270	15
10	-8	3	182	187	10
9	-8	3	225	233	17
8	-8	3	216	-235	15
7	-8	3	255	-268	16
6	-8	3	376	-378	39
5	-8	3	231	-238	18
4	-8	3	142	140	20
3	-8	3	56	42	17
2	-8	3	310	306	39
1	-8	3	69•	-73	•••
0	-8	3	49-	-30	25
-1	-8	3	86	-92	19
-2	-8	3	86	-81	12
-3	-8	3	175	180	10
-4	-8	3	50-	-19	25
-5	-8	3	51-	22	25
-6	-8	3	78	-84	13
-7	-8	3	95	-106	11
-8	-8	3	48•	-46	•••
-9	-8	3	51-	13	26
-10	-8	3	51-	-4	26
-11	-8	3	50-	-24	25
-12	-8	3	49-	36	24
-13	-8	3	46-	-7	23
-14	-8	3	108•	103	•••
-15	-8	3	42•	51	•••
17	-7	3	113•	97	•••
16	-7	3	100	92	10
15	-7	3	51-	41	25
14	-7	3	188	187	12
13	-7	3	128	-121	9
12	-7	3	69	-66	15
11	-7	3	59	50	17
10	-7	3	181	-179	11
9	-7	3	199	211	12
8	-7	3	70	-61	16
7	-7	3	47-	-8	23
6	-7	3	79	-75	11
5	-7	3	53	-59	16
4	-7	3	231	250	15
3	-7	3	61	-52	13
2	-7	3	298	307	23
1	-7	3	92	-88	11
0	-7	3	136	-138	13
-1	-7	3	219	225	14
-2	-7	3	313	-311	45
-3	-7	3	267	248	30
-4	-7	3	70	-72	13
-5	-7	3	315	-323	20
-6	-7	3	159	162	22
-7	-7	3	307	-305	42
-8	-7	3	176	178	19
-9	-7	3	312	298	27
-10	-7	3	132	126	10
-11	-7	3	243	235	36
-12	-7	3	121	-115	18
-13	-7	3	159	-161	19
-14	-7	3	211	-206	30
-15	-7	3	113•	-105	•••
-16	-7	3	33•	1	•••
17	-6	3	50-	-31	25
16	-6	3	196	-192	22
15	-6	3	268	259	14
14	-6	3	73	-79	14
13	-6	3	49-	-14	25
12	-6	3	49-	36	24
11	-6	3	396	-394	23
10	-6	3	188	-196	15
9	-6	3	85	-85	10
8	-6	3	57	44	14
7	-6	3	345	355	22
6	-6	3	376	368	26
5	-6	3	42-	35	21
4	-6	3	94	94	7
3	-6	3	244	-244	20
2	-6	3	403	-409	24
1	-6	3	44	-62	15
0	-6	3	537	-520	40
-1	-6	3	62	-70	11
-2	-6	3	89	90	10
-3	-6	3	224	208	15
-4	-6	3	347	331	28
-5	-6	3	228	223	13
-6	-6	3	41•	38	•••
-7	-6	3	121	-107	11
-8	-6	3	44•	-21	•••
-9	-6	3	50•	-38	•••
-10	-6	3	48•	-28	•••
-11	-6	3	140	138	10
-12	-6	3	113	-113	9
-13	-6	3	49•	40	•••
-14	-6	3	51-	13	25
-15	-6	3	144	-141	9
-16	-6	3	192	186	20
-17	-6	3	94•	-84	•••
-18	-6	3	60•	73	•••
17	-5	3	119	-117	9
16	-5	3	324	-313	24
15	-5	3	48•	-34	•••
14	-5	3	63	64	15
13	-5	3	134	130	9
12	-5	3	428	387	42
11	-5	3	173	-169	26
10	-5	3	272	269	23
9	-5	3	291	-271	16
8	-5	3	120	113	9
7	-5	3	269	264	19
6	-5	3	413	-399	52
5	-5	3	344	354	22
4	-5	3	514	-525	43
3	-5	3	232	-236	29
2	-5	3	332	317	19
1	-5	3	115	113	7
0	-5	3	678	690	83
-1	-5	3	179	192	10
-2	-5	3	152	-167	10
-3	-5	3	203	-202	14
-4	-5	3	477	-496	34
-5	-5	3	228	229	22
-6	-5	3	65	70	10
-7	-5	3	96	96	9
-8	-5	3	44-	-9	22
-9	-5	3	372	-368	24
-10	-5	3	205	-205	11
-11	-5	3	124	-126	10
-12	-5	3	49-	9	24
-13	-5	3	161	155	12
-14	-5	3	174	174	15
-15	-5	3	123•	79	•••
-16	-5	3	119•	73	•••
-17	-5	3	49-	-30	24
-18	-5	3	116•	-124	•••
17	-4	3	51•	56	•••
16	-4	3	192	195	11
15	-4	3	49-	-9	24
14	-4	3	95	-93	10
13	-4	3	46-	-13	23
12	-4	3	95	-94	10
11	-4	3	126	-123	9
10	-4	3	91•	78	•••
9	-4	3	245	-241	17
8	-4	3	37-	19	18
7	-4	3	237	213	37
6	-4	3	453	-457	28
5	-4	3	104	105	11
4	-4	3	72•	-83	•••
3	-4	3	532•	-543	•••
2	-4	3	891•	1129	•••
1	-4	3	230•	240	•••
0	-4	3	520•	577	•••
-1	-4	3	515•	586	•••
-2	-4	3	609•	-641	•••
-3	-4	3	250•	-234	•••
-4	-4	3	714	-724	80
-5	-4	3	166	-164	10
-6	-4	3	35-	-8	18
-7	-4	3	248	252	24
-8	-4	3	359	348	20
-9	-4	3	80	-80	9
-10	-4	3	249	248	23
-11	-4	3	169	-173	9
-12	-4	3	115	109	19
-13	-4	3	201	200	23
-14	-4	3	254	-254	15
-15	-4	3	90	98	11
-16	-4	3	194	-198	12
-17	-4	3	97	-104	10
-18	-4	3	200	187	12
18	-3	3	203•	207	•••
17	-3	3	149	141	10
16	-3	3	100	95	10
15	-3	3	150	150	9
14	-3	3	155	-150	9
13	-3	3	96	-93	8
12	-3	3	172	-169	10
11	-3	3	96	98	12
10	-3	3	108	-106	7
9	-3	3	35•	21	•••
8	-3	3	221	207	34
7	-3	3	414	-416	28
6	-3	3	639•	665	•••
5	-3	3	449•	451	•••
-5	-3	3	313•	327	•••
-6	-3	3	176	171	11
-7	-3	3	471	-452	47
-8	-3	3	268	265	18
-9	-3	3	337	-389	23
-10	-3	3	143	-148	19
-11	-3	3	147	151	16
-12	-3	3	185	-189	18
-13	-3	3	167	167	26
-14	-3	3	52	-54	18
-15	-3	3	46	-35	21
-16	-3	3	41•	-37	•••
-17	-3	3	97	-94	13
-18	-3	3	99	102	14
-19	-3	3	86•	69	•••
18	-2	3	41•	28	•••
17	-2	3	193	-188	11
16	-2	3	133	-132	11
15	-2	3	46-	-35	24
14	-2	3	366	-365	19
13	-2	3	235	226	14
12	-2	3	164	169	21
11	-2	3	365	359	21
10	-2	3	584	575	55
9	-2	3	34•	-8	•••
8	-2	3	36-	7	18
7	-2	3	587•	-561	•••
6	-2	3	568•	-603	•••
-7	-2	3	92•	-88	•••
-8	-2	3	190	-189	21
-9	-2	3	53	45	9
-10	-2	3	79	-78	7
-11	-2	3	126	-117	15
-12	-2	3	166	167	12

TABLE 5-4 (Continued)

H	K	L	F0	FC	σ
-13	-2	3	196	-202	20
-14	-2	3	295	288	19
-15	-2	3	152	149	14
-16	-2	3	49-	2	25
-17	-2	3	137	142	13
-18	-2	3	163	-167	16
-19	-2	3	164*	-151	***
18	-1	3	41*	48	***
17	-1	3	148	-144	11
16	-1	3	153	150	11
15	-1	3	94	82	11
14	-1	3	46-	0	23
13	-1	3	52	49	15
12	-1	3	80	80	9
11	-1	3	193	-190	16
10	-1	3	181	187	12
9	-1	3	136	142	16
8	-1	3	461	-446	45
7	-1	3	20*	-10	***
-8	-1	3	325*	341	***
-9	-1	3	279	269	19
-10	-1	3	1100	1170	204
-11	-1	3	253*	-240	***
-12	-1	3	40-	-26	20
-13	-1	3	255	-251	15
-14	-1	3	493	-475	34
-15	-1	3	223	213	14
-16	-1	3	48-	-34	24
-17	-1	3	125	125	20
-18	-1	3	51-	0	25
-19	-1	3	74*	-87	***
18	0	3	43*	-47	***
17	0	3	68	-73	15
16	0	3	345	345	19
15	0	3	96	-94	16
14	0	3	347	349	24
13	0	3	44*	37	***
12	0	3	621	-628	38
11	0	3	32*	-74	***
10	0	3	936	-958	116
9	0	3	28*	24	***
8	0	3	739	733	90
7	0	3	243*	235	***
-8	0	3	198*	-197	***
-9	0	3	225	218	14
-10	0	3	253	-249	15
-11	0	3	129	131	8
-12	0	3	39-	-27	20
-13	0	3	137	-135	15
-14	0	3	192	-194	11
-15	0	3	85	-83	16
-16	0	3	135	-127	10
-17	0	3	64	57	15
-18	0	3	115	119	10
-19	0	3	41*	-17	***
17	1	3	152	-153	11
16	1	3	175	-174	13
15	1	3	122	-118	19
14	1	3	69	-54	13
13	1	3	147	148	9
12	1	3	69	-67	11
11	1	3	169	171	14
10	1	3	63	-64	9
9	1	3	129	-134	10
8	1	3	311	311	25
7	1	3	431	-427	40
6	1	3	436*	441	***
-8	1	3	944*	-1103	***
-9	1	3	24*	428	***
-10	1	3	896*	-940	***
-11	1	3	144*	-153	***
-12	1	3	468*	449	***
-13	1	3	41*	34	***
-14	1	3	565	538	55
-15	1	3	219	214	19
-16	1	3	62	-66	14
-17	1	3	77	75	13
-18	1	3	99	-103	10
-19	1	3	41*	-38	***
17	2	3	198	200	12
16	2	3	140	-148	12
15	2	3	44*	-46	***
14	2	3	62	60	15
13	2	3	156	-160	9
12	2	3	451	466	37
11	2	3	148	149	9
10	2	3	40-	15	20
9	2	3	501	504	30
8	2	3	489	-472	31
7	2	3	32-	-29	16
6	2	3	114	-107	15
5	2	3	733*	-794	***
-7	2	3	394*	446	***
-8	2	3	111*	141	***
-9	2	3	233*	-221	***
-10	2	3	100	-101	7
-11	2	3	137	136	8
-12	2	3	80	77	9
-13	2	3	75	75	9
-14	2	3	225	229	13
-15	2	3	348	-344	20
-16	2	3	82*	-99	***
-17	2	3	42*	66	***
-18	2	3	161*	-190	***
-19	2	3	194*	269	***
17	3	3	130	127	12
16	3	3	252	248	15
15	3	3	78	-77	13
14	3	3	54	45	18
13	3	3	115	-112	11
12	3	3	188	-180	11
11	3	3	45-	3	22
10	3	3	124	-121	11
9	3	3	41-	-7	20
8	3	3	378	-358	39
7	3	3	188	188	23
6	3	3	178	182	16
5	3	3	222	231	15
4	3	3	785*	850	***
3	3	3	521*	-626	***
-6	3	3	102*	97	***
-7	3	3	222*	-221	***
-8	3	3	404	412	26
-9	3	3	226	226	29
-10	3	3	356*	379	***
-11	3	3	203*	234	***
-12	3	3	169	-177	18
-13	3	3	116	-114	8
-14	3	3	124	-118	16

H	K	L	F0	FC	σ
-15	3	3	243	-240	18
-16	3	3	58*	-49	***
-17	3	3	38*	-18	***
-18	3	3	49*	53	***
-19	3	3	173	172	30
17	4	3	65*	-62	***
16	4	3	77	-75	13
15	4	3	51-	-44	25
14	4	3	49	-61	21
13	4	3	110	105	13
12	4	3	91	86	12
11	4	3	41*	35	***
10	4	3	167	170	10
9	4	3	65	-70	12
8	4	3	96	-99	9
7	4	3	94	87	8
6	4	3	64	-73	9
5	4	3	41*	34	***
4	4	3	446	425	43
3	4	3	271	-255	16
2	4	3	269	-261	15
1	4	3	371*	-365	***
0	4	3	939*	-1149	***
-1	4	3	428*	455	***
-2	4	3	32*	-6	***
-3	4	3	409*	423	***
-4	4	3	796*	897	***
-5	4	3	384*	-387	***
-6	4	3	142	152	13
-7	4	3	41	-14	10
-8	4	3	300	-304	17
-9	4	3	90*	90	***
-10	4	3	279	-284	36
-11	4	3	91	-75	11
-12	4	3	270*	-270	***
-13	4	3	81*	116	***
-14	4	3	110*	112	***
-15	4	3	95	95	14
-16	4	3	373	378	23
-17	4	3	228	-223	14
-18	4	3	70	72	15
-19	4	3	173*	-176	***
17	5	3	100*	87	***
16	5	3	154	-156	10
15	5	3	61	52	17
14	5	3	51-	22	25
13	5	3	143	-144	10
12	5	3	130	128	10
11	5	3	49-	-17	25
10	5	3	216	213	16
9	5	3	60*	59	***
8	5	3	46-	30	23
7	5	3	243	-245	13
6	5	3	307	-296	26
5	5	3	129	-132	8
4	5	3	327	-314	21
3	5	3	374	367	23
2	5	3	377	371	23
1	5	3	177	173	19
0	5	3	756	781	76
-1	5	3	50	-54	9
-2	5	3	168	-164	17
-3	5	3	331	333	19
-4	5	3	565	-581	54
-5	5	3	51	-43	10
-6	5	3	119	-122	7
-7	5	3	253	-261	26
-8	5	3	195	198	12
-9	5	3	380	359	29
-10	5	3	42-	10	21
-11	5	3	187	194	20
-12	5	3	146	-145	9
-13	5	3	279	-283	15
-14	5	3	217*	205	***
-15	5	3	40*	-56	***
-16	5	3	158*	144	***
-17	5	3	90	87	13
-18	5	3	194	-185	20
17	6	3	38*	68	***
16	6	3	78*	86	***
15	6	3	146*	151	***
14	6	3	61*	66	***
13	6	3	86	-90	12
12	6	3	51-	-48	26
11	6	3	402	-411	34
10	6	3	100	-102	13
9	6	3	50-	18	25
8	6	3	49-	-13	24
7	6	3	438	433	24
6	6	3	66	-57	13
5	6	3	46-	15	23
4	6	3	45-	-19	22
3	6	3	171	-165	13
2	6	3	270	247	34
1	6	3	117	-123	11
0	6	3	282	282	18
-1	6	3	100	-105	8
-2	6	3	339	-323	26
-3	6	3	100	110	9
-4	6	3	528	-529	52
-5	6	3	75	72	11
-6	6	3	81	87	10
-7	6	3	172	-169	11
-8	6	3	295	303	16
-9	6	3	169	-174	10
-10	6	3	178	184	10
-11	6	3	127	127	13
-12	6	3	48*	-43	***
-13	6	3	49*	56	***
-14	6	3	261	-272	17
-15	6	3	66	-66	15
-16	6	3	162	-155	10
-17	6	3	88*	77	***
-18	6	3	112*	116	***
15	7	3	30*	32	***
14	7	3	37*	-58	***
13	7	3	62	72	15
12	7	3	50-	6	25
11	7	3	51-	-17	25
10	7	3	51-	3	26
9	7	3	51-	8	26
8	7	3	51-	15	25
7	7	3	138	139	10
6	7	3	172	178	10
5	7	3	49-	0	25
4	7	3	111	103	8
3	7	3	60	-63	15
2	7	3	136	-131	14
1	7	3	58	53	15

H	K	L	F0	FC	σ
0	7	3	190	-186	26
-1	7	3	166	-170	11
-2	7	3	74	-79	15
-3	7	3	73	71	11
-4	7	3	250	260	14
-5	7	3	452	451	33
-6	7	3	205	212	12
-7	7	3	129	-131	13
-8	7	3	60	-64	15
-9	7	3	635	-628	54
-10	7	3	63	-59	15
-11	7	3	49-	-33	24
-12	7	3	115*	-118	***
-13	7	3	439	427	27
-14	7	3	73	-72	14
-15	7	3	51-	-2	25
-16	7	3	122	122	14
-17	7	3	187	-178	22
-18	7	3	136	137	23
13	8	3	126*	134	***
12	8	3	37*	51	***
11	8	3	139	144	10
10	8	3	165	175	10
9	8	3	163	-176	10
8	8	3	103	101	12
7	8	3	203	-202	26
6	8	3	275	-273	19
5	8	3	99	104	11
4	8	3	343	-345	19
3	8	3	147	148	15
2	8	3	41*	31	***
1	8	3	50-	15	25
0	8	3	243	251	14
-1	8	3	49-	27	25
-2	8	3	44*	44	***
-3	8	3	148	-151	13
-4	8	3	60	-65	16
-5	8	3	171	-169	20
-6	8	3	59*	42	***
-7	8	3	143	151	18
-8	8	3	90	-96	11
-9	8	3	56*	48	***
-10	8	3	50-	3	25
-11	8	3	92	-98	11
-12	8	3	187	187	16
-13	8	3	62	69	17
-14	8	3	59	48	18
-15	8	3	70	74	15
-16	8	3	49-	-12	24
-17	8	3	47-	-38	23
-18	8	3	44*	19	***
12	9	3	11*	-19	***
11	9	3	32*	-30	***
10	9	3	36*	-21	***
9	9	3	52	-60	17
8	9	3	49-	-12	25
7	9	3	41*	44	***
6	9	3	51-	17	26
5	9	3	176	182	12
4	9	3	50*	-51	***
3	9	3	52-	18	26
2	9	3	52-	-16	26
1	9	3	125	-130	11
0	9	3	164	168	10
-1	9	3	64	-66	17
-2	9	3	92	92	12
-3	9	3	51-	-4	26
-4	9	3	198	-208	11
-5	9	3	44*	-37	***
-6	9	3	248	-256	16
-7	9	3	129	134	10
-8	9	3	74	70	14
-9	9	3	180	175	11
-10	9	3	281	280	16
-11	9	3	140	-146	9
-12	9	3	95	94	11
-13	9	3	161	-156	10
-14	9	3	179	-178	22
-15	9	3	47-	23	23
-16	9	3	199*	-199	***
-17	9	3	51*	45	***
2	10	3	183*	-196	***
1	10	3	133	-135	10
0	10	3	139	-135	16
-1	10	3	73	-74	15
-2	10	3	147	154	11
-3	10	3	155*	156	***
-4	10	3	58	62	18
-5	10	3	135	138	9
-6	10	3	51-	22	26
-7	10	3	51-	-35	26
-8	10	3	85	85	12
-9	10	3	88	-91	12
-10	10	3	53*	-46	***
-11	10	3	47*	-44	***
-12	10	3	109	-114	10
-13	10	3	49*	39	***
-14	10	3	34*	10	***
-15	10	3	108*	113	***
0	0	-10	27*	-22	***
0	0	-9	194	214	12
0	0	-8	164	-173	8
0	0	-7	91	-82	10
0	0	-6	63	-45	9
0	0	-5	115	110	7
0	0	-4	75	-85	13
0	0	-3	219	209	12
0	0	-2	907	-905	165
0	0	-1	34*	23	***
0	-1	-10	98*	-98	***
0	-1	-9	43-	-34	22
0	-1	-8	156	-166	10
0	-1	-7	185	-190	13
0	-1	-6	77	78	7
0	-1	-5	78	-78	5
0	-1	-4	325	341	18
0	-1	-3	313	321	19
0	-1	-2	24-	9	12
0	-1	-1	344*	338	***
0	-1	0	86*	-90	***
0	-1	1	263*	283	***
0	-1	2	596	-628	62
0	-1	3	267	-246	25
0	-1	4	45	-36	8
0	-1	5	36-	15	18
0	-1	6	721	-758	71
0	-1	7	161	-173	11
0	-1	8	472	469	24
0	-1	9	171	176	17

H	K	L	F0	FC	σ
0	-1	10	147*	142	***
0	-2	-10	115*	131	***
0	-2	-9	40	-39	15
0	-2	-8	66	-55	10
0	-2	-7	225	-230	16
0	-2	-6	40	-39	13
0	-2	-5	418	-410	22
0	-2	-4	264	265	21
0	-2	-3	792	841	81
0	-2	-2	218	215	22
0	-2	-1	831X	927	136
0	-2	0	1023X	-1320	181
0	-2	1	940X	-1095	187
0	-2	2	369	356	21
0	-2	3	205	-202	11
0	-2	4	254	255	30
0	-2	5	435	-439	31
0	-2	6	105	101	6
0	-2	7	38	28	16
0	-2	8	183	187	12
0	-2	9	43-	-23	22
0	-2	10	108*	-120	***
0	-3	-9	99	96	6
0	-3	-8	143	-144	7
0	-3	-7	43	-13	14
0	-3	-6	141	139	7
0	-3	-5	879	931	86
0	-3	-4	451	-448	33
0	-3	-3	889X	-959	88
0	-3	-2	333	339	19
0	-3	-1	178	164	16
0	-3	0	312*	-297	***
0	-3	1	63	8	5
0	-3	2	416	-399	21
0	-3	3	409	-404	24
0	-3	4	136	156	10
0	-3	5	64	49	12
0	-3	6	140	121	16
0	-3	7	526	524	33
0	-3	8	127	-120	10
0	-3	9	181	-193	9
0	-3	10	113*	-156	***
0	-4	-9	82*	-75	***
0	-4	-8	65*	-60	***
0	-4	-7	43-	5	22
0	-4	-6	240	225	15
0	-4	-5	388	383	20
0	-4	-4	181*	161	***
0	-4	-3	1065	-1149	175
0	-4	-2	265	270	16
0	-4	-1	45	-41	9
0	-4	0	127	-118	13
0	-4	1	35-	-21	18
0	-4	2	249	-219	26
0	-4	3	597	577	45
0	-4	4	96	-100	10
0	-4	5	82	-87	9
0	-4	6	209	-207	13
0	-4	7	61	-70	10
0	-4	8	137	135	21
0	-4	9	39-	2	20
0	-5	-8	170	183	9
0	-5	-7	43-	3	21
0	-5	-6	43-	2	22
0	-5	-5	511	-496	35
0	-5	-4	387	-385	20
0	-5	-3	786	781	68
0	-5	-2	107	100	10
0	-5	-1	47	-32	15
0	-5	0	342	-336	17
0	-5	1	137	-144	14
0	-5	2	405	381	21
0	-5	3	700	690	63
0	-5	4	108	101	7
0	-5	5	232	-226	12
0	-5	6	145	134	8
0	-5	7	132	-133	9
0	-5	8	41-	-14	21
0	-5	9	38*	22	***
0	-6	-8	46*	27	***
0	-6	-7	128	128	13
0	-6	-6	113*	-77	***
0	-6	-5	83	-82	7
0	-6	-4	294	-300	27
0	-6	-3	282	282	18
0	-6	-2	383	372	20
0	-6	-1	43	-29	13
0	-6	0	160	161	17
0	-6	1	98	72	9
0	-6	2	464	473	24
0	-6	3	521	-520	56
0	-6	4	334	-343	18
0	-6	5	35*	-23	***
0	-6	6	145	149	8
0	-6	7	267	272	15
0	-6	8	226	-229	16
0	-7	-7	72*	62	***
0	-7	-6	134	138	14
0	-7	-5	77	-82	8
0	-7	-4	188	194	13
0	-7	-3	194	-186	22
0	-7	-2	137	-143	10
0	-7	-1	85	80	11
0	-7	0	93	83	10
0	-7	1	119	117	6
0	-7	2	43-	16	21
0	-7	3	140	-138	13
0	-7	4	320	-327	19
0	-7	5	108	96	8
0	-7	6	41-	-29	21
0	-7	7	37-	-4	18
0	-8	-6	23*	-14	***
0	-8	-5	65	-63	9
0	-8	-4	120	122	6
0	-8	-3	251	251	13
0	-8	-2	151	158	8
0	-8	-1	68	-62	13
0	-8	0	407	-390	27
0	-8	1	66	67	11
0	-8	2	190	-191	19
0	-8	3	42-	-30	21
0	-8	4	219	228	21
0	-8	5	52	-48	10
0	-8	6	33*	-32	***
0	-9	-4	55*	57	***
0	-9	-3	172	168	9
0	-9	-2	74*	-62	***
0	-9	-1	136	-133	7
0	-9	0	69*	11	***

H	K	L	F0	FC	σ
0	-9	1	50	-39	11
0	-9	2	47	50	11
0	-9	3	197	-195	15
0	-9	4	53	-58	8
0	-9	5	114*	121	***
0	-10	-2	133*	-179	***
0	-10	-1	189*	-204	***
0	-10	0	226*	223	***
0	-10	1	96*	103	***
0	-10	2	52*	-61	***
1	-10	-1	59	-51	10
1	-10	0	56	-59	11
1	-10	1	179	-186	10
1	-10	2	129	131	23
1	-10	3	178	192	11
1	-10	4	114*	-120	***
1	-10	5	82*	-86	***
1	-9	-6	148*	164	***
1	-9	-5	162	160	10
1	-9	-4	307	-312	21
1	-9	-3	72	-66	10
1	-9	-2	146	155	7
1	-9	-1	294	295	22
1	-9	0	85	93	17
1	-9	1	263	-260	16
1	-9	2	215	-208	15
1	-9	3	46-	-6	23
1	-9	4	183	196	9
1	-9	5	120	-122	8
1	-9	6	85*	94	***
1	-8	-7	270*	-259	***
1	-8	-6	44-	-26	22
1	-8	-5	37*	-50	***
1	-8	-4	105	112	7
1	-8	-3	47-	27	23
1	-8	-2	53	41	14
1	-8	-1	165	160	13
1	-8	0	87	-89	13
1	-8	1	113	120	10
1	-8	2	278	-294	14
1	-8	3	64	-73	11
1	-8	4	47-	7	23
1	-8	5	45	40	16
1	-8	6	45-	-3	22
1	-8	7	178	-177	11
1	-7	-8	32*	-3	***
1	-7	-7	84	-90	8
1	-7	-6	323	-322	16
1	-7	-5	123	122	6
1	-7	-4	224	237	11
1	-7	-3	170	-170	10
1	-7	-2	53	-42	13
1	-7	-1	459	-478	23
1	-7	0	205	198	17
1	-7	1	438	446	22
1	-7	2	129	131	8
1	-7	3	94	-88	8
1	-7	4	53	56	13
1	-7	5	110	-123	12
1	-7	6	397	-391	20
1	-7	7	105	105	7
1	-7	8	99	98	7
1	-6	-9	30*	26	***
1	-6	-8	121	117	11
1	-6	-7	140	141	7
1	-6	-6	46-	19	23
1	-6	-5	46-	-14	23
1	-6	-4	322	-322	19
1	-6	-3	104	-105	16
1	-6	-2	355	-365	18
1	-6	-1	374	374	19
1	-6	0	484	486	24
1	-6	1	126	-122	10
1	-6	2	70	65	11
1	-6	3	51*	-62	***
1	-6	4	357	353	21
1	-6	5	129	117	13
1	-6	6	174	-182	10
1	-6	7	99	-91	9
1	-6	8	46-	36	23
1	-6	9	73*	93	***
1	-5	-10	53*	79	***
1	-5	-9	61	50	10
1	-5	-8	105	116	7
1	-5	-7	67	58	11
1	-5	-6	171	170	9
1	-5	-5	235	-222	12
1	-5	-4	225	228	11
1	-5	-3	60	-54	10
1	-5	-2	465	-468	24
1	-5	-1	115	119	9
1	-5	0	183	-182	10
1	-5	1	258	-260	27
1	-5	2	368	-363	21
1	-5	3	125	113	6
1	-5	4	380	364	20
1	-5	5	478	474	40
1	-5	6	269	255	23
1	-5	7	355	-366	18
1	-5	8	86	-90	10
1	-5	9	80	-88	12
1	-5	10	69*	78	***
1	-4	-10	167*	-172	***
1	-4	-9	59	41	12
1	-4	-8	86*	71	***
1	-4	-7	46-	-22	23
1	-4	-6	120	-124	6
1	-4	-5	182	180	11
1	-4	-4	727	737	72
1	-4	-3	462	455	37
1	-4	-2	110	-33	17
1	-4	-1	1126X	-1249	200
1	-4	0	68	-63	9
1	-4	1	466	464	37
1	-4	2	290	283	25
1	-4	3	240	240	20
1	-4	4	661	-657	66
1	-4	5	252	252	23
1	-4	6	316	321	18
1	-4	7	111	116	13
1	-4	8	152	-148	12
1	-4	9	56	56	13
1	-4	10	109*	103	***
1	-3	-10	195	-201	10
1	-3	-9	231	-228	11
1	-3	-8	106	114	8
1	-3	-7	330	334	19
1	-3	-6	128	-130	6
1	-3	-5	119	-109	8

TABLE 5-4 (Continued)

H	K	L	F0	FC	σ
1	-3	-4	276	-285	30
1	-3	-3	661	692	67
1	-3	-2	176	-176	9
1	-3	-1	545	-558	55
1	-3	0	105	97	7
1	-3	1	335	-340	19
1	-3	2	93	-69	13
1	-3	3	609	-617	61
1	-3	4	344	-347	17
1	-3	5	160	-150	14
1	-3	6	379	393	19
1	-3	7	233	229	20
1	-3	8	47-	42	23
1	-3	9	230	238	12
1	-3	10	87	-93	13
1	-2	-10	102	85	10
1	-2	-9	265	-259	14
1	-2	-8	82	77	9
1	-2	-7	47	-46	14
1	-2	-6	41-	-13	20
1	-2	-5	260	-258	13
1	-2	-4	243	-258	13
1	-2	-3	369	-360	22
1	-2	-2	734	778	91
1	-2	-1	1100•	1337	•••
1	-2	0	877	-1026	175
1	-2	1	25-	-25	12
1	-2	2	719	-761	91
1	-2	3	562	-576	56
1	-2	4	394	395	24
1	-2	5	121	-134	8
1	-2	6	80	-76	7
1	-2	7	232	-216	12
1	-2	8	90	-86	8
1	-2	9	87•	-84	•••
1	-2	10	202	198	11
1	-1	-10	173	171	13
1	-1	-9	193	183	10
1	-1	-8	583	-607	29
1	-1	-7	96	-92	6
1	-1	-6	321	344	16
1	-1	-5	78	-70	7
1	-1	-4	244	237	12
1	-1	-3	339	336	23
1	-1	-2	446	447	48
1	-1	-1	385•	-547	•••
1	-1	0	8•	-209	•••
1	-1	1	333•	309	•••
1	-1	2	734	759	127
1	-1	3	467	494	39
1	-1	4	645	-681	69
1	-1	5	212	-204	11
1	-1	6	75	-55	9
1	-1	7	93	99	9
1	-1	8	95	-93	9
1	-1	9	158	-159	9
1	-1	10	190	198	13
1	0	-10	38•	53	•••
1	0	-9	156	-153	8
1	0	-8	95	-92	7
1	0	-7	378	413	19
1	0	-6	55	-45	9
1	0	-5	287	-285	17
1	0	-4	304	-315	17
1	0	-3	140	144	7
1	0	-2	95•	-102	•••
1	0	-1	9•	-190	•••
1	0	1	11•	-150	•••
1	0	2	1256•	2047	•••
1	0	3	103•	-103	•••
1	0	4	508•	-513	•••
1	0	5	46•	-49	•••
1	0	6	35•	-13	•••
1	0	7	494•	482	•••
1	0	8	46•	26	•••
1	0	9	153	-152	12
1	0	10	240	-238	15
1	1	-10	98	-100	17
1	1	-9	48-	30	24
1	1	-8	436	434	22
1	1	-7	95	-98	6
1	1	-6	314	319	16
1	1	-5	127	116	8
1	1	-4	676	-732	85
1	1	-3	164	165	8
1	1	-2	572	587	63
1	1	-1	740•	978	•••
1	1	0	237•	-328	•••
1	1	1	671•	-720	•••
1	1	2	911•	-1093	•••
1	1	3	243•	306	•••
1	1	4	538•	654	•••
1	1	5	30•	-1	•••
1	1	6	154	152	8
1	1	7	247	-239	22
1	1	8	45	40	16
1	1	9	39•	-13	•••
1	1	10	100•	-107	•••
1	2	-10	125•	130	•••
1	2	-9	187	180	18
1	2	-8	226	-217	19
1	2	-7	497	-483	26
1	2	-6	122	119	13
1	2	-5	551	570	33
1	2	-4	424	468	32
1	2	-3	940X	-1049	168
1	2	-2	255	233	14
1	2	-1	26-	17	13
1	2	0	171	165	10
1	2	1	300	-287	17
1	2	2	836	-890	119
1	2	3	792	806	81
1	2	4	306	300	31
1	2	5	165•	156	•••
1	2	6	126•	-175	•••
1	2	7	82	-82	10
1	2	8	205	210	11
1	2	9	48-	12	24
1	2	10	52	35	13
1	3	-10	53	43	13
1	3	-9	64	-68	12
1	3	-8	157	-158	9
1	3	-7	45-	-6	22
1	3	-6	304	-307	15
1	3	-5	753	804	75
1	3	-4	169	178	8
1	3	-3	575	-585	49
1	3	-2	100	-101	8
1	3	-1	66	56	5

H	K	L	F0	FC	σ
1	3	0	436	-435	27
1	3	1	50	-30	7
1	3	2	266	277	14
1	3	3	628	-636	47
1	3	4	365	-364	22
1	3	5	441	-424	25
1	3	6	215	-219	11
1	3	7	533•	530	•••
1	3	8	139•	129	•••
1	3	9	47-	-23	23
1	3	10	127•	-129	•••
1	4	-10	87•	-83	•••
1	4	-9	47-	-29	23
1	4	-8	162	161	8
1	4	-7	49	29	14
1	4	-6	93	104	7
1	4	-5	434	-424	23
1	4	-4	244	-235	14
1	4	-3	559	586	48
1	4	-2	132	135	7
1	4	-1	440	443	24
1	4	0	104	83	9
1	4	1	88	-92	6
1	4	2	368	-375	19
1	4	3	371	-365	18
1	4	4	395	381	21
1	4	5	216	-226	11
1	4	6	82	79	8
1	4	7	93	-97	19
1	4	8	47-	2	24
1	4	9	79•	94	•••
1	4	10	74•	-33	•••
1	5	-10	27•	-10	•••
1	5	-9	116	113	9
1	5	-8	147	-161	8
1	5	-7	131	-136	7
1	5	-6	178	-169	15
1	5	-5	325	-311	18
1	5	-4	602	590	40
1	5	-2	348	-327	21
1	5	-3	190	192	15
1	5	-1	398	391	21
1	5	0	585	583	39
1	5	1	41-	-2	20
1	5	2	357	-355	18
1	5	3	187	173	14
1	5	4	59	51	11
1	5	5	463	447	26
1	5	6	274	-276	15
1	5	7	482	-468	33
1	5	8	80	65	14
1	5	9	142	139	21
1	6	-9	139•	143	•••
1	6	-8	46-	0	23
1	6	-7	193	-198	13
1	6	-6	161	-150	8
1	6	-5	261	264	15
1	6	-4	45-	-6	22
1	6	-3	69	-70	9
1	6	-2	318	-311	18
1	6	-1	711	-739	67
1	6	0	787	799	79
1	6	1	424	413	23
1	6	2	90	68	7
1	6	3	121	-123	11
1	6	4	89	-84	11
1	6	5	51	-35	14
1	6	6	111•	-88	•••
1	6	7	115	112	6
1	6	8	91	-86	10
1	6	9	59•	54	•••
1	7	-8	284•	285	•••
1	7	-7	189	196	10
1	7	-6	73•	-73	•••
1	7	-5	252	-248	13
1	7	-4	247	-239	12
1	7	-3	223	225	13
1	7	-2	65•	-69	•••
1	7	-1	112•	82	•••
1	7	0	143•	-66	•••
1	7	1	138	131	10
1	7	2	151	139	8
1	7	3	61	53	12
1	7	4	55	-48	13
1	7	5	113	-107	16
1	7	6	250	250	12
1	7	7	44-	-15	22
1	7	8	101•	-85	•••
1	8	-8	88•	105	•••
1	8	-7	118	115	6
1	8	-6	44-	13	22
1	8	-5	198	-189	10
1	8	-4	43	36	17
1	8	-3	98•	-92	•••
1	8	-2	257	268	18
1	8	-1	120	-106	6
1	8	0	535	-534	30
1	8	1	50	48	15
1	8	2	47	-31	16
1	8	3	47-	15	23
1	8	4	133	125	8
1	8	5	183	176	9
1	8	6	43-	30	21
1	8	7	160•	-152	•••
1	9	-6	36•	31	•••
1	9	-5	150	143	10
1	9	-4	137	139	10
1	9	-3	45-	8	23
1	9	-2	109	-120	12
1	9	-1	210	-201	10
1	9	0	101•	39	•••
1	9	1	63	63	11
1	9	2	104	101	7
1	9	3	140	-130	14
1	9	4	172	-165	16
1	9	5	85•	84	•••
1	9	6	27•	-5	•••
1	10	-5	23•	-21	•••
1	10	-4	68•	-56	•••
1	10	-3	119	112	13
1	10	-2	41-	-6	21
1	10	-1	150	154	16
1	10	0	60•	-11	•••
1	10	1	110	-110	10
1	10	2	177	171	15
1	10	3	145•	-135	•••
1	10	4	128•	-124	•••
2	-10	-1	149	-186	27
2	-10	0	116	134	21

H	K	L	F0	FC	σ
2	-10	1	84•	89	•••
2	-10	2	48-	18	24
2	-10	3	151	-163	25
2	-10	4	66•	-46	•••
2	-10	5	81•	95	•••
2	-10	6	58•	-66	•••
2	-9	-7	40•	-57	•••
2	-9	-6	46-	44	23
2	-9	-5	70	-79	13
2	-9	-4	49-	19	24
2	-9	-3	81•	92	•••
2	-9	-2	195	-219	17
2	-9	-1	85	96	10
2	-9	0	163•	174	•••
2	-9	1	118	135	10
2	-9	2	50-	17	25
2	-9	3	188	-190	15
2	-9	4	263	-273	18
2	-9	5	67•	-84	•••
2	-9	6	272	284	16
2	-9	7	35•	-20	•••
2	-8	-8	34•	44	•••
2	-8	-7	47-	-18	23
2	-8	-6	71	-68	11
2	-8	-5	252	-249	32
2	-8	-4	134•	-143	•••
2	-8	-3	49-	44	25
2	-8	-2	475	508	37
2	-8	-1	87	105	9
2	-8	0	342•	-359	•••
2	-8	1	51•	75	•••
2	-8	2	49-	26	24
2	-8	3	292	306	15
2	-8	4	75•	-78	•••
2	-8	5	209	-208	17
2	-8	6	49-	-20	24
2	-8	7	48-	-24	24
2	-8	8	57•	-64	•••
2	-8	9	86•	-110	•••
2	-7	-9	99•	-91	•••
2	-7	-8	202	-207	17
2	-7	-7	115	122	10
2	-7	-6	77	72	10
2	-7	-5	49-	-31	24
2	-7	-4	281	-281	17
2	-7	-3	73	-79	13
2	-7	-2	170	183	20
2	-7	-1	153	-171	17
2	-7	0	73•	-71	•••
2	-7	1	300	-314	17
2	-7	2	390	404	21
2	-7	3	295	307	18
2	-7	4	48-	65	24
2	-7	5	184	-178	17
2	-7	6	124	-133	23
2	-7	7	88•	87	•••
2	-7	8	167	-173	23
2	-7	9	83•	86	•••
2	-6	-10	137•	140	•••
2	-6	-9	144	-135	10
2	-6	-8	49-	0	25
2	-6	-7	106	116	23
2	-6	-6	58	56	13
2	-6	-5	178	178	13
2	-6	-4	120	-120	7
2	-6	-3	328	-323	17
2	-6	-2	568	-573	41
2	-6	-1	393	400	23
2	-6	0	44-	27	22
2	-6	1	158	154	13
2	-6	2	318	327	22
2	-6	3	390	-409	22
2	-6	4	70•	-96	•••
2	-6	5	100	114	7
2	-6	6	173	162	13
2	-6	7	92	90	9
2	-6	8	49	-54	17
2	-6	9	125	-132	7
2	-6	10	91•	-106	•••
2	-5	-10	37•	-33	•••
2	-5	-9	286	264	17
2	-5	-8	213	208	15
2	-5	-7	79	-82	15
2	-5	-6	93	80	12
2	-5	-5	95	-84	13
2	-5	-4	335	337	30
2	-5	-3	166	-164	18
2	-5	-2	300	294	17
2	-5	-1	150	145	9
2	-5	0	134	-135	10
2	-5	1	193	-190	17
2	-5	2	347	-354	17
2	-5	3	316	317	22
2	-5	4	110	121	20
2	-5	5	103	110	12
2	-5	6	46	-48	15
2	-5	7	75	81	12
2	-5	8	270	269	17
2	-5	9	239	-252	14
2	-5	10	65•	-70	•••
2	-4	-10	48-	-8	24
2	-4	-9	160	151	15
2	-4	-8	349	-341	23
2	-4	-7	61	-44	12
2	-4	-6	123	114	6
2	-4	-5	188	188	11
2	-4	-4	48•	-13	•••
2	-4	-3	38-	-6	19
2	-4	-2	156	151	10
2	-4	-1	139	142	7
2	-4	0	143	139	8
2	-4	1	849	-927	72
2	-4	2	36-	-24	18
2	-4	3	1021	1129	139
2	-4	4	137	115	19
2	-4	5	105	-103	14
2	-4	6	415	-417	25
2	-4	7	47-	-22	23
2	-4	8	277	276	14
2	-4	9	246	251	13
2	-4	10	73•	-80	•••
2	-3	-10	50-	31	25
2	-3	-9	295	-284	25
2	-3	-8	48-	-34	24
2	-3	-7	243	-237	12
2	-3	-6	246	247	13
2	-3	-5	667	662	62
2	-3	-4	333	-339	27
2	-3	-3	367	-360	19

H	K	L	F0	FC	σ
2	-3	-2	281	-279	14
2	-3	-1	123	127	8
2	-3	0	193	194	16
2	-3	1	491	494	49
2	-3	2	436	-416	29
2	-3	3	1027X	-1113	183
2	-3	4	376	392	21
2	-3	5	342	-356	18
2	-3	6	45	-31	18
2	-3	7	45-	10	23
2	-3	8	48-	-1	24
2	-3	9	81•	86	•••
2	-3	10	41•	-47	•••
2	-2	-10	136•	-129	•••
2	-2	-9	191	192	21
2	-2	-8	354	342	18
2	-2	-7	400	-393	20
2	-2	-6	399	-394	22
2	-2	-5	357	-356	20
2	-2	-4	123	127	10
2	-2	-3	388	367	26
2	-2	-2	447	-448	43
2	-2	-1	140	-144	14
2	-2	0	586•	625	•••
2	-2	1	979•	1221	•••
2	-2	2	872X	-957	177
2	-2	3	173•	-168	•••
2	-2	4	113	120	10
2	-2	5	109	112	13
2	-2	6	314	313	16
2	-2	7	176	-169	11
2	-2	8	275	-272	19
2	-2	9	90	-88	23
2	-2	10	73•	71	•••
2	-1	-10	50-	22	25
2	-1	-9	220	220	13
2	-1	-8	101	95	10
2	-1	-7	128	125	9
2	-1	-6	849	-892	107
2	-1	-5	172	-170	13
2	-1	-4	510	556	44
2	-1	-3	434	-459	37
2	-1	-2	433	439	58
2	-1	2	752	774	163
2	-1	3	76	-76	5
2	-1	4	318	317	17
2	-1	5	413	428	21
2	-1	6	818	-850	102
2	-1	7	209	-214	27
2	-1	8	134	133	13
2	-1	9	105	108	8
2	-1	10	61•	55	•••
2	0	-10	92	81	15
2	0	-9	126	-118	11
2	0	-8	46-	0	23
2	0	-7	362	368	18
2	0	-6	344	343	19
2	0	-5	347	353	18
2	0	-4	432	-458	28
2	0	-3	441	-452	36
2	0	-2	852•	-1013	•••
2	0	2	462•	468	•••
2	0	3	110•	101	•••
2	0	4	279•	287	•••
2	0	5	123•	143	•••
2	0	6	32•	4	•••
2	0	7	35•	12	•••
2	0	8	85•	-86	•••
2	0	9	134•	126	•••
2	0	10	71•	-73	•••
2	1	-10	174•	-148	•••
2	1	-9	49-	33	24
2	1	-8	160	145	18
2	1	-7	169	167	14
2	1	-6	626	647	32
2	1	-5	518	-546	26
2	1	-4	325	312	25
2	1	-3	490	503	48
2	1	-2	383	-391	38
2	1	1	538•	616	•••
2	1	2	68•	68	•••
2	1	3	136•	-146	•••
2	1	4	391•	-496	•••
2	1	5	544	553	49
2	1	6	986X	1095	125
2	1	7	246	-246	15
2	1	8	124	-128	10
2	1	9	198	-198	17
2	1	10	41•	14	•••
2	2	-10	183	-174	21
2	2	-9	49-	-11	25
2	2	-8	119	109	11
2	2	-7	157	144	9
2	2	-6	299	-310	15
2	2	-5	448	-456	22
2	2	-4	518	514	36
2	2	-3	934X	1051	167
2	2	-2	170	161	21
2	2	-1	1168•	-1660	•••
2	2	0	897•	-1107	•••
2	2	1	345	-342	23
2	2	2	199•	-182	•••
2	2	3	305	286	15
2	2	4	302	-298	20
2	2	5	228•	231	•••
2	2	6	34•	17	•••
2	2	7	187•	181	•••
2	2	8	70	-67	16
2	2	9	50-	6	25
2	2	10	138	142	15
2	3	-10	50-	-23	25
2	3	-9	377	-361	21
2	3	-8	129	-116	12
2	3	-7	45-	-10	23
2	3	-6	69	73	13
2	3	-5	518	508	40
2	3	-4	433	-454	22
2	3	-3	498	484	26
2	3	-2	310	315	16
2	3	-1	41	-38	9
2	3	0	340	331	21
2	3	1	550	-566	78
2	3	2	109	-97	12
2	3	3	100	-102	9
2	3	4	112	105	13
2	3	5	738	-761	74
2	3	6	83	-94	11
2	3	7	196•	199	•••
2	3	8	63•	-37	•••

H	K	L	F0	FC	σ
2	3	9	237	248	17
2	3	10	112•	-17	•••
2	4	-10	222	217	14
2	4	-9	184	-173	13
2	4	-8	223	-211	25
2	4	-7	46-	28	23
2	4	-6	217	216	14
2	4	-5	103	-93	12
2	4	-4	271	-257	14
2	4	-3	647	-641	54
2	4	-2	103	95	11
2	4	-1	1091X	1231	183
2	4	0	124	-119	11
2	4	1	42•	-29	•••
2	4	2	124	-124	15
2	4	3	267	-261	14
2	4	4	253	-251	23
2	4	5	41•	-51	•••
2	4	6	211	200	15
2	4	7	58	56	18
2	4	8	40•	49	•••
2	4	9	159•	-226	•••
2	4	10	41•	-4	•••
2	5	-10	91•	87	•••
2	5	-9	305	280	27
2	5	-8	119	-111	17
2	5	-7	48-	-27	24
2	5	-6	182	-184	12
2	5	-5	229	-224	16
2	5	-4	67•	64	•••
2	5	-3	160	-167	9
2	5	-2	630	627	36
2	5	-1	130•	-133	•••
2	5	0	376	-378	24
2	5	1	61	55	13
2	5	2	419	406	57
2	5	3	382	371	21
2	5	4	218	-212	12
2	5	5	52	-46	16
2	5	6	126	-116	21
2	5	7	76	80	13
2	5	8	105	-110	8
2	5	9	212	-222	15
2	5	10	120•	118	•••
2	6	-10	44•	6	•••
2	6	-9	75	62	10
2	6	-8	46	-49	18
2	6	-7	72	73	11
2	6	-6	162	171	14
2	6	-5	117	112	19
2	6	-4	99	-84	11
2	6	-3	90	90	9
2	6	-2	184	-167	15
2	6	-1	124	-110	11
2	6	0	68•	-70	•••
2	6	1	287	-272	21
2	6	2	542	536	28
2	6	3	261	247	24
2	6	4	88	84	15
2	6	5	48-	4	24
2	6	6	217	-202	12
2	6	7	49-	-21	25
2	6	8	119	115	20
2	6	9	184	182	14
2	7	-9	66•	-83	•••
2	7	-8	92	84	21
2	7	-7	145	-134	8
2	7	-6	275	260	21
2	7	-5	246	242	13
2	7	-4	160	-168	10
2	7	-3	317	-311	22
2	7	-2	335	-305	36
2	7	-1	396	382	25
2	7	0	169	173	11
2	7	1	55•	-15	•••
2	7	2	474	-459	41
2	7	3	140	-131	22
2	7	4	374	365	19
2	7	5	93	93	10
2	7	6	82	66	20
2	7	7	69•	-50	•••
2	7	8	144	149	17
2	7	9	41•	-46	•••
2	8	-9	101•	125	•••
2	8	-8	61•	52	•••
2	8	-7	190	-186	16
2	8	-6	124	-118	10
2	8	-5	185	170	16
2	8	-4	223	221	15
2	8	-3	94	-81	9
2	8	-2	135	137	11
2	8	-1	110	-101	18
2	8	0	49-	19	25
2	8	1	118•	-109	•••
2	8	2	441	-432	30
2	8	3	49-	31	25
2	8	4	49-	9	25
2	8	5	69	65	14
2	8	6	48-	4	24
2	8	7	48	38	14
2	8	8	32•	-10	•••
2	9	-7	33•	36	•••
2	9	-6	251	-232	28
2	9	-5	48-	41	24
2	9	-4	160	161	15
2	9	-3	197	193	23
2	9	-2	50-	-7	25
2	9	-1	129•	-127	•••
2	9	0	50-	20	25
2	9	1	50•	-48	•••
2	9	2	176	175	18
2	9	3	49-	-16	24
2	9	4	58	-55	13
2	9	5	126	-118	14
2	9	6	132	-129	11
2	9	7	73•	73	•••
2	10	-6	28•	18	•••
2	10	-5	54•	-61	•••
2	10	-4	45-	-30	23
2	10	-3	47-	-44	23
2	10	-2	88	-78	9
2	10	-1	170	172	18
2	10	0	103	101	15
2	10	1	145	145	10
2	10	2	65•	-66	•••
2	10	3	131•	-196	•••

1, $\frac{1}{2}$, $\frac{1}{2}$ and relabelling their -$\underline{b}$, -$\underline{c}$ and -$\underline{a}$ as $\underline{a}$, $\underline{b}$ and $\underline{c}$. This gives x, y, z in terms of their coordinate tables as $\frac{1}{2}$ - y, $\frac{1}{2}$ - z, and 1 - x. This author's choice of axis labels has been preferred because of close comparisons with known monoclinic structures.

Table 5-4 gives the observed structure amplitudes (Fo) and their standard errors (σ) together with the structure factors calculated using the parameters of this author in Table 5-3. The atomic scattering factors for these calculations were taken from (6, Table 3.3.1A): K^+ ref. SX-21(39); Cr^{+++} ref. SX-67A; and O^- ref. SX-31A. The complex scattering factors used during anomalous dispersion calculations were obtained by modifying the above values according to (6, Section 3.3.2).

5.4 Description of the Structure

5.4 A Structure of the Dichromate Ions

The $Cr_2O_7^{-2}$ ion may be thought of as two CrO_4 tetrahedra sharing one corner oxygen atom. The bridging Cr-O distances are equal to each other but are longer than the terminal Cr-O distances. The latter are also equivalent within experimental error. The two crystallographically distinct dichromate ions occur in similar but not identical environments. Fig. 5-3 shows side and end views for each of these ions. The former are perpendicular to the Cr-OB-Cr planes and the latter are parallel to the Cr-Cr vectors.

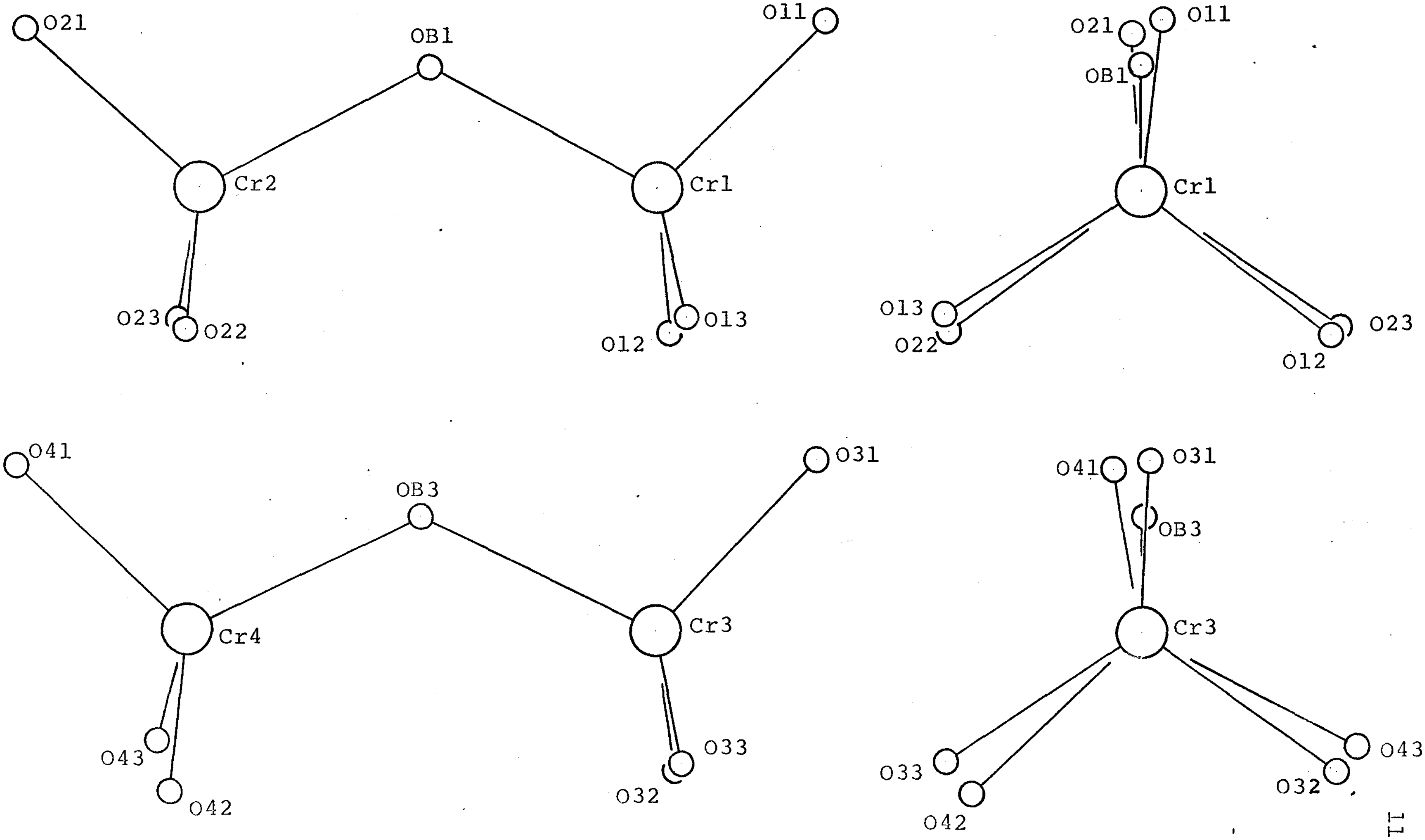

FIGURE 5-3

Side and End Views for the Two Crystallographically Distinct Dichromate Ions

Table 5-5 lists their bond lengths and angles. Values for important distances are quoted both before and after applying corrections for thermal motion assuming that the oxygen atoms are riding on the heavier chromium atoms (21). The standard errors quoted take account of the standard errors in the atom coordinates calculated by least squares refinement and the standard errors in the cell constants. Direction cosines for these bonds with respect to the unit cell axes appear in Sec.5.4 D for comparison with the directions of the principal axes of the thermal ellipsoids. The mean thermally corrected Cr-O (bridge) distance is 1.786 ± .008 Å and the mean corrected Cr-O (terminal) distance is 1.629 ± .010 Å.

The dichromate ions do not quite have an exact C_{2v} or even C_2 symmetry. The projections along the Cr-Cr vectors in Fig. 5-3 indicate a twisting of each dichromate ion away from an exactly eclipsed C_{2v} geometry. The decrease of one of the angles from tetrahedral in each ion (OB1-Cr1-O11 and OB3-Cr3-O31) appears to be a real effect and destroys an exact C_2 symmetry. None of the other O-Cr-O angles differ too significantly from tetrahedral.

The values 124.0° and 127.6° for the bridging angles are significantly different as are the Cr-Cr distances. The twisting away from C_{2v} symmetry is about 5° for the ion containing Cr1-Cr2 and about 10° for the ion containing Cr3-Cr4. This twisting occurs in the same sense for each

TABLE 5-5

Interatomic Distances and Angles for the
Two Crystallographically Distinct Dichromate Ions

Distances	Uncorrected	Thermally Corrected	Distances	Uncorrected	Thermally Corrected
Cr1-Cr2	3.144(2) Å	3.144 Å	Cr3-Cr4	3.189(2) Å	3.189 Å
Cr1-OB1	1.776(3)	1.781	Cr3-OB3	1.780(3)	1.788
Cr2-OB1	1.784(3)	1.790	Cr4-OB3	1.775(3)	1.784
Mean Corrected Cr-O (Bridge) = 1.786(8) Å					
Cr1-O11	1.614(3)	1.624	Cr3-O31	1.618(4)	1.633
O12	1.622(3)	1.634	O32	1.620(4)	1.634
O13	1.610(4)	1.626	O33	1.614(3)	1.629
Cr2-O21	1.583(3)	1.602	Cr4-O41	1.613(4)	1.627
O22	1.632(3)	1.642	O42	1.604(3)	1.619
O23	1.625(3)	1.638	O43	1.633(3)	1.643
Mean Corrected Cr-O (Terminal) = 1.629(10) Å					
OB1-O11	2.71		OB3-O31	2.72	
O12	2.77		O32	2.78	
O13	2.79		O33	2.78	
O21	2.75		O41	2.77	
O22	2.77		O42	2.79	
O23	2.78		O43	2.76	
O11-O12	2.64		O31-O32	2.65	
O13	2.67		O33	2.66	
O12-O13	2.64		O32-O33	2.65	
O21-O22	2.64		O41-O42	2.63	
O23	2.64		O43	2.66	
O22-O23	2.64		O42-O43	2.62	
O12-O23	3.35		O32-O43	3.54	
O13-O22	3.41		O33-O42	3.49	

Angles		Angles	
Cr1-OB1-Cr2	124.0(1)°	Cr3-OB3-Cr4	127.6(2)°
OB1-Cr1-O11	106.1(1)	OB3-Cr3-O31	106.6(2)
O12	109.4(1)	O32	109.7(1)
O13	110.8(1)	O33	110.1(1)
O11-Cr1-O12	109.5(1)	O31-Cr3-O32	109.8(2)
O13	111.7(1)	O33	110.6(1)
O12-Cr1-O13	109.2(2)	O32-Cr3-O33	110.1(1)
OB1-Cr2-O21	109.6(1)	OB3-Cr4-O41	109.7(1)
O22	108.5(1)	O42	111.2(2)
O23	109.5(1)	O43	108.4(1)
O21-Cr2-O22	110.2(1)	O41-Cr4-O42	109.7(2)
O23	110.6(1)	O43	109.9(2)
O22-Cr2-O23	108.4(1)	O42-Cr4-O43	107.9(1)

ion with respect to their similar environments. Likewise the unique angles OB1-Cr1-O11 and OB3-Cr3-O31 are in analogous positions for the two ions. Details of the environments of the two dichromate ions appear in Tables 5-6 and 5-7. Further discussion of the dichromate ion stereochemistry is given in Sec. 5.5 D.

5.4 B Ionic Packing to Form the Structure

The structure consists of a three dimensional array of K^{+1} and $Cr_2O_7^{-2}$ ions. The dichromate ion orientations in the array are described by reference to the "backbone" of the group (consisting of the bridging oxygen and the two terminal oxygen atoms which form a line nearly parallel to the Cr-Cr vector), and by reference to the "feet" of the group (consisting of the remaining four oxygen atoms).

Fig. 5-4 shows the arrangement of K^+ and $Cr_2O_7^{-2}$ ions projected down c. Atom labels correspond to those of Table 5-3. Atoms with primes are related to the unprimed ones by inversion in the centres of symmetry at $0\ \frac{1}{2}\ \frac{1}{2}$ or $\frac{1}{2}\ \frac{1}{2}\ \frac{1}{2}$. Roman numerals denote layers in the structure parallel to the plane of b and c. These layers are described later in the text.

The groups containing Cr1-Cr2 in each unit cell form a row (A) of dichromate ions whose members repeat by the translation along c (out of the plane of Fig. 5-4). The potassium ions K1 and K2 lie between successive dichromate ions

FIGURE 5-4

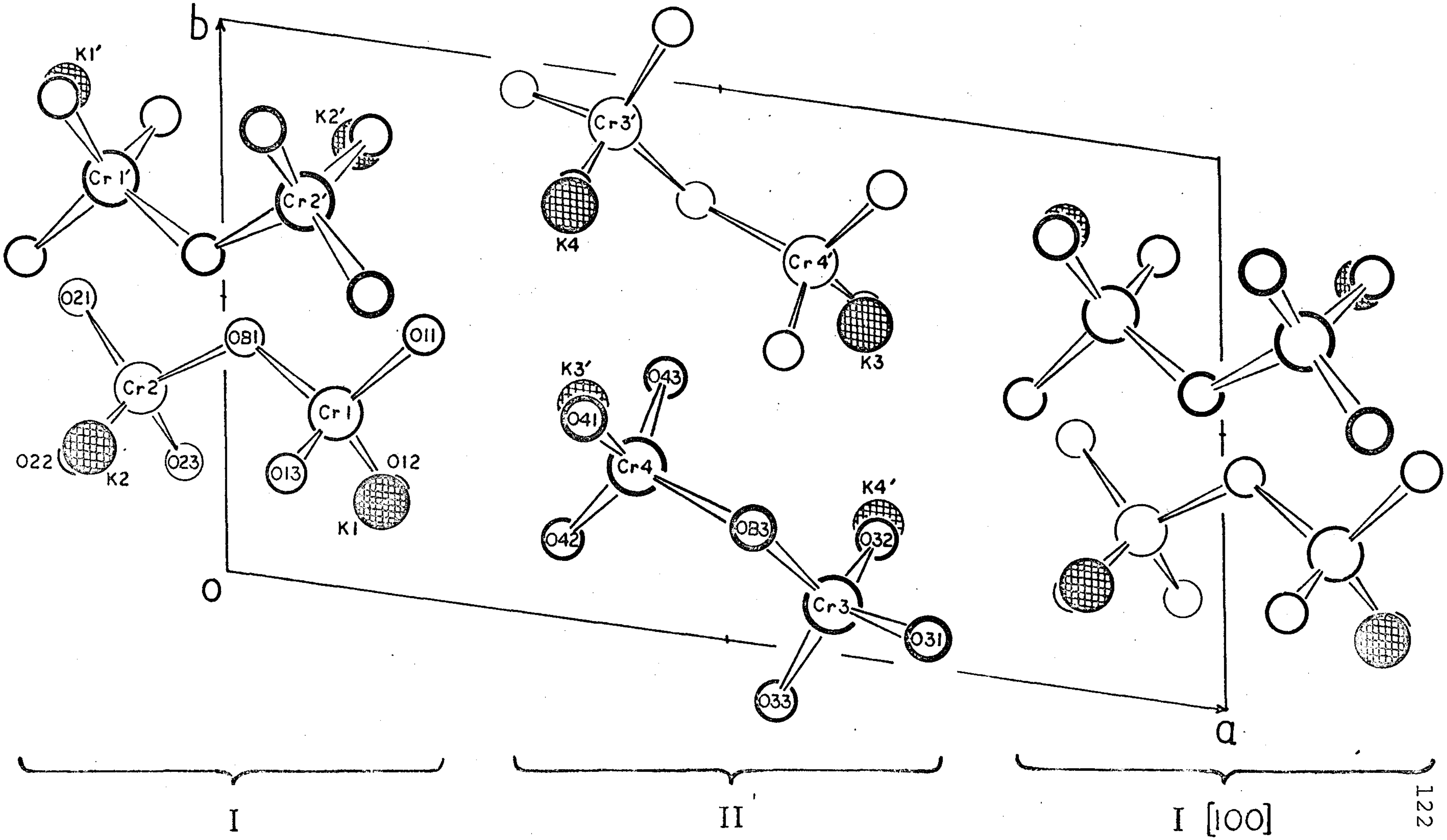

Structure of Triclinic $K_2Cr_2O_7$ projected down [001].

of row A and are approximately coplanar with the four feet oxygen atoms of the dichromate ions. The arrangement of such a row is shown schematically in Fig. 5-5. The groups containing $\mathrm{Cr1}'$-$\mathrm{Cr2}'$ together with $\mathrm{K1}'$ and $\mathrm{K2}'$ form a similar row (B) along the *c* direction related to row A by inversion through the centre of symmetry at $0\,\frac{1}{2}\,\frac{1}{2}$. The B row backbones fit into the troughs between the backbones of two adjacent dichromate groups in row A and vice versa. The backbones of one row do not rest exactly in the centre of the troughs of the other row, but instead are displaced such that any dichromate ion in one row is paired more closely to one particular dichromate ion in the adjacent row. The groups Cr1-Cr2 and $\mathrm{Cr1}'$-$\mathrm{Cr2}'$ in Fig. 5-4 are a close pair. The pairing may be thought of as a distortion from an exactly centred arrangement by sliding the backbones of one row along the trough direction of the interlocking row and translating one row relative to the other along the row direction.

Applying the *b* translation to these interlocking rows, a layer (I) is generated parallel to the plane of *b* and *c*. This layer contains the sequence of rows ABAB...etc. The contact A:B is between interlocking backbones; the contact B:A is between the flat planes of oxygen feet and potassium ions of the two rows, and occurs so that the oxygen feet of one row straddle the potassium ions of the other.

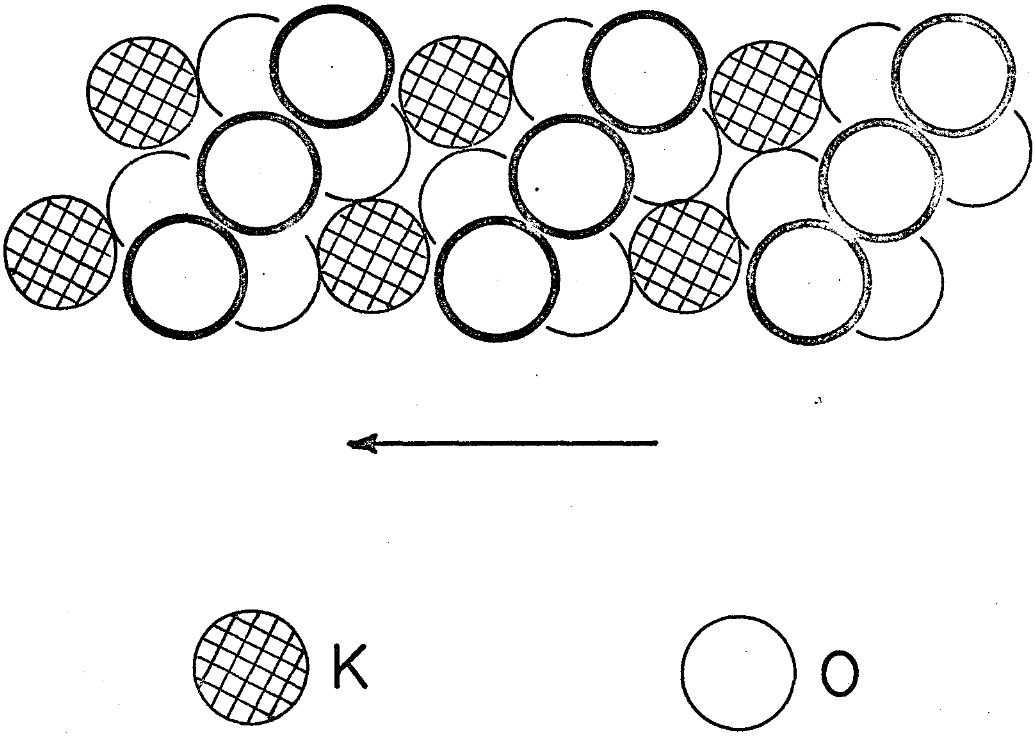

FIGURE 5-5

Schematic Diagram Showing a Row Formed by Potassium and Dichromate Ions. The vector denotes the unit cell translation by which members of the row repeat. The text gives further description of these rows and a description of how they pack next to each other to form layers in the structure.

The two layers are crystallographically distinct. However, the layer marked II in Figure 5-4 has nearly the same construction as layer I . The rows C and D which form layer II are found to run along the $\underline{b}$ direction whereas the analogous rows (A and B) in layer I run along the $\underline{c}$ direction. In layer II an example of the analogous close paired dichromate ions are Cr3-Cr4 in row D and Cr3$'$-Cr4$'$ O$\bar{1}$1 in row C.

The failure of the layers to be strictly identical cannot be pictured as a small distortion of any crystallographic symmetry relationship between them. This is because the transformation necessary to generate layer II and then layer I (100) from the original layer I cannot correspond to a possible space group symmetry operation. The actual generation can be pictured as: 1) a rotation of $+90^\circ$ about $\underline{a}^*$ and a translation of $\frac{1}{2}\,\underline{a} + \frac{1}{2}\,\underline{b} + \frac{1}{2}\,\underline{c}$ giving II from I, and 2) a rotation of -90° about $\underline{a}^*$ and a translation of $\frac{1}{2}\,\underline{a} - \frac{1}{2}\,\underline{b} - \frac{1}{2}\,\underline{c}$ giving I(100) from II.

Fig. 5-6(a) and (b) show the unit cell contents viewed down the $\underline{c}$ and $\underline{b}$ axes. Here the dichromate ions are schematically drawn as space filling tetrahedra. The 90° rotation of one layer relative to the next is evident from these two diagrams. These figures together with Fig. 5-4 show how the atoms O11 and O31 protrude somewhat outside

FIGURE 5-6

Structure of Triclinic $K_2Cr_2O_7$ projected

(a) down [001]; and
(b) down [010].

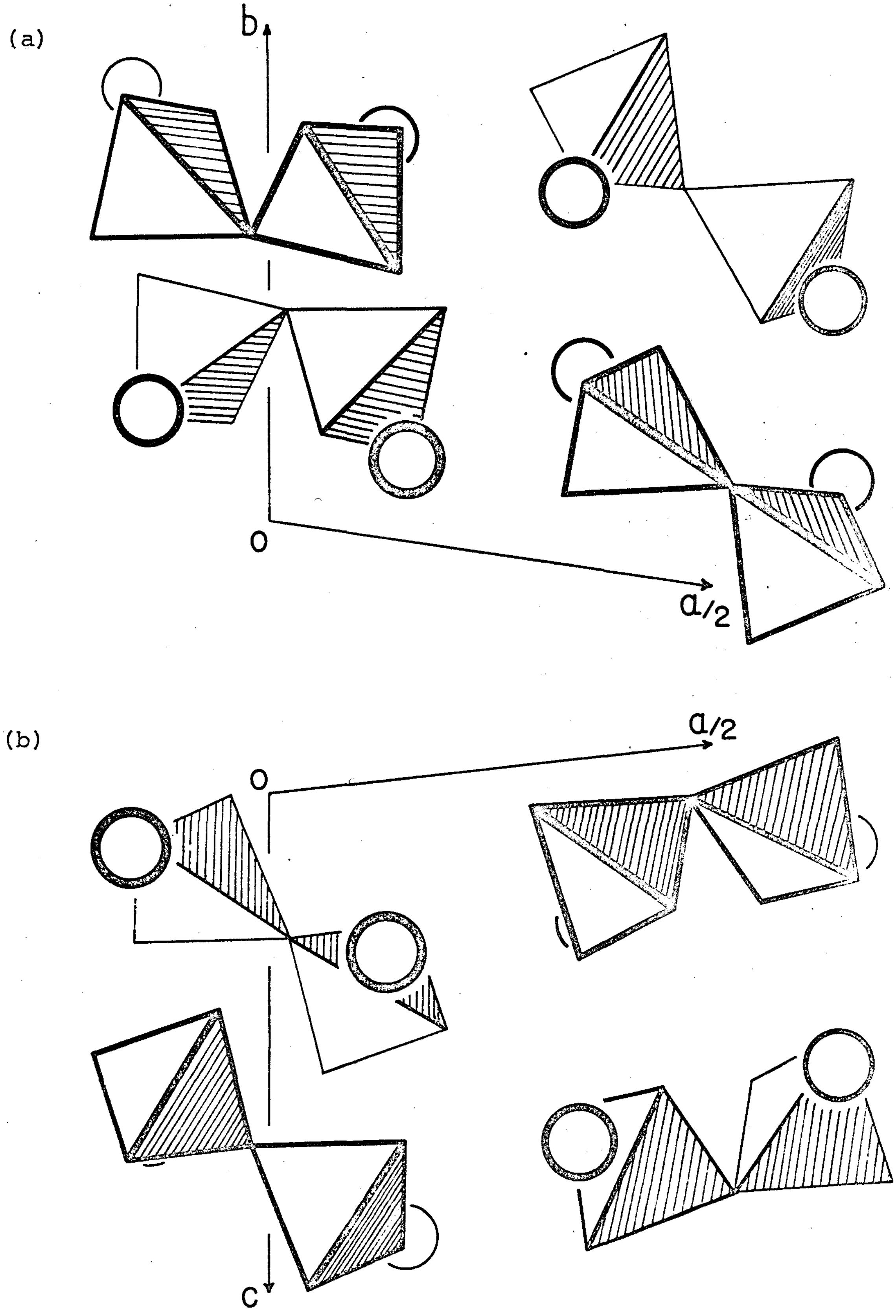

their respective layers, suggesting that forces between adjacent layers may be the cause of the decrease from tetrahedral for the angles OB1-Cr1-O11 and OB3-Cr3-O31 (see Section 5.4 A).

5.4 C Structural Environments

The K^+ ions are surrounded by oxygen atoms in the structure. Table 5-6 gives the interatomic distances for the four crystallographically distinct K^+ ions and their oxygen neighbours. The table is constructed to allow comparison of analogous contacts in the similar layers I and II.

For reference the K atoms in contact with each dichromate group are listed below.

1) $Cr_2O_7^{-2}$ group Cr_1-Cr_2 :

K1	K1 00$\bar{1}$	K1'	K1' 0$\bar{1}$0
K2	K2 00$\bar{1}$	K2'	K2' 0$\bar{1}$0
K3'			
K4	K4' $\bar{1}$00		

2) $Cr_2O_7^{-2}$ group Cr_3-Cr_4:

K1	K1' 1$\bar{1}$1		
K2			
K3	K3 0$\bar{1}$0	K3'	K3' 001
K4	K4 0$\bar{1}$0	K4'	K4' 001

The distances may be derived from Table 5-6.

TABLE 5-6

Oxygen Environments of Potassium Ions*

K1		K2		K3		K4	
Intralayer Distances (Å):							
O11	3.82	O21 001	3.63	O31 010	3.70	O41	3.25
O12 001	2.83	O22	2.80	O32	2.88	O42 010	2.94
O13	2.74	O23 001	2.73	O33 010	2.70	O43	2.74
O23 001	2.87	O13	2.75	O43	2.71	O33 010	2.83
O21'	2.82	O11'	2.93	O41'001	2.67	O31'001	2.97
O22'0$\bar{1}$0	2.83	O12'0$\bar{1}$0	2.83	O42'	3.34	O32'	2.82
O23'0$\bar{1}$0	2.97	O13'0$\bar{1}$0	3.64	O43'	2.68	O33'	
OB1 001		OB1	3.86	OB3	3.59	OB3 010	3.90
OB1'		OB1'	2.96	OB3'001		OB3'001	2.86
Pseudo 2 Fold Related Pairs				Pseudo 2 Fold Related Pairs			
Analogous Pairs In Each Layer							
Interlayer Distances (Å):							
O41	2.89	O31 $\bar{1}$00	3.14	O11'100	2.79	O21'	3.29
O42	3.07	O32 $\bar{1}$00	2.89	O12'100	2.84	O22'	2.76
O31'0$\bar{1}$1	2.84	O41'001		O21 101		O11	3.09

* Blank entries indicate distances are >4.00 Å.

In addition there are some O-O distances between neighbouring dichromate groups comparable with some of the K-O distances listed above. Such O-O distances less than 3.3 Å are given in Table 5-7. There are other values in the range 3.30 to 3.40 Å too numerous to list.

5.4 D Anisotropic Thermal Parameter Analysis

The anisotropic temperature factors given in Table 5-3 have been analyzed to determine the directions and magnitudes of the atomic motions along the three principal axes of the thermal ellipsoids. The results are given in Table 5-8. The table shows that the Cr atoms undergo almost isotropic thermal motion. Comparing the directions of the Cr-O bonds with the directions of the principal axes of vibration for the oxygen atoms, it can be seen that the smallest thermal displacements are generally coincident with the bond directions. The largest displacements occur in directions which suggest that the dichromate ions are librating about their Cr-Cr axes. Estimates of the RMS libration angle give about 7° which is in agreement with the corresponding maximum librational modes found in analogous structures (e.g. 6.4° in $K_2S_2O_7$ (3); 5.7° in $K_2CH_2(SO_3)_2$ (24); and 6.8° in $K_2NH(SO_3)_2$ (60).).

5.5 Discussion and Conclusions

5.5 A Comparison of Cell Constants and Space Groups for Related Structures

Table 5-9 gives the crystal data found in the literature for several compounds which might have structures

TABLE 5-7

Oxygen-Oxygen Distances Between Dichromate Ions*

OB1 - O13'	3.30 Å
O11 - O32'	3.04
O11 - O22'	3.16
O12 - O31'0$\bar{1}$0	3.19
O13 - O13'0$\bar{1}$0	3.22
O13 - O22'0$\bar{1}$0	3.29
O21 - O41'$\bar{1}$00	3.25
O22 - O42'$\bar{1}\bar{1}$0	3.17
O22 - O31 $\bar{1}$0$\bar{1}$	3.21
O23 - O23'0$\bar{1}\bar{1}$	3.21
O31 - O41'0$\bar{1}$0	3.24
O32 - O33'0$\bar{1}$0	3.22
O33 - O33'0$\bar{1}$0	3.30
O43 - O43'	3.15

---

*Only one member of each pair of symmetry related distances is listed.

TABLE 5-8

Principal Axes Analysis for Anisotropic Temperature Factors

Atom	R.M.S. Displacements (A)	Associated Direction	Direction Cosines ($x10^3$) With Respect To		
			a	b	c
K1	0.171		-684	-331	671
	0.154		343	-941	-270
	0.147		-643	66	-690
K2	0.211		193	-792	-600
	0.165		-913	-238	286
	0.151		-360	563	747
K3	0.207		- 91	832	-564
	0.162		211	525	758
	0.147		973	-179	-328
K4	0.198		-418	-796	354
	0.159		-471	2	-821
	0.147		777	-606	-446
Cr1	0.146		107	-847	540
	0.138		-783	364	640
	0.126		-613	-387	-547
		Cr1-Cr2	-765	117	-558
Cr2	0.142		-690	-395	612
	0.135		177	560	747
	0.125		-701	728	-260
Cr3	0.148		257	567	701
	0.140		-431	-557	713
	0.124		-865	607	- 22
		Cr3-Cr4	-885	576	170
Cr4	0.147		-340	-489	-712
	0.134		192	727	-658
	0.124		-921	482	244
OB1	0.189		-601	212	845
	0.149		794	93	476
	0.139		- 87	973	-243
		Cr1-OB1	-686	570	-483
		Cr2-OB1	665	361	502
O11	0.207		-241	-362	916
	0.172		684	-804	-190
	0.143		689	471	352
		Cr1-O11	569	624	331

(continued next page)

TABLE 5-8 (Continued)

Principal Axes Analysis for Anisotropic Temperature Factors

Atom	R.M.S. Displacements (Å)	Associated Direction	Direction Cosines ($x10^3$) With Respect To		
			a	b	c
O21	0.238		-605	- 87	842
	0.202		474	634	451
	0.150		-640	768	-294
		Cr2-O21	-602	757	-371
O12	0.206		201	788	-572
	0.181		818	42	458
	0.129		540	-614	-681
		Cr1-O12	561	-644	-639
O23	0.225		52	867	-495
	0.163		-998	194	102
	0.149		- 22	-459	-863
		Cr2-O23	482	-585	-735
O13	0.236		181	-793	-599
	0.175		-966	109	-150
	0.145		-184	-599	787
		Cr1-O13	-435	-510	751
O22	0.191		-622	154	-710
	0.177		422	-861	-428
	0.142		-660	-486	559
		Cr2-O22	-534	-555	630
OB3	0.219		460	815	- 72
	0.160		-161	102	993
	0.135		873	-570	98
		Cr3-OB3	-722	563	572
		Cr4-OB3	866	-470	267
O31	0.229		470	805	-155
	0.199		-381	334	908
	0.135		796	-490	390
		Cr3-O31	732	-292	576
O41	0.213		634	463	450
	0.190		309	-854	469
	0.152		-709	236	760
		Cr4-O41	-572	385	808
O32	0.207		659	-658	-540
	0.202		740	272	462
	0.160		133	702	-703
		Cr3-O32	341	545	-774

(continued next page)

TABLE 5-8 (Continued)

Principal Axes Analysis for Anisotropic Temperature Factors

Atom	R.M.S. Displacements (Å)	Associated Direction	Direction Cosines ($\times 10^3$) With Respect To a	b	c
O43	0.209		111	492	820
	0.168		859	-595	97
	0.146		500	635	-565
		Cr4-O43	198	732	-649
O33	0.221		193	99	-991
	0.192		938	-441	52
	0.160		-287	-892	-121
		Cr3-O33	-352	-792	-328
O42	0.216		-102	540	-840
	0.192		870	-479	-415
	0.157		-482	-692	-348
		Cr4-O42	-487	-621	-453

TABLE 5-9

Comparison of Cell Constants and Space Groups

Material	Space Group	a(Å)	b(Å)	c(Å)	α(°)	β(°)	γ(°)	Reference
$K_2Cr_2O_7$								
Room Temp.	P$\bar{1}$ (C_i^1)	13.37	7.38	7.44	90.75	96.21	97.96	This Work
		13.47	7.41	7.49	90.85	96.22	98.00	K and S (45)
		13.40	7.40	7.52	90.84	96.17	98.00	K,I and B (53)
High Temp. $\gtrsim 260^\circ$C	$P2_1/n$(C_{2h}^5)	13.45	7.52	7.55	90	91.68	90	K and S (45)
Room Temp. Metastable	C2/c (C_{2h}^6)	13.06	7.37	7.43	90	91.85	90	K and S (45)
Z + P Form	$P2_1/a$(C_{2h}^5)	12.94	7.35	7.47	90	91.92	90	Z and P (61)
$(NH_4)_2Cr_2O_7$	C2/c (C_{2h}^6)	13.26	7.54	7.74	90	93.20	90	B and W (49)
$K_2S_2O_7$	C2/c (C_{2h}^6)	12.35	7.31	7.27	90	93.12	90	L and T (3)
$K_2CH_2(SO_3)_2$	C2/c (C_{2h}^6)	12.56	7.77	7.25	90	90.50	90	T (24)
$K_2NH(SO_3)_2$	C2/c (C_{2h}^6)	12.43	7.46	7.18	90	91.18	90	C and J (60)
$Rb_2Cr_2O_7$								
Room Temp.	P$\bar{1}$ (C_i^1)	13.49	7.65	7.74	86.13	98.43	91.00	K and S (45)
Room Temp.	$P2_1/n$(C_{2h}^5)	13.62	7.62	7.67	90	93.37	90	K and S (45)
$Ca_2P_2O_7$								
β-Form	$P4_1$ (C_4^2)	24.14	6.68	6.68	90	90	90	W (62)

related to triclinic $K_2Cr_2O_7$. Structures have now been determined for all but $P2_1/n$ and C2/c $K_2Cr_2O_7$, and the two $Rb_2Cr_2O_7$ forms. Detailed comparisons of the known structures suggest possible forms for those of other symmetries yet to be solved. The solved C2/c structures are all quite similar and it is probable that the unsolved C2/c form of $K_2Cr_2O_7$ is isostructural with the known ones. The $K_2Cr_2O_7$ room temperature structure determined by Zhukova and Pinsker (61) for thin film crystals using electron diffraction is completely different from any other known structure in the table. If their structure, cell, and space group are correct, this might correspond to a fourth form of $K_2Cr_2O_7$. Since there is a systematic pattern in all the other known structures, the Zhukova and Pinsker structure is somewhat suspect. Because of its dissimilar nature it is not a useful example to discuss in the comparisons which follow.

5.5 B Relation to the Monoclinic C2/c Structures

Five of the structures listed in Table 5-9 have space group C2/c. Fig. 5-7 compares the symmetry elements in C2/c to three other centrosymmetric subgroups useful in the following discussions. These include monoclinic $P2_1/n$ (C_{2h}^5), and triclinic $C\bar{1}$ (C_i^1) and $P\bar{1}$ (C_i^1).

Fig. 5-8 compares the [001] and [010] projections of a typical C2/c structure with similar projections of

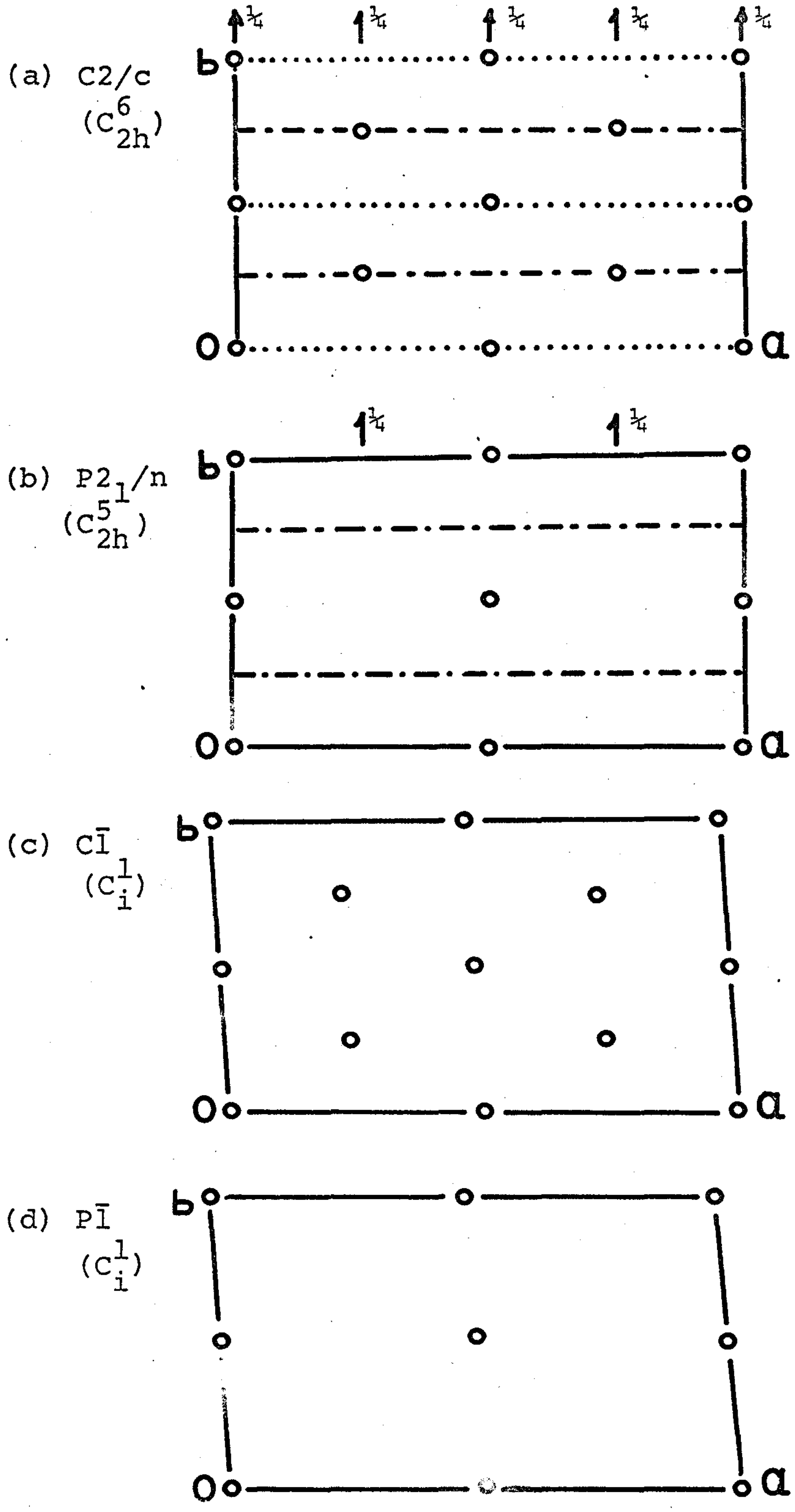

FIGURE 5-7

Space group comparison. The International Table symbol convention (4, Tables 4.1.6 and 4.1.7) has been used to describe those symmetry elements present in each case.

FIGURE 5-8

Comparison of C2/c and $P\bar{1}$ Structures:

(a) C2/c down c,

(b) C2/c down b,

(a)

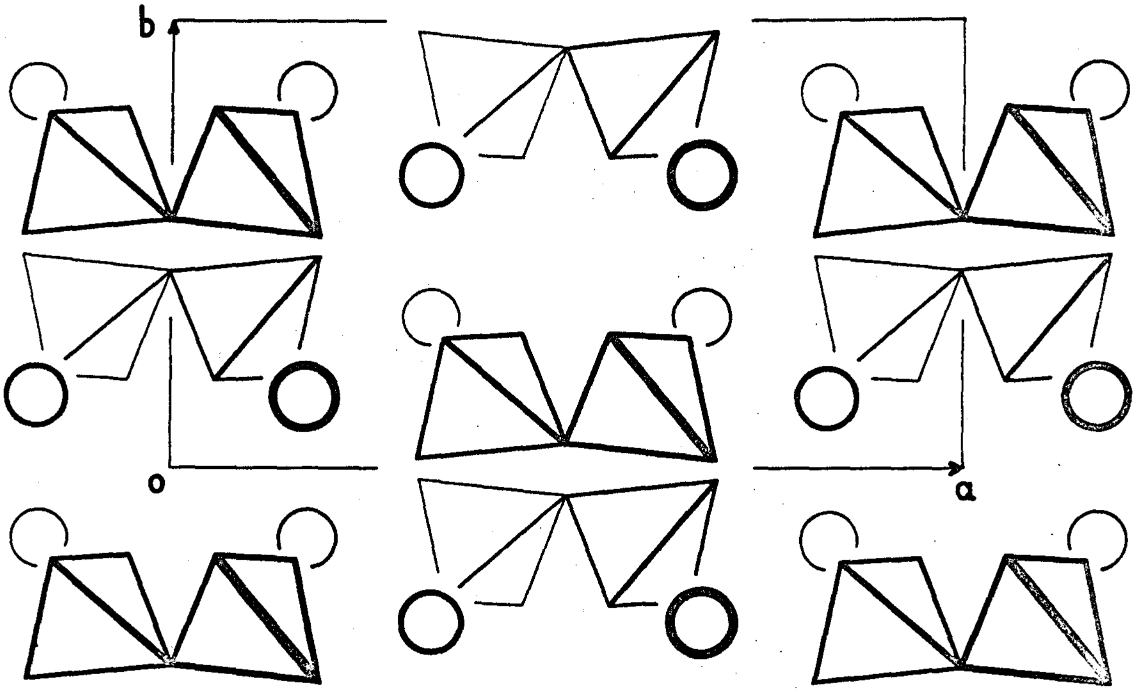

(b)

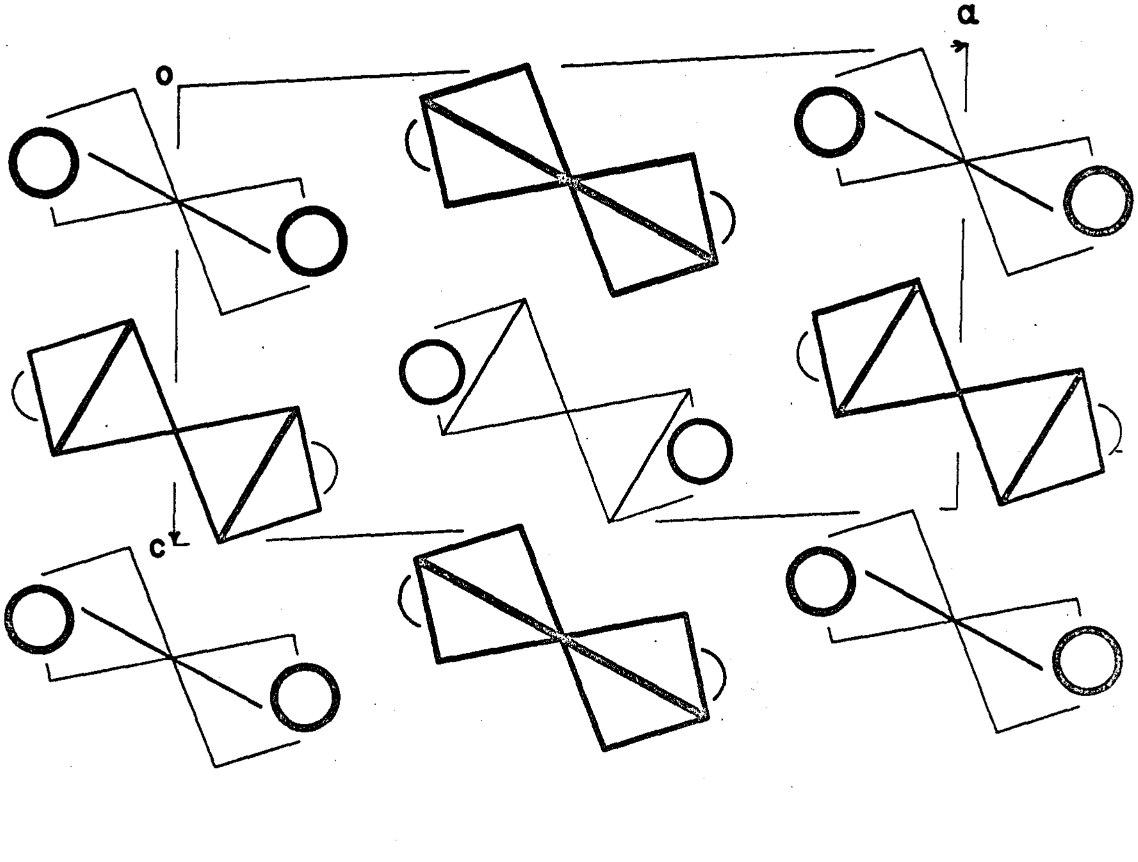

FIGURE 5-8 (continued)

Comparison of C2/c and P$\bar{1}$ Structures:

(c) P$\bar{1}$ down c,

(d) P$\bar{1}$ down b.

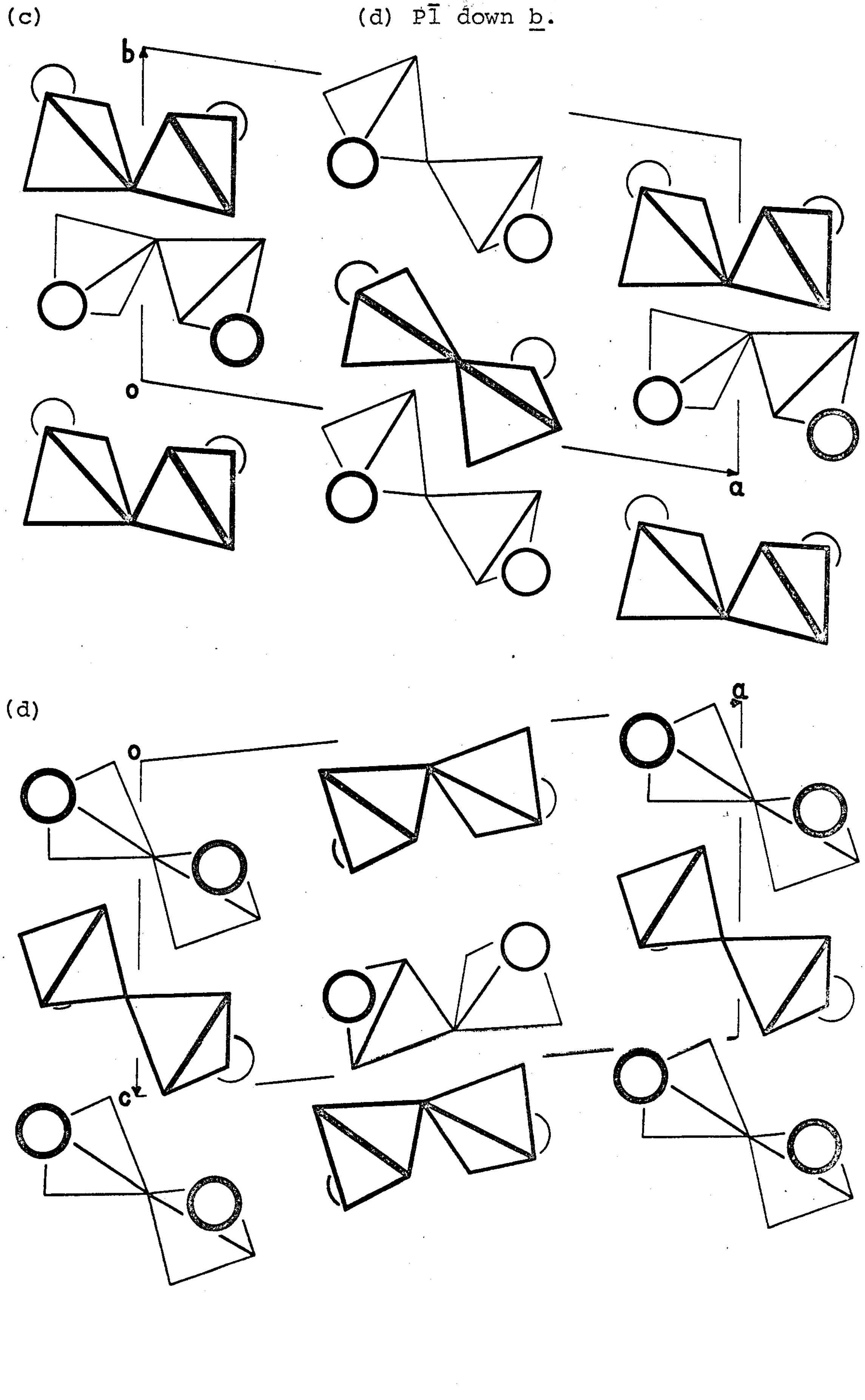

P$\bar{1}$ $K_2Cr_2O_7$. Both structures can be described in terms of rows of cations and anions interlocking backbones to form layers which stack perpendicular to $\underline{a}^*$. This has been the descriptive approach used in Sec. 5.4 B and it can be followed again to describe the C2/c structure.

Layer I in C2/c is formed by two rows, A and B, which interlock backbones in a manner similar to P$\bar{1}$. Each row of anions and cations is similar to the row shown in Fig. 5-5. However in C2/c the two halves of each anion in a row are related by a 2 fold symmetry axis with the bridging atom restricted to lie on the symmetry axis. These 2 fold axes also relate pairs of cations in each row. When two of these rows A and B interlock backbones, there is a c glide operation as well as a centre of symmetry relating the two rows. The 2 fold axes and c glide planes in C2/c ensure that each row is centred in the plane of $\underline{b}$ and $\underline{c}$, and also ensure that the backbones of one row fit exactly in the centre of the troughs between the backbones of the next row. Hence no pairing of anions is possible in C2/c. This is in contrast to P$\bar{1}$ where there is a sliding of the backbones of one row along the trough direction and a translation along the row direction (compare layers I for Figs. 5-8 (b) and (d)). The essential difference between P$\bar{1}$ layer I and C2/c layer I is that C2/c has 2 fold axes and c glide planes which P$\bar{1}$ does not have. Only the inversion centres within the layer are common to C2/c and $P\bar{1}$(see Figs. 5-7 (a) and (d)).

In C2/c there is a second layer, II, which is related to layer I by the C centering. The C centering requires that layer II be identical to layer I. It also requires that the rows which interlock backbones to form layer II must run along the same direction as those rows forming layer I. The $P\bar{1}$ layer II, while quite similar to layer I, is not identical by symmetry to layer I and the rows forming layer II run approximately at right angles to those forming layer I. The $P\bar{1}$ layer arrangement does not even exhibit an approximate C centering. Hence the arrangement of adjacent layers is quite different for the C2/c and $P\bar{1}$ structures and seems surprising in view of their many similarities. An explanation follows of how this large difference can occur between the layer arrangements of the C2/c and $P\bar{1}$ structures.

It has already been pointed out above that the 2 fold axes and c glide planes in C2/c produce small but distinct differences between the C2/c and $P\bar{1}$ type layers. Fig. 5-9 (a) shows the appropriate views of the $P\bar{1}$ layers for comparison with the [001] C2/c projection, and Fig. 5-9 (b) shows those for comparison with the [010] C2/c projection. The latter comparison especially illustrates how the absence of 2 fold axes and c glide planes in both of the $P\bar{1}$ layers results in a close pairing of Cr_2O_7 ions. This close pairing observed for both of the crystallographically distinct $P\bar{1}$ layers is a key point in explaining how the 90° relationship between

FIGURE 5-9

Comparison of C2/c and $P\bar{1}$ Layers

(a)

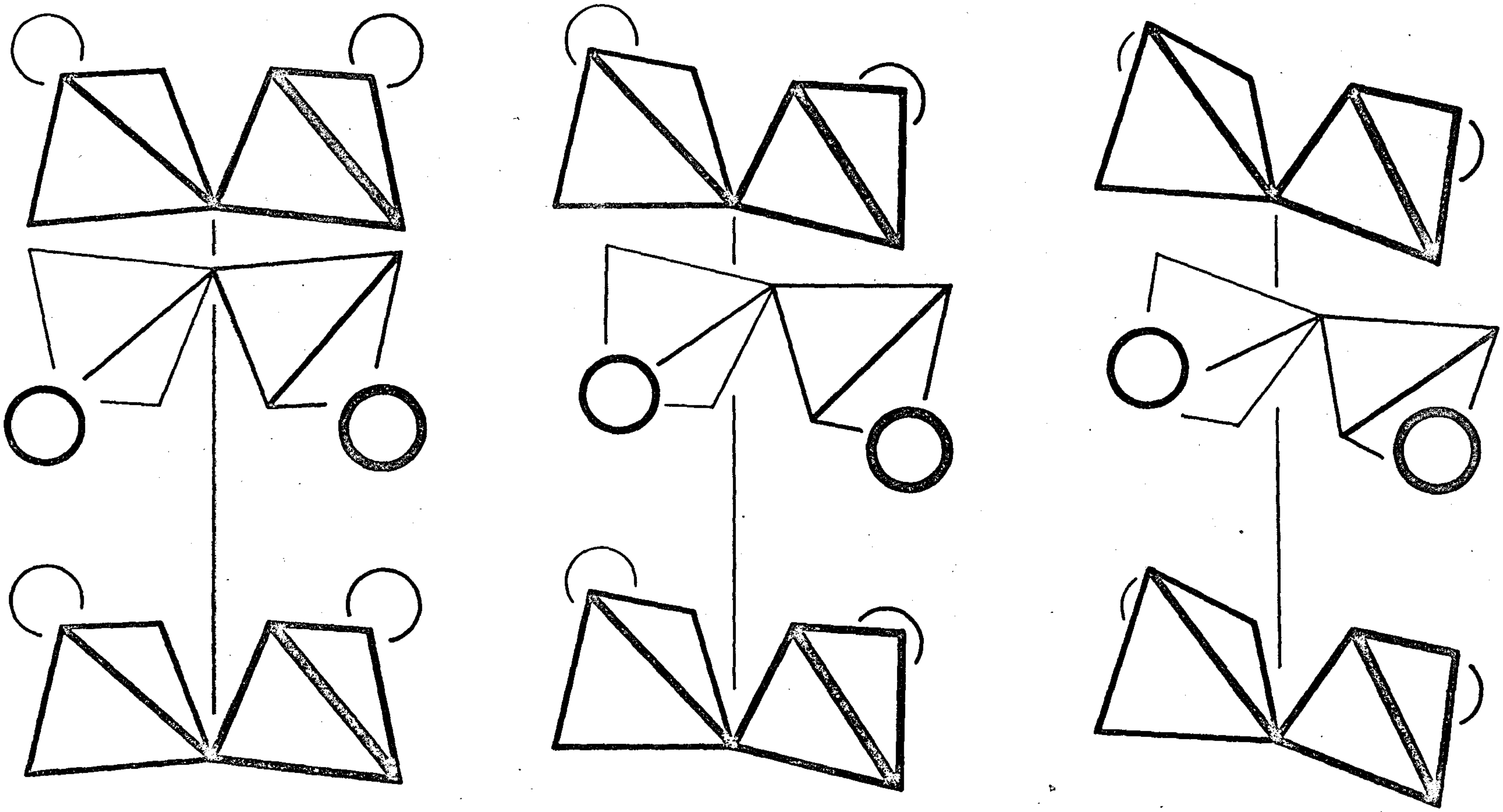

C2/c DOWN c

$P\bar{1}$ I DOWN c

$P\bar{1}$ II ALONG b

FIGURE 5-9 (continued)

Comparison of C2/c and P$\bar{1}$ Layers

(b)

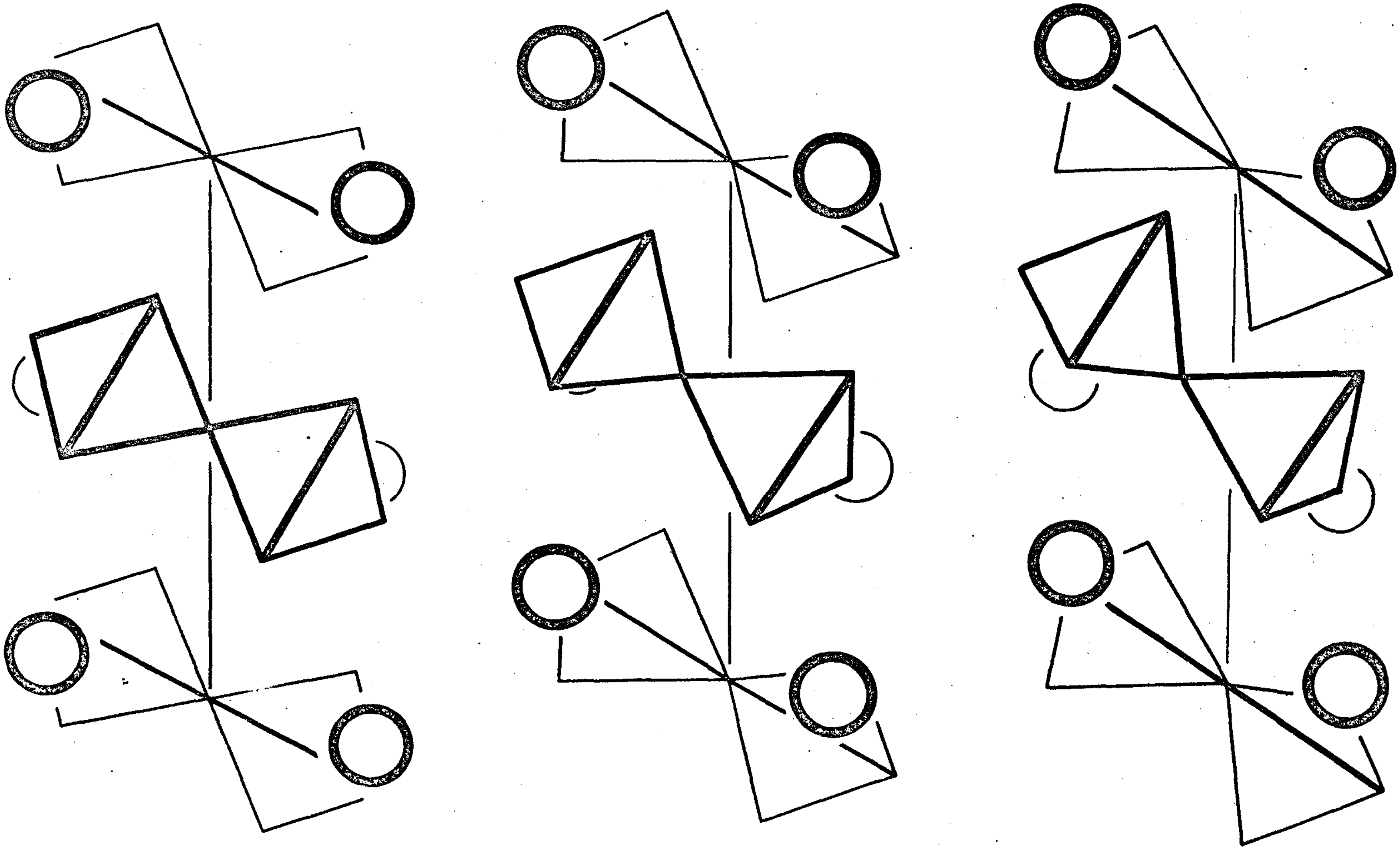

C2/c DOWN b   P$\bar{1}$ I DOWN b   P$\bar{1}$ II DOWN c adjacent layers can occur.

Fig. 5-10 illustrates qualitatively how the packing of adjacent layers can occur so differently in the C2/c and P$\bar{1}$ structures. These diagrams show projections perpendicular to the layers. They show for each of (a) C2/c and (b) P$\bar{1}$: (i) how the atoms are arranged on the front face of layer I, and (ii) how these are overlapped by the atoms on the back face of layer II. Each layer face consists of an approximately planar arrangement of red oxygen and green potassium atoms. Those oxygen atoms belonging to the same dichromate ion appear in contact. Each such oxygen pair contains one terminal backbone oxygen and one foot oxygen. The remaining feet and bridging oxygen atoms of the anions lie within the layers and are not shown.

Fig. 5-10 (a) (i) shows the front face of layer I for C2/c. The rows A and B which run along $\underline{c}$ are marked. The contact A:B shows the interlocking backbones while the contact B:A shows the arrangement of adjacent planes of potassium atoms and feet oxygen atoms. It is important here to notice that across the contact B:A there is formed along $\underline{c}$ a zig-zag chain of equally spaced K atoms related by one of the c glide planes. Between such chains are parallel zig-zag chains of equally spaced oxygen atom pairs belonging to interlocking dichromate groups, again related by a c glide plane. In C2/c layer II is identical to layer I and

(a) C2/c (b) $P\bar{1}$

(i) Projection down $\underline{a}^*$ showing front face of layer I

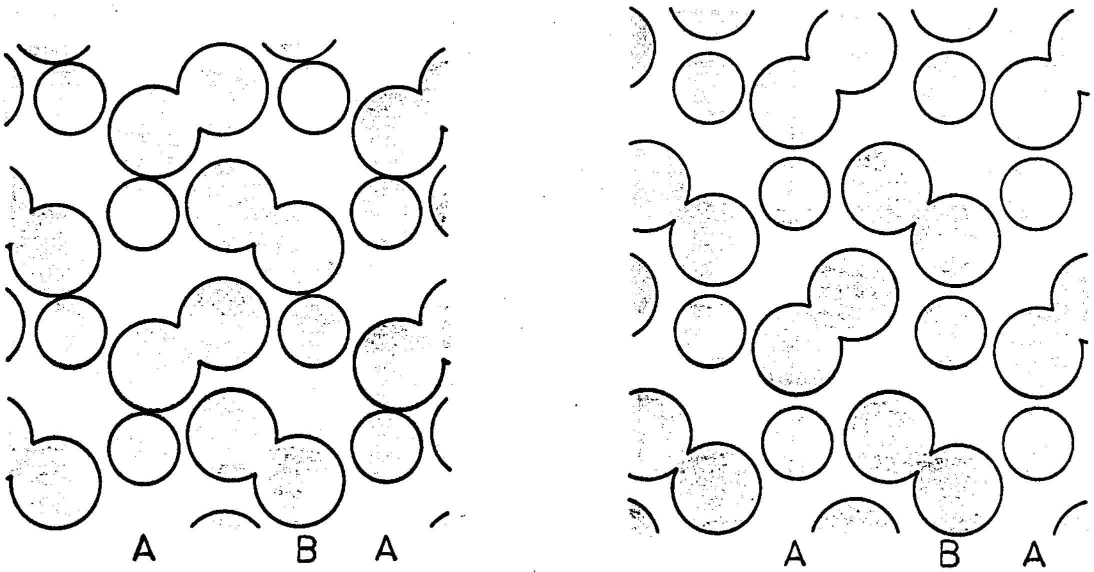

(ii) Back face of layer II overlapping front face of Layer I

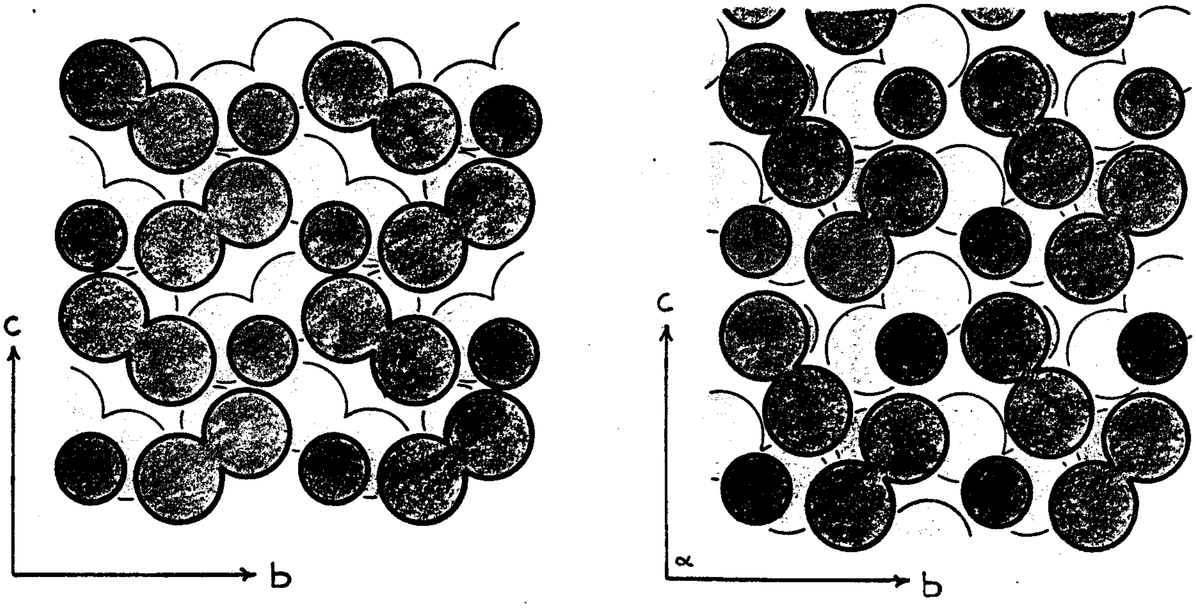

FIGURE 5-10

Comparison of C2/c and $P\bar{1}$ adjacent layer packing the back face of layer II is identical to the inversion of the front face shown for layer I. Fig. 5-10 (a) (ii) shows how layer II overlaps layer I with the zig-zag chains of equally spaced K atoms on the back face of layer II fitting over the zig-zag chains of equally spaced oxygen atom pairs in the front face of layer I, and vice versa. This overlap arrangement is a reasonable one since one expects to find contacts between potassium ions and the oxygens of the dichromate ions when the two layers pack adjacent to one another. Since the two types of zig-zag chains must be parallel when they overlap, the orientation of layer II is the same as that of layer I in the C2/c crystal structure.

Quite a different situation arises in $P\bar{1}$. Fig. 5-10 (b) (i) shows the front face of $P\bar{1}$ layer I for comparison with Fig. 5-10 (a) (i). Similar zig-zag chains of K atoms and of oxygen atoms running along c̲ are formed across the row contacts. However in $P\bar{1}$ the close pairing allowed through the absence of the 2 fold axes and c glide planes results in one member of any chain being displaced closer to one of its neighbouring members. With such displacements it becomes possible to pick out other zig-zag chains of unequally spaced K and O atoms running along b̲.

Since layer II is nearly identical to layer I, it too will possess on its faces two different directions in which zig-zag chains can be found. Assuming that $P\bar{1}$ layer II will make contact with layer I by aligning zig-zag K atom chains over chains of oxygen atoms, there are now seen to be two orientations for which layer II might accomplish this. Briefly, these two ways are: (A) K chains along $\underline{c}$ over oxygen chains along $\underline{c}$, and (B) K chains along $\underline{b}$ over oxygen chains along $\underline{c}$.

Case (A) would result in at least an approximate C centering relation between layers I and II. Case (A) could also arise with an n glide relation since the approximate c glide within the $P\bar{1}$ layers plus an n glide combine to give an approximate C centering.

The structure analysis of $K_2Cr_2O_7$ at room temperature indicates that case (A) is not observed. Case (B) on the other hand would give the $P\bar{1}$ structure an apparent interchange in the roles of the unit cell $\underline{b}$ and $\underline{c}$ axes for the two different layers. This approximate 90° relation is found in the $P\bar{1}$ $K_2Cr_2O_7$ structure determination. Fig. 5-10 (b) (ii) shows this observed overlap arrangement. The comparison of the two different layer structures has led to an understanding of how two quite different overlap arrangements can occur, and these ideas will be used in Sec. 5.5 C to speculate on the structures of other phases of $K_2Cr_2O_7$.

The differences between the C2/c and $P\bar{1}$ structures can be summarized as an absence in $P\bar{1}$ of the following C2/c symmetry elements: 2 fold axes, c glide planes, C centering, n glide planes, 2_1 fold screw axes, and the second class of inversion centres (i.e. the ones between layers, see Fig. 5-7). Only the first class of inversion centres remains. The absence of the last four elements in this list result in quite drastic changes in the way layer II is arranged with respect to layer I. The absence of 2 fold axes and c glide planes produce less drastic differences within individual layers, but their absence nevertheless results in the close pairing which in turn allows adjacent $P\bar{1}$ layers to stack with different orientations.

While case (B) contacts are observed in triclinic $K_2Cr_2O_7$, it is certainly possible that similar triclinic compounds might show case (A) contacts with C or n symmetry relating adjacent layers. One other example of case (B) contacts has been found in the structure of β-$Ca_2P_2O_7$ (62) which has the noncentrosymmetric tetragonal space group $P4_1$. Here, four layers per cell stack adjacent to one another, each at right angles to the next in accord with the 4_1 screw axis. Case (A) contacts occur for all the known C2/c structures of Table 5-9. The choice of layer contact scheme is probably in delicate balance with the extent to which the c glide planes and 2 fold axes are missing within the layers, which in turn reflects the specific anion cation interactions that form the layers.

5.5 C Speculation on the Structures of Other $K_2Cr_2O_7$ Phases

Klement and Schwab (45) have identified a monoclinic $K_2Cr_2O_7$ phase which is metastable at room temperature and has space group C2/c (C^6_{2h}) or Cc (C^4_s) . They favour C2/c on the basis of expected similarity to the structures of $K_2S_2O_7$ and $(NH_4)_2Cr_2O_7$, and there is no evidence arising from this present work to invalidate this choice. One might expect C2/c, the highest symmetry, to be the highest temperature phase but this need not be so. The C2/c phase is probably isostructural with $K_2S_2O_7$ and $(NH_4)_2Cr_2O_7$.

Klement and Schwab have also studied the high temperature ($\gtrsim 260^{\circ}C$) $K_2Cr_2O_7$ phase and report monoclinic $P2_1/n$ (C^5_{2h}) symmetry. This space group is a subgroup of C2/c obtained by removing 2 fold axes, c glide planes and one set of inversion centres (see Fig. 5-7). The C centering which occurs as a combination of the c and n glide planes is also absent.

Assuming that the $P2_1/n$ structure also has rows of $Cr_2O_7^{-2}$ and K^+ ions interlocking backbones to form layers which stack up $\underline{a}^*$, one can speculate what the structure looks like using packing and symmetry arguments. In $P2_1/n$ the arrangement within the layers is not restricted by any c glide planes or 2 fold axes and the $P2_1/n$ layers can be distorted from the C2/c configuration. The n glide planes and 2_1 screw axes still relate the layers I and II and ensure that the rows forming adjacent layers are parallel,i.e. a type (A) contact between the zig-zag oxygen and potassium chains in adjacent faces.

It is therefore proposed that adjacent interlocking rows in $P2_1/n$ will show a sliding of rows along the trough direction and a translation along the row direction. This will give a close pairing of dichromate ions and potassium ions like that seen in the $P\bar{1}$ layers. The extent of these distortions from the equally spaced C2/c arrangement is expected to be less than that observed in $P\bar{1}$, and the choice of type (A) contacts between layer faces is favoured with n glide and 2_1 screw axes relating adjacent layers. Verification of these proposals must await a solution of the $P2_1/n$ $K_2Cr_2O_7$ high temperature structure, or alternatively that of room temperature $P2_1/n$ $Rb_2Cr_2O_7$ since these two are expected to be isostructural.

A fourth possible centrosymmetric space group allowing an analogous two layered structure might be non primitive triclinic $C\bar{1}$ (C_i^1). The only symmetry elements remaining from C2/c are the C centering and the two sets of inversion centres (see Fig. 5-7). With the absence of c glide planes and 2 fold axes within the layer, close pairing would be possible. The C centering ensures that the rows forming adjacent layers would be parallel. However, when close pairing occurs, as for $P\bar{1}$ and as speculated for $P2_1/n$, the zig-zag chains on the layer faces begin to resemble zig-zag ridges and valleys due to the sliding of the backbones of one row along the trough direction of the interlocking row. If any sliding is present, the C centering tends to put zig-zag ridge of layer II on top of zig-zag ridge of layer I and valley opposite valley. This would produce open regions between adjacent layers and would not be a favourable packing arrangement. The n glide relation as in $P2_1/n$ does allow ridges to overlap valleys and seems preferable to any $C\bar{1}$ form. If this objection to $C\bar{1}$ were overcome by limiting the amount of sliding, the structure reapproaches the high symmetry C2/c type of arrangement. Hence the speculated $C\bar{1}$ structure, while possible, seems less likely than either the proposed $P2_1/n$ form or the observed $P\bar{1}$ form. No reports on the existence of any $C\bar{1}$ form are known to the author.

A comparison of the packing schemes in $P\bar{1}$ $K_2Cr_2O_7$ and in $P4_1$ β-$Ca_2P_2O_7$ (62) shows considerable similarity. The structure of β-$Ca_2P_2O_7$ also has layers formed by rows of Ca and nearly eclipsed pyrophosphate ions interlocking backbones. These layers are reported to have local non crystallographic centres of symmetry. The layers are related to one another by a 4_1 screw axis giving an exact 90° rotation between adjacent layers. Because the 4_1 screw axis requires four layers per unit cell, the a axis is twice as long as in the corresponding two layer packing arrangements (see Table 5-9). In view of the similarities in their general packing schemes, it might even be possible for a dichromate structure to occur with the β-$Ca_2P_2O_7$ $P4_1$ type arrangement, but no form with this space group has yet been reported.

5.5 D Discussion of the Dichromate Ion

A preliminary description of the $Cr_2O_7^{-2}$ ions and their symmetry appears in Sec. 5.4 A. It remains to discuss the observed stereochemistry for the dichromate ion in $P\bar{1}$ $K_2Cr_2O_7$ and to compare it with the pyrosulfate ion, $S_2O_7^{-2}$, as found in C2/c $K_2S_2O_7$. This comparison is not ideal since the data comes from two structures with different symmetries and packing arrangements. The dichromate ion in C2/c $(NH_4)_2Cr_2O_7$ (49) with C_2 crystallographic symmetry is unfortunately not known with sufficient accuracy to make its inclusion in the comparison very meaningful. Some points of comparison may also be made between the dichromate ion and the pyrophosphate ion $P_2O_7^{-4}$ geometry found in β-$Ca_2P_2O_7$ (62). The latter comparison however cannot be representative of all pyrophosphate ion geometries since they have been found with quite different configurations in other structures (63).

The bond lengths and angles in $Cr_2O_7^{-2}$ have been listed in Table 5-5. The two crystallographically distinct dichromate ions have been found with twists of 5° and 10° away from an exactly eclipsed configuration when viewed along the Cr-Cr directions (see Fig. 5-3). In C2/c the $S_2O_7^{-2}$ ion only has crystallographic symmetry C_2 but is within experimental error of being exactly eclipsed and having C_{2v} symmetry. The pyrophosphate ions in β-$Ca_2P_2O_7$ are found with slight twists away from an exactly eclipsed configuration.

It is difficult to say with certainty whether the twisting of the dichromate ion is a property of the free ion itself, or whether the effect is a distortion away from an eclipsed configuration caused by external forces on the ion in the crystal packing. The fact that the K-K vectors do not coincide with the backbone directions in Fig. 5-9 (a) and (b) might explain the twisting of the dichromate groups. By the same argument one might expect the same twisting for the ions in a C2/c structure. None is found for the C2/c x-ray structures involving sulfur compounds since they show C_{2v} symmetry within experimental error. The ammonium dichromate structure is not accurate enough to examine this proposal for a C2/c dichromate ion. Although no free ion data[†] is available for $Cr_2O_7^{-2}$ a crystal packing explanation seems necessary to explain the two different angles of twist observed for two distinct dichromate ions. Certainly the pyrophosphate ion twisting is variable among

---

[†] Some work has been done (67) but no data on twisting is reported.

different structures. Chlorine heptoxide molecules, Cl_2O_7 however show a twist of about 15° from an eclipsed configuration even in the gaseous state (51). O-O and Cl-O repulsions between opposite halves of the molecule are suggested as the cause of this effect in Cl_2O_7.

The dichromate ion has been observed with Cr-O-Cr bridging angles of $124.0 \pm 0.1^\circ$ and $127.6 \pm 0.2^\circ$ compared to $124.2 \pm 0.5^\circ$ for the S-O-S bridge angle, and $130.5 \pm 0.8^\circ$ and $137.8 \pm 0.8^\circ$ in the β-$Ca_2P_2O_7$ pyrophosphate ions. The two different angles for the dichromate ions again probably arise from different forces in the crystal packing.

For each dichromate ion, the two bridge Cr-O bonds are equal within experimental error (mean $1.786 \pm .008$ Å) as are the terminal Cr-O bond distances (mean $1.629 \pm .010$ Å). The bridge S-O distances in the pyrosulfate ion are equivalent by symmetry and again the terminal S-O bonds seem equal within experimental error. Comparison of the bond angles, however, reveals some different features for the stereochemistry of these two ions.

Table 5-10 compares these angles along with data for other C2/c structures with analogous ions containing sulfur, namely $CH_2(SO_3)_2^{-2}$ (24) and $NH(SO_3)_2^{-2}$ (60). The first three sets of angles involve the bridge atom and all show a decrease from tetrahedral in the pyrosulfate type ions, whereas they remain close to tetrahedral for the

TABLE 5-10

Comparison of Angles (°) for Related Anions Involving Sulfur and Chromium

Analogous Angle Names Used in This Work	$P\bar{1}$ Cr_2O_7 I	$P\bar{1}$ Cr_2O_7 II	C2/c S_2O_7	C2/c $CH_2(SO_3)_2$	C2/c $NH(SO_3)_2$
OBi-Cri-Oi1	106.1	106.6	101.3	102.4	102.9
OBi-Crj-Oj1	109.6	109.7			
OBi-Cri-Oi2	109.4	109.7	106.2	106.3	106.5
OBi-Crj-Oj2	108.5	111.2			
OBi-Cri-Oi3	110.8	110.1	106.1	107.3	107.0
OBi-Crj-Oj3	109.5	108.4			
Oi1-Cri-Oi2	109.5	109.8	113.6	113.2	112.8
Oj1-Crj-Oj2	110.2	109.7			
Oi1-Cri-Oi3	111.7	110.6	115.5	113.8	114.0
Oj1-Crj-Oj3	110.6	109.9			
Oi2-Cri-Oi3	109.2	110.1	112.8	112.8	112.3
Oj2-Crj-Oj3	108.4	107.9			
Cri-OBi-Crj	124.0	127.6	124.2	119.7	125.5

dichromate ions. The one exception for the dichromate cases is the backbone angle of about 106° which has been suggested as due to packing forces since it occurs only on the one end of the Cr_2O_7 ions which protrudes the most out of the layers. The pyrosulfate angles analogous to this one exception both decrease for the two halves of the ion more than the other O-S-O angles to about 102° possibly for the same reason since each half of the ion receives equal forces from the adjacent layers in C2/c . On the other hand, McDonald and Cruickshank (52) have recently suggested that these distortions are of intraionic origin.

The second three sets of angles in Table 5-10 involve only terminal oxygen atoms. These all open from tetrahedral for the pyrosulfate types whereas they remain quite close to tetrahedral for chromium cases. The opening of the terminal O-S-O angles (and consequent decrease in the OB-S-O angles) has been suggested (3) as due to repulsion between the three charged oxygen atoms when the fourth oxygen is more distant. The fact that the terminal O distances are longer for Cr than for S (1.63 Å compared to 1.44 Å) might account for such repulsions not being as effective in opening the terminal O-Cr-O angles in $Cr_2O_7^{-2}$ ions. Weaker repulsive forces are expected since the terminal O-O distances are about 2.65 Å in $Cr_2O_7^{-2}$ compared to about 2.43 Å in $S_2O_7^{-2}$. The sum of O-O van der Waals radii (2 , Table 7-20) is 2.80 Å. Similar data for the pyrophosphate ion in β-$Ca_2P_2O_7$ shows an opening of terminal O-P-O angles with terminal O-O distances of about 2.53 Å.

In Cruickshank's theory of bonding in tetrahedral arrangements (1) the presence of such angle distortions can result in a further increase in the π-bonding strength and hence a slight shortening of the bond from its value in a purely tetrahedral environment. This tendency has been described in connection with X_nSO_{4-n} type ions in Chapter 3, particularly Table 3-5. The mean S-O (terminal) distance of 1.437 ± .004 Å (3) in the $S_2O_7^{-2}$ type ions is a shortening from the SO_4^{-2} ion S-O distance of 1.49 Å (1) as expected with the angle distortions present. However the mean Cr-O (terminal) distance of 1.629 ± .010 Å suggests that much less of a shortening occurs here from the reported 1.65 Å value for the CrO_4^{-2} ion (65). A much smaller shortening, if any, would be expected here since no appreciable angle changes have occurred from terminal oxygen repulsions. The 0.02 Å shortening itself may be in doubt since not much accurate data is available for Cr-O distances in CrO_4^{-2} ions. In any case the observed opening of terminal O-S-O angles in $S_2O_7^{-2}$ ions contrasts with the nearly tetrahedral values for terminal O-Cr-O angles and is a significant difference in the stereochemistries of these analogous sulfur and chromium ions.

The great similarity seen for the configurations of the $Cr_2O_7^{-2}$ and $S_2O_7^{-2}$ ions would suggest that Cruickshank's theory of π-bonding in tetrahedral complexes is applicable as well to chromium in tetrahedral arrangements. A reason why terminal O-Cr-O angles do not open appreciably from tetrahedral has been suggested. The fact that they do not deviate appreciably from tetrahedral means that arguments favouring any increases in the π-bonding strength are not as applicable for chromium-oxygen cases as for sulfur-oxygen cases.

It can be questioned whether the closing of the OB-S-O and OB-Cr-O angle values for the backbone oxygen atoms results in any significant decrease in the S-O or Cr-O bonds. In the C2/c structures these values (102°) decrease from tetrahedral even more than do the OB-S-O (feet) angles (106.5°) suggesting that additional distortions may be present. Indeed, if any terminal oxygen atoms should be unique in the symmetry of the bonding, one would expect it to be the terminal backbone oxygens since they lie in the same plane as the longer bridge bonds connecting the two halves of the ion. A slight shortening has been detected for the unique terminal oxygen bond length in the pyrophosphate ion in β-$Ca_2P_2O_7$ ($1.497 \pm .011$ Å compared to $1.529 \pm .016$ Å). Similar differences may also exist in the $K_2S_2O_7$ pyrosulfate ion, but experimental errors make any such trend in the data uncertain. No significant differences among the terminal Cr-O bond lengths are noted. The short Cr2-O21 distance of 1.602 Å seems unique but this can be explained by the fact that O21 only has one potassium ion contact less than 3.25 Å.

The occurrence of angle distortions for these unique oxygen atoms solely for one half of each dichromate ion (angles OB1-Cr1-O11 and OB3-Cr3-O31) correlates with the fact that O11 and O31 protrude from the layers while O21 and O41 do not. This suggests that the angle effect is due to external forces arising from the crystal packing rather than internal forces of bonding within the ion. From analogy with the gaseous Cl_2O_7 results (51), McDonald and Cruickshank (52) have suggested these distortions to be intraionic effects. They describe the distortion as a tilt of the 3 fold axis of the SO_3^- group away from the OB-S direction, and cite this as an example of bent X-O (bridge) bonds (64).

The less accurate structure determination of triclinic $K_2Cr_2O_7$ recently reported by Kuzmin, Iliukhin, and Belov (53) gives misleading information about the dichromate ion geometry. While their bridging angles of 122° and 127° compare reasonably well with the present results, they report bridging Cr-O distances of 1.72 Å and 1.85 Å in one ion, and 1.74 Å and 1.84 Å in the other. Terminal Cr-O distances likewise show wide spreads of 1.53 Å to 1.68 Å in one ion, and 1.51 to 1.63 Å in the other. Similar wide spreads among bond lengths were observed in early stages of the present refinement, even with an agreement index R as low as 0.12 or so, and particularly when refinement was attempted with only portions of the intensity data included. Hence these discrepancies in $Cr_2O_7^{-2}$ ion stereochemistry may be attributed simply to the lower accuracy available in the structure refinement of these other authors.

CHAPTER 6 SUMMARY

Cesium methylsulfonate crystallizes in space group Pnma with cell constants a = 9.526, b = 6.264, and c = 8.692 Å. Three dimensional x-ray diffraction intensity data have been collected photographically and the solved structure has been refined by least-squares procedures to give a weighted agreement index (R) of 0.12. All but the hydrogen positions were determined in the structure analysis. The structure is related to, but is not identical with, that of the isoelectronic compound barium sulfate. A comparison of these two structures has indicated the differences in crystal packing arising from the differences between the methylsulfonate and sulfate ions. The methylsulfonate ion has been found within the accuracy of this analysis to have C_{3v} symmetry with S-O = 1.47 ± 0.02 Å, S-C = 1.85 ± 0.04 Å (both corrected for thermal motion), O-S-O = 112 ± 1°, and O-S-C = 107 ± 2°. The stereochemistry of the methylsulfonate ion has been compared with that of a series in which methyl groups are substituted for the oxygen atoms of a sulfate ion. The results for the methylsulfonate ion and for other members of this series are in accord with the predictions of Cruickshank (1) about the nature of the bonding in groups of this type with sulfur as the central atom. This work on the structure determination of cesium methylsulfonate has recently been published elsewhere (31).

A rerefinement of two independently measured sets of room temperature intensity data for lithium hydrazinium sulfate failed to resolve some slight differences between the two reported x-ray structures. In addition to allowing for anisotropic thermal motion of all the large atoms, some attempts were made to refine hydrogen atom positions with the x-ray data but these latter efforts were inconclusive. Above 160°C the observed systematic absences together with the structure analysis show that the space group is $Pbn2_1$, and hence remains the same as that of the room temperature structure. The high temperature structure refinement indicated that no very significant changes occur from the room temperature structure for the heavy atom positions. Although sample deterioration at high temperatures prevented the collection of very accurate intensity data, the accuracy available ought to have shown any changes which might occur above 160°C in the positions of these large atoms. If the structure above 160°C should be distinctly different from the room temperature structure, it must differ primarily in the hydrogen configurations, which could not be observed, or possibly in the nitrogen or lithium atom z coordinates which could not be too accurately determined with the available high temperature data.

The crystal structure of triclinic potassium dichromate has been solved using single crystal x-ray diffraction techniques. The cell constants are a = 13.367, b = 7.376, c = 7.445 Å, $\alpha = 90.75^\circ$, $\beta = 96.21^\circ$, and $\gamma = 97.96^\circ$ with four formula units per cell. Anomalous dispersion experiments and least squares refinement of three dimensional intensity data to an agreement index R of 0.054 have confirmed the space group to be centrosymmetric $P\bar{1}$. The structure can be described in terms of rows of potassium and dichromate ions fitting together to form layers which stack next to one another parallel to the (100) face. The solved structure is similar in some ways to monoclinic C2/c structures like ammonium dichromate and potassium pyrosulfate, but distinct differences are observed particularly in the way in which adjacent layers in the two types of structure stack next to one another. Through detailed examination of the C2/c and $P\bar{1}$ layers, an explanation has been proposed as to how both the C2/c layer arrangement and the $P\bar{1}$ layer arrangement (with its 90° relation between layers) can each occur. Ideas arising from this explanation suggest possible structures for other phases of potassium dichromate and some predictions about these forms have been given. The dichromate ion has been described as two CrO_4 tetrahedra sharing one corner oxygen atom. Small distortions have been detected which prevent the ion from having exact

C_{2v} or even C_2 symmetry. The Cr-O (bridge) bonds are equivalent (1.786 ± 0.008 Å) as are the Cr-O (terminal) bonds (1.629 ± 0.010 Å) within experimental errors. The Cr-O-Cr bridging angles are 124.0 ± 0.1° and 127.6 ± 0.2° for the two crystallographically distinct ions. The O-Cr-O angles are essentially tetrahedral (109.5°). A comparison has been made with other similar ions where sulfur occurs in place of chromium. A discussion is presented on the possibility that Cruickshank's theory, which has previously been used to explain the bonding in these ions involving sulfur, might also be applicable for cases involving chromium. A preliminary report of this work on the structure of triclinic potassium dichromate has previously been presented elsewhere (66).

APPENDIX I

THE SCATTERING FACTOR FOR A SPHERICALLY SYMMETRIC ATOM ROTATING ABOUT AN AXIS

In cesium methylsulfonate and lithium hydrazinium sulfate, contributions to the structure factors have been calculated for hydrogen atoms using a dynamic model for the CH_3 groups and the NH_3 portion of the N_2H_5 groups. The structure factor contribution from each such hydrogen atom rotating about an axis at radius r from a centre (x_c, y_c, z_c) is (5, Section 6.3.3.6)

$$F_H(hk\ell) = f_H(hk\ell)\ J_o(2\pi tr)\ \exp 2\pi i(hx_c + ky_c + \ell z_c)$$

where t is the distance in the reciprocal lattice from the point (h,k,ℓ) to the axis through the origin parallel to the axis of rotation, and $f_H(hk\ell)$ is the usual scattering factor for a hydrogen atom. $J_o(x)$ is the zeroth order Bessel function of the first kind given by

$$J_n(x) = \sum_{k=0}^{\infty} \frac{(-1)^k\ x^{n+2k}}{2^{n+2k}\ k!\ (n+k)!} \quad (n=0,1,2...)$$

i.e. $$J_o(x) = \sum_{k=0}^{\infty} \frac{(-1)^k\ x^{2k}}{2^{2k}\ (k!)^2} .$$

Hence the contributions from these rotating hydrogen atoms may be included in eqn.[2-3] by replacing the scattering factor $f_i(hk\ell)$ by $f_H(hk\ell)\ J_o(2\pi tr)$ with the desired values of t and r, and using the coordinates $(x_c y_c z_c)$ in the exponential factor.

Padmanabhan and Balasubramanian (41) for their dynamic model of rotating NH_3 groups in LiHzS report using the hydrogen atom structure factor contribution

$$F_H(hk\ell) = \sum_{j=1}^{N} f_j(hk\ell)\ J_o(x_j)$$

where

$$x_j = \frac{4\pi r}{\lambda} \sin\Theta \sin\alpha$$

and where α is the angle between the plane containing the rotating atoms and the plane of reflection. Their Bessel function argument x_j so defined agrees with the argument $2\pi rt$ used above. However, the factor

$$\exp 2\pi i\ (hx_c + ky_c + \ell z_c)$$

is missing in both of their quoted expressions and they fail to define any coordinates for the centre of the rotating group. Such an omission in the actual calculations would mean that the rotating groups had been incorrectly centred at the unit cell origin. On the other hand, this omission could well be a misprint.

APPENDIX II

OBSERVED $LiN_2H_5SO_4$ STRUCTURE FACTOR DATA OF VAN DEN HENDE AND BOUTIN (43)

H	K	L	FO	H	K	L	FO	H	K	L	FO	H	K	L	FO	H	K	L	FO
0	2	0	20	4	6	0	54	9	7	0	6	3	9	1	12	8	1	1	2
0	4	0	32	4	7	0	15	10	1	0	20	3	10	1	11	8	2	1	30
0	6	0	55	4	9	0	10	10	3	0	10	4	1	1	10	8	3	1	7
0	8	0	14	4	10	0	15	10	5	0	18	4	2	1	23	8	4	1	19
0	10	0	15	5	1	0	14	0	2	1	61	4	3	1	8	8	5	1	10
1	1	0	30	5	2	0	35	0	4	1	29	4	4	1	32	8	6	1	4
1	2	0	38	5	3	0	18	0	6	1	11	4	5	1	6	8	7	1	10
1	3	0	66	5	4	0	15	0	8	1	20	4	6	1	26	8	8	1	22
1	5	0	42	5	5	0	7	0	10	1	7	4	8	1	26	9	0	1	33
1	6	0	10	5	6	0	9	1	0	1	41	4	10	1	12	9	1	1	12
1	7	0	13	5	7	0	6	1	1	1	40	5	0	1	34	9	2	1	3
1	8	0	19	5	8	0	25	1	2	1	33	5	1	1	25	9	4	1	5
1	9	0	19	5	9	0	23	1	3	1	7	5	2	1	25	9	5	1	20
1	10	0	7	5	10	0	16	1	4	1	11	5	3	1	21	9	6	1	17
2	0	0	15	6	0	0	10	1	5	1	14	5	4	1	10	9	7	1	8
2	1	0	61	6	1	0	39	1	6	1	21	5	5	1	6	10	1	1	9
2	2	0	9	6	2	0	8	1	7	1	22	5	6	1	36	10	3	1	19
2	4	0	15	6	3	0	11	1	8	1	18	5	7	1	16	10	4	1	3
2	5	0	37	6	4	0	9	1	9	1	14	5	9	1	16	10	5	1	6
2	6	0	18	6	5	0	35	1	10	1	11	5	10	1	10	0	0	2	100
2	7	0	29	6	6	0	12	2	1	1	65	6	2	1	17	0	2	2	39
2	9	0	8	6	7	0	22	2	2	1	19	6	3	1	29	0	4	2	22
2	10	0	12	6	9	0	10	2	3	1	22	6	4	1	13	0	6	2	26
3	1	0	26	7	4	0	25	2	4	1	18	6	5	1	15	0	8	2	10
3	2	0	46	7	5	0	20	2	5	1	28	6	6	1	10	0	10	2	28
3	3	0	5	7	7	0	12	2	6	1	14	6	7	1	20	1	1	2	10
3	4	0	4	7	8	0	10	2	7	1	29	6	8	1	16	1	2	2	13
3	5	0	15	7	9	0	10	2	8	1	5	6	9	1	13	1	3	2	22
3	6	0	8	8	0	0	39	2	9	1	23	6	10	1	4	1	4	2	18
3	7	0	30	8	1	0	4	2	10	1	7	7	0	1	16	1	5	2	16
3	8	0	32	8	2	0	29	3	0	1	32	7	1	1	27	1	6	2	13
3	9	0	10	8	4	0	11	3	1	1	25	7	2	1	21	1	7	2	26
3	10	0	11	8	6	0	21	3	2	1	24	7	3	1	7	1	8	2	23
4	0	0	30	8	8	0	5	3	3	1	16	7	4	1	12	1	9	2	9
4	1	0	7	9	2	0	21	3	4	1	27	7	5	1	15	2	0	2	31
4	2	0	18	9	3	0	27	3	5	1	27	7	6	1	9	2	1	2	21
4	3	0	26	9	4	0	15	3	6	1	25	7	7	1	20	2	2	2	4
4	4	0	30	9	5	0	9	3	7	1	17	7	8	1	5	2	3	2	14
4	5	0	15	9	6	0	7	3	8	1	14	7	9	1	5	2	4	2	11

H	K	L	FO
2	5	2	22
2	6	2	13
2	7	2	12
2	8	2	12
2	9	2	18
2	10	2	8
3	1	2	16
3	2	2	15
3	3	2	16
3	4	2	14
3	5	2	17
3	6	2	0
3	7	2	21
3	8	2	28
3	10	2	8
4	0	2	28
4	1	2	15
4	2	2	17
4	3	2	11
4	4	2	17
4	5	2	5
4	6	2	37
4	7	2	17
4	8	2	10
4	9	2	6
4	10	2	17
5	1	2	6
5	2	2	19
5	3	2	15
5	4	2	12
5	5	2	5
5	6	2	7
5	7	2	7
5	8	2	19
5	9	2	12
5	10	2	11
6	1	2	14
6	3	2	4
6	4	2	6
6	5	2	22
6	6	2	11
6	7	2	13
6	8	2	10
6	9	2	11
7	1	2	29
7	2	2	10
7	3	2	6
7	4	2	9
7	5	2	14
7	6	2	9
7	7	2	17
7	8	2	15
8	0	2	14
8	1	2	7
8	2	2	10
8	4	2	14
8	5	2	6
8	6	2	14
8	7	2	9
9	2	2	16
9	3	2	10
9	4	2	13
9	6	2	4
10	0	2	10
10	1	2	15
10	2	2	8
10	3	2	9
10	4	2	3
0	2	3	40
0	4	3	13
0	6	3	16
0	10	3	11
1	0	3	32
1	1	3	20
1	2	3	25
1	3	3	8
1	4	3	13
1	5	3	16
1	6	3	22
1	7	3	12
1	8	3	5
1	9	3	13
1	10	3	6
2	1	3	45
2	2	3	11
2	3	3	22
2	5	3	23
2	6	3	10
2	7	3	17
2	9	3	14
2	10	3	6
3	0	3	34
3	1	3	32
3	2	3	17
3	3	3	5
3	9	3	2
4	1	3	3
4	2	3	32
4	3	3	8
4	4	3	36
4	5	3	3
4	8	3	15
5	0	3	31
5	1	3	31
5	3	3	2
5	4	3	4
5	5	3	9
5	6	3	17
5	7	3	15
5	8	3	6
5	9	3	2
6	1	3	10
6	2	3	2
6	3	3	22
6	4	3	8
6	5	3	13
6	6	3	3
6	7	3	23
6	8	3	11
7	0	3	13
7	1	3	13
7	2	3	13
7	3	3	10
7	4	3	12
7	5	3	17
7	6	3	12
7	7	3	11
8	1	3	2
8	2	3	18
8	3	3	4
8	4	3	16
8	5	3	2
8	6	3	6
9	0	3	22
9	1	3	9
9	2	3	1
9	3	3	1
9	4	3	8
0	0	4	40
0	2	4	13
0	4	4	14
0	6	4	23
0	8	4	10
1	1	4	5
1	2	4	10
1	3	4	17
1	5	4	7
1	6	4	6
1	7	4	16
1	9	4	14
2	0	4	10
2	1	4	29
2	2	4	7
2	3	4	5
2	4	4	6
2	5	4	18
2	7	4	16
2	8	4	8
2	9	4	8
3	1	4	8
3	2	4	25
3	3	4	14
3	4	4	11
3	5	4	15
3	6	4	9
3	7	4	16
3	8	4	13
3	9	4	7
4	0	4	46
4	1	4	4
4	2	4	12
4	3	4	7
4	4	4	6
4	6	4	27
4	7	4	7
5	1	4	8
5	2	4	14
5	3	4	19
5	4	4	13
5	5	4	8
5	6	4	3
5	7	4	4
6	0	4	2
6	1	4	13
6	2	4	6
6	5	4	26
6	6	4	6
6	7	4	13
7	1	4	13
7	2	4	11
7	3	4	4
7	4	4	9
8	0	4	9
8	1	4	4
8	2	4	4
8	3	4	3
0	2	5	11
0	4	5	9
0	6	5	11
1	0	5	4
1	1	5	5
1	2	5	3
1	3	5	4
1	4	5	9
1	5	5	7
1	6	5	18
1	7	5	7
2	1	5	17
2	2	5	4
2	3	5	6
2	4	5	4
2	5	5	7
2	6	5	6
2	7	5	20
3	0	5	8
3	1	5	5
3	2	5	5
3	4	5	5
3	5	5	14
3	6	5	6
3	7	5	10
4	1	5	3
4	2	5	8
4	4	5	13
4	6	5	8
5	0	5	28
5	1	5	4
5	2	5	3
5	3	5	7
5	5	5	6
6	1	5	5
6	2	5	6
6	3	5	12
6	4	5	6
7	0	5	4
0	0	6	28
0	2	6	3
0	4	6	9
1	1	6	3
1	2	6	4
1	3	6	11
1	4	6	7
2	0	6	3
2	1	6	19
2	2	6	5
2	3	6	2
3	2	6	12

APPENDIX III

VERIFICATION OF A RESULT USED IN SECTION 5.3

This appendix will show the approximate equivalence for small Δ_1, Δ_2 of the intensities from the following:

I The P1 structure factor summation function for the two arguments $\underline{X}_1 = \underline{x} + \underline{\Delta}_1$ and $\underline{X}_2 = -\underline{x} + \underline{\Delta}_2$ each with unit weight

and

II The P$\bar{1}$ structure factor summation function for the two arguments $\underline{X}_1{}' = \underline{x} + \underline{\Delta}_1$ and $\underline{X}_2{}' = \underline{x} - \underline{\Delta}_2$ each with 1/2 weight.

Comparison will be made of the intensities arising in these two cases and that from a simple P$\bar{1}$ case with argument $\underline{X}_1{}'' = \underline{x}$.

Proof

The P1 function is

$$F(\underline{h}) = A + iB = \sum_i \omega_i \, [\cos 2\pi \, \underline{X}_i \cdot \underline{h} + i \sin 2\pi \, \underline{X}_i \cdot \underline{h}] \ .$$

The P$\bar{1}$ function is

$$F(\underline{h}) = A = \sum_i \omega_i \, [2 \cos 2\pi \, \underline{X}_i \cdot \underline{h}] \ .$$

Case I gives

$$F(\underline{h}) = \cos 2\pi \, (\underline{x} + \underline{\Delta}_1) \cdot \underline{h} + i \sin 2\pi \, (\underline{x} + \underline{\Delta}_1) \cdot \underline{h}$$
$$+ \cos 2\pi \, (-\underline{x} + \underline{\Delta}_2) \cdot \underline{h} + i \sin 2\pi \, (-\underline{x} + \underline{\Delta}_2) \cdot \underline{h} \ .$$

Case II gives

$$F(\underline{h}) = \cos 2\pi\ (\underline{x} + \underline{\Delta}_1)\cdot\underline{h}$$
$$+ \cos 2\pi\ (\underline{x} - \underline{\Delta}_2)\cdot\underline{h}\ .$$

Since cos z = cos(-z) the difference between the two cases is

$$i\ [\sin 2\pi\ (\underline{x} + \underline{\Delta}_1)\cdot\underline{h} + \sin 2\pi\ (-\underline{x} + \underline{\Delta}_2)\cdot\underline{h}]$$

$$= i\ [\sin \underline{x}\cdot\underline{h}\ (\cos \underline{\Delta}_1\cdot\underline{h} - \cos \Delta_2\cdot\underline{h})$$
$$+ \cos \underline{x}\cdot\underline{h}\ (\sin \underline{\Delta}_1\cdot\underline{h} + \sin \underline{\Delta}_2\cdot h)]\ .$$

When both Δ_1 and Δ_2 are small $\cos \underline{\Delta}_1\cdot\underline{h} \approx \cos \underline{\Delta}_2\cdot\underline{h}$, $\sin \underline{\Delta}_1\cdot\underline{h} \approx \underline{\Delta}_1\cdot\underline{h}$, and $\sin \underline{\Delta}_2\cdot\underline{h} \approx \underline{\Delta}_2\cdot\underline{h}$ giving a difference of only

$$i\ (\underline{\Delta}_1 + \underline{\Delta}_2)\cdot\underline{h}\ \cos \underline{x}\cdot\underline{h}$$

which is small when Δ_1 and Δ_2 are small. Hence the two cases differ by only a small imaginary term. They give rise to nearly equivalent intensities since the small difference occurs for B and the square makes little difference to the expression $I = (A^2 + B^2)$ when B is small itself as in a pseudo-centrosymmetric structure.

The simple $P\bar{1}$ case for the argument $X_1'' = \underline{x}$ with unit weight gives $F(\underline{h}) = A = 2 \cos 2\pi\ \underline{x}\cdot\underline{h}$ which differs only in the A term from cases I and II by a factor of $\frac{1}{2}(\cos 2\pi\underline{\Delta}_1\cdot\underline{h} + \cos 2\pi\ \underline{\Delta}_2\cdot\underline{h})$. While this factor is close to unity for small Δ_1, Δ_2, the difference in $F(\underline{h})$ occurs now in the A term. The intensity $I = (A^2 + B^2)$ is sensitive to even small changes in A since A is usually not small itself.

Hence cases I and II give nearly identical intensities. For non identically zero Δ_1, Δ_2, both cases have intensities similar to but probably noticeably different from the simple case corresponding to the isotropic $P\bar{1}$ model. These proofs have bearing on the arguments of Section 5.2 C.

BIBLIOGRAPHY

1. D. W. J. Cruickshank. J. Chem. Soc. 5486 (1961).
2. L. Pauling. The Nature of the Chemical Bond. Cornell University Press, Ithica, New York. 1960.
3. H. Lynton and M. R. Truter. J. Chem. Soc. 5112 (1960).
4. International Tables for X-ray Crystallography. Vol. I. Kynoch Press, Birmingham, England. 1952.
5. International Tables for X-ray Crystallography. Vol. II. Kynoch Press, Birmingham, England. 1959.
6. International Tables for X-ray Crystallography. Vol. III. Kynoch Press, Birmingham, England. 1962.
7. R. W. James. The Optical Principles of the Diffraction of X-rays. G. Bell and Sons Ltd., London. 1962.
8. H. Lipson and W. Cochran. The Determination of Crystal Structures. G. Bell and Sons Ltd., London. 1962.
9. M. J. Buerger. X-ray Crystallography. John Wiley and Sons Inc., New York. 1942.
10. M. J. Buerger. Vector Space. John Wiley and Sons Inc., New York. 1959.
11. M. J. Buerger. Crystal-structure Analysis. John Wiley and Sons Inc., New York. 1960.
12. M. J. Buerger. The Precession Method. John Wiley and Sons Inc., New York. 1964.

13. C. Kittel. Introduction to Solid State Physics. John Wiley and Sons Inc., New York. 1956.

14. A. L. Patterson. Z. Krist. 90, 517 (1935).

15. E. A. Robinson. Private Communication.

16. V. Silberberg. M. A. Thesis. University of Toronto. 1962.

17. J. A. Bearden. X-ray Wavelengths. U. S. Atomic Energy Commission, Div. of Tech. Information Extension, Oak Ridge, Tennessee. 1964.

18. R. J. Blume. Rev. Sci. Instr. 32, 598 (1961).

19. W. C. Hamilton. Acta Cryst. 18, 502 (1965).

20. M. Merrington and C. M. Thompson. Biometrica 33, 73 (1946).

21. W. R. Busing and H. A. Levy. Acta Cryst. 17, 142 (1964).

22. M. A. James and W. A. Wood. Proc. Roy. Soc. London, Ser. A, 109, 598 (1925).

23. Chu Chia-hsuan, Cheng Yu-fen, and Shen Chin-chuan. Sci. Sinica Peking, 14, 1541 (1965).

24. M. R. Truter. J. Chem. Soc. 3393 (1962).

25. A. I. M. Rae and E. N. Maslen. Acta Cryst. 15, 1285 (1962).

26. S. R. Hall and E. N. Maslen. Acta Cryst. 18, 301 (1965).

27. C. J. Brown and D.E.C. Corbridge. Acta Cryst. 21, 485 (1966).

28. D. E. Sands. Z. Krist. 119, 245 (1963).

29. C. L. Coulter, P. K. Gantzel, and J. D. McCullough. Acta Cryst. 16, 676 (1963).

30. I. C. Zimmermann, M. Barlow, and J. D. McCullough. Acta Cryst. 16, 883 (1963).

31. J. K. Brandon and I. D. Brown. Can. J. Chem. 45, 1385 (1967).

32. F. Sommer and K. Weise. Z. anorg. allgem. Chem. 94, 51 (1916).

33. R. Pepinsky, K. Vedam, Y. Okaya, and S. Hoshino. Phys. Rev. 111, 1467 (1958).

34. J. D. Cuthbert and H. E. Petch. Can. J. Phys. 41, 1629 (1963).

35. R. Blinc, M. Schara, and S. Poberaj. J. Phys. Chem. Solids 24, 559 (1963).

36. I. D. Brown. Acta Cryst. 17, 654 (1964).

37. J. H. Van den Hende and H. Boutin. Acta Cryst. 17, 660 (1964).

38. N. Niizeki and H. Koizumi. J. Phys. Soc. Japan 19, 132 (1964).

39. J. Vanderkooy, J. D. Cuthbert and H. E. Petch. Can. J. Phys. 42, 1871 (1964).

40. R. S. Krishnan and K. Krishnan. Proc. Indian Acad. Sci. 61A, 122 (1965).

41. V. M. Padmanabhan and R. Balasubramanian. Acta Cryst. 22, 532 (1967).

42. W. D. MacClement, M. Pintar, and H. E. Petch. (in press, Can. J. Phys.).

43. J. H. Van den Hende and H. Boutin. Private Communication.

44. E. Mitscherlich. Ann. Physik 28, 116 (1833).

45. U. Klement and G. Schwab. Z. Krist. 114, 170 (1960).

46. G. S. Rao. J. Indian Inst. Sci. 41A, 47 (1959).

47. V. S. Podisko. Tr. Inst. Kristallogr. AN SSSR 9, 327 (1954).

48. V. F. Parvov and A. V. Shubnikov. Kristallografiya 9, 435 (1964). (Translation in Soviet Physics-Cryst. 9, 361 (1964).).

49. A. Bystrom and K. Wilhelmi. Acta Chem. Scand. 5, 1003 (1951).

50. G. A. Barclay, E. G. Cox, and H. Lynton. Chemistry and Industry, 178 (1956).

51. B. Beagley. Trans. Faraday Soc. 61, 1821 (1965).

52. W. S. McDonald and D. W. J. Cruickshank. Acta Cryst. 22, 43 (1967).

53. E. A. Kuzmin, V. V. Iliukhin, and N. V. Belov. Doklady Akad. Nauk SSSR 173, 1078 (1967). (Translation in Soviet Physics - Doklady. To be Published. 1967).

54. A. V. Shubnikov. Z. Krist. 50, 19 (1911).

55. A. V. Shubnikov. Z. Krist. 76, 469 (1931).

56. P. Groth. Chemische Kristallographie 2, 586 (1908).

57. P. L. Stedehouder and P. Terpstra. Physica 10, 113 (1930).

58. B. Gossner and F. Mussgnug. Z. Krist. 72, 476 (1930).

59. M. E. Straumanis, T. Ejima, and W. J. James. Acta Cryst. 14, 493 (1961).

60. D. W. J. Cruickshank and D. W. Jones. Acta Cryst. 16, 877 (1963).

61. L. A. Zhukova and Z. G. Pinsker. Kristallografiya 9, 44 (1964). (Translation in Soviet Physics-Cryst. 9, 31 (1964).).

62. N. C. Webb. Acta Cryst. 21, 942 (1966).

63. B. E. Robertson. Ph.D. Thesis. McMaster University, 1967.

64. F. L. Hirshfeld. Israel J. Chem. 2, 87 (1964).

65. G. Collotti, L. Conti, and M. Zocchi. Acta Cryst. 12, 416 (1959).

66. J. K. Brandon and I. D. Brown. Bull. Am. Phys. Soc. 12, 671 (1967).

67. R. G. Kidd. Can. J. Chem. 45, 605 (1967) .